5G Millimeter Wave Frequencies And Mobile Networks

A Technology Whitepaper on Key Features and Challenges

June 14, 2019

Notice and Disclaimer –

The statements and viewpoints expressed in this White Paper are those of the IWPC mmWave Working Group as of the release date noted on the cover page. Except as expressly stated, they may not reflect the views of individual IWPC members. The IWPC mmWave Working Group has endeavored to provide information that is current and accurate as of the Release Date, but it does not warrant that all information is complete and error-free. Nor does it undertake to update this white paper based upon new information and developments, though it may elect to do so in its sole discretion and without notice. All information in this white paper is provided on an "AS IS" basis. The IWPC disclaims all express and implied warranties relating to the contents of this white paper.

The IWPC has not investigated or made an independent determination regarding title or non-infringement of any technologies that may be described or reference in this white paper. Persons seeking to implement such technologies are solely responsible for making all assessments relating to title and non-infringement of any technology, standard, or specification referenced in this document and for obtaining appropriate authorization to use such technologies, standards, and specification, including through the payment of any required license fees. IWPC and the IWPC Logo are trademarks of the IWPC.

Table of Contents

Table of Figures

1. Whitepaper Objectives

The use of mmWave frequency bands for mobile terrestrial networks is one of the new aspects introduced in 3GPP Release 15, which includes the first definition of a 5G standard. While mmWave frequencies have been used in the past for satellite, LMDS, or 802.11ad transmissions, this is the first time that mmWave frequencies will be used for point-to-multipoint mobile networks supporting handheld devices, among other use cases.

There have been many positive advancements in the areas of mmWave in the last few years, although many debatable topics still persist in the industry. Of particular interests are the reliability coverage offered by mmWave, robustness of the wireless connections, and device impacts in terms of power consumption, thermal dissipation, practical peak throughput expected performance, etc.

This whitepaper intends to provide a comprehensive end-to-end wireless system technology review of all the areas impacting the implementation and deployment of mmWave frequencies for mobile networks and propose certain architectures and configuration that may help overcome some of mmWave shortcomings as it relates to coverage or device constraints. This information may be beneficial to the overall wireless industry, especially with the upcoming initial mmWave deployments in the US and other parts of the world. Furthermore, the information provided in this paper may serve to identify and highlight areas where further technological advancement may be required in the future.

This paper does not intend to cover topics related to business case, costs associated with deployment of mmWave frequencies, or incremental cost to support mmWaves in smartphones.

2. Executive Summary

3GPP Release 15 introduces 5G technology intended to address the stated ITU-2020 goals including higher spectral efficiency, greater numbers of users, higher data rates, reduced end-to-end latency, a more consistent user experience, higher device connection densities, prolonged device battery life, service-based core network, etc. While many of the fundamental 5G technology components build on 4G technology, there are several technological advancements that are new in 5G. Among these new features is support for mmWave frequency bands, otherwise known as FR2 in 3GPP vocabulary. This inclusion of mmWave frequencies is an important aspect of 5G technology, which attempts to alleviate mobile network capacity constraints in certain areas, or address new use cases related to factory automation, fixed wireless access, vehicular connectivity, and potentially many others.

This whitepaper provides a comprehensive review of key technological features required to support mmWave frequency deployment, particularly for mobile network applications and handheld devices like smartphones. Subsequent versions of this whitepaper will address other potential use cases, as 3GPP support for those uses cases materializes. Particular attention has been paid to technology features such as beamforming or enhanced dual-connectivity (EN-DC) between 5G mmWave bands and LTE sub-6GHz

bands, which are meant to address the key limitations of mmWave spectrum (i.e. reduced coverage when compared to sub-6GHz frequencies, potential high device power consumption or thermal dissipation, reliability of connection, etc.). Furthermore, the whitepaper focuses on UE implementation, as it pertains to power consumption, thermal dissipation, and other UL transmit power intricacies related to mmWaves when compared to sub-6GHz-bands. In addition, this paper summarizes the latest status of mmWave frequency allocation around the world, as well as the current and planned work within 3GPP to support such frequencies, both of which are key to establishing a large-scale ecosystem paramount to success of any technology, as demonstrated by certain sub-6GHz bands that have benefited from unified global deployments.

Propagation coverage of mmWave frequencies has been a much-debated topic in recent times, driven in part by the lack of building material data as well as accurate tools and methods with which to model. Given the potential for varying building surfaces to greatly and differently impact the reflective properties of mmWaves depending upon the UE location, it is difficult to develop accurate coverage prediction models without access to a reliable and consistent database of building materials. In an effort to provide a realistic view of mmWave coverage, the simulation analysis included in the whitepaper takes a dual-track approach. Specifically, the UL coverage simulations included here are based on both the best-case max UE transmit power as well as a more realistic 50% percentile UE transmit power. This approach is deemed more realistic not only because 4G/5G mobile networks are UL coverage limited, but also because it is unlikely that handheld devices, like smartphones, will have a constant line-of-site with a mmWave gNB. Furthermore, co-location between mmWave and sub-6GHz bands is assumed, as this allows for a much more practical and optimal EN-DC deployment between mmWave and sub-6GHz bands.

The simulation coverage analysis in this whitepaper focuses largely on dense urban areas, which are assumed to more likely be congested today as well as being among the first areas targeted for mmWave deployments in the US and potentially elsewhere. Unfortunately, simulation analysis in this paper does not consider mobility related to user movement, which may have a detrimental aspect on overall mmWave performance when compared to sub-6GHz frequencies, due to lack of support for such a feature in two different simulation tools used in this paper. Results show that mmWave frequency deployments in a stand-alone (i.e. SA) configuration would require 2.5-3 times the site density when compared to mid-band sub-6GHz 5G bands in order to achieve similar outdoor coverage. Understandably, a higher number of sites may be required if indoor mmWave coverage is desired, as outdoor-to-indoor coverage using mmWave seems unrealistic. It should also be mentioned that the sub-6GHz inter-site distance used in the paper is approximately 300 to 450 meters, which is typical for metro/dense urban areas, although lower than other deployment morphologies such as suburban or rural areas. It is, therefore, expected that mmWave outdoor coverage for these other morphologies (i.e. suburban or rural areas) may require higher site densities in order to ensure full coverage (i.e. potentially up to 10 times).

The deployment of EN-DC combination between mmWave and LTE sub-6GHz would require approximately 1.8x more sites than sub-6GHz bands in dense urban areas to ensure comparable outdoor coverage between the two options, as network would become DL coverage constrained under such

configuration. In this case, a dedicated LTE UL channel bandwidth of 20-40MHz would be required to support the DL peak speeds of 1-2Gbps offered by mmWave for TCP type applications, or overall optimal mmWave DL capacity deployment distribution. Deployment of mmWave frequencies in an EN-DC combination with sub-6GHz bands would also alleviate some of device power consumption concerns associated with UL mmWave transmission, as UL data would utilize the LTE channel. However, the availability of large UL channel bandwidths in single sub-6GHz bands, up to 40MHz, may be quite challenging for most operators. Therefore, such deployments may need to support inter-band UL carrier-aggregation on sub-6GHz bands (i.e. two independent Tx chains in UL), which can pose issues for a device's battery life. Of course, there are multiple assumptions that impact a simulation coverage analysis, and various tools may offer different outcomes even for the same deployment environment. Therefore, coverage measurements in real mmWave frequency deployed networks using commercial smartphones would be a welcome addition not only for this whitepaper, but for the overall calibration of simulation tools as well.

The reliability and robustness of mmWave connections on handheld devices is of great technical interest, given the related impacts on key factors associated with a well-run mobile network, such as coverage predictability and deterministic user behavior. To that end, increasing the number of antenna elements/panels on handheld devices in a distributed manner increases the probability of connection robustness. Preliminary analysis has shown that increasing the number of antenna modules on UE side to three separate entities located at different sides of the phone yields a 39% increase in DL spectral efficiency, or 13% DL spectral capacity. However, such designs may pose additional challenges in terms of the device size, cost, power consumption, and thermal dissipation.

The form factor of mobile UEs and the interaction with the user and the environment strongly constrain the practical implementation of UE antennas and achievable spherical coverage. This paper analyzes the performance of various potential mmWave UE antenna technologies, such as phased arrays, fixed high-gain switched antennas, and reactive beam steering. These UE antenna solutions are analyzed to look at performance, potential cost, ease of implementation, and size implications. While the phased array provides the most flexible and best performing beam-forming solution, it may not be the most optimal solution for UE implementation where cost and size are at a premium. Alternatively, a switched array of high-gain antennas may offer the simplest system implementation, and a relatively low-cost solution due to the use of a single IC RF chipset implementation. But, this solution requires a higher-power PA and requires low-loss, multi-throw switches. Reactive beam steering also offers a low-cost approach, as a single IC can provide the RF front end and the tunable reactive terminations. A reactive beam steering approach is more complex than the switched array, but less complex than a phased array, as it may not require low-loss, multi-throw switches and the overall combined antenna system is smaller than a high-gain antenna switched approach. Irrespective of UE antenna technology selection, it is critical to pay careful attention to the proper integration of mmWave antennas into the mechanical structure of the UE in order to maintain the radiating properties of the system. This is mainly due to the susceptibility of mmWave antennas to a mobile terminal's environment or materials, including the device casing, glass, chassis, or even a user's hand, etc. all of which can distort the radiated patterns. The multi-band

requirements, be it in the form of support for several mmWave bands or co-integration of mmWave with sub-6GHz frequencies in the same design, will also have an impact on overall mobile UE antenna system design in order to achieve certain levels of performance, and may well drive the need for innovative solutions in tuning and/or re-configurability throughout the RF front-end signal chains.

The UL transmission challenges of mmWave bands are reflected in the 3GPP's MPR large power reduction allowances and the relatively lenient ACLR specification as compared to sub-6GHz band, which suggest that the current technology has more difficulty with keeping mmWave transmissions as "clean" and contained as sub-6GHz transmissions. Other factors related to large channel bandwidths, frequent beam management due to limited cell size on mmWave systems, or power handling efficiency of transmit paths related to those frequencies may have an additional impact on overall power consumption. To overcome some of those challenges, system-on-chip integration of RF front-end architectures supporting mmWave frequencies is seen as a beneficial approach. Such solutions are believed to recover up to 37% of UL RFFE power consumption when compared to stand-alone component integration architectures. Other more generic technical solutions such as bandwidth part channel allocation or cross-slot scheduling may also have a positive impact. Overall, the subject of mmWave frequency total power consumption and thermal dissipation, particularly on the UE, is a very complex multi-disciplinary topic that depends greatly on the selected implementation approach. To that end, it is believed that developing user data profiles that allow for a more unified and holistic power consumption per bits/sec transmission/reception would benefit the entire industry in terms of product performance evaluation and efficiencies related to specific optimization techniques.

Equipment certification for mmWave also presents a new paradigm, as all of RF conformance tests have to be executed in an over-the-air environment under far-field conditions, compared to sub-6GHz frequencies that use mostly conducted methodologies. The test and measurement industry has made significant progress in addressing over-the-air mmWave frequency test complexities and implementation challenges through innovative solutions that reduce both the RF chamber size requirements and the time required to execute the related tests. As of this writing, the device RF exposure certification is based on the FCC's October 3rd 2018 interim guidance, which uses 4-seconds as the time window and 4 cm2 as averaging area for 28 GHz and 39 GHz. There is no current indication that the FCC will make any announcements with respect to mmWave RF exposure, as there have been no other revised test procedures/KDBs released to date.

The deployment of mmWave frequency for mobile wireless networks is in its infancy and a lot will be learned from the initial 2019-2020 deployments in the USA and/or other countries. Hopefully, these lessons will help in the evaluation of the multi-disciplinary technology complexities associated with mmWave point-to-multipoint mobile wireless networks, as well as the associated performance under real-world deployment scenarios. In addition, it is hoped that these learnings will help spur further technological advancements to improve the performance and reliability as well as alleviate some coverage constraints inherent in mmWave frequencies.

3. Introduction

The introduction of 5G heralds a new area of technological advancement intended to address a variety of use cases, some of which may have not been possible to serve in the past, and opens new frontiers for the wireless industry. While mobile broadband has constituted the dominant use case for mobile operators so far, 5G intends to also deal with other large categories of use cases, such as Massive IoT and critical communications.

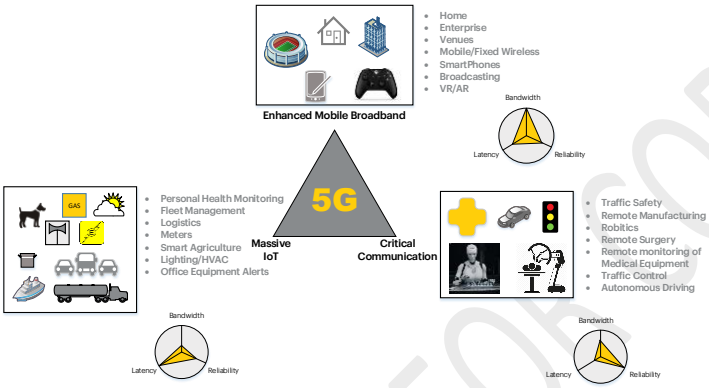

Figure 3-1 5G Use case categories

Each of those categories present their own specific requirements in terms of throughput, latency, reliability and density of connection, and other performance indicators, which may substantially increase the complexity of mobile networks. Furthermore, all these use cases would further exacerbate capacity constraints already experienced in mobile network, as increased data traffic will impose additional demands on those networks [1][2].

Faced with those data traffic challenges and a shortage of spectrum in already established sub-6GHz 4G frequency bands, 3GPP Release 15 defines a new range of frequencies above 24GHz, which are specific to 5G technology, to help overcome some of the current capacity congestions as well as to address very time sensitive use cases. While mmWave frequencies have been used in the past in other scenarios, this is the first time that such frequencies will be used for mobile terrestrial networks. Having said that, mobile networks pose a different set of requirements compared to previous scenarios where mmWave were deployed, particularly related to mobility, customer expectations in terms of device battery life, reliability and predictability of operation in terrestrial environments, etc.

To address some of those requirements, initial 5G mmWave 3GPP specifications rely on several technological advancements related to massive MIMO, beamforming techniques, antenna designs, power management schemas, chipset processing power increase, etc to overcome fundamental limitations related to coverage, reliability of wireless link, and power consumption associated with mmWave frequencies. Furthermore, network architectures associated with centralized eNB/gNB implementation like C/V/C-RAN may further help with beamforming techniques to ensure a more robust wireless link while ensuring smother user mobility experience. Understandably, there is a high level of complexity associated with such combination of multi-domain technological advancements integrated into a single system,

which in turn may lead to uncertainties as to what level of performance to expect with mmWave frequencies in a mobile network deployment. Some of those uncertainties were also experienced as part of some of initial mmWave 5G deployments in the US [95][96]. Very preliminary evaluation of those deployments by various independent analysts found that while such networks can offer very high user speeds, all be it with very few or even single user in the network, connectivity reliability, coverage, and stability of the service remains an issue. Of course these are early days, and with time, resources, and investment technology has shown that it can overcome various challenges. Despite all these, there are still differences of opinion in the industry as to what the viability of technology and business case might be for mmWave deployment in large scale mobile networks.

To that end, this whitepaper is intended to provide a comprehensive review of all the technological facets related to 5G mmWave frequencies starting with use cases, global frequency allocation, 3GPP current status and future expected developments, coverage analysis, implementation considerations in both gNB and UE side, regulatory, as well as equipment testing methodologies. It is therefore very much hoped that such extended information will help the readers to obtain a more accurate perspective on this topic and help identify future work in the area.

This whitepaper is organized into several sections. Section 4 describes potential business use cases that can be addressed by mmWave frequency technologies, where eMBB, industrial automation, vehicular connectivity, and fixed wireless access are of primary focus. Efforts have been made for each of those use cases to define application throughput and latency requirements and how mmWave frequencies address those needs. Section 5 summarizes the current status of 3GPP Rel. 15 specifications as it relates to mmWave frequencies (i.e. FR2) in terms of bands, RF specifications, as well as advancements expected as part of 3GPP Release 16. Section 6 presents current mmWave spectrum allocation around the globe, as well as expected auctions in the near future. Section 7 focuses on mmWave coverage analyses with special focus on dense urban areas where most current network capacity constraints are present. The analysis compares mmWave coverage versus mid-band sub-6Ghz bands using scenarios of co-located sites and both maximum and 50% percentile UE transmit power settings. Furthermore, this section explores scenarios of dual-connectivity between mmWave DL and sub-6GHz UL frequencies, in order to overcome some of mmWave's coverage shortcomings while ensuring expected performance. Section 8 addresses implementation aspects related to mmWave both from the gNB access point as well as UE perspective. This section also provides analysis related to single user and sector expected peak throughput performance as a function of channel bandwidths, MIMO configuration, etc. Additionally, information is provided on the first wave of products intended for eMBB use case, both in eNB/gNB and UE spaces. Section 9 addresses regulatory aspects associated with mmWave frequency transmission and equipment certification. Information is provided for US, European, as well as Asian regions. Section 10 focuses on testing methodologies related to mmWave frequencies, as those high frequencies pose specific challenges not present in sub-6 GHz frequencies. And finally, section 11 summarizes the main findings of this whitepaper and recommends future work in this area to better understand expected performance. The whitepaper also offers additional detailed information in the form of an appendix section.

4. mmWave Use case for Mobile Access Networks

This section of the paper introduces four user cases where the applicability of mmWave may be pertinent. The key to successful deployment of these use cases is the integration of single high capacity but coverage limited mmWave network and devices, serving diverse verticals such as automotive, smart manufacturing and many other Internet of Things (IoT), virtual reality (VR), and augmented reality (AR). The diversity of service requirements in terms of capacity, speed, latency, and reliability leads the necessity of mmWave deployment in certain areas of the 5G network, but may not in all areas simply because of massive deployment cost.

4.1. Enhance Mobile Broadband

Current mobile networks suffer from congestion, particularly at dense urban areas, special venues or event, or certain market geographies. According to a new study of 80 wireless network operators across the globe by Helsinki-based research firm Rewheel, Verizon was the operator with the highest yearly average network capacity utilization, at 57% in 2017 [46]. AT&T and T-Mobile in the U.S. ranked among the top 10 operators in terms of higher network capacity usage. AT&T is using 32% of its network capacity while T-Mobile is using 28% and Sprint is using 15% of its network capacity, as shown in Table 4-1.

Mobile network operator name - country code	Country population 2017	Annual data volume Terabytes 2017	Monthly mobile data usage per capita Gigabytes 2017	Aggregate Downlink Busy Hour throughput Gbit/s 2017 year average	Radio network capacity utilization 2017 year average, existing FDD & SDL & 2.5/2.6 GHz TDD spectrum holdings, existing macro site grid, 4x4 MIMO, 256 QAM, downlink		Fixed-to-mobile broadband substitution potential Incremental 200 GB/month MBB connections expressed as a % of country population that can be carried by operator existing macro site grid capacity (up to 80% utilisation in 5% most loaded macro site sectors)					
					5% most loaded sectors	50% least loaded sectors	with existing FDD & SDL & 2.5/2.6 GHz TDD spectrum holdings	AND add existing 2.3 GHz TDD spectrum holdings	AND add massive MIMO on existing 2.3/2.5/2.6 GHz TDD	AND add massive MIMO on existing 2.3/2.5/2.6/ 3.4-3.8 GHz TDD	OR add massive MIMO on existing 2.3/2.5/2.6 and on **40 MHz** of 3.4-3.8 GHz TDD	OR add massive MIMO on existing 2.3/2.5/2.6 and on **100 MHz** of 3.4-3.8 GHz TDD
Verizon-US	325,719,200	5,562,215	1.4		57%	4%			0%			
Play-PL	37,972,964	612,758	1.3		55%	4%			0%			
FreeMobile-FR	66,989,083	570,570	0.7		39%	3%			0%			
Vodafone-IE	4,784,383	105,297	1.8		35%	3%			1%			
ATT-US	325,719,200	5,143,349	1.3		32%	2%			2%			
Vodafone-AU	24,450,561	258,000	0.9		31%	2%			1%			
3-UK	65,808,573	785,359	1.0		30%	2%			1%			
DNA-FI	5,503,297	529,441	8.0		29%	2%			7%			
T-Mobile-AT	8,772,865	313,503	3.0		29%	2%			3%			
3-AT	8,772,865	500,000	4.7		28%	2%			10%			
T-Mobile-US	325,719,200	2,724,879	0.7		28%	2%			1%			
Meteor-IE	4,784,383	56,386	1.0		26%	2%			1%			
Orange-PL	37,972,964	438,000	1.0		25%	2%			1%			
KDDI-JP	127,484,450	2,251,467	1.5		25%	2%			2%			
Optus-AU	24,450,561	279,199	1.0		22%	2%			1%			
NTTdocomo-JP	127,484,450	3,395,550	2.2		22%	2%			3%			
Elisa-FI	5,503,297	637,200	9.6		22%	2%			34%			
TDC-DK	5,748,769	178,573	2.6		22%	2%			3%			
O2-UK	65,808,573	401,489	0.5		21%	2%			4%			
KT-KR	50,982,212	1,260,352	2.1		21%	2%			9%			
Telia-FI	5,503,297	407,746	6.2		20%	2%			9%			
Polkomtel-PL	37,972,964	700,000	1.5		20%	2%			6%			
Telstra-AU	24,450,561	494,013	1.7		19%	1%			3%			
3-DK	5,748,769	123,089	1.8		19%	1%			6%			
T-Mobile-PL	37,972,964	359,242	0.8		17%	1%			1%			
BouyguesTelecom-FR	66,989,083	598,794	0.7		16%	1%			2%			
Tele2-SE	9,995,153	233,067	1.9		16%	1%			4%			
Sprint-US	325,719,200	2,269,557	0.6		15%	1%			8%			
SKTelecom-KR	50,982,212	1,611,711	2.6		15%	1%			13%			
A1-AT	8,772,865	229,577	2.2		15%	1%			8%			
LGUplus-KR	50,982,212	830,139	1.4		14%	1%			3%			

Table 4-1 Top Wireless Operator Network Capacity Utilization

It is important to note that the capacity utilization figures for the top 5% most loaded sectors are substantially higher than the figures for the 50% least loaded sectors, which again points to the argument that network capacity congestion may not be a wide spread phenomenon. The real-time Internet traffic volume map in Figure 4-1 shows traffic indeed is condensed only in certain areas but not everywhere.

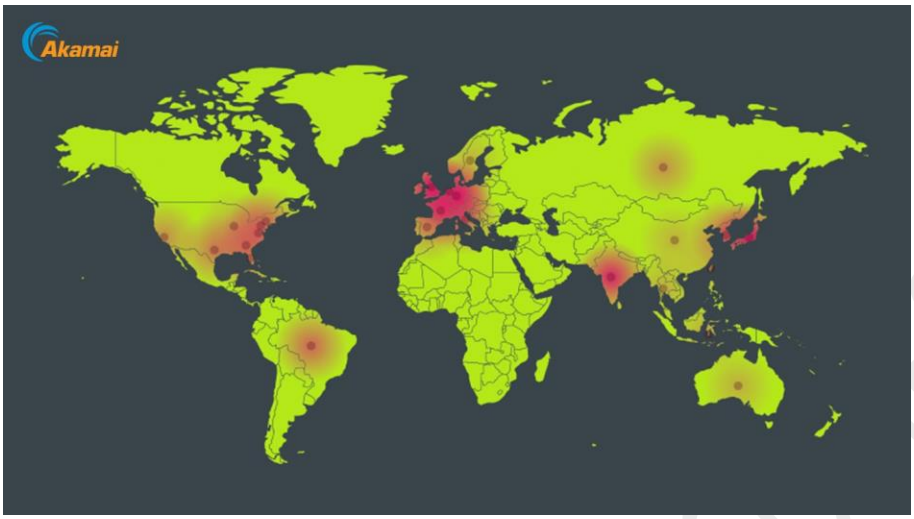

Figure 4-1 Akamai Real-Time Internet Traffic Heat Map

To relieve these top 5% congested sites, mmWave could be deployed there as part of broadband mobile network deployment, be in in a collocated with sub-6GHz frequencies as part of macro nodes or independent small cells at furniture street levels.

Variations in user throughputs during the day has also been used an argument to justify deployment of mmWave as part of mobile broadband networks. According to new study done across 77 counties by Open Signal, 4G download speeds vary between 31.2 Mbps and 5.8 Mbps (i.e. Figure 4-2), faster at the best hour of day compared with the slowest hour of the day [47]. Cities see the greatest speed swings which indicates 5G can help relieve the daytime congestion there since mmWave 5G could add new high capacities.

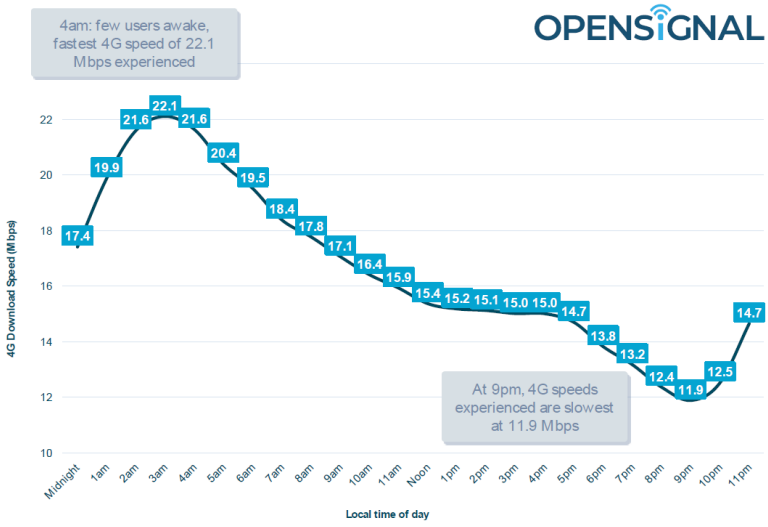

Figure 4-2 Download Speed Variation during Time of Day [47]

Projected mobile traffic increase is another factor which will compound the current congestion issues experienced in mobile networks. Therefore, for operators that do not possess sufficient sub-6Ghz frequencies to address future traffic growth mmWave frequencies may be the only option to do so.

A recent report by Cisco states that consumer mobile data traffic will grow 7-fold from 2017 to 2022, a compound annual growth rate of 48% [1].

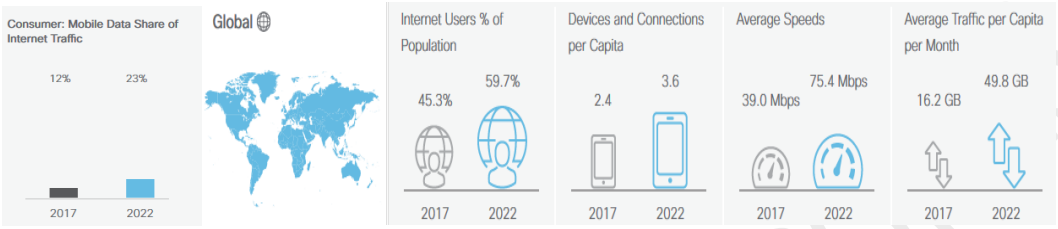

Figure 4-3 Global Internet Traffic Trend and Mobile Data Share [1]

The above trend is on-going with two contributing factors. One factor is the number of wireless broadband connections continues to increase due to increasing percentage of population use Internet and increasing device per capita. The second factor is the content of mobile application offerings is going to higher data rates, such as 4K video and all the realities (VR, AR, XR). Six hundred and fifty million mobile devices and connections were added in 2017. Global mobile devices and connections in 2017 grew to 8.6 billion, up from 7.9 billion in 2016 [1]. Globally, mobile devices and connections will grow to 12.3 billion by 2022 at a CAGR of 7.5 percent. By 2022, there will be 8.4 billion handheld or personal mobile-ready devices, as shown in the Figure 4-4.

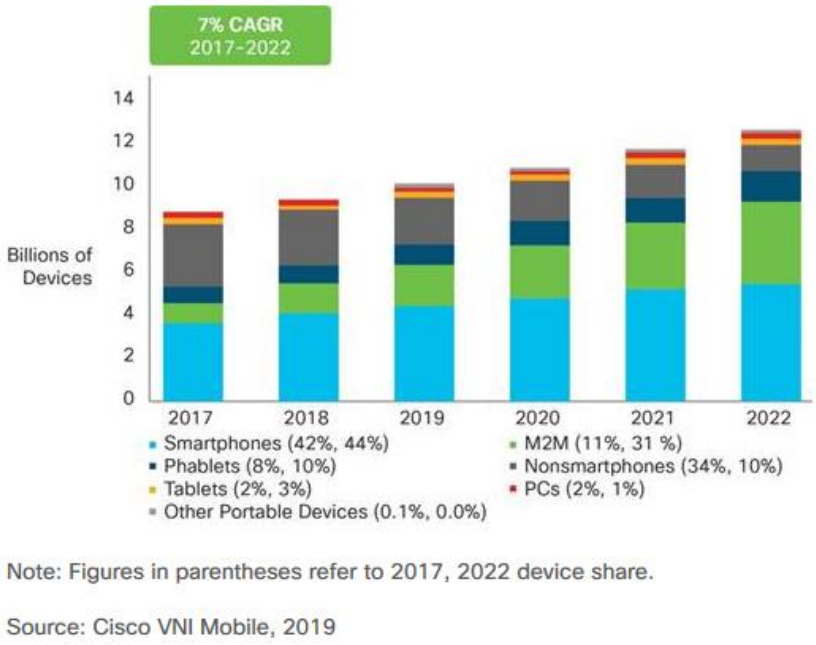

Figure 4-4 Global Mobile Devices and Connections Growth [1]

In the sub-sections below, we will look at projected bandwidth requirement for each of these applications, which belong to relatively high throughput realm of applications.

4.1.1. High Definition Mobile Video

Video has been a predominant application on mobile devices. It has already been integral part of daily life among all ages. Current statistics suggests 60% of all mobile traffic is video. Cisco VNI report predicts that the video traffic will further increase to 79% by 2022 [1]. Ericsson also predicts similar video forecast where video traffic increases from 60% in 2018 to (74%) by 2024 [2].

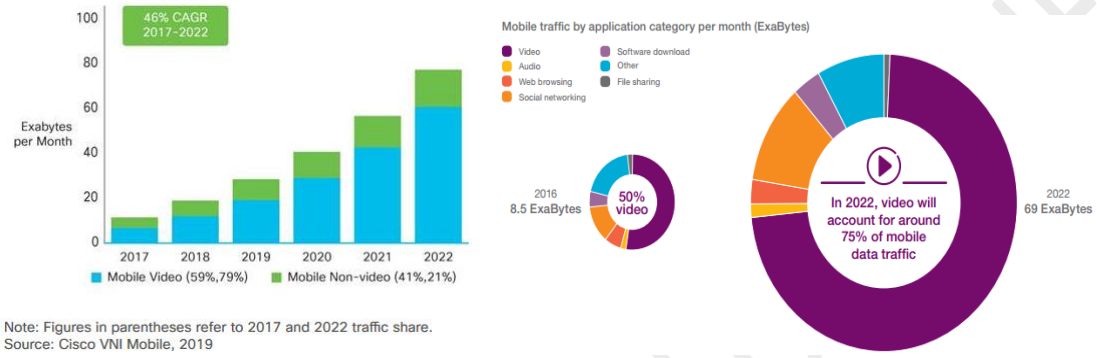

Figure 4-5 Video Predictions

Looking more closely at the requirements for video playing on mobile devices (i.e. smartphones), it is well understood that the requirements are heavily dependent on display parameters. Figure 4-6 below provides the throughput requirement for video across various devices.

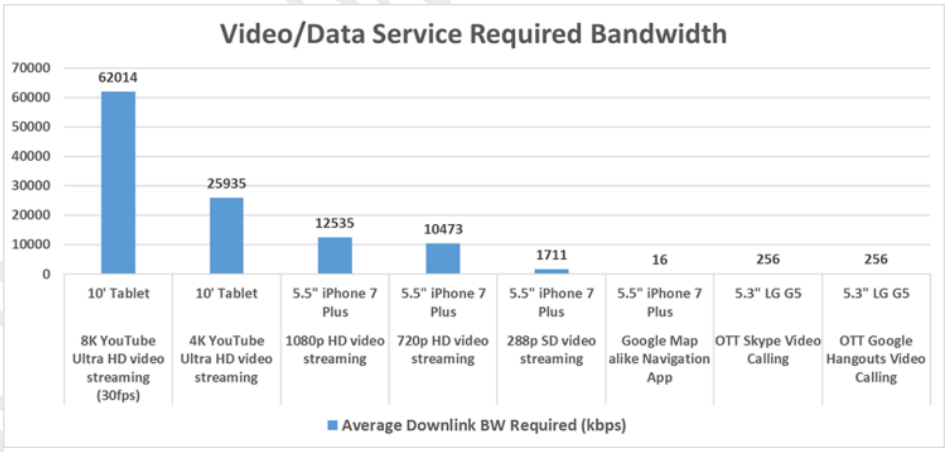

Figure 4-6 Video Bandwidth Requirements

As seen above, the smartphone / tablet requirements for video is well below 100Mbps, even with streaming of 8K Ultra HD picture quality, but still 5 times of 1080p HD.

Besides streaming standard video formats, it is expected that 360-degree immersive video applications supporting 4K/8K quality may also be increasing. This may require higher throughput beyond 100Mbps.

Capturing 4K/8K standard and 360 deg video pose an important throughput requirement on uplink as well. 4K/8K video capture would need minimum of 15-60Mbps uplink throughput, while 360-degree video would require 4-5 times higher uplink throughput for a 4k/8K video quality due to stream captures from multiple different cameras/lens for later stitching into 1 post processed video.

4.1.2. Enhanced AR/VR/XR Experience

Augmented reality (AR) is a live direct or indirect view of a physical, real-world environment whose elements are augmented (or supplemented) by computer-generated sensory input such as sound, video, graphics or GPS data. AR devices could be in various form factors such as Glasses, handheld devices, laptops as well as large screens. These AR devices helps overlaying key information over the surroundings. AR applications are expected to require ultra-low latencies, between 5 to 20ms [68][69], while may pose moderate to high downlink throughput requirements. It should be noted that some of the AR use cases would also require high UL throughput for sending real time / live video back to the cloud for content processing and getting results. Some AR use cases of interest could be:

Figure 4-7 AR Applications

- Fashion industry: Allows users to virtually choose and try various clothing and makeup options
- Furniture industry: Allows users to virtually identify most suitable furniture to match their interior / exterior.
- Tourism industry: AR device can identify the attractions and provide relevant information about its history, things to go etc.
- Navigation: Helps users to see points of interest around themselves.

On the other hand, virtual reality (VR) refers to software generated realistic images, sounds and other sensations that replicate a real environment (or create an imaginary setting), and simulate a user's physical presence in this environment. VR can be implemented on various form factors including smartphones, Gaming consoles, TVs, etc. Some of the key use cases are:

Figure 4-8 VR Applications

- Gaming: Various forms of gaming including outdoor sports, adventures, etc.
- Training: Used to train user with specific functions such as flying aircrafts, sports training, fitness, etc.

VR, AR, XR are being touted as the first wave of applications requiring 5G eMMB networks and speeds. The chart below shows the required bandwidth for VR services with peak throughput reaching up to 1Gbps. It should be noted that less than 40ms latency is required to have a good audio-haptic coordination and less than 10ms to have a good visual-haptic coordination [70][85].

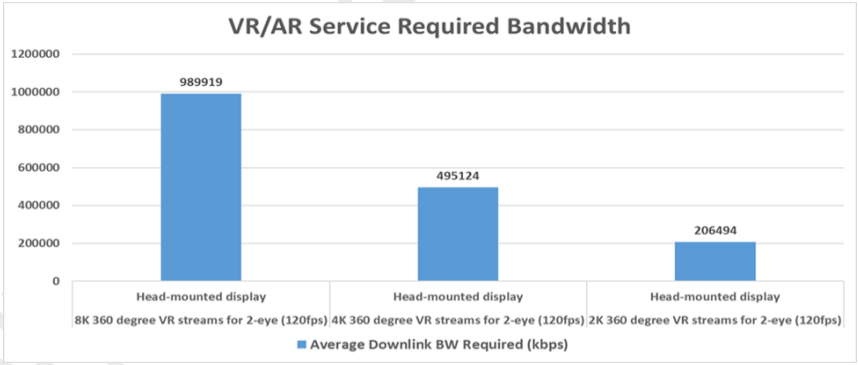

Figure 4-9 AR/VR Bandwidth Requirements

Such throughput requirement may also depend on implementation specifics. Qualcomm/NEXTVR Keynote at MWC 2017 indicated that bandwidth of 100Mbps per user is sufficient to achieve a high-quality immersive VR experience [16].

As for market feature penetration, VR headsets expected to reach 100M by 2021 based on Cisco VNI forecast. Another source, BI Intelligence predicts VR handset shipments to reach 55 Million in 2022. Analyst Chetan Sharma predicts 13.4 million cellular VR devices by 2025, accounting 15% of total consumer traffic.

All these innovations in AR and VR will place new demands on the network in terms of its quality in speed and latency and mostly important on the overall network capacity. Globally, augmented and virtual reality traffic is expected to grow nearly 12-fold from 22 petabytes per month in 2017, to 254 petabytes per month in 2022, as depicted in Figure 4-10.

Figure 4-10 AR and VR Mobile Data Traffic [1]

These are relatively modest numbers when compared to total number of smartphones, or total internet traffic. However, if materialized, it may well be an application that would pose capacity and speed constraint on mobile networks, especially at sport of special venues where AR/VR seems to be most attractive for consumer space.

4.2. Connected Vehicle

Connected vehicle, commonly referred to as V2X (vehicle-to-everything) technology, allows vehicles to directly communicate with each other, roadside infrastructure, and other road users. The example applications are road safety, traffic efficiency, smart mobility and automatous driving, vehicle infotainment for passengers, etc as depicted in Figure 4-11.

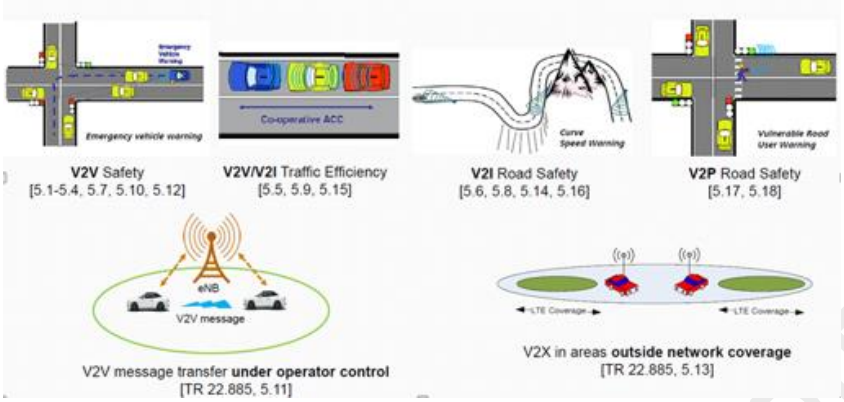

Figure 4-11 Examples of Use Cases for Vehicular Communication

There are several components of V2X, including vehicle-to-vehicle (V2V), vehicle-to-infrastructure (V2I), vehicle-to-pedestrian (V2P) communications. Each application may invoke one or more components of V2X.

High Doppler effect is one of the technical challenges that need to be considered when mmWave frequencies are considered for V2X use case, as Doppler effect is known to be more than 10 times greater at 28-60 GHz compared with sub-6GHz wireless systems [134]. This is mainly due the frequency differences between the two (i.e. Doppler effect is proportional to the transmitted wave frequency).

4.2.1. V2V Use Case

The Department of Transportation (USDOT) has proposed support of V2V in all new light vehicles back in 2017 but no final rule has been issued [136][137]. Automated and assisted driving in these new V2V capable vehicles involve various layers of information processing at the vehicle. For example, layer 4 data about the surrounding vehicles is exchanged among neighboring vehicles in Figure 4-12 [8]. Those data exchange helps for the coordination of the trajectories (e.g. lane change, platooning, emergency break, passing-by of emergency vehicle) among vehicles.

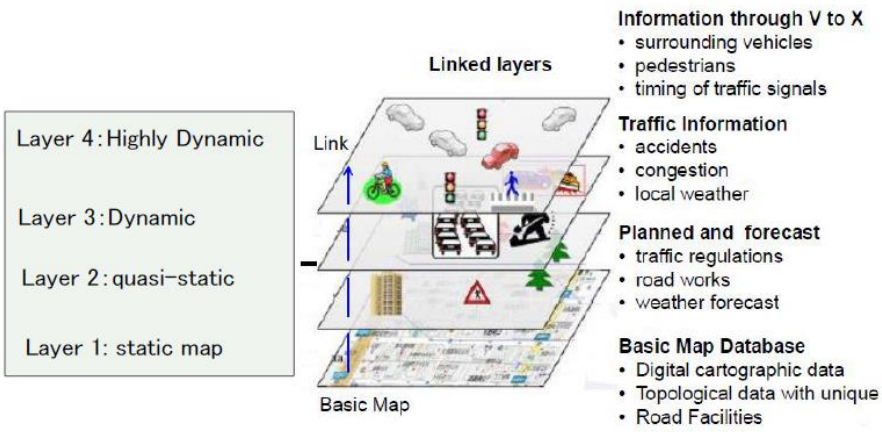

Figure 4-12 Layers of Information exchange in vehicle operation [8]

Figure 4-13 illustrates some of the latency / throughput requirements [9]. For example, it is estimated that V2V information exchange requires up to 1Mbps and within 5-10ms in the case of cooperative maneuver planning and prediction. For cooperative perception function, V2V requires up to 10-20Mbps within 10-50ms. The required reliability is expected at 90-95% [136][137].

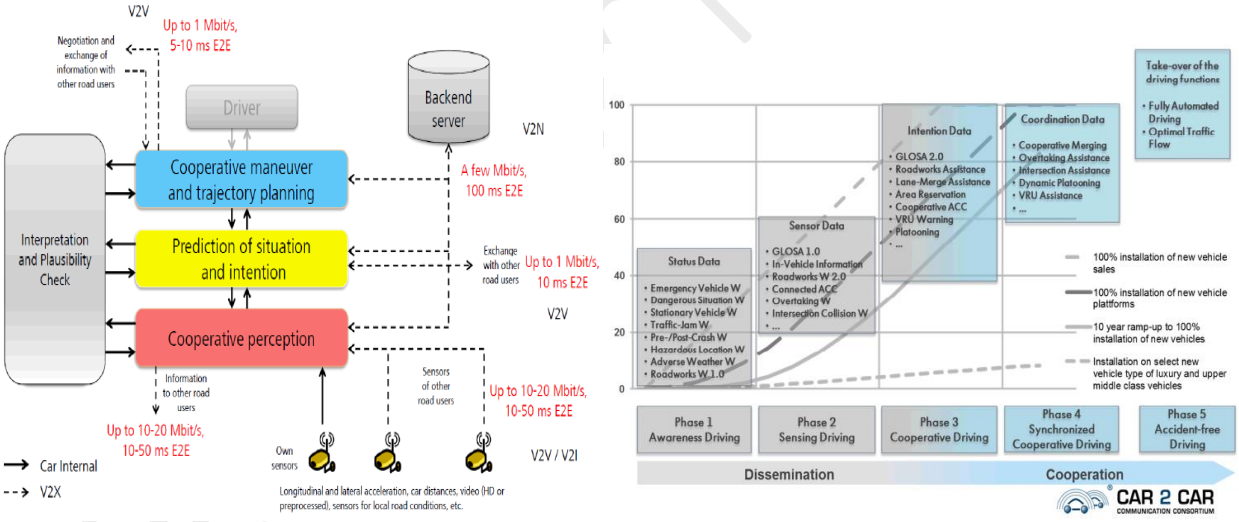

Figure 4-13 5GPPP Bandwidth/Latency Requirements in Vehicle operation

It should be noted that there has been no clear requirements set forth by automotive industry on autonomous driving for the network operators to support. Having said that, Figure 4-14 below illustrates a high level requirement from Toyota on overall requirement. Red region indicates strict requirements in terms of throughput, latency and reliability [8].

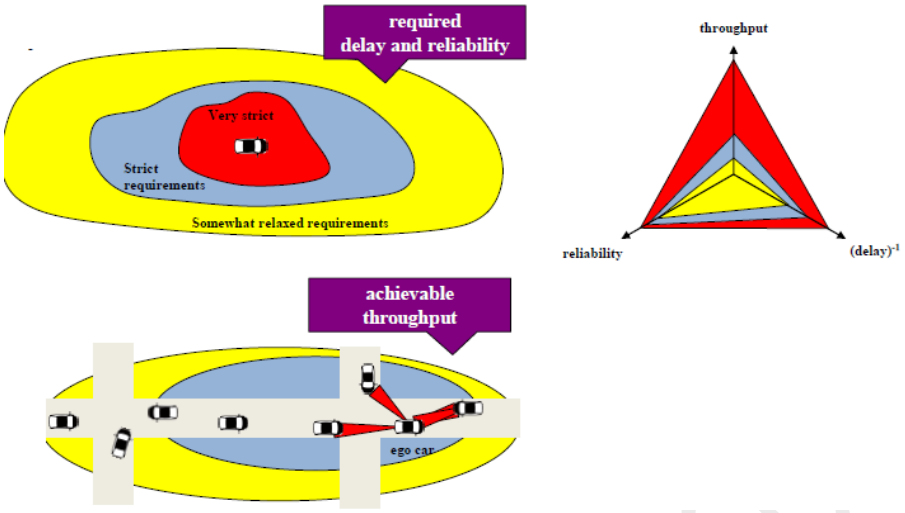

Figure 4-14 Regions of Performance Requirement Severity by Toyota [8]

A recent research paper shows it is feasible to support V2V use cases with 5G mmWave [78]. However, further research and trials need to be conducted to fully vet the viability of cellular mmWave technology for V2V.

4.2.2. V2I Use Case

V1I topic is also another area that has drown the interest of research and industry communities. A recent 5GAA white paper analyzed the cellular V2I architectural solutions and evaluated them against Intersection Movement Assist (IMA) use case [50]. Even though mmWave was not the focus of 5GAA white paper, the evaluation result is still very much relevant to network capacity and congestion subject.

The considered deployment model for IMA is as illustrated in **Figure 4-15**, in particular the intersection area is considered as 50-meter radius from the center of the intersection whereas the transmitter vehicles considered are those located at most 150 meters from the center of the intersection.

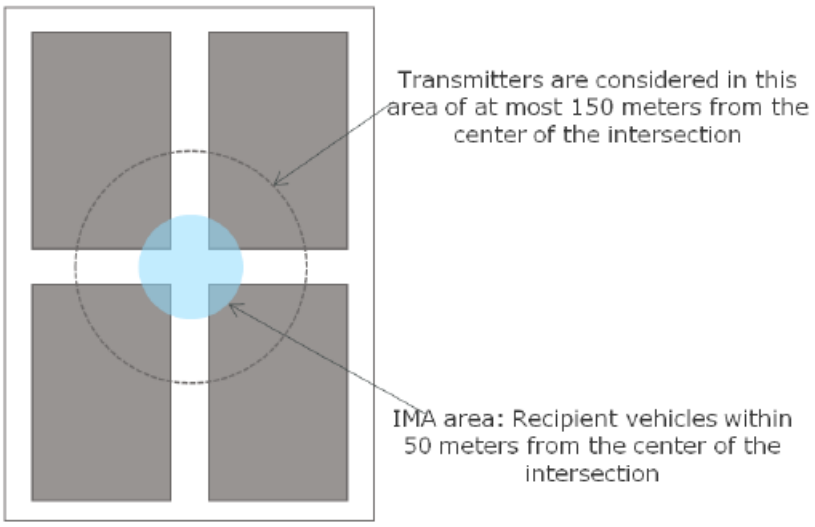

Figure 4-15 IMA Use Case [50]

Figure 4-16 shows the packet delivery rate (PDR) vs transmission distance from the intersection area. The PDR is provided for two conditions, one with traffic jam condition where 280 vehicles are in the intersection area and one with light traffic condition where only 60 vehicles are in the area.

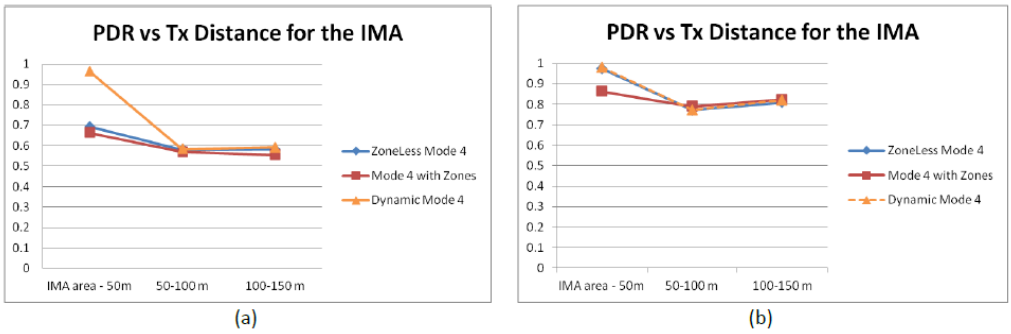

Figure 4-16 (a) High Congestion Condition (b) Low Congestion Condition [50]

The PDR goes down to 60% in high congestion condition while stays at 80% in low congestion condition at the distance of 50-100m. The throughput required for each vehicle in the IMA case is expected around 1.3 Mbps, latency is about 10ms and reliability is >99% [136][137]. If mmWave spectrum is deployed for IMA use case, the high capacity may help ease the congestion condition and improves PDR.

4.2.3. V2P Use Case

The same recent 5GAA white paper analyzed the cellular V2X architectural solutions and evaluated them against Vulnerable Road User (VRU) discovery use case [50]. In this case, a UE app (running on a pedestrian user UE) periodically sends short notifications to the network, then the network sends awareness

messages to a cluster of neighboring cars to warn about the presence of VRUs in the area, as shown in Figure 4-17.

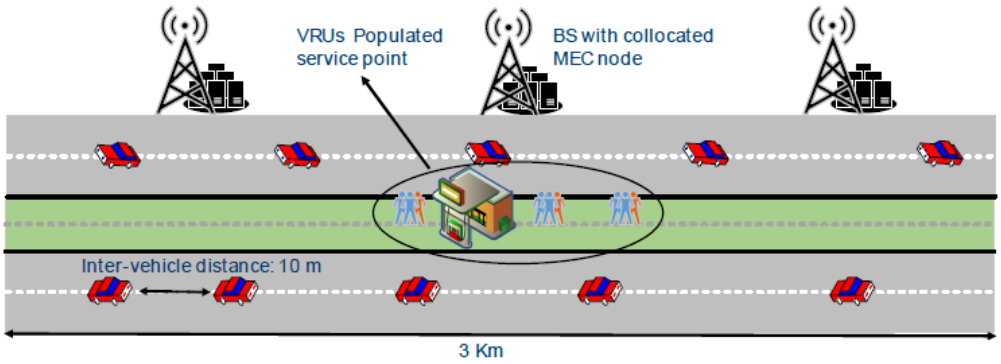

Figure 4-17 VRU Discovery Use Case [50]

Figure 4-18 shows the average radio transmission induced latency, in the case of MEC, increases from 20ms with 50 VRUs to 40ms with 90 VRUs. The throughput required for each VRU is expected between 5-10kbps, latency is below 100ms and reliability is required at 90-95% [136][137]. Large channel bandwidths associated with mmWave spectrum may address high capacity and low latency requirements associated with VRU use case, while at the same time improving its safety margins.

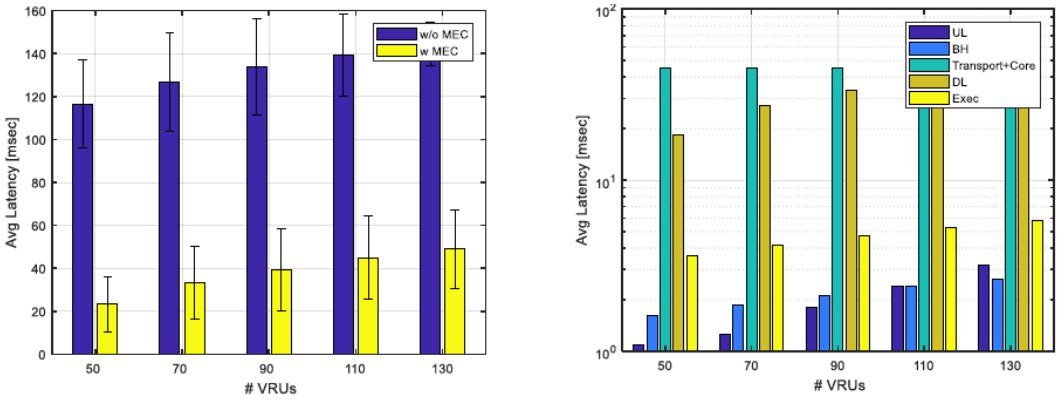

Figure 4-18 (left) Avg E2E Latency (right) Latency Breakdown of All Delay Components [50]

4.3. Industrial Automation

Industrial automation is another potential area where mmWave can help improve production efficiency and safety. It involves connecting industrial automation sensors, devices and equipment with cloud-based systems to gain business value.

Industrial automation IoT market size is projected to be $196B by 2022 [12]. Analyst Chetan Sharma projects that by 2025, Smart factory would account for 4.5% of total enterprise traffic.

Figure 4-19 Industrial Automation Use Case

Industry 4.0 use case based on robotics and slow-moving robots may be an area of interest. These paradigms would use a variety of techniques (i.e. imaging, sensing, XR) to increase production efficiencies in which computers and robots continually optimize production and maintenance in highly flexible factories and plants. In such cases, which could be predominantly indoor, implementation of mmWave bands for the purpose of achieving very high wireless data throughput slow-moving robots in a separate (i.e. possibly private and dedicated) network may be a more plausible scenario for implementing mmWave on devices. Such type of devices would operate in environments where mmWaves propagation characteristic may not be affected drastically, like outdoor or indoor/indoor application) while not suffering by impact of close proximity human attenuations. Furthermore, such devices may not be too restrictive from a power consumption, multi-antenna location, or beamforming performance. Equipped with advanced device designs, edge computing, mmWave cellular networks could provide highly capacity connectivity, enabling factories to become less dependent on wires and more flexible. By capturing information in real-time and enabling remote control of machinery and automatically adapt to shop-floor events, increasing efficiency can be achieved by manufacturers for their customers.

3GPP SA1 working group has defined some key target performance for various automation use cases in Table 4-2 below. ZVEI electrical industry group has more automation performance values in Table 4-3.

Service	End-to-End Latency	Jitter	Survival time	Availability	Experienced Data Rate	Connection Density
Factory automation - Motion Control	1 ms	1 µs	0 ms	99,9999%	10 Mbps	100 000/km^2
Factory automation	10 ms	100 µs	0 ms	99,99%	10 Mbps	100 000/km^2
Process automation –Remote Control	50 ms	20 ms	100 ms	99,9999%	100 Mbps	1 000/km^2
Process automation Monitoring	50 ms	20 ms	100 ms	99,9%	1 Mbps	10 000/km^2

Table 4-2 Performance requirements for Industrial Automation [61]

Use case (high level)		Availability	Cycle time	Typical payload size	# of devices	Typical service area
Motion control	Printing machine	>99.9999%	< 2 ms	20 bytes	>100	100 m x 100 m x 30 m
	Machine tool	>99.9999%	< 0.5 ms	50 bytes	~20	15 m x 15 m x 3 m
	Packaging machine	>99.9999%	< 1 ms	40 bytes	~50	10 m x 5 m x 3 m
Mobile robots	Cooperative motion control	>99.9999%	1 ms	40-250 bytes	100	< 1 km²
	Video-operated remote control	>99.9999%	10 – 100 ms	15 – 150 kbytes	100	< 1 km²
Mobile control panels with safety functions	Assembly robots or milling machines	>99.9999%	4-8 ms	40-250 bytes	4	10 m x 10 m
	Mobile cranes	>99.9999%	12 ms	40-250 bytes	2	40 m x 60 m
Process automation (process monitoring)		>99.99%	> 50 ms	Varies	10000 devices per km²	

Source: ZVEI

Table 4-3 Performance Requirements for Industrial Automation [76]

Factory automation is one use case where products are manufactured, assembled, tested or packed in many discrete steps (automotive, general consumer electronic, goods production). In-time deliveries of messages and high reliability are very important to avoid interruptions in the manufacturing process. Redundancy, security and functional safety are also very important for factory automation. Typically, every manufacturing step involves many sensors and actuators controlled by a single Programmable Logical Controller (PLC). Many of these PLCs use wired connections which are often stressed by repeated movements and/or rotations and other harsh conditions. More and more devices, especially sensor and actuator nodes, could be connected using mmWave technology to improve productivity and increase availability compared to wired sensors/actuators at difficult locations. One example of such mass market product is IWR6x, a 60GHz sensor portfolio introduced by Texas Instruments [60]. Given the connection density is very high in this use case, mmWave may provide the needed capacity and minimize the end-to-end latency for the factory network as shown in Figure 4-20.

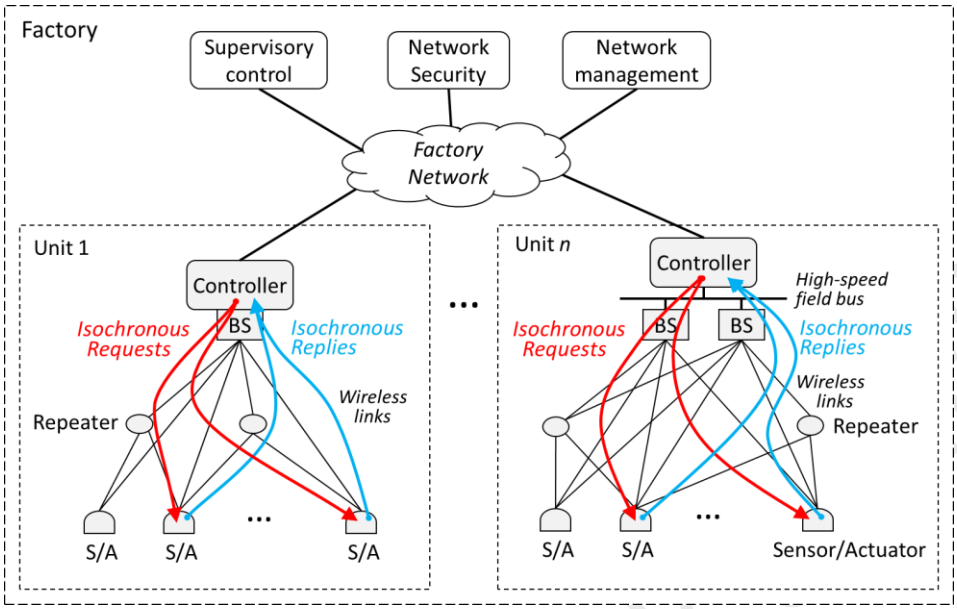

Figure 4-20 Communication Path for Factory Automation [61]

Process automation is another use case where it is used for continuous production processes to make large quantities or batches of a certain product. It requires deterministic behavior and therefore require typical latency of 50ms. It can cover relatively large areas and so wide wireless transmissions ranges are required with modest to high connection density. End-to-end throughput, security and availability becomes more important, but real–time communication requirements decrease. Again, smaller number of devices with each has high throughput requires network with high total capacity which mmWave can provide.

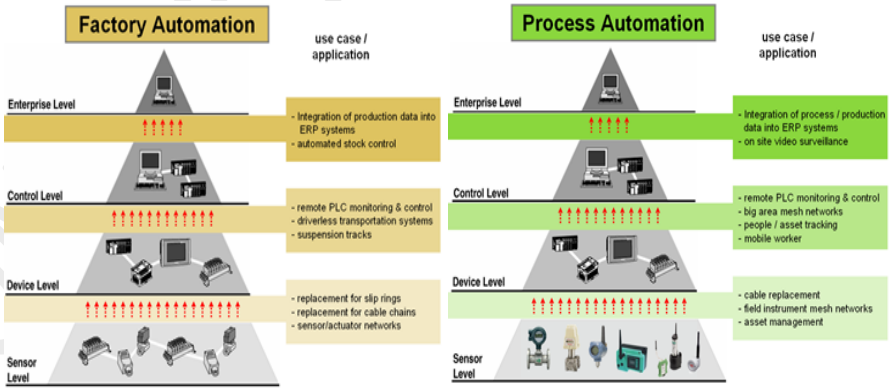

Figure 4-21 Examples of Automation Hierarchy

High level of automation may require higher number of connection in industrial automation use cases, as estimated in Figure 4-22 by Ericsson.

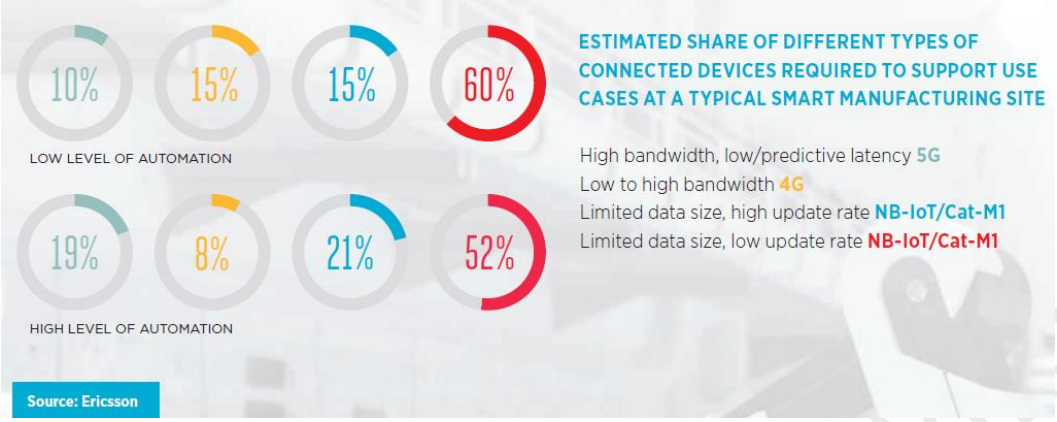

Figure 4-22 Mobile IoT Connection Type Estimation [59]

By testing the technologies in its own factories, Ericsson has found that Mobile IoT and mmWave networks can support a wide range of different manufacturing use cases, making it possible to securely and efficiently optimize manufacturing variables with a single cellular communication system.

In both use cases above, mmWave performance may experience degradation where wireless signal gets blocked due to many moving objects on the factory shop-floor. Even robotic arm could block line-of-sight between sensor on the factory line and PLC. The higher power consumption on the sensor and device may also be another challenge. Many of these issues of mmWave is investigated in the IEEE paper [62] and subsequent sections in this white paper. Some of these mmWave deployments may be in the form of private dedicate network so that user has more configuration control of the network to support specific requirements associated with these use cases.

4.4. Fixed Wireless Access

While the mmWave bands are extremely challenged in morphology losses and building penetration, they are well suited for Line of Sight (LOS) of Gigabyte capacity links to buildings. Historically mmWave frequencies have been used for backhaul applications. More recently mmWave has been considered for Fixed Wireless Access (FWA) which provides Internet access to homes (e.g. apartments) and businesses (e.g. universities, hospitals, retail shopping malls, etc.) using wireless network technology rather than fixed lines. It will use 5G concepts such as dual-connectivity and mmWave spectrum and beamforming to bolster wireless broadband fiber-equivalent connectivity.

There are three different segments of the FWA market in the North America [5][93][94]. The first segment is nomadic and temporary demand. Examples include special events, festivals, etc. This represents a flexible, quick and cost-effective solution even though the main challenge is to get adequate backhaul for temporary cells. The second segment is broadband access in urban area. Due to high civil work cost in dense urban, the wireless connectivity with high throughput and low latency could be a cost-effective solution. The third segment is rural area coverage [71][82][90][93]. The high-power transmission and beamforming antenna technologies are required to enable reach-out of rural.

Figure 4-23 depicts two of the common scenarios being explored today in the 28 and 39 GHz spectrum for the second segment use case.

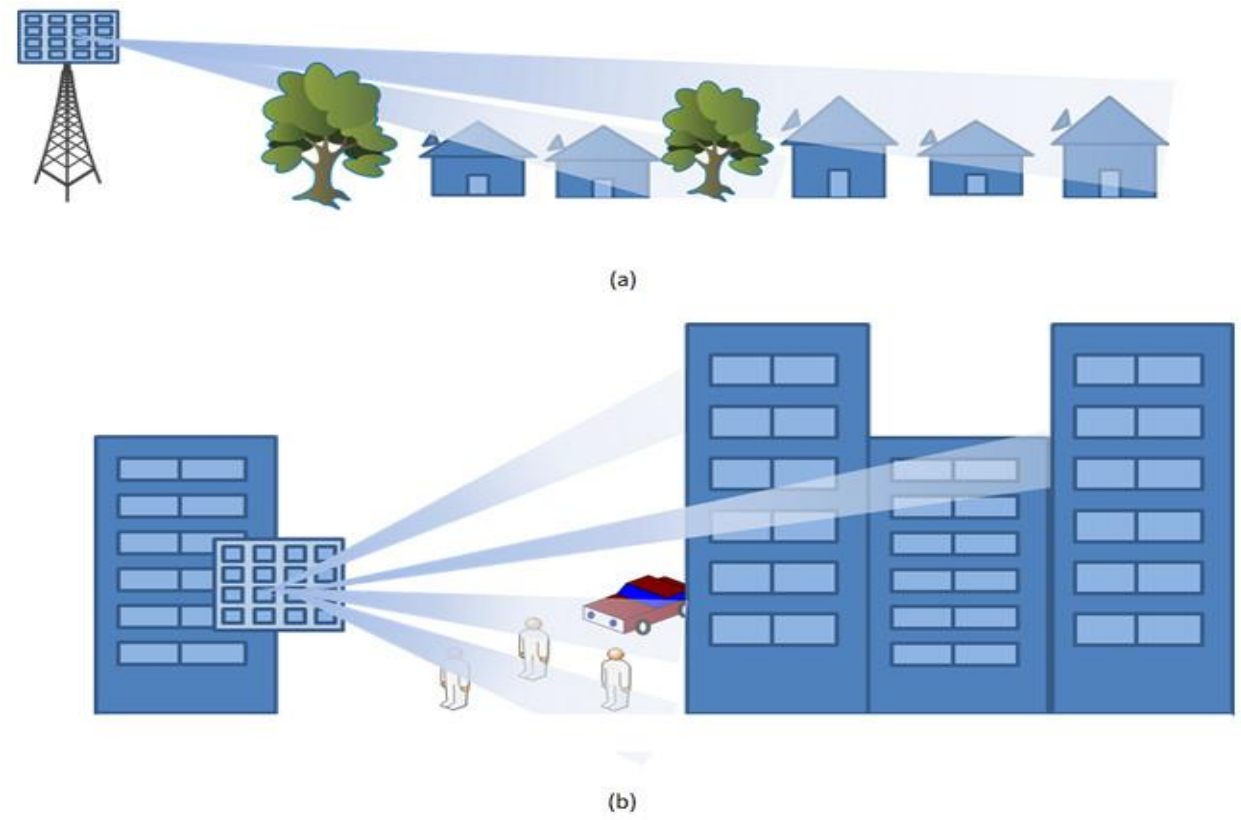

Figure 4-23 Outdoor deployment (a) Suburban fixed wireless, (b) Dense urban fixed and mobile wireless [6]

Figure 4-23(a) illustrates an FWA use case, where the system tries to deliver high bandwidth data to homes in a suburban environment. In such a case the base station could be on a utility pole or tower and is required to cover a large area to produce a positive business case. In the initial deployments, it is assumed that the coverage is outdoor to outdoor, whereby the customer premises equipment (CPE) is mounted outdoors and the link may be engineered to ensure the best over the air connection. Given that the antenna is pointing down and users are fixed, it may not require a large amount of vertical steering range, but the transmitted power may be quite high, in excess of 65 dBm EIRP to maximize the coverage and leverage existing infrastructure.

Figure 4-23(b) illustrates a dense urban scenario, where the base station will be mounted lower to the ground on a building rooftop or façade, possibly evolving to streetlight or other street level mounting in the future. In any case this type of base station will require vertical scanning ability to deliver signals across the entire building elevation and eventually to mobile or nomadic users on the ground (pedestrians and vehicles) as mobile devices emerge. In this case the transmitted power may not need to be so high as in the suburban case, although low E glass has proven to be a significant problem for outdoor to indoor penetration. As shown, the system needs more flexibility in the beam scanning range, in both horizontal

and vertical axis. The major takeaway here, is that there is not a-one-size fits all solution. Deployment scenario will determine beamforming architecture and architecture will influence the choice of RF technology.

The Carmel Group predicted FWA to grow significantly over the next few years, as depicted in Figure 4-24.

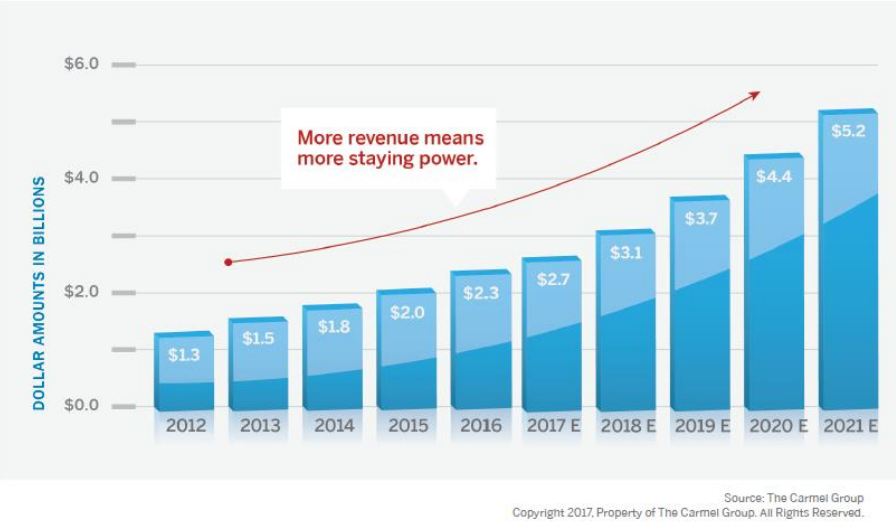

Figure 4-24 Fixed Wireless Access business growth [7]

The revenue projection depends on customer subscriptions roughly double, from 4.0 million in 2016 to 8.1 million in 2021 and average monthly customer billing increases from $51 to $58 [7]. FWA could potentially introduce a significant change in wireless services.

In October 2018, Verizon launched its *5G Home* fixed wireless Internet service in four cities (Sacramento, CA; Los Angeles, CA; Houston, TX; and Indianapolis, IN), using roughly 400MHz of its 28GHz spectrum holdings with typical speed of 300Mbps [52] based on a proprietary 5GTF technology. As of late 2018, Verizon announced its plans to upgrade its pre-standard 5GTF mmWave FWA to the 3GPP standard in the second half of 2019 [53] [57]. According to VentureBeat those four-city 5G Home network won't expand much beyond its current footprint until then [77].

AT&T has also evaluated mmWave frequencies for FWA deployments in the past few years. AT&T stated on its 2018 Q4 earnings call that they expect 5G to be a suitable wireless replacement for fixed broadband in three to five years [55].

4.5. Use Case Summary

Four use cases where mmWave frequencies can be applied are discussed in this section. Although the early uses cases for mmWave will focus on mobile broadband (i.e. eMBB) and fixed wireless services, mWave frequencies have the potential to trigger a major wave of innovation across a variety of other use cases, such as autonomous driving, smart manufacturing, etc.

This version of whitepaper focuses on the mobile broadband use case, as that represents the first deployment of mmWave frequencies in mobile networks, with initial deployment by VZN in two US cities in Q2 2019. Furthermore, that use case may pose some of the most technical challenges for mmWave deployments due to their unpredictability of propagation as well as challenges related to UE implementation of mmWave frequencies. Therefore, it is believed that most of the industry needs at this stage may be about obtaining a better understanding of all topics related to mmWave deployments for the purpose of eMBB use case. Subsequent version of this paper will address other use cases associated with mmWave technology.

5. 3GPP Definition for FR2

This section will direct its focus towards the 3GPP aspects / requirements of mmWave deployments, more commonly knowns as FR2 (Frequency range 2).

5.1. Core Specifications

3GPP Release-15 is the first release for NR (New Radio), and is intended to satisfy the ITU IMT-2020 criteria for 5G. While NR is largely an evolution of LTE, it does have several major new features, including support for higher frequency, mmWave bands. 3GPP divided the NR bands into two Frequency Ranges, FR1 for bands below 6 GHz, and FR2 for mmWave bands. In Rel-16, the FR1 range is being extended to 7.125 GHz to allow NR to be used for unlicensed bands in the 6 GHz region.

Frequency range designation	Corresponding frequency range
FR1	410 MHz – 7125 MHz
FR2	24250 MHz – 52600 MHz

Table 5-1 3GPP Frequency ranges

3GPP Rel. 15 defines only four bands in the FR2 range, in the 24 GHz, 28 GHz, and 38 GHz ranges. All are defined as TDD to enable reciprocity-based beamforming. Notably excluded is the 60 GHz band, which is the focus of the IEEE 802.1AD (WiGig) set of standards, although there have been 3GPP Study Items on extending FR2 to include higher frequencies, including 60 GHz.

Operating Band	Uplink (UL) operating band BS receive UE transmit	Downlink (DL) operating band BS transmit UE receive	Duplex Mode
	F_{UL_low} – F_{UL_high}	F_{DL_low} – F_{DL_high}	
n257	26500 MHz – 29500 MHz	26500 MHz – 29500 MHz	TDD
n258	24250 MHz – 27500 MHz	24250 MHz – 27500 MHz	TDD
n260	37000 MHz – 40000 MHz	37000 MHz – 40000 MHz	TDD
n261	27500 MHz – 28350 MHz	27500 MHz – 28350 MHz	TDD

Table 5-2 mmWave Bands

The primary practical difference in 3GPP's treatment of FR1 and FR2 is that FR1 bands have their Core and Performance specification primarily based on conducted measurements, while FR2 band have specifications based on OTA measurements. Higher frequency bands rely more on multiple antenna techniques (i.e. beamforming) to compensate for higher propagation losses, so the antenna systems are much more critical to overall system performance than with FR1. There would also be technical challenges with attempting to design UEs with accessible antenna connectors for multi-antenna arrays. As will be discussed further in Section 10, OTA measurements bring additional concerns and complexities, but they also reflect real field usage better than conducted measurements would.

The following section surveys 3GPP's RF specifications for NR in FR2, as presented in TS 38.101-2, and contrasts them with the corresponding specifications for NR in FR1, from TS38.101-1.

5.2. Core Specifications

The tables below compare key specifications between NR in FR1 and FR2.

5.2.1. Operating Bands and Channel Arrangements

As noted earlier, 3GPP defines only 4 bands for FR2. In general, there are fewer option for FR2 – two Numerologies, no support for UL 256QAM, only four channel bandwidths. There are 15 classes of intra-band CA defined (more than for FR1). But there are only 5 inter-band NR CA combinations defined, and they all combine an FR2 band (24 GHz or 28 GHz) with and FR1 band (600 MHz, 800 MHz, 3.5 GHz, or 5.0 GHz). Three of the CA combos (28 GHz with 3.5 or 5.0 GHz) are also defined as NR-DC (NR Dual Connectivity) combinations, which would allow use with uncoordinated gNBs.

There are also many, many combinations defined for EN-DC (LTE-NR Dual Connectivity) involving FR2 bands, which will be the primary use case for 5G NR for early deployments.

In the US, Verizon is launching FWA using 28 GHz, using their semi-proprietary 5GTF standard, not 3GPP EN-DC. AT&T is launching both FWA and "mobile 5G" using 39 GHz n260, in EN-DC combinations with their existing LTE sub-6GHz bands. T-Mobile is building out both NR and LTE in its 600 MHz spectrum, and plans to deploy B71/n71 EN-DC there. And Sprint is adding NR to its existing 2.5 Ghz LTE network, and is launching B41/n41 EN-DC. All of these operators have also defined other EN-DC combinations covering practically all of their band holding.

Parameter	FR1	FR2
Numerologies (SCS)	3 (15, 30, 60 kHz)	2 (60, 120 kHz) (Also, 240 kHz for SS/PBCH block)
UL Modulations	Pi/2 BPSK, QPSK, 16 QAM, 64 QAM, 256 QAM	Pi/2 BPSK, QPSK, 16 QAM, 64 QAM
Number of Bands	32 (as of Dec 2018)	4 (3 @ ~28 GHz, 1 @ 39 GHz)
Channel Bandwidth	12 different CBWs	4 (50, 100, 200, 400 MHz)
Intra-Band Carrier Aggregation	12 Classes (up to 8 CCs, and up to 400 MHz aggregate BW)	15 Classes (up to 8 CCs, and up to 1.2 GHz aggregate BW)

	Contiguous and Non-Contiguous	Contiguous and Non-Contiguous
Inter-Band Carrier Aggregation (within FR)	Many defined	None defined
Inter-Band Carrier Aggregation (across FRs)	5 defined: • 3 combining n257 (28 GHz) with various 3.5-5.0 GHz bands • CA_n71-n257 (600 MHz + 28 GHz) • CA_n8-n258. (800 MHz + 24 GHz)	
NR-DC	3 combinations of n257 (28 GHz) with various 3.5-5.0 GHz bands (same combos as with CA)	
EN-DC	Many combinations, including with NR in FR1, FR2, and both FR1 and FR2.	

Table 5-3 FR1/FR2 Operating Bands and Channel Arrangements

5.2.2. Transmitter Characteristics

FR2 Maximum Power is specified in terms of EIRP (Effective Isotropic Radiated Power) which includes both passive antenna gain and beamforming gains. As a result, power measurements are no longer just a single scalar value as they are with conducted measurements, they are now a spherical field, reflecting the antenna gains and beamforming across the full range of angles. Because of this, the maximum power specification are given not as a single value with a tolerance, but in terms of peak EIRP, and a given %-ile CDF value.

Power Classes for FR2 have explicit use case assumptions listed. Handheld UEs (PC3) are the primary concern of this paper, but Vehicular (PC2) and High-Power non-handheld (PC4) are both mobile use cases as well. In addition to different values, these power classes use different %-ile CDF definitions for their specification as well, to reflect the different use cases.

The Minimum Peak EIRP represents the EIRP at the best (highest gain) angle in the spherical field. This would represent the case where the device is “aimed” in the correct direction. For handsets, a metric more representative of general usage is the 50%-ile EIRP. Handsets have a minimum peak EIRP spec of 22.4dBm (for 28 GHz bands), but a 50%-ile EIRP spec of only 11.5 dBm, which is a 9dB difference. And the 50%-ile definition means than in ½ of the angular directions, the EIRP will be even less than 11.5dBm.

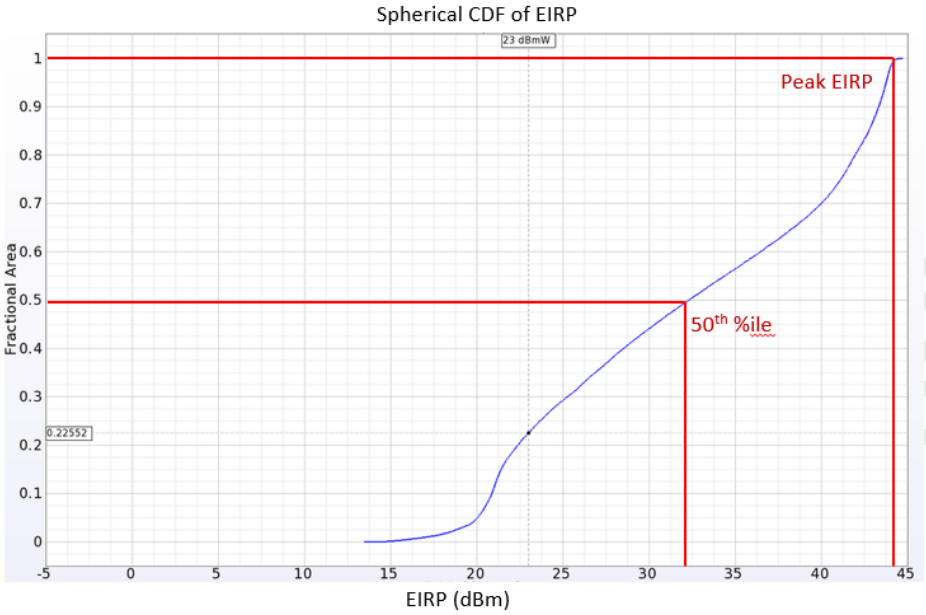

Figure 5-1 Example of Spherical CDF with 50th %-ile and Peak EIRPs

The MPR (Maximum Power Reduction) allowances for FR2 are considerably more generous than for FR1. For FR2, only Pi/2 BPSK transmissions contained entirely within the inner 1/3 or ½ of the channel, are required to support the full nominal power. All other allocations have some allowance for power reduction. The allowance are more generous than for FR1, and are especially large for CP-OFDM transmissions – up to 9 dB for 64QAM CP-OFDM in FR2.

Another major difference between FR1 and FR2 is the ACLR specification. NR in FR1, like in LTE, must meet a -30 or -31 dBc ACLR specification. But for FR2, the ACLR specification is -17 dBc for 28 GHz bands, and -16 dBc for 38 GHz n260. This is a huge difference – FR1 is allowed to leak only ~1/1000th of the channel power into adjacent channels. But FR2 is allowed to leak ~1/50th of the power into adjacent channels.

The implication of the relatively loose ACLR specification for FR2 is that Occupied Bandwidth is effectively the limiting factor for FR2 RF spectrum emissions. Occupied Bandwidth specifies that 99% of the power must fall within the nominal channel bandwidth, which means that ~1/100th of the power may leak into other channels. Assuming the leakage were symmetrical, and all fell into the 1st adjacent channels, that would be 1/200th of the power, which is an ACLR of -23 dBc, considerably more stringent than the ACLR spec.

The larger MPR allowances, and looser ACLR specification, suggest that current technology has more difficulty with keeping FR2 transmissions as “clean” and contained as FR1 transmission are.

These issues illustrate that transmit quality and emissions continue to be challenges for FR2 transmission. 3GPP was overly ambitious with the channel design that utilizes 95% of the nominal mmWave channels, leaving only 5% for guardband.

Parameter	FR1	FR2
Power Class	Two classes PC3 – 23 dBm baseline PC2 – 26 dBm HPUE	Four Classes, with explicit use case PC1 – Fixed Wireless Access PC2 – Vehicular PC3 – Handheld UE PC4 – High-Power non-handheld
Maximum Output Power	Specified as conducted power at antenna connector • Maximum Output Power (23 or 26 dBm) • Simple Tolerance (typically +/- 2dB)	Specified as EIRP • Minimum Peak EIRP (20.6-22.4 dBm for handheld) • Maximum EIRP (43 dBm for handheld) • Minimum spherical 50 %-ile EIRP (8-11.5 dBm for handheld) • UEs supporting multiple bands have relaxation of peak and spherical (<2 dB)
Maximum Power Reduction (MPR)	0 – 6.5 dB, depending on several factors. (Increased allowances for MCS, for outer allocations, and for CP-OFDM) Pi/2 BPSK and QPSK allocation entirely within inner portion of channel get 0 dB MPR, all others get some allowance.	0 – 9.0 dB, depending on several factors. (Increased allowances for MCS, for outer allocations, and for CP-OFDM) Pi/2 BPSK allocations entirely within inner portion of channel get 0 dB MPR, all others get allowance.
Additional Maximum Power Reduction (A-MPR)	Varies by NS values. A-MPR is usually in addition to MPR backoff.	One defined: NS_201 for n258 0 – 5.0 dB additional backoff Total backoff is MAX(MPR, A-MPR)
Minimum Output Power	-33 to -40 dBm, depending on CBW	-13 dBm for handhelds. (“beam locked mode”)
Transmit ON/OFF Mask	10 µs transient period	5 µs transient period
Absolute Power Control Tolerance	+/- 9 dB	+/- [12] dB high side of power range

		+/- [14] dB low side of power range
Relative Power Control Tolerance	+/- (2 to 8) dB Depending on absolute power and step size	+/- (3 to 11) dB Depending on absolute power and step size
Occupied Bandwidth	99% of integrated mean power must fall within nominal channel bandwidth	
ACLR	30 dB for PC3 31 dB for PC2	17 dB for 28 GHz bands 16 dB for 39 GHz band

Table 5-4 FR1/FR2 Transmitter Characteristics

5.2.3. Receiver Characteristics

Like the transmission specifications, the Receiver specifications for FR2 assume OTA measurements, and are defined in terms of EIS (Equivalent Isotropic Sensitivity). Peak Sensitivity values are similar to FR1 values, but the 50%-ile CDF EIS values are 11-12 dB worse. And half of all angular directions will be worse than 50%-ile.

Parameter	FR1	FR2
Reference Sensitivity	Varies by band and SCS -89.7 dBm for n41 30 kHz, 50 MHz	Varies by band and Power Class For handsets on 28 GHz bands (50 MHz CBW) • -88.3 dBm peak • -77.4 dBm 50 %-ile EIS For handsets on 39 GHz bands (50 MHz CBW) • -85.7 dBm peak • -73.1 dBm 50 %-ile EIS

Table 5-5 FR1/FR2 Receiver Characteristics

5.3. Rel-16 New directions for FR2

Rel-15 represents the first release of the 3GPP standards for FR2 (mmWave), but work continues with enhancements in Rel-16. Much of the work is the routine addition of new band combinations of CA and DC, as well as new combinations of Supplemental Uplink (SUL). But there are also Work and Study Items to improve the technology.

One set of Study Items is investigating enhancement to NR for URLLC, specifically targeting Factory Automation, Transportation, and Electrical Power Distribution use cases. These studies are specifically looking at both FR1 and FR2. A primary objective of this work is, "Higher reliability (up to 1E-6 level), higher availability, time synchronization down to the order of a few µs where the value can be 1 or a few us depending on frequency range, short latency in the order of 0.5 to 1 ms."

3GPP is also continuing with Phase 3 of V2X work in Rel-16, and is specifically looking at FR2 applications for V2X. Four specific use cases are the subject of the Rel-16 work: vehicles platooning, extended sensors, advanced driving and remote driving.

There are studies on Improving Power Savings, and on improving MIMO operation, particularly in FR2. And finally, there is a study on extending FR2 beyond the current upper limit of 52.6 GHz, specifically including the 60 GHz band.

Acronym and Title	Description

FS_NR_L1enh_URLLC
Study on physical layer enhancements for NR UR Low Latency Cases
 	
FS_NR_IIOT
Study on NR Industrial Internet of Things (IoT)
	Investigate enhancements to URLLC (Ultra Reliable Low Latency Communications), considering both FR1 and FR2 as well as TDD and FDD, with the already existing solutions for NR as the baseline.
	
	• New Release 16 use cases with higher requirements
	  ○ Factory automation
	  ○ Transport Industry
	  ○ Electrical Power Distribution

FS_IIIOT_CM Study on channel modeling for indoor industrial scenarios	Develop a channel model to support studies on URLLC/IIOT enhancements for industrial scenarios and use cases. • Determine a suitable description of the scenario and frequency bands up to 100GHz that should be supported. • Define a new industrial propagation scenario and determine propagation parameters and, if required, new model components. Use 38.901 as the starting point. ○ Priority should be given to channel modeling for frequency ranges below 52.6GHz, which can be captured in the TR upon completion of the corresponding model.
FS_NR_V2X Study on NR Vehicle-to-Everything (V2X)	SA1 has identified 25 use cases for advanced V2X services and they are categorized into four use case groups: vehicles platooning, extended sensors, advanced driving and remote driving. NR V2X is destined as 3GPP V2X phase 3 and would support advanced V2X services beyond services supported in LTE Rel-15 V2X. Sidelink frequencies for FR1 and FR2 (i.e. up to 52.6 GHz) unlicensed ITS bands and licensed bands are considered in the

	study. The target is to have a common sidelink design for both FR1 and FR2.
FS_NR_UE_pow_sav Study on UE power saving in NR	The objective is to study UE power saving framework taking into consideration of latency and performance in NR as well as network impact. The objective of the UE power saving study includes the following: • Identify techniques for UE power saving study with focus in RRC_CONNECTED mode • Study the UE power consumption reduction in RRM measurements in synchronous and asynchronous network deployment • Study the enhancement of higher layer procedures for UE power saving
NR_SUL_combos_R16 Band combinations for SA NR supplementary uplink (SUL), NSA NR SUL, NSA NR SUL with UL sharing from the UE perspective (ULSUP)	All new SUL configurations including of SA NR SUL, NSA NR SUL and NSA NR SUL with UL sharing from the UE perspective (ULSUP) will be defined under this WI • Specify the band-combination specific RF requirements for all listed SUL configurations • Analyze combinations that have self-desensitization • Add conformance testing in RAN5 specifications
DC_R16_wBLTE_xBNR_yDLzUL Dual Connectivity (EN-DC) of w LTE band (yUL/zDL) and x NR band (1DL/1UL)	All new EN-DC configurations Multiple WIs for different combination numbers.
NR_CA_R16_intra NR intra band Carrier Aggregation	NR CA intra-band configurations are fundamental part of all higher order combinations and all new intra-band configurations will be defined under this WI • Specify the configuration specific RF requirements for all listed NR intra-band CA combinations • Analyze combinations that have self-desensitization • Add conformance testing in RAN5 specifications
NR_eMIMO Enhancements on MIMO for NR	To specify the enhancements identified for NR MIMO. The detailed objectives are as follows. • Enhancements on MU-MIMO support: • Enhancements on multi-TRP/panel transmission including improved reliability and robustness with both ideal and non-ideal backhaul: • Enhancements on multi-beam operation, primarily targeting FR2 operation
FS_NR_beyond_52GHz Study on NR beyond 52.6 GHz	This study item includes the following objectives for frequency range between 52.6 GHz and 100 GHz: • Identify target spectrum ranges • For 60GHz bands, TR 38.805 can be a reference. • Identify potential use cases and deployment scenarios

	• Identify NR design requirements and considerations on top of regulatory requirements

Table 5-6 Release 16 enhancements

5.4. UL in SUL or EN-DC. Does mmWave still need to carry UL signaling?

Most early deployments of 5G NR will use Dual Connectivity between LTE and NR (EN-DC), with the network signaling primarily carried over the LTE connection, primarily so that the NR radio layer can be deployed without requiring the deployment of a 5G Core Network. EN-DC has both the benefits and complexities of multiple radio channels, which is especially useful for FR2 because of the varied coverage in mmWave. Connections can be anchored on lower frequency LTE cells, with the higher throughput of mmWave available opportunistically.

Once 5G Cores are deployed, it will no longer be strictly necessary to use EN-DC for signaling reasons, but it may still be desirable to use multiple channels to provide frequency diversity and higher throughputs. So it is useful to compare the different schemes for a UE to use multiple channels and bands, namely, EN-DC, Carrier Aggregation (CA), and Supplemental UL (SUL).

EN-DC is a form of Dual Connectivity, where there is no assumption of coordinated scheduling between the two connections. The radio layer at the UE must be able to handle all combinations of allocations, on both UL and DL, between the multiple channels, without relying on help from the network.

Carrier Aggregation (CA) uses a single logical connection, made up by aggregating multiple carriers. The assumption is that the scheduling of the carriers is coordinated by the eNB or gNB, so known limitation on the UE can be scheduled around.

Supplemental Uplink (SUL) is also a single logical connection, but is more limited than CA. With SUL, in addition to higher frequency bidirectional channels, a UE can use a lower frequency channel for UL transmission. But there is an important restriction – the UE cannot transmit simultaneously on the SUL and normal channels if both are within FR1, so the scheduling must be coordinated. The main advantage of SUL over CA is simplicity – there is no need for either simultaneous Rx or Tx.

Currently, in Rel-15, SUL combinations are only defined for FR1 channels. For an FR2 connection, there are fewer advantages to SUL. In conditions where a lower frequency UL channel is needed, an FR2 DL connection may not be reliable enough either, so CA may be a better choice since it includes DL on the lower frequency channel. And since there are fewer interactions and restrictions between simultaneous FR1 and FR2 transmissions, the advantages of the simplicity of SUL are less valuable with FR2 – the separate RF Front Ends make it easier for the UE to transmit simultaneously and without coordination between FR1 and FR2 channels. Moreover, FR2 connections use TDD and rely heavily on beamforming, so channel reciprocity and the use of SRS on UL are very important, so UL on the FR2 channel will always be needed.

In summary, even when 5G core signaling is usable by both UE and the network and EN-DC is not necessary, there will still be some conditions where the use multiple channels is advantageous. SUL has fewer advantage with FR2 channels than with FR1, so CA or DC may be more suitable, since they provide robustness on both DL and UL, and the simplicity of SUL is less attractive.

6. mmWave Spectrum Allocation

The previous section elaborated the transmitter and receiver performance in FR2 spectrum. This section will dive deep into the global availability of mmWave spectrum across various operators.

6.1. Standard Body Update

There are four new 5G/NR bands defined by 3GPP in Release 15. They are listed as followed:

NR operating band	Uplink (UL) and downlink (DL)	Duplex mode
n257	26500–29500 MHz	TDD
n258	24250–27500 MHz	TDD
n260	37000–40000 MHz	TDD
n261	27500–28350 MHz	TDD

Table 6-1 mmWave Bands

There are spectrum bands being considered by national regulators that were not considered by 3GPP specifications at end of July 2018:

- 64–86 GHz, or parts thereof.

Note that various parts of the 64–86 GHz range are considered differently in different regions. For instance, 64–71 GHz is set aside for unlicensed use in North America and is under consideration in CEPT (66–71 GHz); 66–76 GHz and 81–86 GHz are under study in ITU-R as a possible range for IMT-2020, to be decided at WRC-19.

6.2. North America Spectrum Update

According to the GSA report, titled “Spectrum for Terrestrial 5G Networks: Licensing Developments Worldwide,” as of December 14 of 2018, regulator in Canada is considering plans to release 26GHz, 32GHz and 80GHz for mobile use by 2021.

In the rest of this section we’re going to see a bit of detail on the road trip FCC took when it conducts its 5G mmWave auction in the recent months.

According to an AT&T survey in 2017, the amount of mmWave spectrum availability could be 43550MHz in the US alone with both licensed and shared spectrum, as depicted in Figure 6-1.

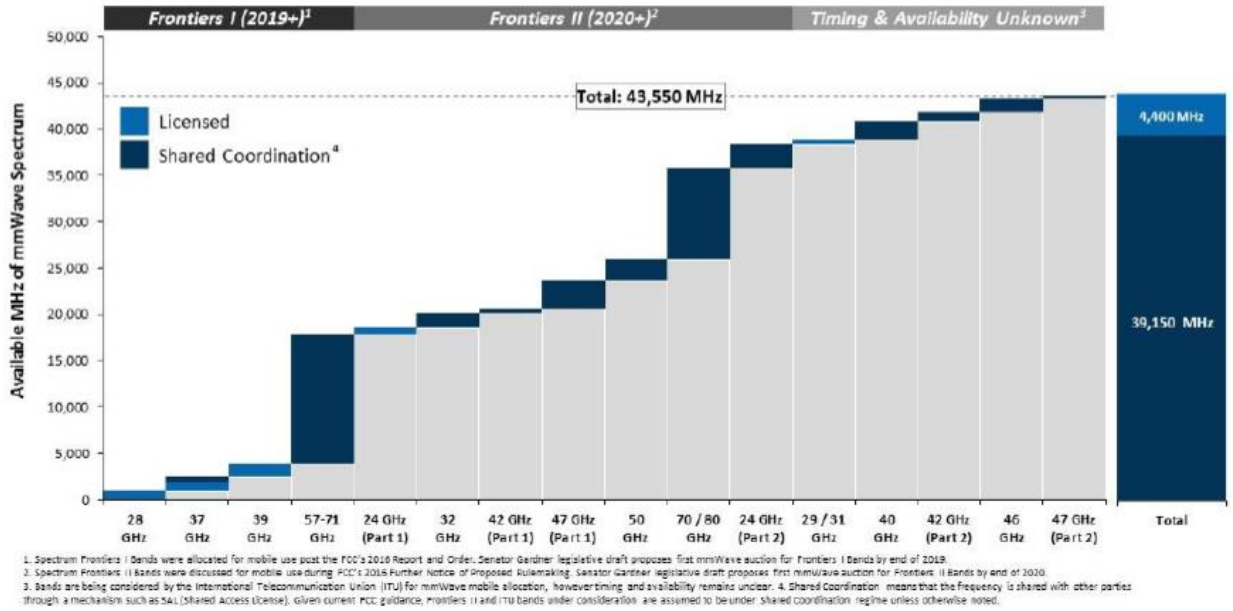

Figure 6-1 U.S, mmWave Spectrum Allocation [48]

U.S. carriers are pushing for the FCC to release additional millimeter wave spectrum, and in response the agency has scheduled the world's first millimeter wave spectrum auction for November 2018. The bidding started on spectrum in the 28 GHz band, which will be followed by bidding for spectrum in the 24 GHz band.

The 28 GHz auction is two 425 megahertz blocks by county. The blocks are 27.500 – 27.925 GHz (L1) and 27.925 – 28.350 GHz (L2). The FCC authorized both fixed and mobile operations in the 28 GHz band. Initial authorizations will have a term not to exceed ten years from the date of initial issuance or renewal.

The 24 GHz auction is seven 100 megahertz blocks. The lower segment (24.25 – 24.45 GHz) is licensed as two 100-megahertz blocks (Blocks A and B). The upper segment (24.75 – 25.25 GHz) is licensed as five 100-megahertz blocks* (Blocks C – G). The FCC authorized both fixed and mobile operations in the 24 GHz band. Initial authorizations will have a term not to exceed ten years from the date of initial issuance or renewal.

The FCC is making 1.55 gigahertz of spectrum available through these two auctions. These auctions will be followed by a 2019 auction of three more millimeter-wave spectrum bands—37 GHz, 39 GHz, and 47 GHz. The FCC auction rules include:

- The spectrum will be auctioned in 100 megahertz blocks based on Partial Economic Areas to enable a simultaneous auction;

- The bidding will follow an incentive auction mechanism considering contiguous blocks;
- And a pre-auction process "that allows incumbent licensees to rationalize their holdings."

Between the three mmWave bands, the FCC is opening up a total of 3.4 gigahertz of high-band frequencies. Prior to November 2018 auction, here are some charts showing the current ownership situation around the millimeter wave bands.

First, the analysts at Wall Street research firm Oppenheimer offer a relatively cohesive look at some of the most popular millimeter wave bands and who owns them. If the FCC owns the spectrum, then it can be auctioned.

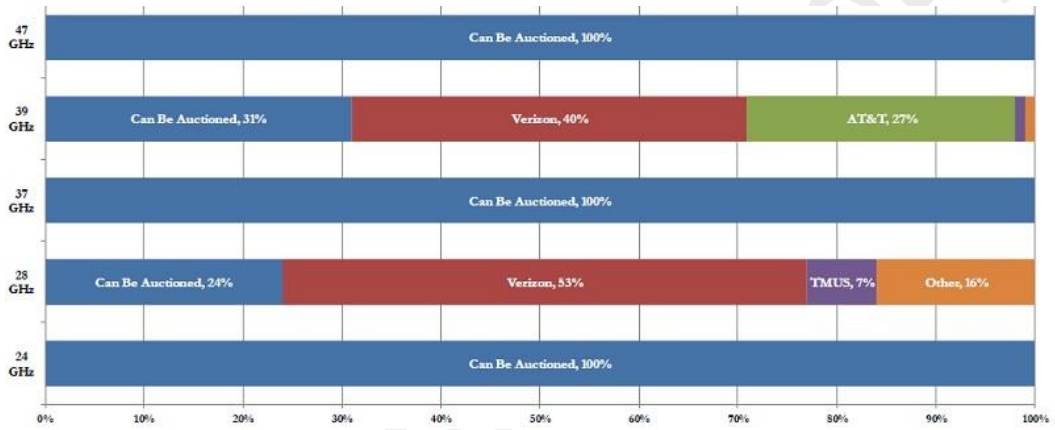

Figure 6-2 mmWave band ownership

Secondly, Allnet [13] shows the aggregate millimeter wave ownership across all bands:

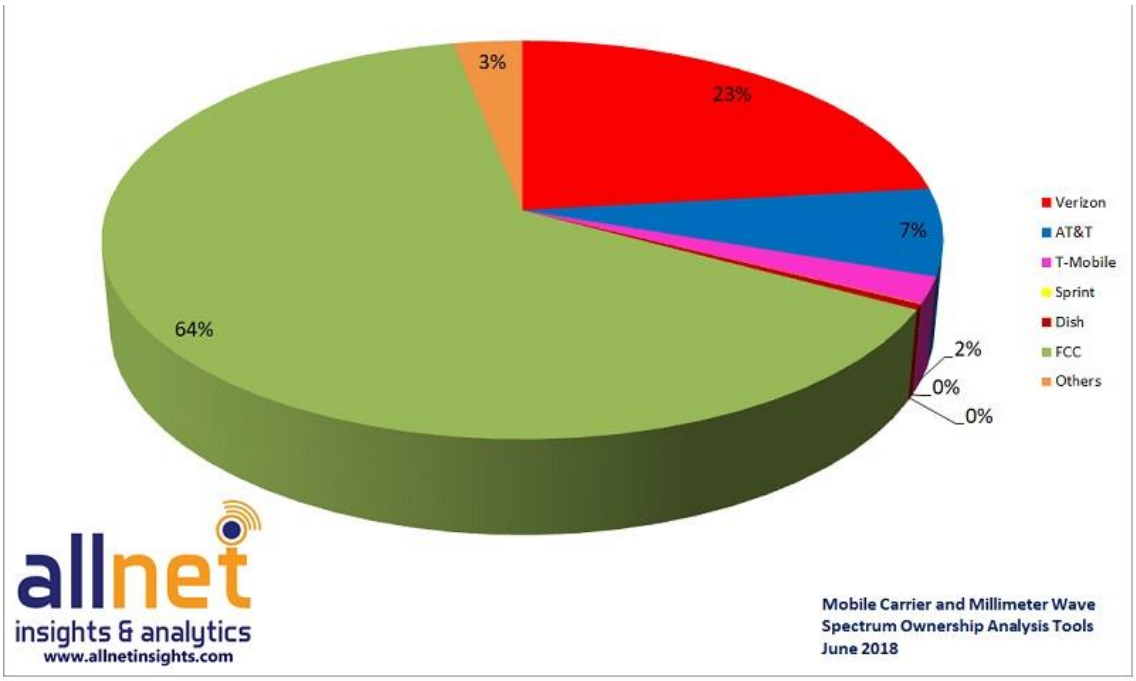

Figure 6-3 Aggregate mmWave spectrum ownership

Allnet breaks that information down into the individual bands, including 24 GHz which is 100% owned by the FCC and is going through the auction process right now.

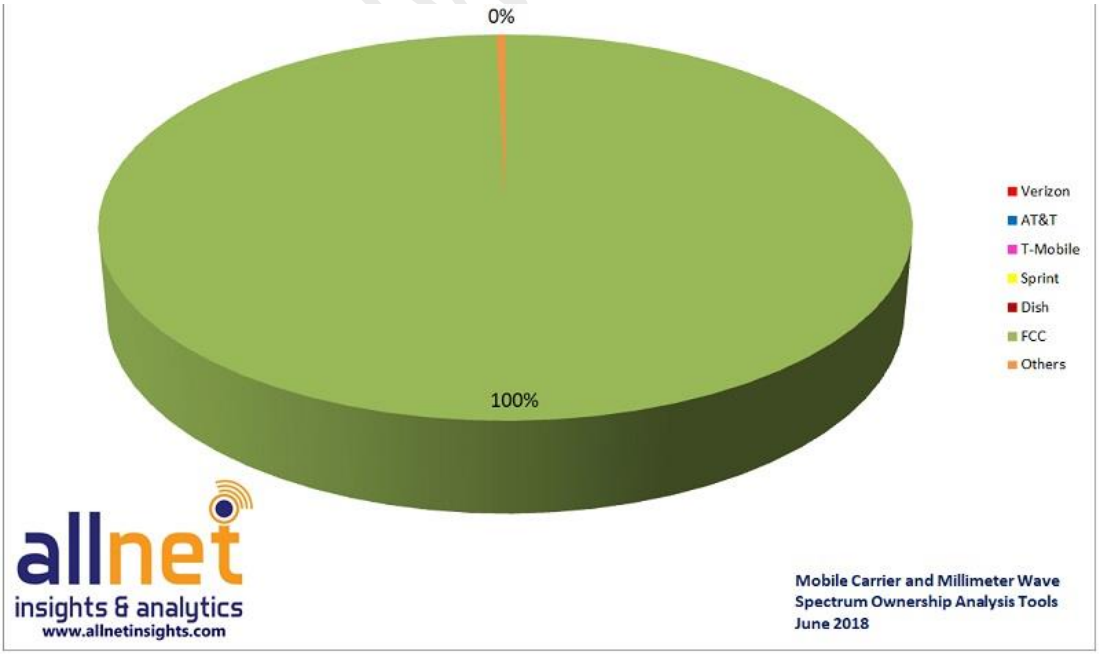

Figure 6-4 mmWave spectrum ownership – 24GHz

For 28-31 GHz, the FCC used to own about 25%, and the auction process is completed now.

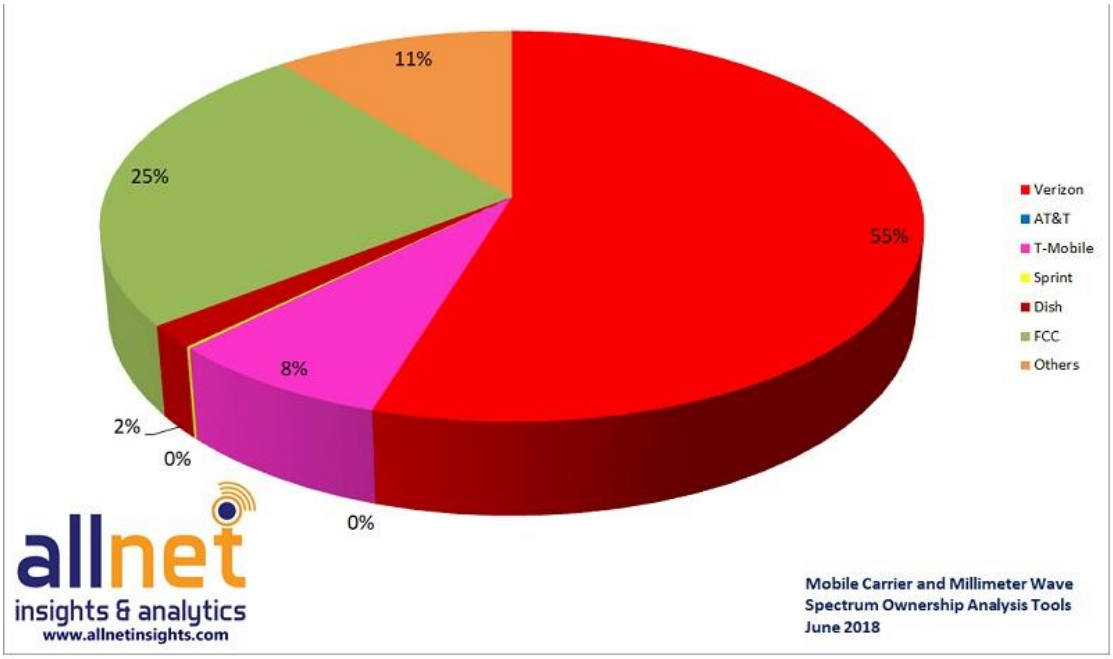

Figure 6-5 mmWave spectrum ownership – 28-31 GHz

The FCC still owns 100% of 37 GHz.

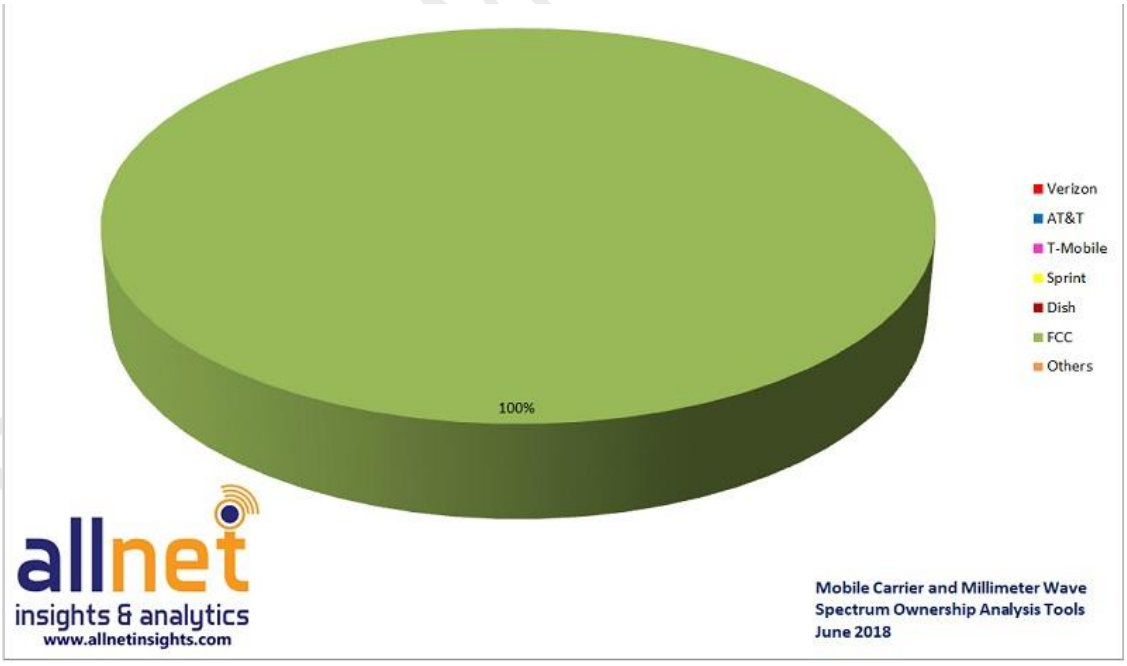

Figure 6-6 mmWave spectrum ownership – 37GHz

For 39 GHz, the FCC owns about 32%.

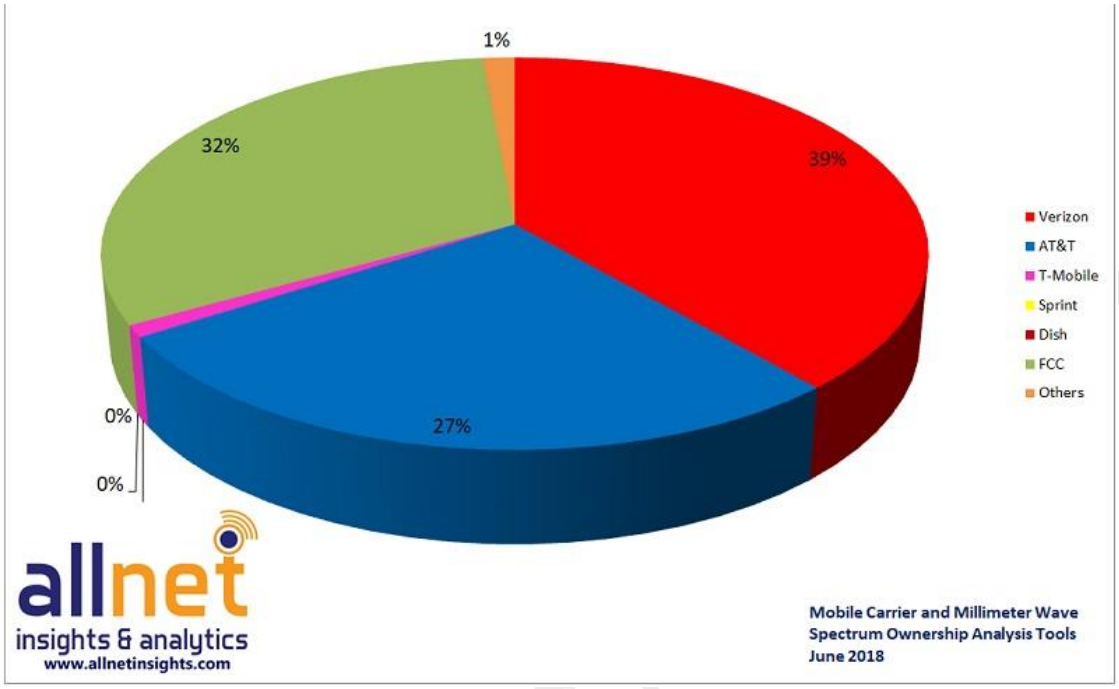

Figure 6-7 mmWave spectrum ownership – 39 GHz

The FCC still owns 100% of 47 GHz.

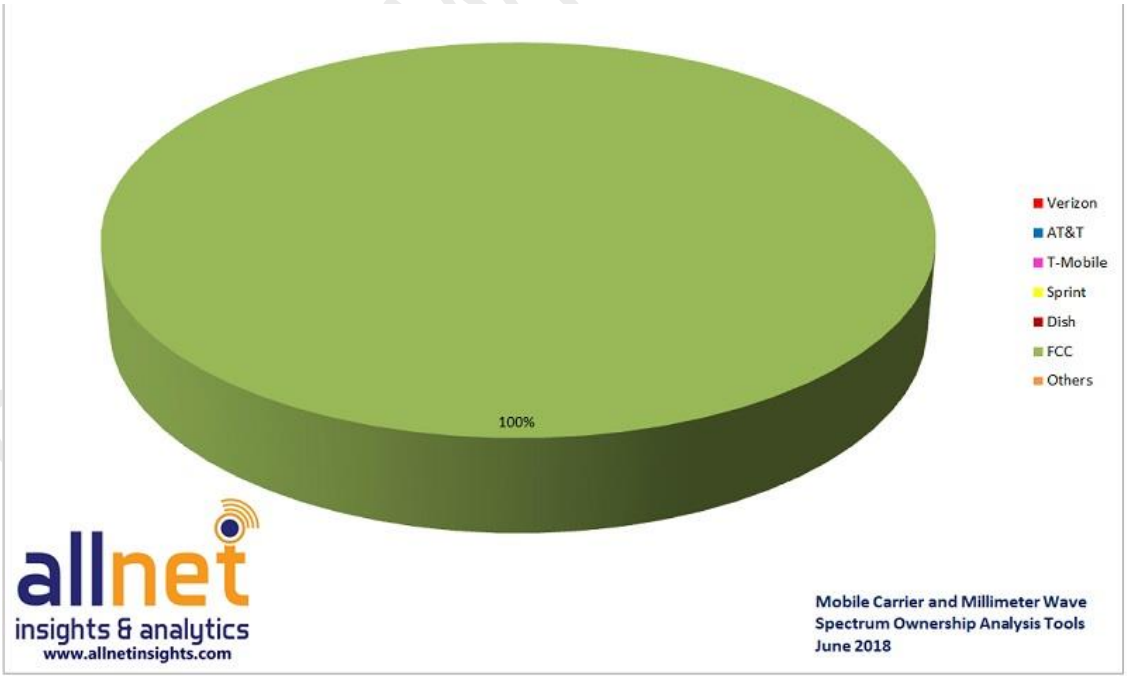

Figure 6-8 mmWave spectrum ownership – 47 GHz

6.3. Asia Pacific Spectrum Update

A recent GTI mmWave white paper gives us more update on the progress many GTI operators made within their own regulatory countries [51]. In July 2017, the Ministry of Industry and Information Technology of China approved 5G technology trials in both 26GHz and 37GHz. In June 2018, South Korea auctioned its 28GHz band to three operators each with 800MHz. The Ministry of Internal Affairs and Communications of Japan announced it will award four operators each with 400MHz in 28GHz by March 2019. In the coming years, we expect to see the number of allocated mmWave spectrum specifically for 5G services will grow rapidly.

According to the GSA report, titled "Spectrum for Terrestrial 5G Networks: Licensing Developments Worldwide," as of December 14 of 2018, regulators in more than 10 Asia Pacific countries were "either formally considering introducing certain spectrum bands for terrestrial 5G services, holding consultations regarding suitable spectrum allocations for 5G, have reserved spectrum for 5G, have announced plans to auction frequencies or have already allocated spectrum for 5G use." in the range of mmWave. Table 6-2 lists each related mmWave spectrum allocation range and time table.

Region	Country	Spectrum (GHz	Spectrum Range (GHz)	Quarter/Ye
Asia-Pacific	Australia	26	24.25–27.5	Q3 2020
Asia-Pacific	China	26	24.25–27.5	
Asia-Pacific	China	37	37–43.5	
Asia-Pacific	Hong Kong	26	24.25–27.5	Q2 2019
Asia-Pacific	Hong Kong	28	27.5-28.35	Q2 2019
Asia-Pacific	India	26	24.25–27.5	
Asia-Pacific	India	28	27.5–29.5	
Asia-Pacific	India	30	29.5–31.3	
Asia-Pacific	India	32	31.8–33.4	
Asia-Pacific	India	42	37–43.5	
Asia-Pacific	Indonesia	26	24.25–27	2022
Asia-Pacific	Indonesia	28	27–29.5	2022
Asia-Pacific	Japan	28	27–29.5	Q1 2019
Asia-Pacific	New Zealand	28	24.25–28.35	2020
Asia-Pacific	Singapore	28	24.25–29.5	
Asia-Pacific	South Korea	28		Q2 2018
Asia-Pacific	Taiwan	28		
Asia-Pacific	Thailand	26		
Asia-Pacific	Thailand	28		
Asia-Pacific	Vietnam	26	24.25–27.5	
Asia-Pacific	Vietnam		27–43.5	

Table 6-2 Asia Pacific mmWave Spectrum Allocation Projection

6.4. Europe Spectrum Update

In late 2018, the European Commission issued regulatory requirements for 5G use of 26GHz and Italy has already auctioned this band to five operators with each to have 200MHz bandwidth [51].

According to the GSA report, titled "Spectrum for Terrestrial 5G Networks: Licensing Developments Worldwide," as of December 14 of 2018, regulators in 17 European countries were "either formally considering introducing certain spectrum bands for terrestrial 5G services, holding consultations regarding suitable spectrum allocations for 5G, have reserved spectrum for 5G, have announced plans to auction frequencies or have already allocated spectrum for 5G use." in the range of mmWave. Table 6-3 lists each related mmWave spectrum allocation range and time table.

Region	Country	Spectrum (GHz	Spectrum Range (GHz)	Quarter/Ye
Europe	Belgium	26		2021
Europe	Belgium	32	31.8–33.4	2022-2027
Europe	Belgium	42	40.5–43.5	2022-2027
Europe	Bulgaria	26	24.25–27.5	
Europe	Czechia	26		
Europe	France	26		2020
Europe	Germany	26		
Europe	Greece	26	24.5–26.5	1Q 2017
Europe	Hungary	26		
Europe	Ireland	26		
Europe	Italy	26	26.5-27.5	Q4 2018
Europe	Norway	26		
Europe	Poland	26		
Europe	Portugal	26		
Europe	Romania	26	24.25–27.5	
Europe	Russia	28	25.25–29.5	
Europe	Slovakia	26		
Europe	Slovakia	29		
Europe	Sweden	26	24.25–27.5	
Europe	UK	26		
Europe	UK		66-71	

Table 6-3 European mmWave Spectrum Allocation Projection

7. mmWave Coverage Analysis

mmWave is now becoming a focus of testing and deployment by many operators due to the support of large bandwidths and 3GPP 5G-NR standardization. It is therefore important to fully understand the coverage aspects of mmWave, particularly in case of handheld devices and how can it be put to use to improve overall user experience. This section will look at various coverage related aspects in more details.

7.1. mmWave Link Budget

Link budget in the mmWave frequencies could be complicated due to varied antenna configurations, and gains/losses depending on the types of deployment. It is therefore best to first look at the MCL, which excludes implementation / deployment parameters as typically used in 3GPP simulations. The Table 7-1 below illustrates the MCL derivation of a 28GHz system for a handheld device:

	Data channel	
	Uplink	Downlink
Total BW	200MHz (100x2)	400MHz (100x4)
MCS	QPSK	QPSK
PRBs per CC	66	66
Throughput (Mbps)	5	50
Transmitter		
100% min EIRP	22.4	60
50% min EIRP	11.5	
Receiver		
Thermal Noise Density (dBm/Hz)	-174	-174
Receiver Noise Figure (dB)	6	10
Occupied Channel BW (MHz)	95.04	95.04
Effective Noise power	-88.22093572	-84.22093572
Required SINR	-0.9	-3
Rx BF Gain (dBi)	29	8
Implementation Margin (dB)	0	0
Receiver Sensitivity	-118.1209357	-95.22093572
MCL (with 100% min EIRP)	137.5106358	149.2003358
MCL (with 50% min EIRP)	126.6106358	

Table 7-1 28GHz Link Budget

The assumptions for the above MCL analysis are based on vendor and 3GPP inputs (for EiRPs, Noise figure, etc.). The MCL analysis does not include implementation losses, penetration losses, reflection coefficients, shadow fading etc as these are deployment specific and should be considered as part of that activity.

As seen from the Table 7-1 above, mmWave system is UL limited. The UL MCL with 11.5dBm UE EIRP (50%-ile peak) is **126.6dB** for sustaining 5Mbps throughput on shared data channel. Similarly the DL MCL for the shared data channel is **149.2dB** for sustaining 50Mbps throughput. The 50Mbps (DL) number was used based on the throughput requirements for most eMBB applications as discussed in section 4. The 5Mbps UL was based on 5% TCP Ack [99] to DL traffic and additional UL data needs. The UE EIRP results in more than 10dB delta in overall UL MCL between 100% min Peak EIRP and 50% min Peak EIRP. The control channel MCL is expected to be 10-15dB higher than the data channels.

An additional link budget from Nokia using their own product specifications is shown below (Table 7-2). AEUB, AEUD/E and CMP are some of Nokia's mmWave supported products.

Sample mmWave RF Link Budget

	AEUB		AEUD/E		CMP	
Operating band [GHz]	28.0		28.0		28.0	
Channel bandwidth [MHz]	100		100		100	
Number of channels	2	2	2	2	2	2
DL/UL TDD ratio	80/20		80/20		80/20	
	DL	UL	DL	UL	DL	UL
Cell-edge user throughput [Mbps]	100	5	100	5	100	5
Total output power (all carriers) [dBm]	31	23	28	23	31	23
Antenna gain (incl. beamforming gain) [dBi]	29	0	23	0	24	0
Total EIRP (all carriers) [dBm]	60	23	51	23	55	23
EIRP (per carrier) [dBm]	57	20	48	20	52	20
RX Antenna gain [dBi]	0	29	0	23	0	24
Required SNR at cell edge [dB]	7.6	-0.9	7.6	-0.9	7.6	-0.9
MCS	16QAM	QPSK	QPSK	QPSK	QPSK	QPSK
Noise Figure [dB]	7	6	7	6	7	6
Receiver sensitivity [dBm]	-79.5	-90.2	-79.5	-90.2	-79.5	-90.2
Shadowing margin [dB]	10.5	10.5	10.5	10.5	10.5	10.5
Maximum Allowable Path Loss [dB]	126.0	128.7	117.0	122.7	121.0	123.7
Body loss (blockage margin) [dB]	0	0	0	0	0	0
Interference Margin [dB]	6.0	2.6	6.0	2.6	6.0	2.6
MAPL (with margins) [dB]	120.0	126.1	111.0	120.1	115.0	121.1

NOKIA

11 © 2018 Nokia

Table 7-2 Nokia Link Budget [17]

The DL MAPL using CMP product is ~121dB while supporting higher UL MAPL of ~124dB. It is important to note that the above link budget does not account for body/hand blockage and other penetration / diffraction losses.

As seen from the sample link budgets above, the MAPL numbers could vary depending on the assumptions made. The typical / 3GPP numbers are MCL based and does not account for any of the over the air losses/blockages. Nokia MAPL numbers does not account for hand/body loss but accounts for shadow fading. Also, the Nokia MAPL numbers illustrate that the system would DL limited while the typical/3GPP numbers demonstrate UL limited system.

In the following subsections, we will look at the key link budget parameter settings that were used above to determine the MCL/MAPL. The parameter values are based on vendor / 3GPP work in this area.

7.1.1. gNB Parameter Settings

gNB parameters are critical for analyzing the coverage and capacity of any given network. mmWave gNB is required to support beamforming for improving coverage. At the mmWave frequency, the wavelength is shorter and hence can support a large number of antenna elements, typically ranging from 128, 256 to 512. With this large number of antennas, support of Digital beamforming is not feasible due to the need for a high number of RF chains which in turn increases cost, power consumption and heat dissipation. Most deployments are expected to support Analog beamforming. Hence, it would support only single layer operation since the phase/amplitude of all the antenna element are controlled using a single RF chain with Analog BF. However, many implementations may also support Hybrid beamforming which

could implement 2-4 RF chains, resulting in support for MU-MIMO operation. For the purpose of link budget analysis, single layer operation shall be considered. The expected antenna array gain is ~24-29dB. The max conducted Tx power is ~31dBm, resulting in an overall peak EiRP to be ~55-60dBm. The noise figure of the receiver is expected to be ~5-7dB.

7.1.2. UE Settings (for Smartphones)

UE simulation parameter assumptions in the link budget are equally important to determine accurate coverage. In order to avoid variability in link budget due to unknown parameters such as penetration loss, hand/body blocking, reflection etc, it makes sense to just define generic parameters and determine MCL. Other impairments can be accounted across different simulation runs as needed.

Below (Table 7-3) are the key assumptions for the UE Receiver as well as UE Transmitter, compiled based on data from multiple sources, including 3GPP. 3GPP however gives freedom to manufacturers to balance between number of antenna elements per panel, number of panels, feed power and number of beams as long as the minimum peak EiRP/EIS and minimum sum of solid angle spatial coverage is fulfilled.

UE Receiver Parameters	**Values**
Frequency	28GHz
Noise Figure	10 dB
# of Ant Arrays	1
# of Ant Elements	4
Element Gain	4 dB
Effective Antenna Array Gain	8 dB

UE Transmitter Parameters	**Values**
Frequency	28GHz
Max Tx power	20 dBm
# of Ant Arrays	1
# of Ant Elements	4
Element Gain	4 dB
Effective Antenna Array Gain	8 dB
Min Peak EiRP	**22.4 dBm**
Min Peak EiRP (50%)	**11.5 dBm**

Table 7-3 UE Tx-Rx Parameters – Link Budget

The mmWave operation requires the support for beamforming at the transmitter and at the receiver for the reliability of the airlink. The mmWave UEs too therefore need to implement antenna arrays to support

beamforming, unlike sub-6GHz UE. The handheld UEs are expected to implement multiple antenna arrays (mostly 3) around the edges of the phone. The number of arrays (3) in mobile devices is driven by the need to have one array, at least, uncovered by handheld operations. However, at a given time, only one antenna array is expected to be active to limit the power consumption and at the same time, possibly avoid hand blocking. Each array is expected to support approximately 4 antenna elements with an element gain of ~4dB each. The peak UE EiRP as defined in 3GPP for handheld devices is 22.4dBm while the 50%-ile EiRP is expected to be ~11.5dBm. The UE receiver Noise figure is expected to be ~10dB.

7.1.3. Technology Components

Previous subsections discussed various UE and gNB RF parameters for the link budget. Apart from those RF parameters, there are technological parameters too that have impact on link budget numbers. Below are the list of key technology parameters.

DL/UL slots	4:1
Waveform (DL/UL)	CP-OFDM
Channel Coding (PDSCH/PUSCH)	NR LDPC
SCS	120KHz
MIMO	Rank 1 SU-MIMO
MCS	QPSK
System BW (DL/UL)	400MHz
PRBs	66PRBs per 100MHz CC
DL Throughput	50 Mbps
UL Throughput	5 Mbps

Table 7-4 Technology parameters – Link Budget

As seen in the Table 7-4 above, most of these parameters (such as DL/UL slots, channel coding, SCS) would dictate the throughput requirement. Other parameters such MCS, PRB, MIMO also impact throughput target but these are also impacted by RF environment.

7.1.4. Other Link Budget Components

The basic link budget (MCL) parameters discussed in previous subsection can be further complemented with real world / practical losses to determine real user experience. These components are mostly frequency dependent and hence important to analyze for mmWave deployments.

7.1.4.1. Propagation losses

The total over the air propagation loss between transmitter and the receiver without any physical blockage, involves Freespace path loss, atmospheric attenuation (Oxygen and Water Vapor) and Rain attenuation. Besides these, foliage could also pose additional losses at mmWave frequency range. This subsection will look at all of these losses and quantify the difference as compared to sub-6GHz.

As we know, the Freespace path loss can be calculated using the formula:

$$FSPL = 20log_{10}(d) + 20log_{10}(f) + 20log_{10}\left(\frac{4\pi}{c}\right)$$

A key component of this formula besides the distance (d), is the frequency (f). So, as the frequency increases, the overall freespace path loss increases. A chart below (i.e. Figure 7-1) from R&S [18] illustrates the path loss vs distance for some mmWave frequencies as compared to sub-6GHz. For a typical mmWave coverage distance of 200m, the mmWave propagation loss could be ~30dB additional as compared to low band channel (850MHz) and ~18dB additional compared to 3.5GHz.

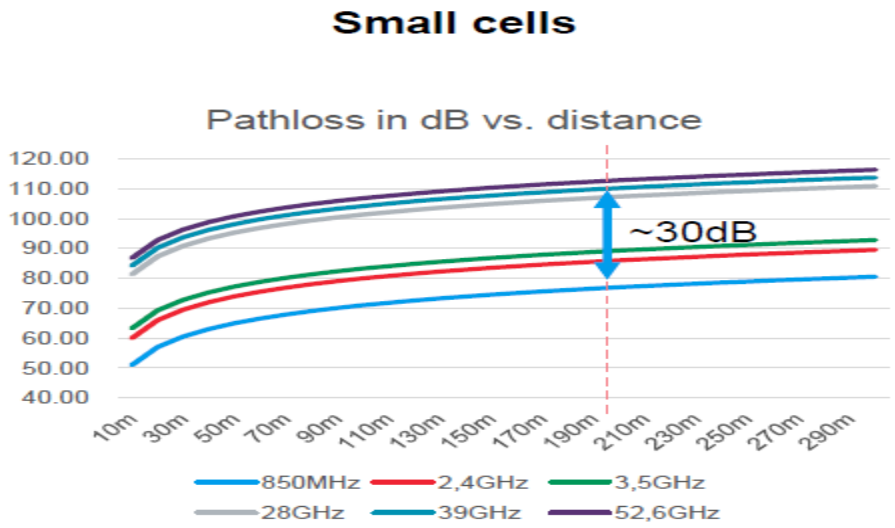

Figure 7-1 Pathloss vs Distance comparison – R&S

Besides Freespace loss, Electromagnetic waves are also absorbed in the atmosphere, depending on the wavelength. The two compounds that are responsible for the majority of signal absorption are oxygen (O2) and water vapor (H2O).

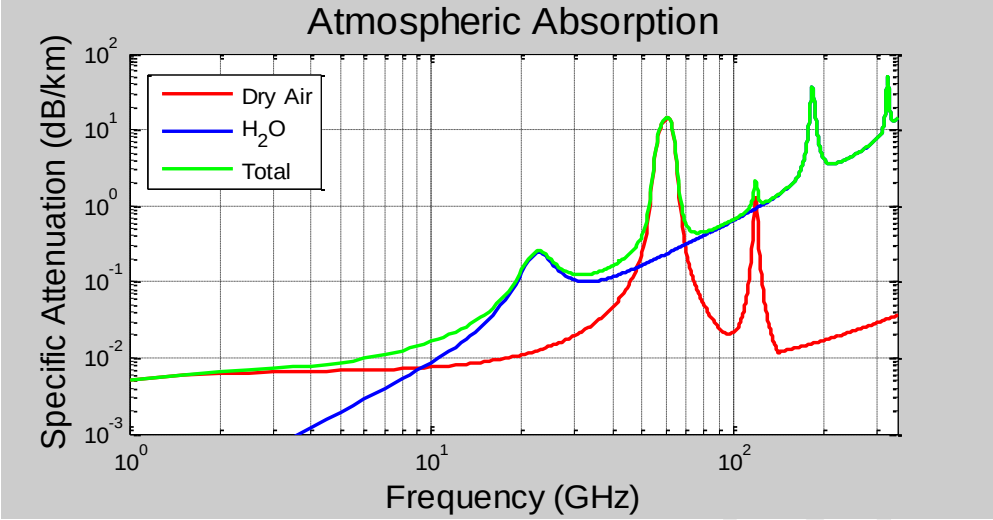

Figure 7-2 Atmospheric Absorption [19]

The atmospheric absorption at mmWave frequencies is higher with some frequencies as seen above in Figure 7-2 but for 28GHz, it would be ~0.1 dB/Km (H2O: 0.09dB/Km & O2: 0.02dB/Km [20]).

The rain attenuation could vary based on geographic location depending on amount of rain probability and density in mm/hr. The rain attenuation could be high in some cases but mostly minor for the mmWave cell sizes i.e 4dB/200m @110mm/h [21] or <3dB/Km @ 10mm/hr (28GHz) [20]. The loss due to snow and fog is insignificant at 28GHz i.e 0.4dB/Km and 0.5 dB/Km respectively.

Besides over the air losses, Foliage loss could be significant at mmWave frequencies. It depends on the type of trees and its depth. Figure 7-3 below illustrates the loss due to foliage across GHz frequency range. At high frequencies, the higher tree depth could result in more than 10 dB of attenuation.

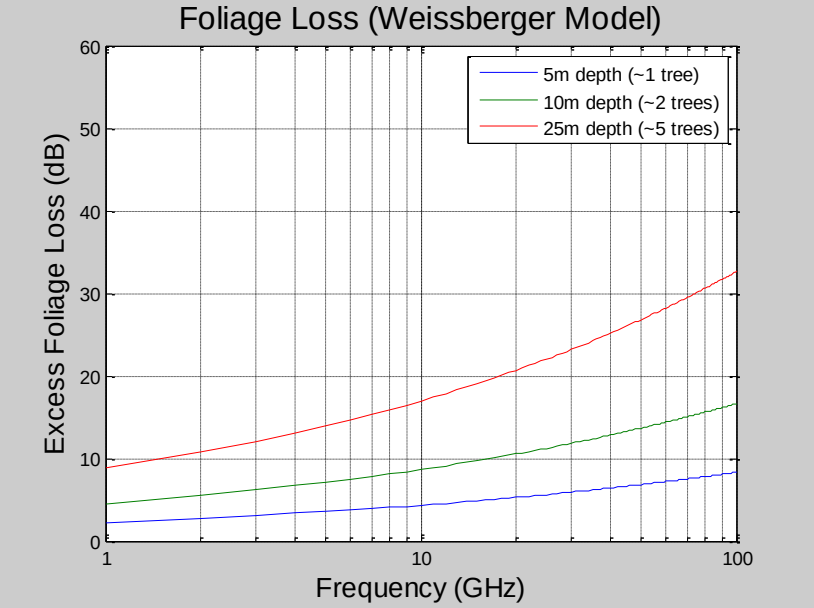

Figure 7-3 Foliage Attenuation – Remcom [19]

Samsung had tested tree losses and Figure 7-4 below illustrates the details. An average of 7dB/m for a single tree was measured [20].

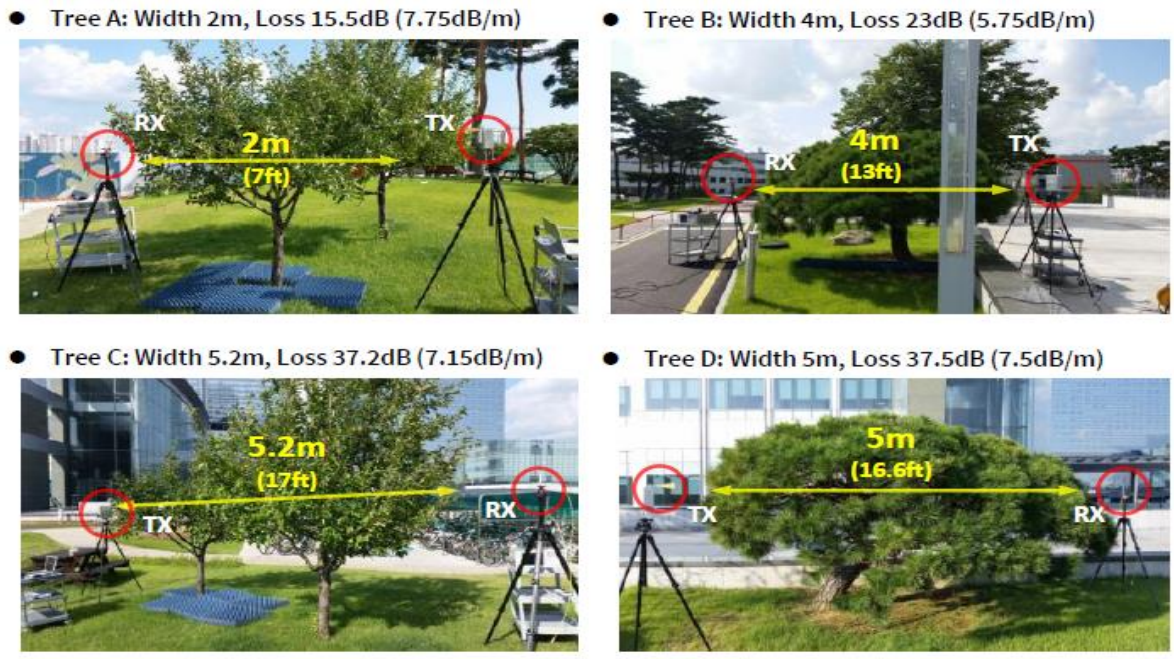

Figure 7-4 Foliage Attenuation - Samsung

Another similar study on foliage attenuation comparison between 2.9GHz and 29GHz was performed by Qualcomm. Figure 7-5 below has the results [22].

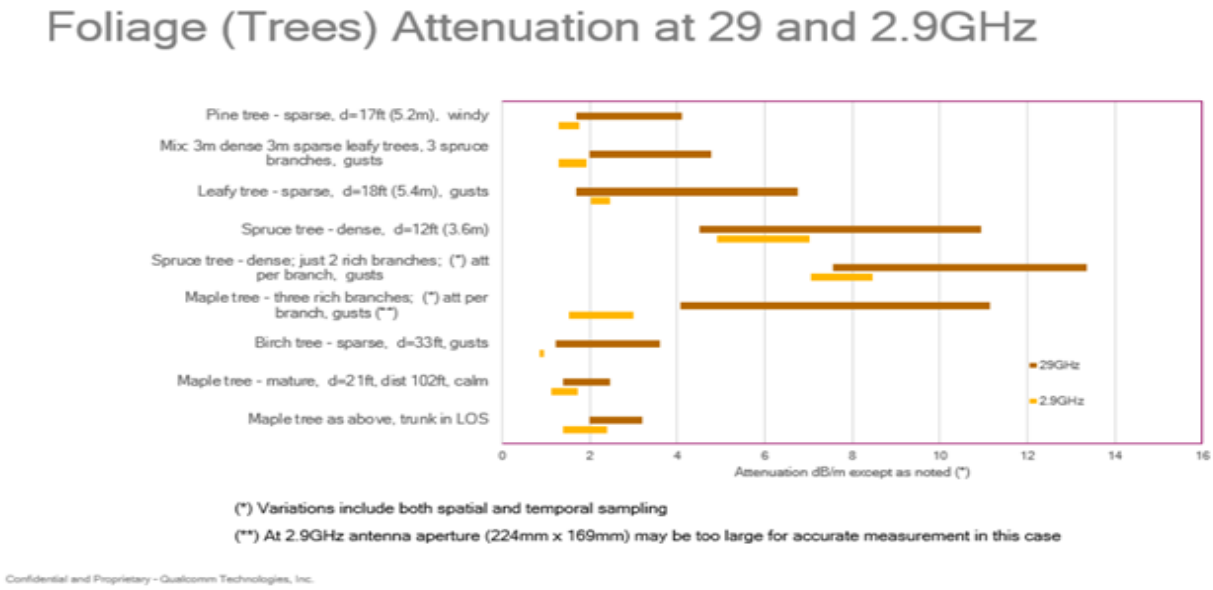

Figure 7-5 Foliage Loss - Qualcomm

It illustrates that (under gusty wind conditions) the leaf density from the conifer, more frequently produces heavy link losses and more so at higher frequencies. On an average, ~4dB/m of additional attenuation at mmWave frequencies can be seen from the above study.

However, the effect of foliage can be relaxed by utilizing alternate propagation paths / reflections and hence the overall loss may not linearly increase with distance.

7.1.4.2. Penetration losses

The penetration losses for mmWave frequencies could vary depending on the material. Below (Figure 7-6) are the measurements performed by Nokia [23]. It shows that losses through softer material may be less significant but other harder materials like cement, brick etc have losses in excess of 20dB.

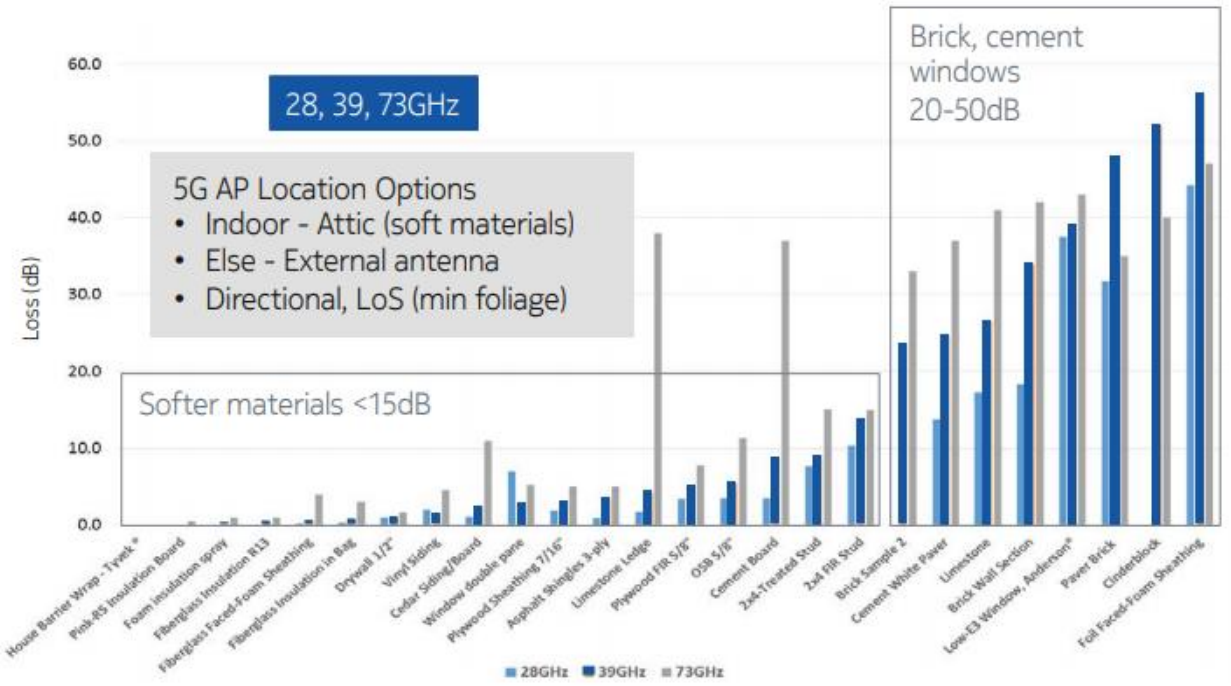

Figure 7-6 Penetration Losses – Nokia [23]

Low emissivity or low-e glass, which has a thin metal oxide coating to reflect energy from the inside and outside in order to make home / offices more energy efficient as well as cutting UV rays from the sun. However, these glasses pose a challenge at mmWave frequencies due to higher penetration losses. As seen in the Figure 7-6 above, Low-e glass has a penetration loss of ~40dB. This would almost act as an isolator. This is a major problem, particularly in downtown areas where the most network capacity congestion exists and needs mmWave hotspot solution. However, the absoprtion losses seen with low emission glass structures can be very useful for in-building 5G deployments. When deployed for in-building scenarios, the mmWave frequency band will improve overall capacity as the signal will experience minmum bleeding from the inside-out and from outside-in, which will ultimately result in better coverage and quality for in-building scenarios.

Another testing was performed by NYU wireless at different locations (ORH, WWH, MTC) in New York City [24].

COMPARISON OF PENETRATION LOSSES FOR DIFFERENT ENVIRONMENTS AT 28 GHZ. THICKNESSES OF DIFFERENT COMMON BUILDING MATERIALS ARE LISTED. BOTH OF THE HORN ANTENNAS HAVE 24.5 DBI GAINS WITH 10° HALF POWER BEAMWIDTH.

Environment	Location	Material	Thickness (cm)	Received Power - Free Space (dBm)	Received Power - Material (dBm)	Penetration Loss (dB)
Outdoor	ORH	Tinted Glass	3.8	-34.9	-75.0	40.1
	WWH	Brick	185.4	-34.7	-63.1	28.3
Indoor	MTC	Clear Glass	<1.3	-35.0	-38.9	3.9
	WWH	Tinted Glass	<1.3	-34.7	-59.2	24.5
		Clear Glass	<1.3	-34.7	-38.3	3.6
		Wall	38.1	-34.0	-40.9	6.8

Figure 7-7 Penetration Loss – Glass – NYU [24]

The Figure 7-7 shows that the tinted glass on these sample buildings cause 25-40 dB loss while the clear glass is <4dB at 28GHz frequency.

Qualcomm had also performed similar study on penetration losses. Below (Figure 7-8) are the results [22].

Summary of Out-to-In Propagation Loss

•Measured penetration losses for various materials

Residential 1	
Material	Loss
Vinyl siding	~6-7 dB
Stone siding	~35 dB
Window glass	~10 dB
Plastic blinds	~2 dB

Residential 2	
Material	Loss
Plywood	~8-10 dB
Hollow sheetrock	~1-2 dB
Wood exterior wall/panel	~10 dB
Brick exterior	~30 dB
Metal doors/window frames	high

Residential & Commercial	
Material	Loss
Commercial Tinted Window	10-20 dB
Clear glass	2.5 dB
Residential Home Exterior	~9 dB

•Results consistent with other industry sources

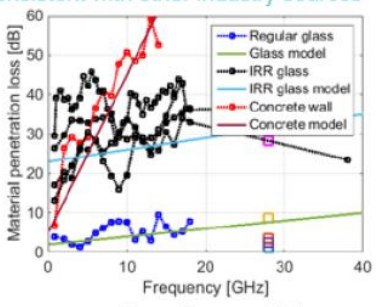

Sources: Samsung and Nokia

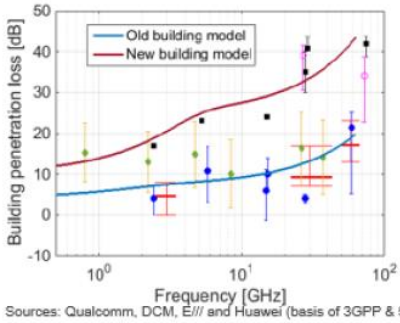

Sources: Qualcomm, DCM, E/// and Huawei (basis of 3GPP & 5GTF O2I model)

Confidential and Proprietary - Qualcomm Technologies, Inc.

Figure 7-8 Penetration Losses – Qualcomm [22]

As seen from the chart above, the penetration loss indoors could be more than 10dB in both residential and commercial setting, depending on the type of materials used.

Another data point from Pivotal Commware on Low E-Glass is shown in the Figure 7-9 below

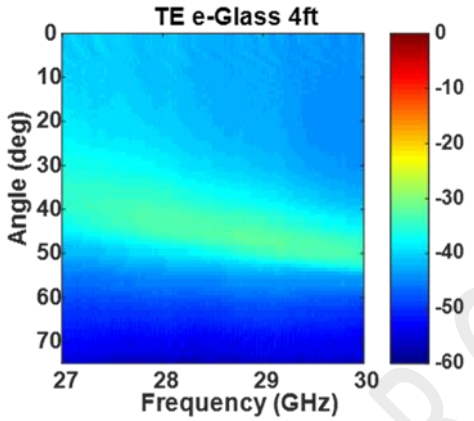

Figure 7-9 e-glass insertion loss for a TE polarized wave as a function of angle of incidence and frequency.

It shows the typical insertion loss through a 4 ft e-glass window for TE polarized light (the electric field vector is transverse to the plane of incidence). As can be seen in the figure, loss starts at about -40 dB at normal incidence (0 degrees) and gets worse as angle increases.

To summarize, penetration through Low-e / tinted glass, cement and brick wall which is common in downtown locations, is very challenging for mmWave deployments.

7.1.4.3. Reflection and Diffraction losses

Reflection impact at mmWave is similar to what it is at lower frequencies (sub-6GHz) except with some materials like Wood and plaster board as seen in the Figure 7-10 below.

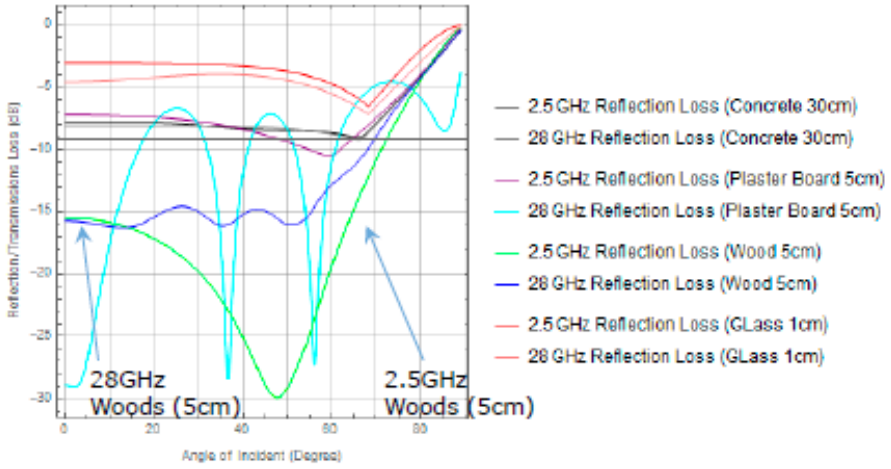

Figure 7-10 Reflection Loss: 2.5 vs 28 GHz – Softbank [25]

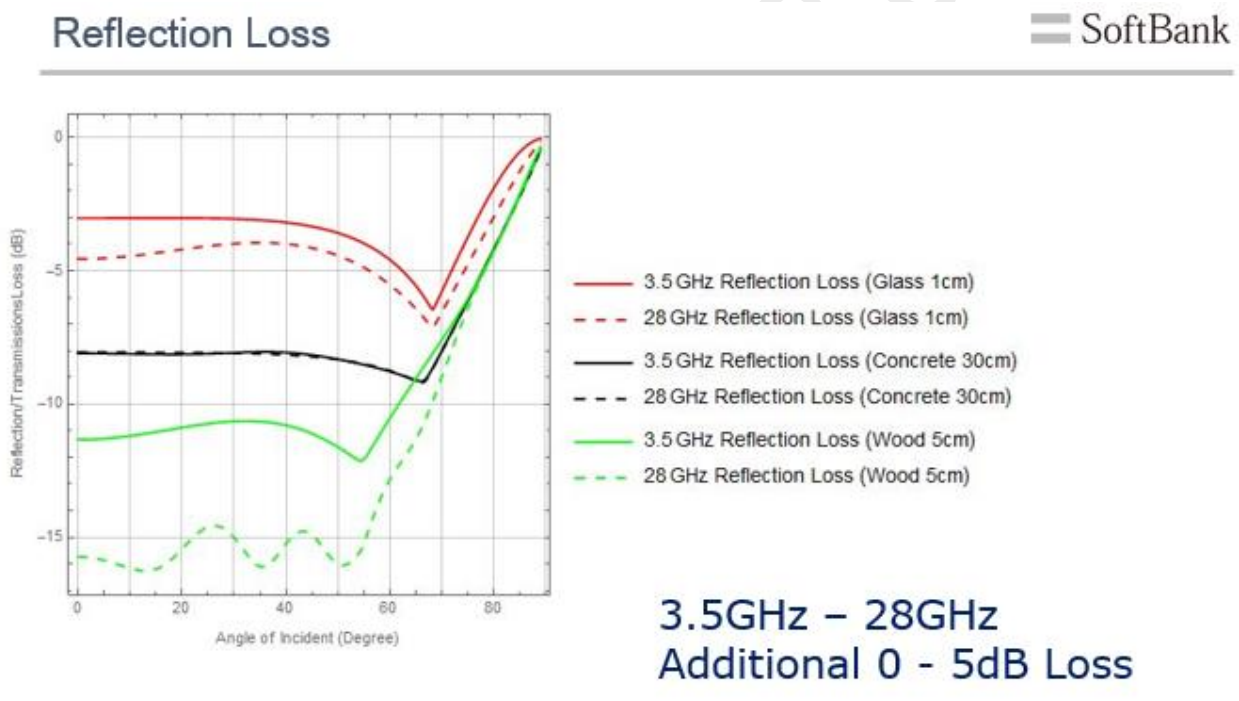

Figure 7-11 Reflection Loss: 3.5 vs 28 GHz – Softbank [26]

Softbank data in Figure 7-11 [26] shows 0-5dB reflection loss delta at 28GHz as compared to 3.5GHz. The reflection from wood show different characteristics even between 2.5GHz and 3.5GHz as seen from above 2 charts.

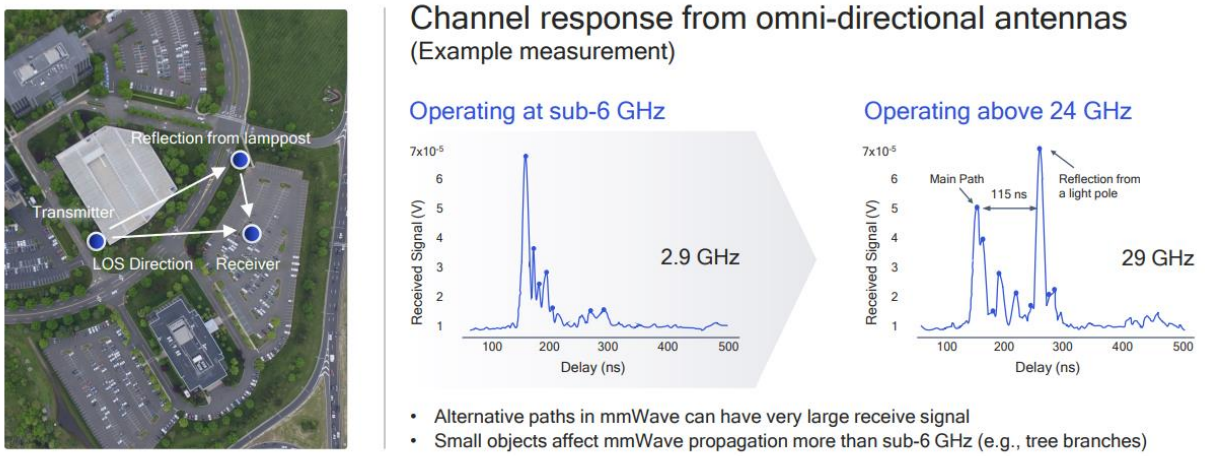

Figure 7-12 Reflection measurement – Qualcomm [27]

Based on measurements performed by QCOM (Figure 7-12), reflection could also potentially benefit mmWave multipath propagation. The reflection coefficient is a function of various reflection material properties. As seen above, the multipath signal due to reflection from a light pole is better than LOS signal. Initial real mmWave network performance evaluation by Signals Research Group [123] has shown that the Building reflections has a positive impact but unpredictable and cannot quantify easily.

Besides reflections, it is equally important to look at diffraction characteristics. As shown in the Figure 7-13 below, mmWave pose less diffraction, resulting in higher diffraction loss. The diffraction loss would be higher if the receiver is close to the wall of buildings or any other obstructions.

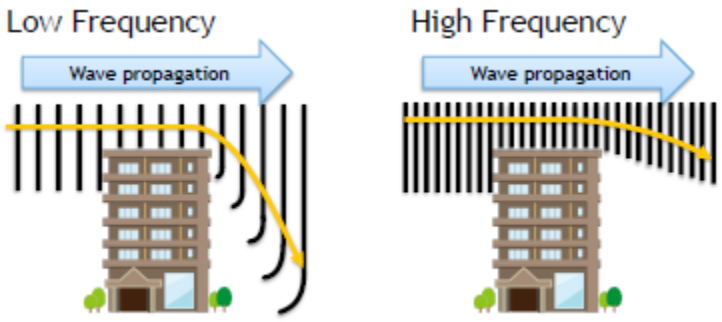

Figure 7-13 Diffraction at High Frequency [25]

Figure 7-14 Diffraction Loss – Softbank [26]

(TE: Horizontal Polarization, TM: Vertical Polarization)

Softbank data above in Figure 7-14 shows an additional loss of 15-20 dB as compared to 3.5GHz due to diffraction.

7.1.4.4. Body losses

mmWave systems are susceptible to self-blockage, which is shadowing from the user itself in the form of hand blocking and blockage from other body parts. This can cause a significant blockage of the user equipment (UE) antennas depending on the antenna position relative to the hand / body.

A study performed by Qualcomm on hand blockage measurement. The test (uncontrolled) was performed where people could walk by/past the UE at normal pedestrian speeds and at different distances (people could get as close as 0.5 m from the UE). The results are in Figure 7-15.

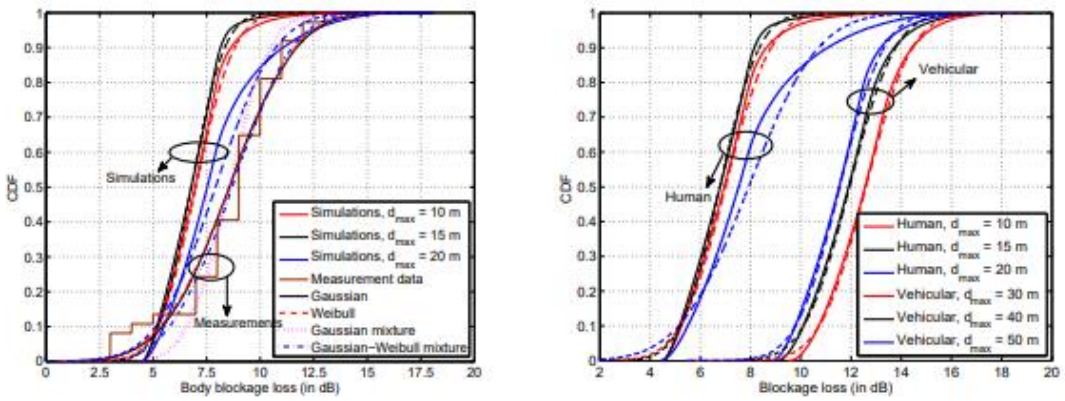

(a) CDF of human body blockage loss with simulations using the dynamic blockage methodology, measurements using the experimental prototype, and model fits to measurement data. (b) CDF of human body and vehicular blockage loss with simulations using the dynamic blockage methodology.

Figure 7-15 Body Blockage Loss – Qualcomm [45]

The results above based on measurement and statistical modelling suggests the body blockage loss of ~8dB based on 50%'ile on the CDF curve [45].

Initial real mmWave network performance evaluation by Signals Research Group [123] has also shown that quick body movements has an impact on device performance.

Another study [63] was performed by a team at Chalmers University of Technology and Royal institute of Technology in Sweden. They has used a 60MHz communication link for understanding human body shadowing. Their simulations assumed a 20X20m room with varied shadowing objects moving freely around. The results were as follows. In the Figure 7-16, the density of 1 person per $20m^2$ represented the office space and 1 person per $1.5m^2$ represented a public hotspot scenario.

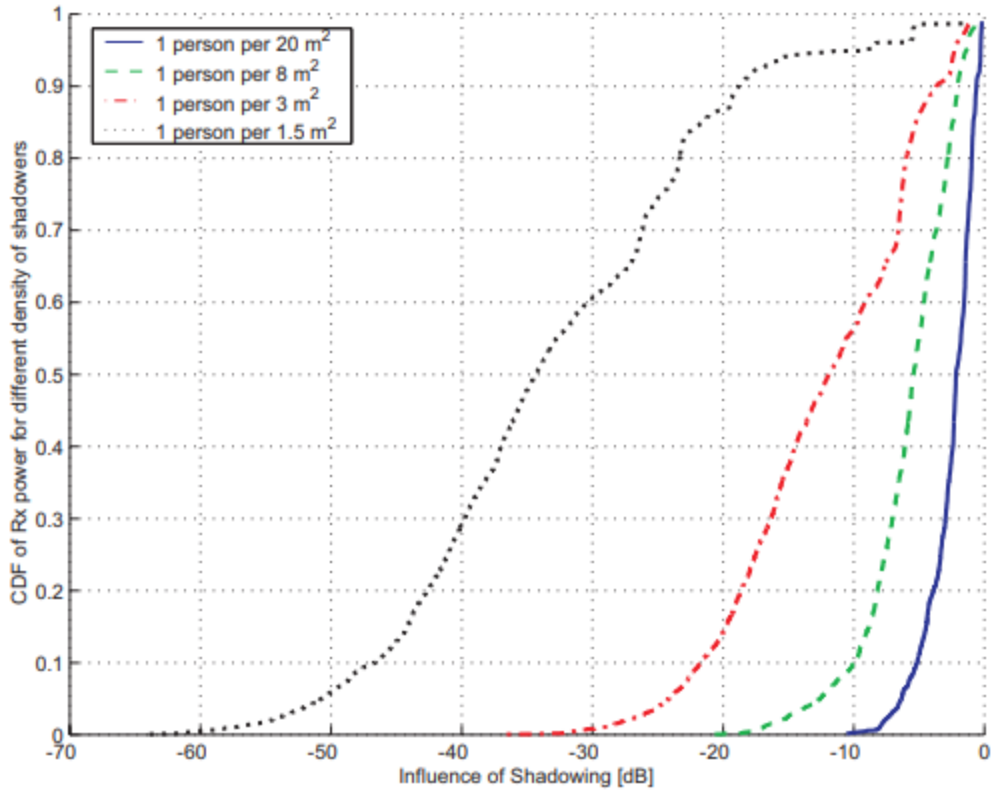

Figure 7-16 CDF of normalized received power for different shadowing densities.[63]

The Figure 7-16 represents that as more people moving inside the room, the probability of rays being attenuated increases. For more moderate/low shadowing density (1person per 20m^2), a user will experience more than 6dB power loss for 10% of the time. With shadowing density of 1person per 20m^2, the 50%'ile loss is ~35dB at 60GHz.

It should also be noted that the Impact of body blockage / loss increases as the beam becomes narrower, making it more complex to characterize. It is therefore important to further study the impact of body loss on mmWave systems accounting specific scenario.

7.1.4.5. Handheld losses

Characterizing handheld losses is critical for mobile devices, particularly for mmWave frequencies as a large area of the UE could be easily covered and blocked by hand or parts of the human body. There are various factors in determining loss such as hand grip, hand size, skin properties, beamwidth of the beam, UE antenna design, dipoles/patches and definition of measurement coverage area. As reported in one of the Qualcomm paper [28] Figure 7-17, the chart (right) below shows the impact of handblocking (in Landscape and portrait mode) using a typical UE design with multiple linear subarray units of four antenna elements (on the Top and Long edges of the device). The presence of hand in upper right chart (Landscape

mode) and in the lower right chart (Portrait mode) is indicated by dark blue areas as compared to freespace receiver gain plot in lower left.

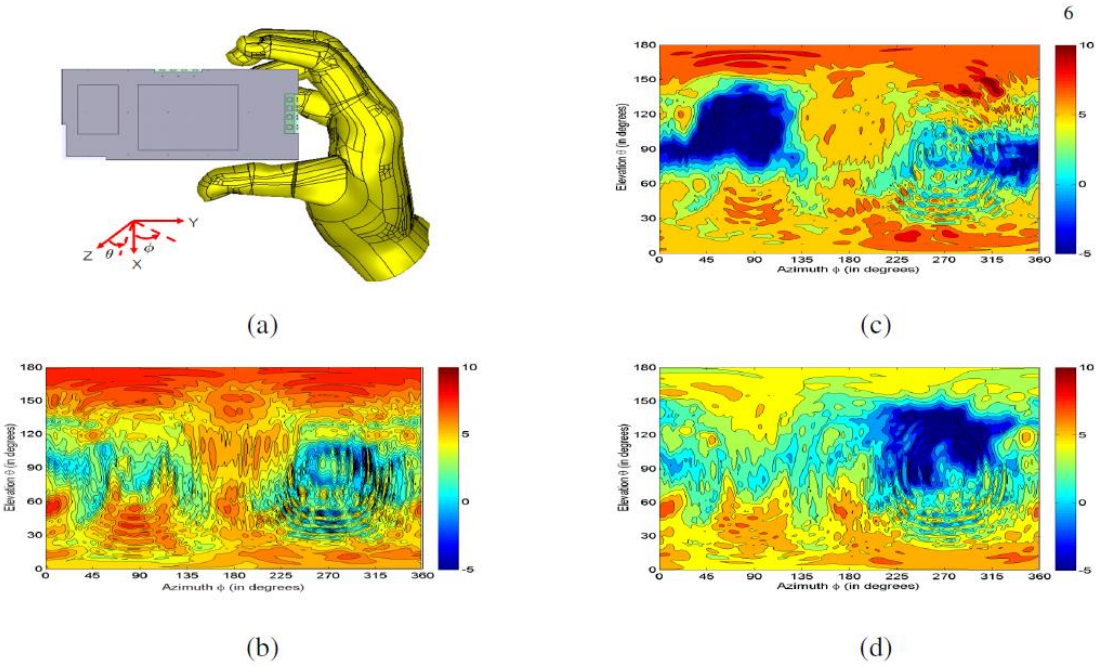

Fig. 1. (a) A typical UE design with multiple subarrays (Top and Long edges) in Landscape mode. Received gain as a function of azimuth and elevation angles for the UE design at 28 GHz in (b) Freespace mode, and with hand blocking in (c) Landscape and (d) Portrait modes.

Figure 7-17 Hand blocking impact heat map – Qualcomm [28]

3GPP models assume hand blockage loss to be 30dB flat. Qualcomm did analysis for hand blockage loss using a smartphone form factor with multiple subarrays. The results based on measurement and statistical modelling show ~15dB of loss at 50%'ile of CDF (see Figure 7-18 below).

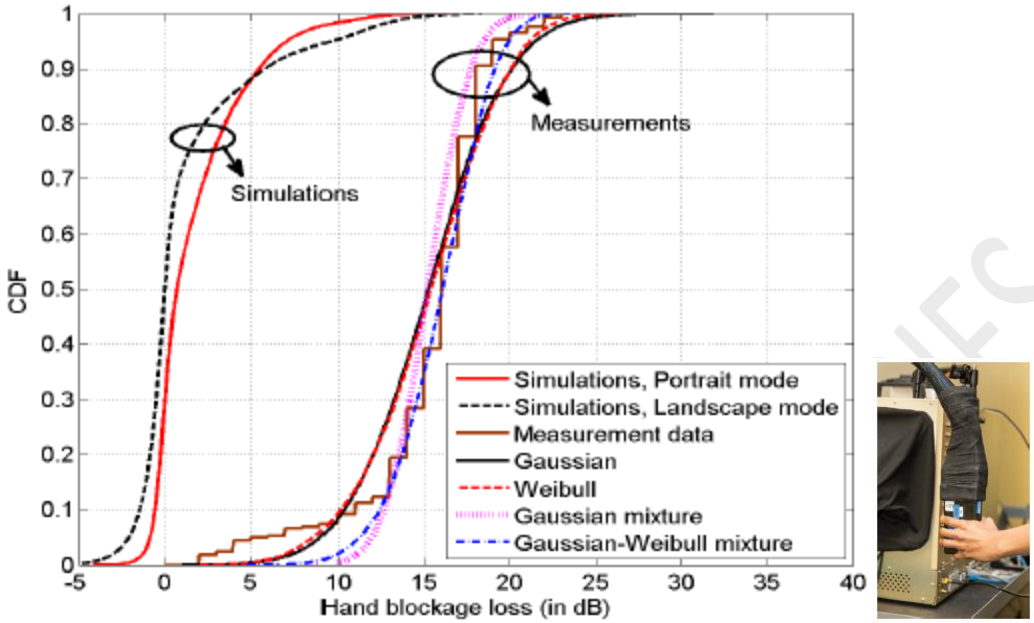

Figure 7-18 Hand blockage loss – Qualcomm [29]

Initial real mmWave network performance evaluation by Signals Research Group [123] has also shown that in an extreme case of using both hands firmly placed over the entire back of the phone would result in 20 dB drop in signal strength. Phone orientation may have an impact as well. However, normal holding of the phone may not have as big of an impact.

Furthermore, recently Qualcomm repeated similar analysis using a commercial grade device and mmWave hand phantom. The setup is shown in the Figure 7-19 below.

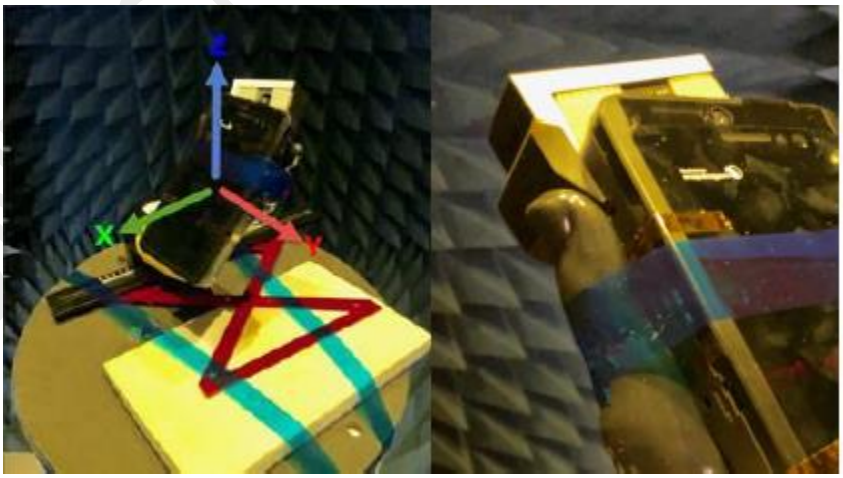

Figure 7-19 Updated hand blockage setup - Qualcomm

The test procedure involved picking an area around the peak gain and comparing radiation patterns with and without the hand blockage to analyze loss / gain. The measurements were performed for 3 different beams (0°, +30° and -30°) using 1x4 Patch (V&H) and 1x2 Dipole. The results are shown in Figure 7-20 and Figure 7-21 for Patch array and Dipole array respectively.

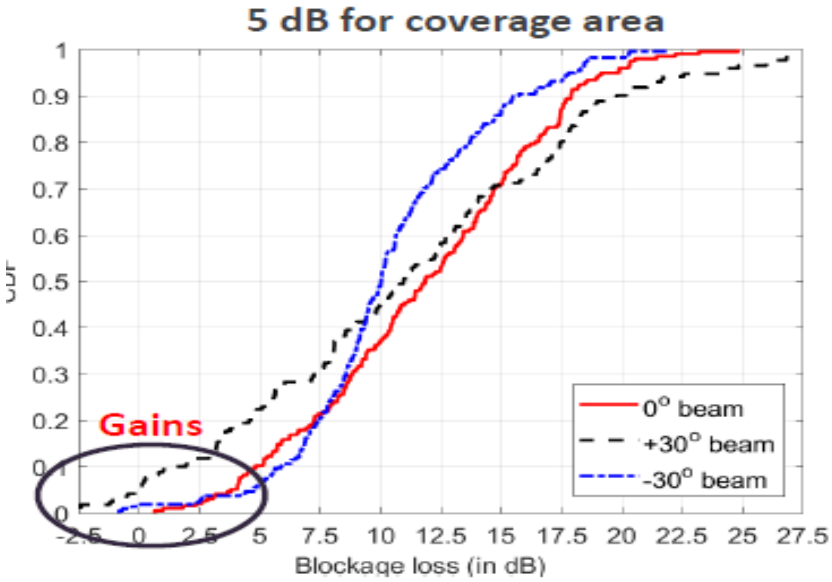

	0° beam	+30° beam	-30° beam
Median (in dB)	11.86	10.96	10.03
10th percentile (in dB)	4.87	1.61	5.88
90th percentile (in dB)	17.92	19.99	15.70
Mean and Std	(11.80, 4.96)	(11.11, 7.11)	(10.42, 4.00)

Figure 7-20 Updated Hand blockage loss - Patch Array - Qualcomm

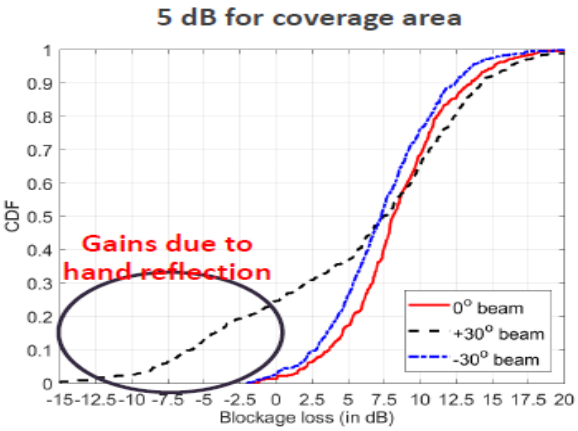

	0° beam	+30° beam	-30° beam
Median (in dB)	8.11	7.45	7.31
10th percentile (in dB)	3.70	-5.85	2.77
90th percentile (in dB)	13.56	14.32	12.46
Mean and Std	(8.41, 3.84)	(5.78, 7.80)	(7.42, 3.87)

Figure 7-21 Updated Hand blockage loss - Dipole array - Qualcomm

Depending on the antenna type and placement, the median hand blockage loss ranges between ~8 to 12dB. It should also be noted from the results that there could be instances where the hand grip help with reflections, resulting in gain in certain scenarios / directions.

More measurements from vendors are needed to fully understand its impact in real environment and real UE form factors.

7.1.4.6. mmWave Reflectors

As seem from previous subsections, there are significant impact of losses at mmWave frequencies. Besides using the beamforming capabilities to mitigate many of the losses, there is still a need for additional solutions to help improve the non-line of sight communication. One of the solution for improving mmWave propagation characteristics is the use of Reflectors.

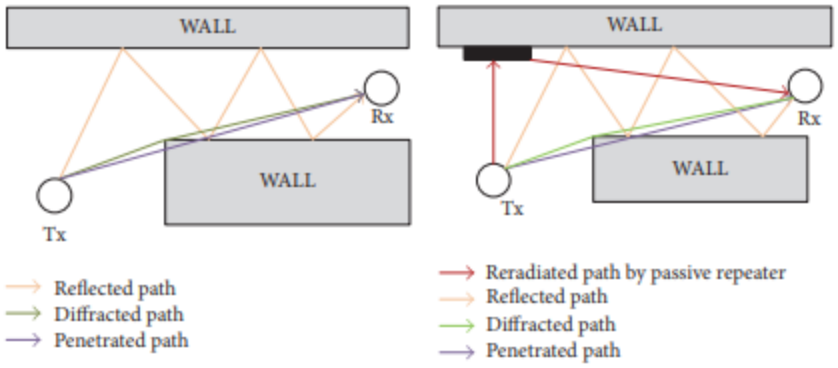

Figure 7-22 Propagation procedure with or without passive repeater [64]

In the fig above, the left part illustrates the challenges at the receiver due to diffraction / NLOS condition. Reflector on the right figure helps improving the signal reception. The reflectors are a kind of passive repeaters that include planar array of patch antenna elements to reflect the special beam direction and shape with certain tuning when primary source illuminates it. These planar reflect arrays provide benefits of deployment convenience, lower mass/weight lower cost and improved coverage/user experience. The reflector is beneficial even more in the indoor use cases where are there are many obstructed paths between transmitter and the receiver.

7.2. Simulation Results on mmWave Coverage

The previous section provided an insight on expected link loss in an ideal scenario. This sub-section would account for additional deployment gains/losses to determine overall mmWave coverage, particularly focused on dense urban areas. First, the paper summarizes some of the key coverage simulation findings published by various entities. However, most of that work assumes favorable LOS operation, optimal transmit power as well as CPE type form factors. To further understand the coverage topic, this paper analyses outdoor dense urban coverage offered by mmWaves and compares it to mid-band sub-6GHz bands for two top tier US markets. Both DL and UL coverages are analyzed as well as benefits of EN_DC between mmWave and sub-6GHz mid-bands are compared.

7.2.1. Third Party mmWave Coverage Analysis

Below (Figure 7-23) are the simulation results from Qualcomm [27]. They had calibrated their simulation tool based on Qualcomm's channel measurements and testing. The simulations were run for different environments / different cities around the world based on actual site locations, provided by the operators. The mmWave BSs were co-sited with these actual 2G/3G/4G BSs to determine the mmWave coverage. The results are as follows:

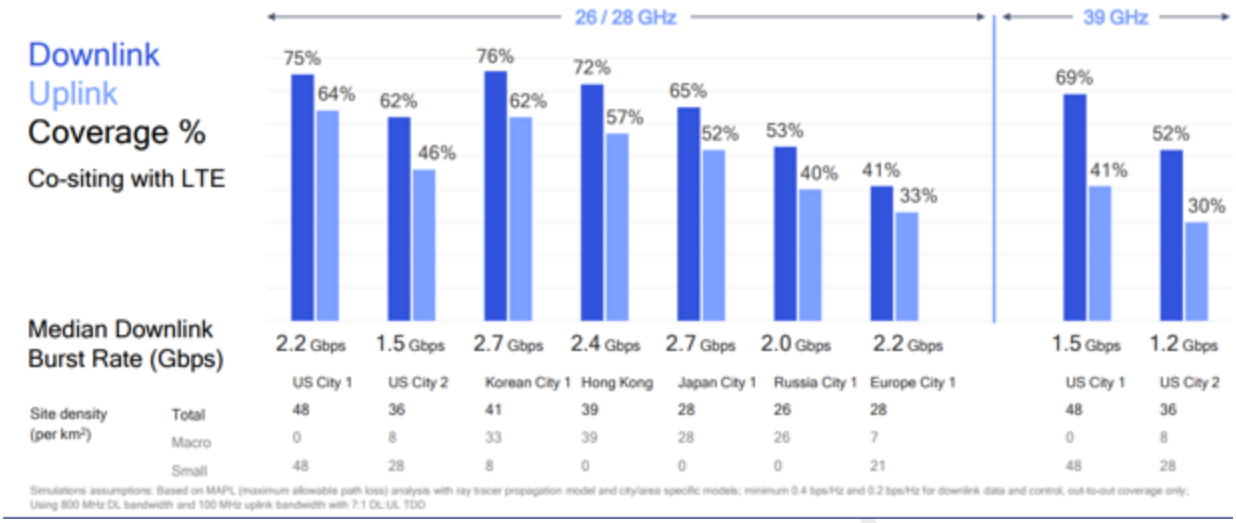

Figure 7-23 mmWave Coverage, co-siting with LTE – Qualcomm [27]

In some places like US City 1 where there are lot of small cells, mmWave can provide ~75% of blanket DL coverage. While in some other cities like Europe city 1, mmWave can provide ~41% DL coverage since the original sites deployments may be sparse. Such cities may require additional sites for blanket coverage or concentrate on hotspot deployments.

KT had also performed similar coverage analysis for the 2018 Winter Olympics (Figure 7-24), where they had co-sited mmWave with the existing LTE cells. Based on the data [30], mmWave deployment for outdoor coverage required 4.6 times more sites as compared to sub-6GHz 4G deployment.

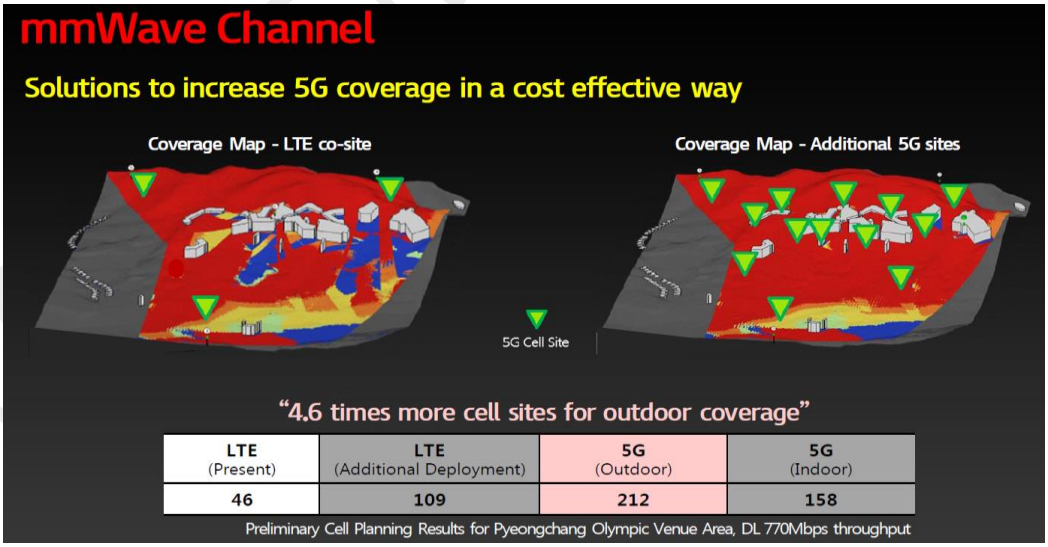

Figure 7-24 mmWave Coverage – KT [30]

Ericsson had performed comparative study (Figure 7-25 below) between mmWave and sub-6GHz link budget. The chart shows throughput vs pathloss. The sub-6GHz assumed regular macro deployment while mmWave assumed to be dense and opportunity based deployment. As seen below, the mmWave boost system capacity to nearly double in the cell center condition due to its wider channel BW.

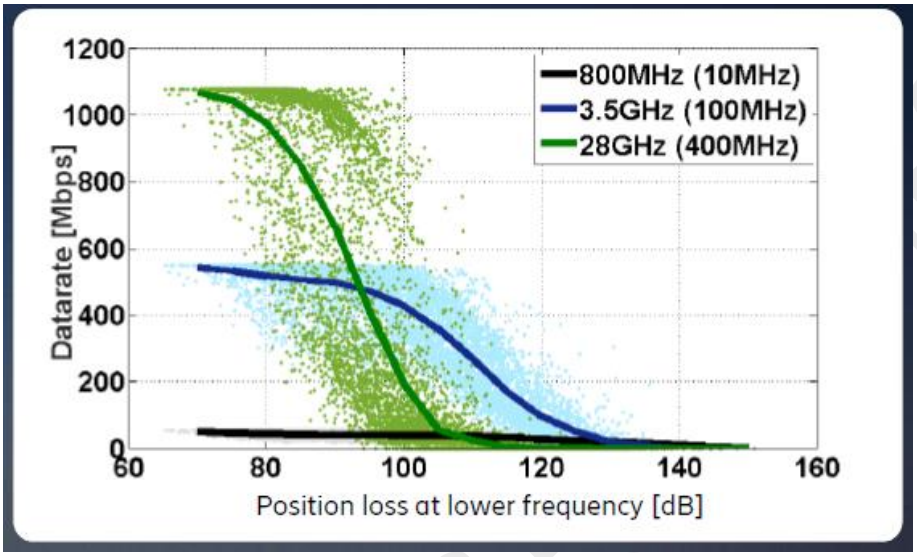

Figure 7-25 Throughput vs Pathloss comparison - Ericsson

From a field testing perspective, PCTEL had performed measurements on mmWave frequency (28GHz) using their scanner. The Table 7-5 below depicts the free space path loss of a signal source as collected. The source was radiating at a 17 dBm power level and was around 15ft (4.6 m) in height. Measurements done at different distance shows the drop in power level in line of sight (LOS) conditions.

LOS Propagation profile ~28GHz mmWave spectrum

Transmit Power	Received power @5 meters from site	Received power @10 meters from site	Received power @20 meters from site	Received power @50 meters from site	Received power @100 meters from site
17 dBm	-41 dBm	-51 dBm	-58 dBm	-67 dBm	-80 dBm

Table 7-5 Received Power measurement

While the data measured above was only for up to 100 meters using a scanning receiver on the receiving side, it provides a good field indication of the signal level drop with respect to distance as small as 100 meters for line of sight propagation. The cellular industry is accustomed to designing macro sites for cell radius of distances up to 5 kms for LTE and introduction of these mmWave frequency bands creates a paradigm shift.

As discussed in section 7.1.4, the phenomena of reflection, refraction and diffraction encountered by the transmitted signal through various structures, depending on the building material, also creates a huge

complexity with respect to designing mobility for 5G deployments in mmWave spectrum. In the data illustrated in Figure 7-26 and Figure 7-27 below, which was collected in the largest US metro urban canyon, moving only two blocks away from the signal source results in a signal loss of approximately 20 dBm due to the shadowing of a glass building. This also resulted in the loss of signal in one direction but simultaneouly, the signal level and quality level measured in the opposite direction is high and sustainable for up to eight city blocks. This mechanism of high absoprtion loss with buildings made of low emission glass, phenomenon of reflections, refraction and diffraction from various other buildings complicates the design of 5G mobile networks. Operators will have to take into account the seasonality and topology to a higher degree vs sub-6 GHz networks for their propogation models and will be need to collect real life data to tune their models using highly calibrated receiving equipment to ensure that they are able to design and optimize the network to meet their 5G rollout goals.

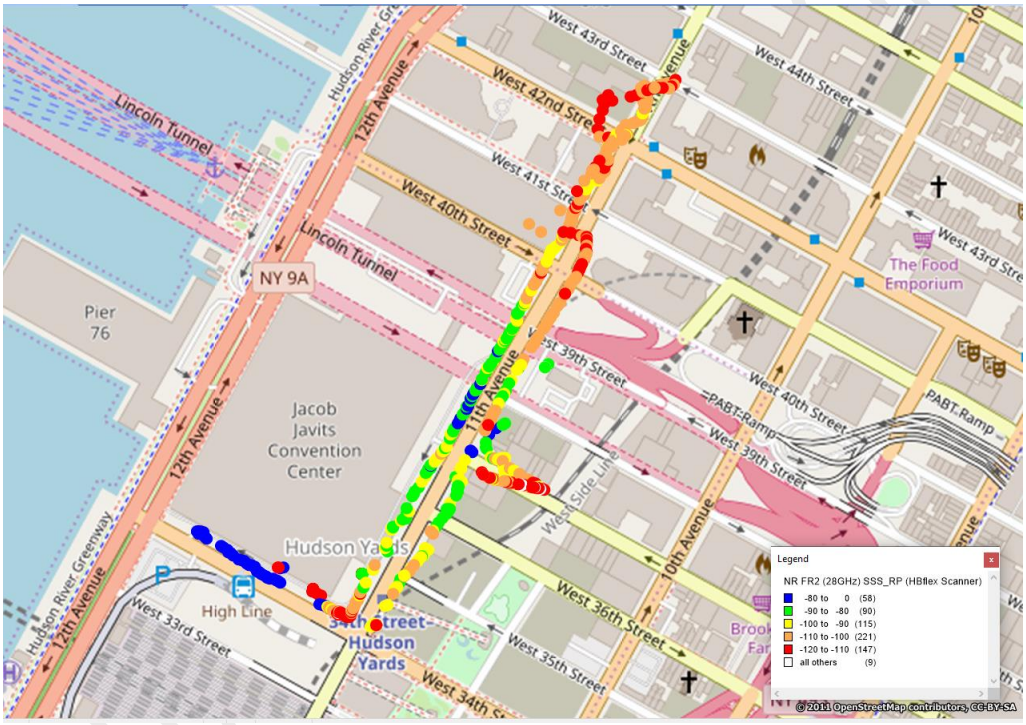

Figure 7-26 Strongest Secondary Sync Signal Received Power (SSS RP)

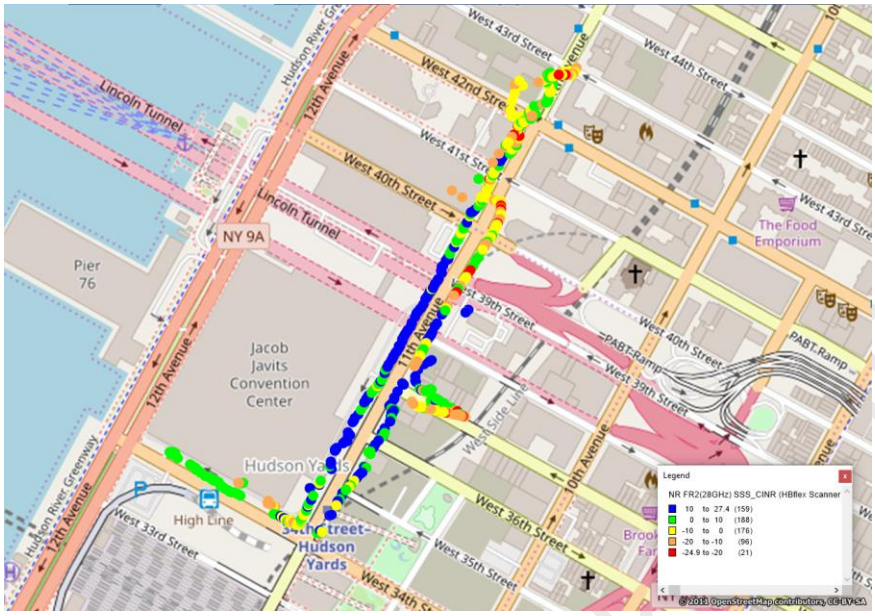

Figure 7-27 Strongest Secondary Sync Signal Carrier to Noise Ratio (CINR)

Most simulation work on mm-wave network analysis are usually simplified and does not account for real world / practical use cases, which can lead to significant deviation in performance. This whitepaper has used the inputs from various vendors and generated additional results accounting for practical handset use cases.

7.2.2. Dense Urban / Metro Tier 1 Market Coverage Analysis

The Simulation test cases generated specifically for this whitepaper address both coverage and capacity scenarios for two major tier 1 downtown areas.

7.2.2.1. Market 1 Analysis

For coverage analysis of the first market, Atoll was used to generate simulation results. These simulations include a test network of 190 sites with three sectors (Macro + Small cells) in a 6.6 Sq. Km. area of a dense urban US market. The mmWave sites were co-sited with Sub-6GHz at an ISD of 300m. The test simulation methodology does not account for UE mobility and the results are based on outdoor stationary environment. The results illustrated for Market 1 are at Cell level. The simulation assumptions are discussed in the following subsections.

7.2.2.1.1 gNB parameter settings

- The mmWave sites are assumed to have 400 MHz channel at 28 GHz.
- The propagation model was based on 3GPP 38.900 and used TDD DL/UL frame configuration 2 alike slot format.
- The location and height of mmWave sites was assumed to be same as sub-6GHz sites.

- The gNB supported MU-MIMO of max 2 layers in Downlink and no MU-MIMO / SU-MIMO on UL. The max MCS on DL and UL was 256QAM and 64QAM respectively.
- The system was configured with 50% loading.

7.2.2.1.2 UE parameter settings

Two UE configurations were used for the purpose of these simulation;

1. 1T/1R module with a max EiRP of 23 dBm (Ideal case)

2. 1T/1R module with a 50%'ile EiRP of 11.5 dBm (Practical case).

Configuration 2 (i.e. 50% percentile of UT EiRP) provides a more accurate representation on mobile networks performance when compared to UE max EiRP case, as it is very unlikely the smartphones will line-of sight with the mmWave gNB all the time. When line-of-sight is not possible, gNB/UE will rely on reflected signals to establish a link, and that link will be much less than optimal. The UE noise figure was assumed to be 7dB.

7.2.2.1.3 Standalone mmWave results – Market 1

The results of the simulations are as follows:

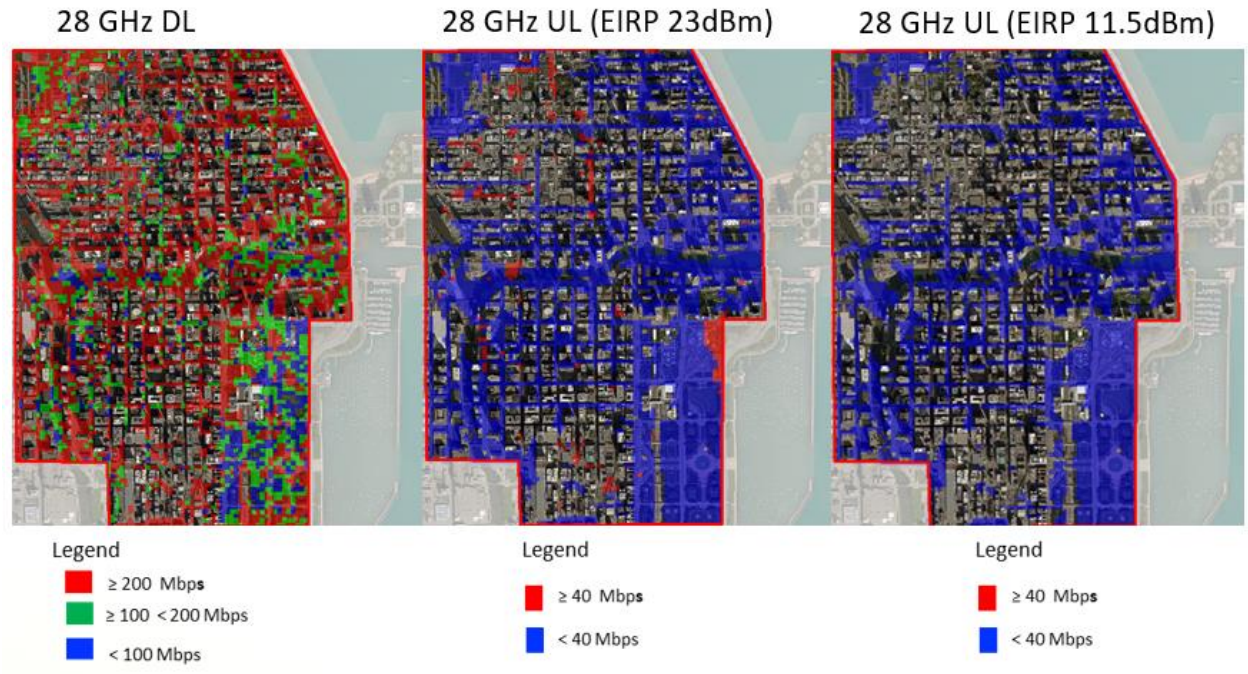

Figure 7-28 mmWave Coverage map

The coverage plot is shown in Figure 7-28. As it can be seen, coverage hole exists with mmWave coverage due to co-siting the cells with sub-6GHz outdoors, which is expected.

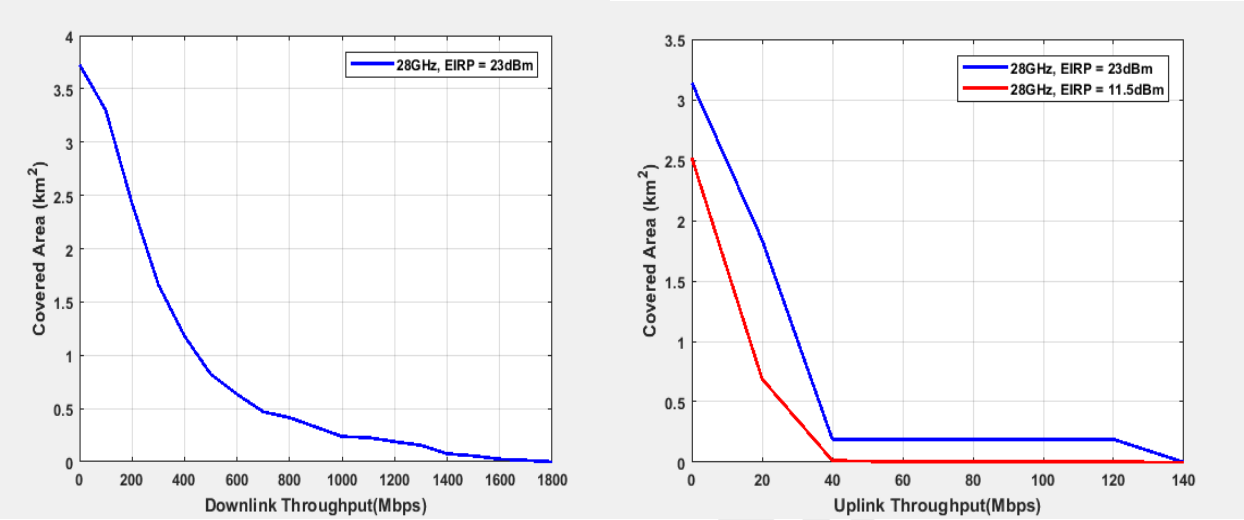

Figure 7-29 mmWave Throughput vs Coverage chart

The left chart above illustrates the DL mmWave coverage and cell throughput. As seen from the chart, mmWave DL covers 3.7 Sq. Km. of 6.6 Sq. Km. total area which is ~44% smaller coverage area. The max DL sector throughput was ~1.8Gbps outdoors. The chart on the right shows cell throughput vs coverage for the UL scenarios (11.5dBm EiRP and 23dBm EiRP). As it can be seen, using the ideal UE EiRP case would result in a coverage total of 3.1 Sq Km area (47% of total coverage area) while the more practical scenario of 11.5dBm UE EiRP would limit the total coverage area to 2.5 Sq Km (38% of total coverage area). This would result in UL limited system with coverage delta of 32% between downlink and uplink.

From the capacity/throughput perspective, below are the sector throughput CDF.

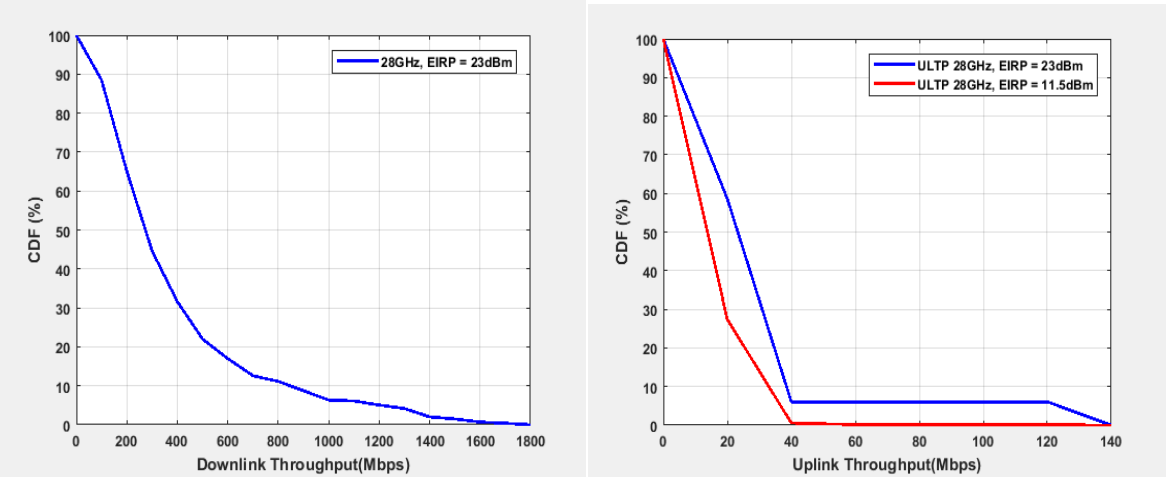

Figure 7-30 mmWave Throughput CDFs

At 50%-ile, the DL sector throughput is ~275Mbps, while the peak DL sector throughput in this case is 1.8Gbps. The 50%'ile UL sector throughput is ~13Mbps for realistic EIRP scenario and the best case UE EIRP scenario, the UL sector throughput was ~22Mbps@50%'ile. The peak UL throughput noted was ~140Mbps.

7.2.2.1.4 Comparative Coverage between mmWave and sub-6GHz mid band

This sub-section will now dive into mmWave coverage in comparison with Sub-6GHz mid band. The mmWave assumptions are the same as in the previous sub-section (i.e. 400MHz channel bandwidth, etc). For Sub-6GHz, the simulation assumed 100MHz channel BW, TDD FC2 alike slot configuration, 256QAM DL MCS, 64QAM UL MCS, 8 Layer DL MU-MIMO. The Sub-6GHz UE max EiRP was assumed to be 19.3dBm (50%'ile, number based on real network measurements). The UE supported 1Tx and 2Rx for Sub-6GHz channel. It should be mentioned that most of mid-band sub-6GHz smartphone solutions support 4 antennas on UE side nowadays. However, that scenario was not analyzed as part of current work.

The Figure 7-31 below shows the coverage heat map of mmWave and Sub-6GHz DL and UL.

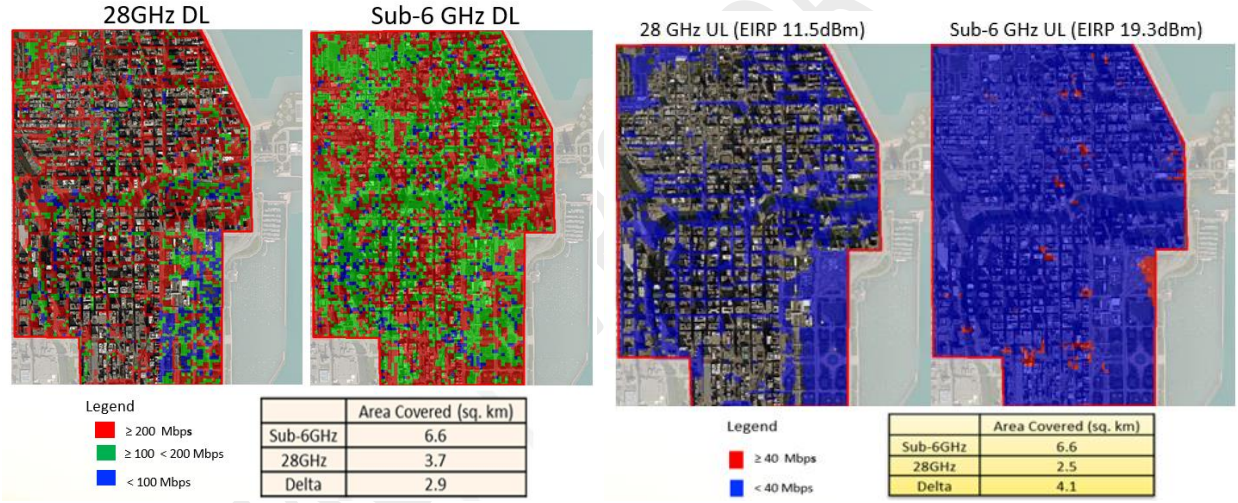

Figure 7-31 28GHz vs Sub-6 GHz coverage plot

As it can be seen, Sub-6GHz maps shows full blanket outdoor (100%) coverage, while mmWave DL coverage is ~44% lower than Sub-6GHz. The UL using 50%'ile EiRP for mmWave and Sub-6GHz shows that mmWave UL coverage is ~62% lower. Another view of throughput vs. coverage area is shown below (Figure 7-32) in the chart, illustrating the mmWave performance vs Sub-6GHz. The mmWave could yield higher throughput on DL/UL when compared to sub-6GHz mid-band only for in a coverage area of less than 2 Sq Km (i.e. compared to a total of 3.7 Sq. Km that mmWave covers).

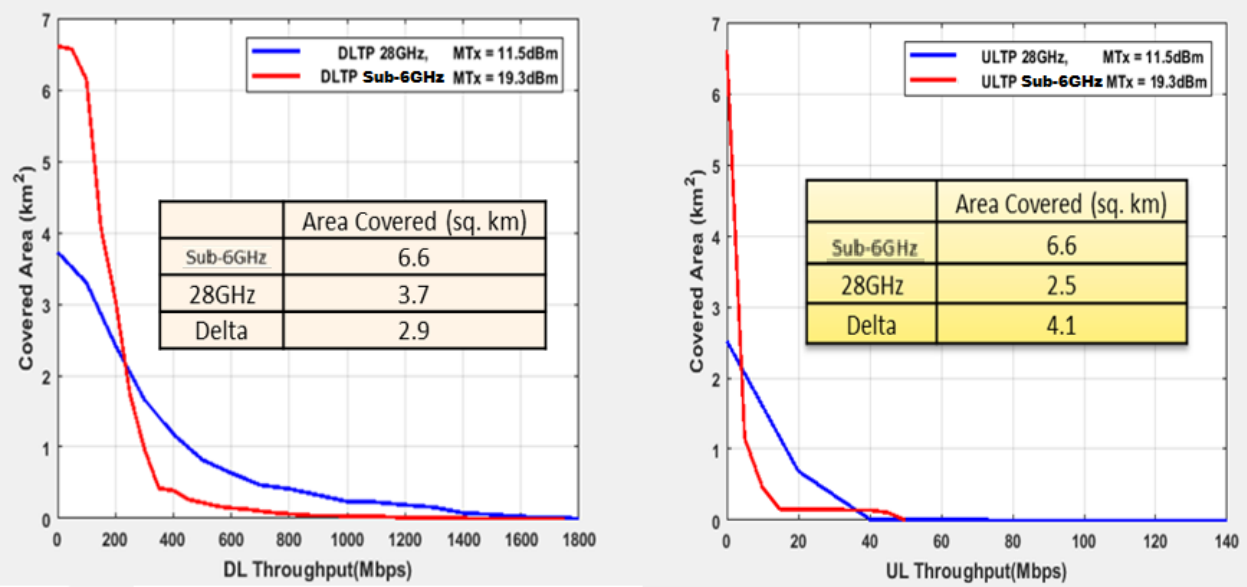

Figure 7-32 mmWave vs Sub-6GHz Throughput / Coverage plot

Below chart in Figure 7-33 illustrates the throughput CDF comparison between Sub-6GHz and mmWave. Based on mmWave UL with 50%'ile EIRP, a standalone mmWave network would require ~-3X sites to match the coverage of sub-6GHz. The DL throughput delta at 50%-ile is ~100 Mbps, while the UL delta at 50%-ile is ~15 Mbps. The peak DL throughput is similar but mmWave could provide 1.8X higher peak UL throughput.

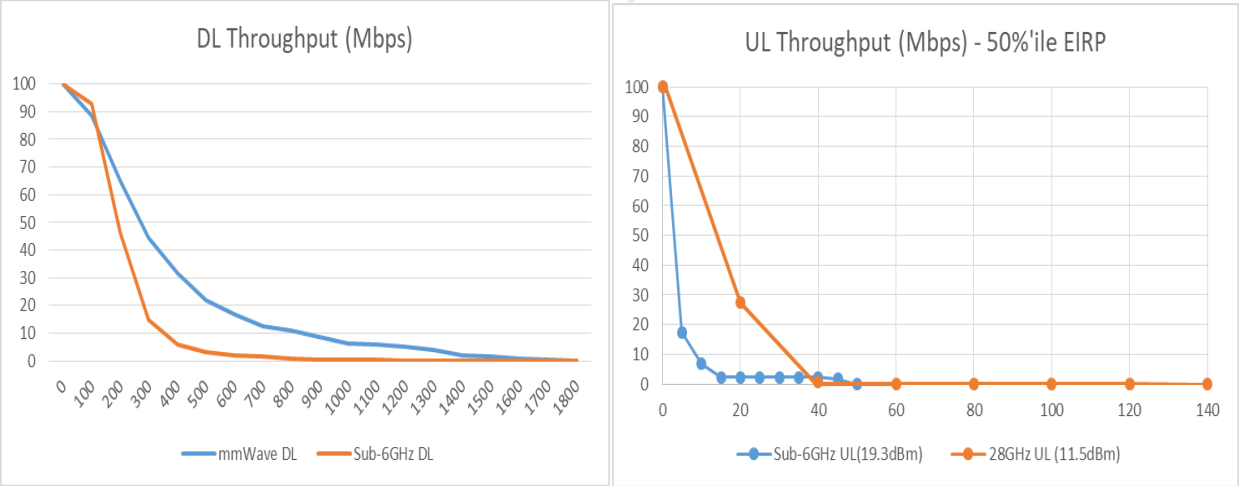

Figure 7-33 DL/UL Throughput CDF

However, it should be noted that the simulations assume peak MCS of 256QAM in DL and 64QAM in UL for mmWave, which may potentially be challenging to achieve with most current systems. Also, it should be noted that the coverage area of Sub-6GHz is higher and hence the overall CDF throughput values are lower when compared to mmWave coverage area.

7.2.2.2. Market 2 Analysis

For coverage analysis of the second market, Remcom used Wireless InSite®'s full three-dimensional ray-tracing model, X3D, to evaluate SINR and throughput over an area of approximately 1.3 square kilometers in downtown Boston. The simulations included analysis at 28 GHz as well as a mid-band sub-6 GHz frequency, using gNB sites provided by a tier 1 U.S. wireless carrier. The gNB inter-site distances (ISD) varied from less than 300 meters to more than 500 meters, with a mean of approximately 435 meters. The locations of the sites were based on a sub-6GHz deployment and the 28GHz gNBs were co-sited at the same locations. This allowed for a direct comparison between the frequency bands in order to estimate the reduction in coverage and the resultant increase in the gNB sites that would be required to cover an area at millimeter wave bands.

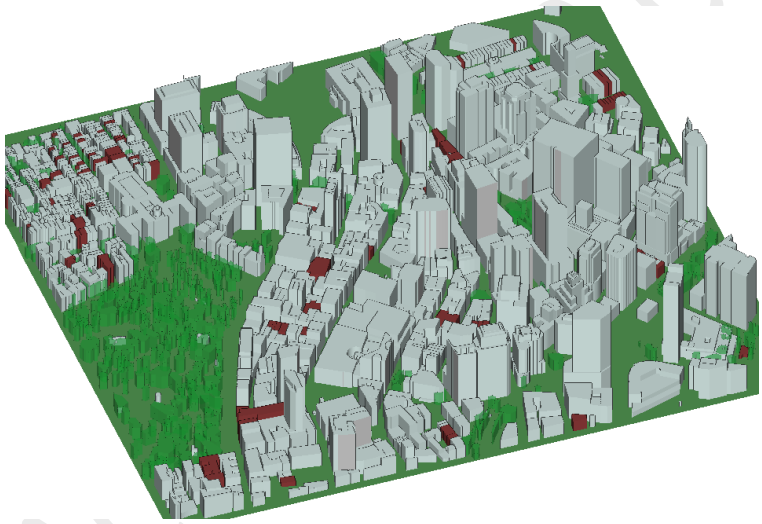

Figure 7-34-Coverage Analysis of Dense Urban Scene in Downtown Boston

The focus of this study was on enhanced mobile broadband (eMBB) in a dense urban setting. Because millimeter waves are not expected to penetrate into structures very effectively, the comparison was limited to outdoor locations within the scene. The simulation methodology did not account for UE mobility, which though important for both bands, would be expected to have a more negative impact on the higher frequency. As described earlier in this paper, key elements of the scenario that affect signal propagation are multipath and shadowing from structures, losses from penetration through trees, and differences in the path loss and atmospheric attenuation, all of which result in higher losses at millimeter waves than at the sub-6 GHz frequency. To compensate for these losses, the 28 GHz base stations were simulated with MIMO antennas that had larger numbers of elements and a wider bandwidth. Coverage analysis results were then compared to those for a sub-6GHz deployment in order to determine basic trends in the additional required base stations that would be needed to achieve coverage at 28GHz.

7.2.2.2.1. gNB Parameter Settings

The gNB sites were defined using the specifications in Table 7-6 below, using assumptions provided by a Tier 1 U.S. carrier based on current data and expectations for 5G New Radio. For both 28 GHz and sub-6 GHz, the transmitter power was defined as 43 dBm for consistency in the comparison. Both included large MIMO antenna arrays, with the 28 GHz sites defined to have 16x16 arrays with cross-polarized patch antennas (512 total elements), and the sub-6 GHz sites defined to have 8x8 arrays with cross-polarized patch antennas (128 total elements). These arrays were physically laid out in the simulation using patch antennas spaced approximately half a wavelength apart as shown in Figure 7-35, with ±45-degree polarized components at each location. Including effective gain of the antennas and the array, this resulted in peak EIRP of 73 dBm and 67 dBm, respectively. The 28 GHz sites also had a larger bandwidth of 400MHz as compared to 100MHz at the sub-6GHz frequency.

Specification	**28 GHz**	**Mid-Band Sub-6GHz**
Locations	*Sites provided by Tier 1 U.S. Wireless Carrier	
Array Configuration	16x16, cross-pol (512 total elements)	8x8, cross-pol (128 total elements)
Polarization	Cross-Pol Beams (±45°)	
Transmit Power (dBm)	43 dBm	
Element Gain (dB)	Approx. 6dB (patch array)	
Peak Array Gain (dB)	30 dBi	24 dBi
Peak EIRP (dBm)	73 dBm (per polarization)	67 dBm (per polarization)
Noise Figure (uplink)	5dB	5dB
SCS	120 kHz	30 kHz
DL/UL Slots	4:1	4:1
System Bandwidth	400 MHz	100 MHz

Table 7-6 Specifications for gNB

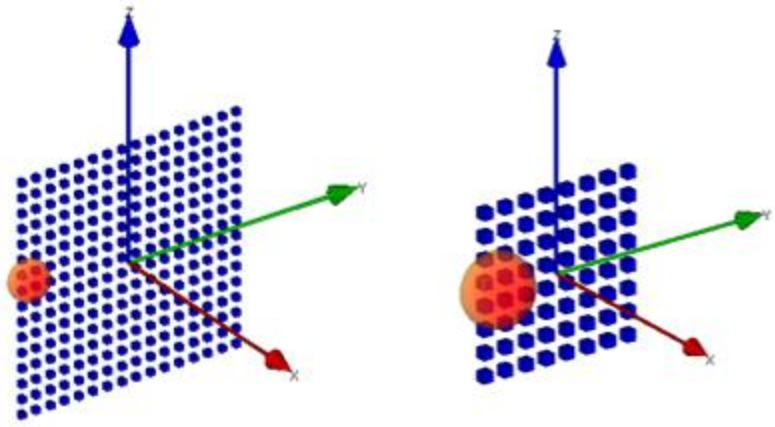

Figure 7-35 MIMO Arrays for 28GHz (left) and Sub-6GHz (right)

7.2.2.2.2. UE Settings (for Smartphones)

The user equipment (UE) for the simulations were defined according to specifications provided in Table 7-7. UE's were placed uniformly throughout the scene at an assumed height of 1.5 meters above the ground. For uplink simulations, two EIRP levels were evaluated:

- A maximum power case (ideal)
- A 50th percentile case (conservative)

Key differences for the two frequency bands included a slightly higher noise figure for downlink at 28 GHz, as well as lower EIRP for the full and 50th percentile uplink EIRP levels.

Specification	**28 GHz**	**Mid-Band Sub-6GHz**
Array Configuration	2 isotropic xpol beams (represents 4 elements)	Isotropic cross-pol antennas (2 elements)
Polarization	Cross-Pol (±45°)	Cross-Pol (±45°)
EIRP: Max (dBm)	23 dBm	26 dBm
EIRP: 50% (dBm)	11.5 dBm	19.3 dBm
Noise Figure (downlink)	10dB	8dB

Table 7-7 Specification for UE

7.2.2.2.3. MIMO Analysis

For both frequencies, beamforming was used to maximize the signal-to-noise ratio for each uplink and downlink channel. Both the gNB's and the UE's employed Maximum Ratio Transmission (MRT) at the transmitter and Maximal Ratio Combining (MRC) at the receiver for both uplink and downlink. These are adaptive MIMO beamforming and combining techniques, respectively, that provide an optimal channel

for a single layer, assuming perfect channel state information. In the analysis, simulations used the complex channel matrices between each transmitting and receiving MIMO antenna element to apply these techniques to predict both the received power as well as interference from neighboring base stations. These calculations provided an ideal estimate for a single stream. Basic assumptions were then applied to include throughput from additional layers, as described in the next section.

7.2.2.2.4. Throughput Analysis

Throughput was estimated from the signal-to-interference-plus-noise ratios (SINR) calculated from the ray-tracing simulations. For the downlink simulations, interference from neighboring base stations were included in the analysis, whereas for uplink only noise was included, assuming negligible interference between UEs. Throughput estimates included the following assumptions:

- TDD with 4:1 ratio of downlink to uplink
- Upper limits on MCS for uplink and downlink:
    - For sub-6GHz, downlink MCS up to 256 QAM and uplink MCS up to 64 QAM
    - For 28 GHz, downlink MCS up to 64 QAM and uplink MCS up to 16 QAM
- Limits for multiple layers:
    - For sub-6 GHz, up to 4 layers for downlink, and up to 2 layers for the uplink
    - For 28 GHz, up to 2 layers for downlink, and only a single layer for the uplink

For uplink and downlink at each frequency, SINR thresholds were established for switching to increasingly higher modulation and coding schemes (MCS). These thresholds were extended to allow additional layers by assuming that for a given MCS, a second layer could be added if SINR were 6 dB above the single-layer threshold, and four layers (sub-6 GHz downlink only) could be included if SINR were 12 dB above the single-layer threshold. This logic was then merged in across all of the supported MCS's for uplink and downlink in the two frequency bands. The final set of thresholds was reviewed with a tier 1 wireless carrier for consistency with observations in the field. This approach did not take into account multipath channel conditions for the additional layers, so represented an ideal estimate for throughput, but served the purpose of allowing a comparison between the FR1 and FR2 coverage results.

Once the MCS was established for the channel between the base station and each UE location, the throughput was estimated using the equation for approximate data rate provided in 3GPP TS 38.306 v15.5.0 [125], *User Equipment (UE) radio access capabilities (Release 15)*. For sub-6 GHz a bandwidth of 100 MHz was assumed, and for 28 GHz, a bandwidth of 400 MHz was assumed. Throughput calculations did not explicitly include mobility; the SINR thresholds used to determine MCS were based on estimates assuming stationary UE's or slowly-moving pedestrians.

7.2.2.2.5. Propagation Environment

The effects of the propagation environment on coverage are affected by the frequency in a number of ways. Some of the critical effects fall into the following categories:

- Path loss, which increases with frequency and also includes some absorption effects
- Reflections, scattering, and shadowing from structures and terrain

- Penetration through foliage

Most of these effects tend to reduce the signal more significantly at millimeter waves than at sub-6 GHz bands. The Wireless InSite® ray-tracing model used in the simulations incorporated all of these effects.

Material properties impact multipath and shadowing interactions with buildings, terrain, and foliage within the scene. The Wireless InSite® downtown Boston scenario used in this study included three different building materials and some properties for terrain and foliage. Some of the high-level specifications for these material properties are given in Table 7-8. Material properties for terrain and buildings were based on frequency-specific properties described by ITU-R recommendations [126] and [127]. Foliage loss was modeled using the foliage penetration loss model developed by Weissberger [128].

Feature	Material Type	Mid-band Sub-6 GHz		28 GHz	
		Relative Permittivity	Conductivity (S/m)	Relative Permittivity	Conductivity (S/m)
Terrain	Medium dry earth	13.7	0.1458	5.7	6.5
Buildings	Brick	4.44	0.001	4.44	0.001
	Concrete	5.32	0.06622	5.31	0.4838
	Glass	6.27	0.01221	6.27	0.2287
Foliage	Weissberger Foliage Penetration Loss Model	(Not Applicable)			

Table 7-8 Material Properties for Terrain, Structures & Foliage

7.2.2.2.6. Comparative Coverage between mmWave and sub-6GHz

Based on the parameter settings above, these sections analyze the coverage simulation results for DL and UL using mmWave and Sub-6GHz frequencies.

7.2.2.2.6.1. Downlink Analysis

The results of downlink simulations are given in Figure 7-36 and Figure 7-37, below. Plots on the left show the SINR, while those on the right show the throughput, first for the sub-6GHz band, and then for the 28 GHz band. As discussed earlier, the locations of the sites were provided by a tier 1 U.S. carrier and represent a sub-6 GHz deployment. A portion in the Northwest corner of the scene was omitted from coverage statistics, because it is served by a site outside of the area. In order to get a direct comparison between the two frequency bands, the 28GHz gNB's were co-sited with the sub-6GHz sites. As expected, there is a drop in the coverage due to the additional path loss and other factors described earlier in this whitepaper.

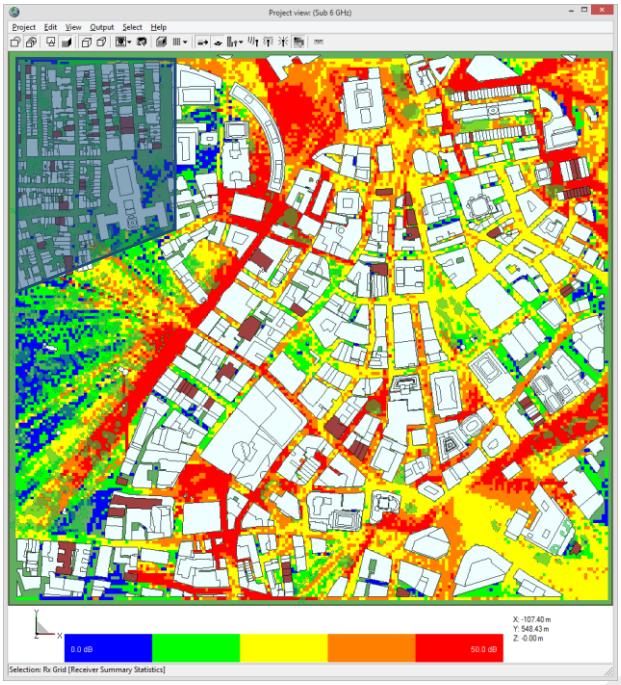

(a) Sub-6 GHz SINR

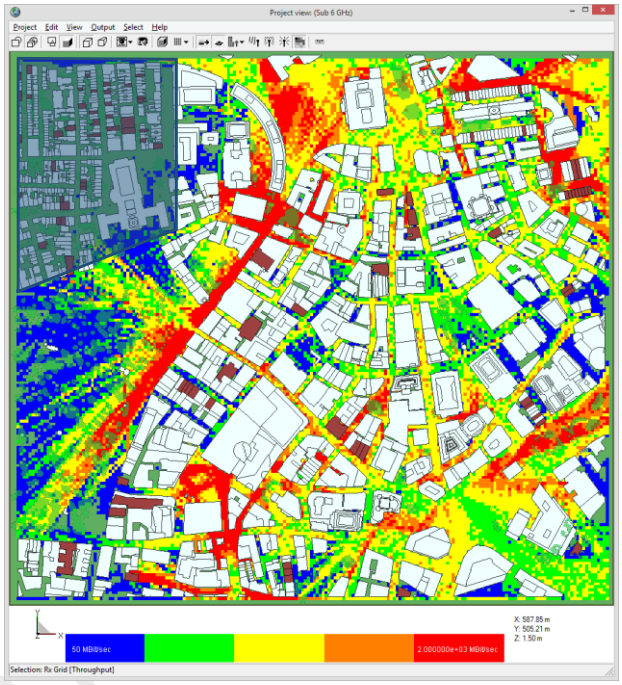

(b) Sub-6 GHz Throughput Coverage

Figure 7-36 Comparing SINR and Peak Throughput for Downlink at Sub-6 GHz

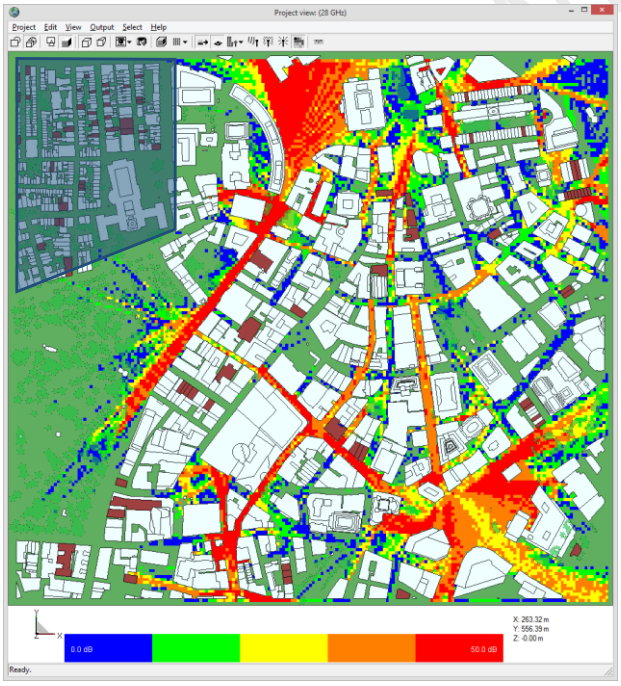

(c) 28 GHz SINR

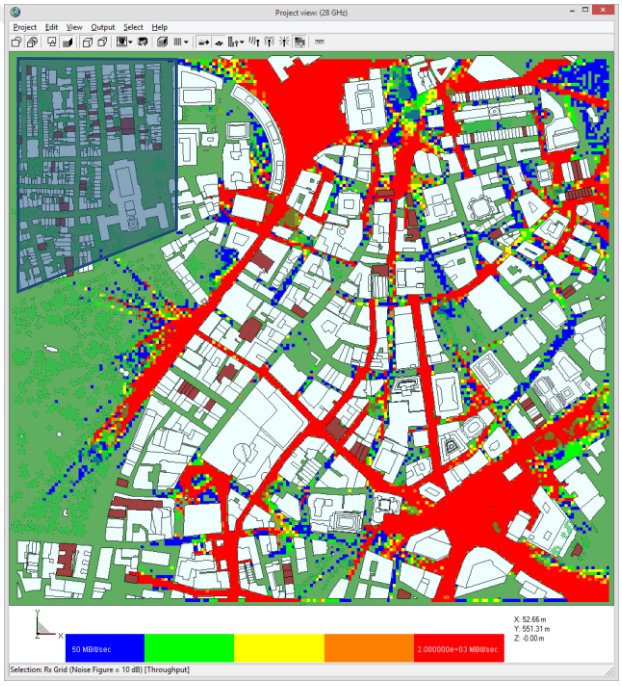

(d) 28 GHz Throughput Coverage

Figure 7-37: Comparing SINR and Peak Throughput for Downlink at 28 GHz

Overall coverage results for two selected throughput thresholds are given in Table 7-9. For the sub-6 GHz band, using a threshold of 50 Mbps as the minimum throughput for coverage, approximately 94% of the area is covered, and almost half of the area is able to achieve peak downlink throughput of 1000 Mbps. Using the same threshold, simulation results for the 28 GHz band show approximately 55% of the area to be covered, and approximately a third able to achieve peak downlink throughput of 1000 Mbps. These results suggest that a deployment at this band would require almost twice as many sites to achieve the same level of coverage, given the assumptions used in the simulations.

Frequency	% Coverage	
	> 50 Mbps	> 1000 Mbps
Mid-band Sub-6 GHz	93.8%	47.0%
28 GHz	54.7%	35.3%

Table 7-9 Downlink Percentage of Area Covered by Each Frequency Band

A cumulative distribution of the downlink throughput throughout the area (outdoor only), is shown in Figure 7-38. This is consistent with observations earlier in this white paper, showing less coverage for the 28 GHz band. There are some areas, however, where the 28 GHz band is able to get higher throughput than the sub 6-GHz band. These are areas where the SINR and channel conditions are sufficient that the system is able to achieve the highest MCS of 64 QAM and 2 layers within its 400 MHz band, allowing it to out-perform the 100 MHz bandwidth of the sub-6GHz frequency.

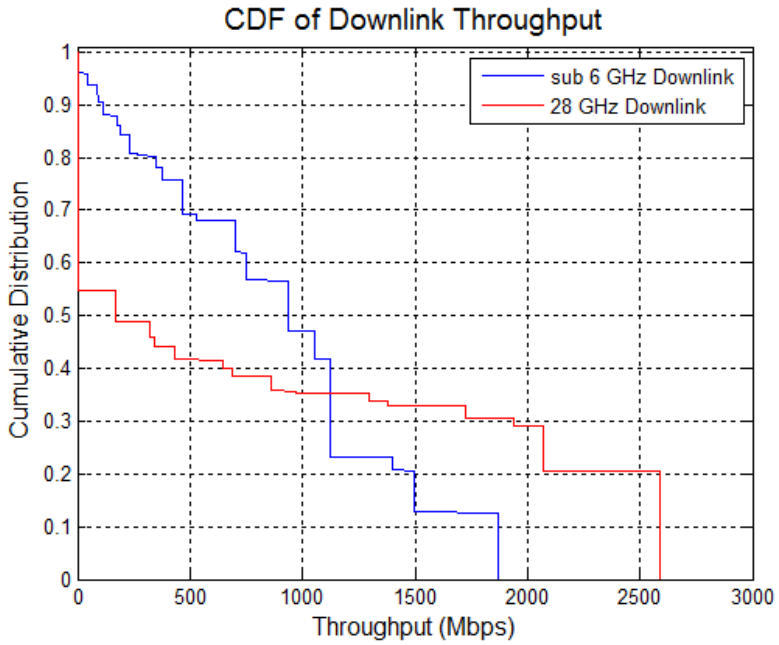

Figure 7-38: Comparison of the Cumulative Distribution of Downlink Throughput

Based on the results in Table 7-9, for a DL SLA of 50Mbps, mmWave would require approximately 2x the number of sites to cover same area as sub-6GHz.

7.2.2.2.6.2. Uplink Analysis

The results of uplink simulations are given in Figure 7-39 and Figure 7-40 below. In this figure, both plots are throughput, with those on the left showing the results for the 50th percentile EIRP, and those on the right showing the results for the maximum UE power. As observed for the downlink simulations, there is a noticeable drop in coverage between the sub-6 GHz results (Figure 7-39) and the 28 GHz results (Figure 7-40). This is as expected as the systems are co-sited in order to support a direct comparison of coverage, without any additional densification to offset the higher path loss of the 28 GHz band.

Overall uplink coverage results for two selected throughput thresholds are given in Table 7-10. For the sub-6 GHz band, using a threshold of 7 Mbps as the minimum throughput for coverage, approximately 75% to 84% of the area is covered. A threshold of 7Mbps is considered accounting 5Mbps of User data (TCP Ack + some UL data) and control overhead of 2Mbps. Initial real mmWave network performance evaluation by Signals Research Group [123] has shown that a constant 1-2Mbps of UL data was used independent of user data. Using the same threshold at 28 GHz, approximately 24% to 33% of the area is covered. These results suggest that a deployment at this band could require 2.5 to 3 times as many sites to achieve the same level of coverage, given the assumptions used in the simulations.

Frequency	Threshold	% Coverage	
		> 7 Mbps	> 100 Mbps
Mid-band Sub-6 GHz	50th Percentile EIRP	75.2%	47.1%
	Peak (ideal) EIRP	83.9%	57.3%
28 GHz	50th Percentile EIRP	24.3%	17.4%
	Peak (ideal) EIRP	33.3%	27.0%

Table 7-10 Uplink Percentage of Area Covered by Each Frequency Band

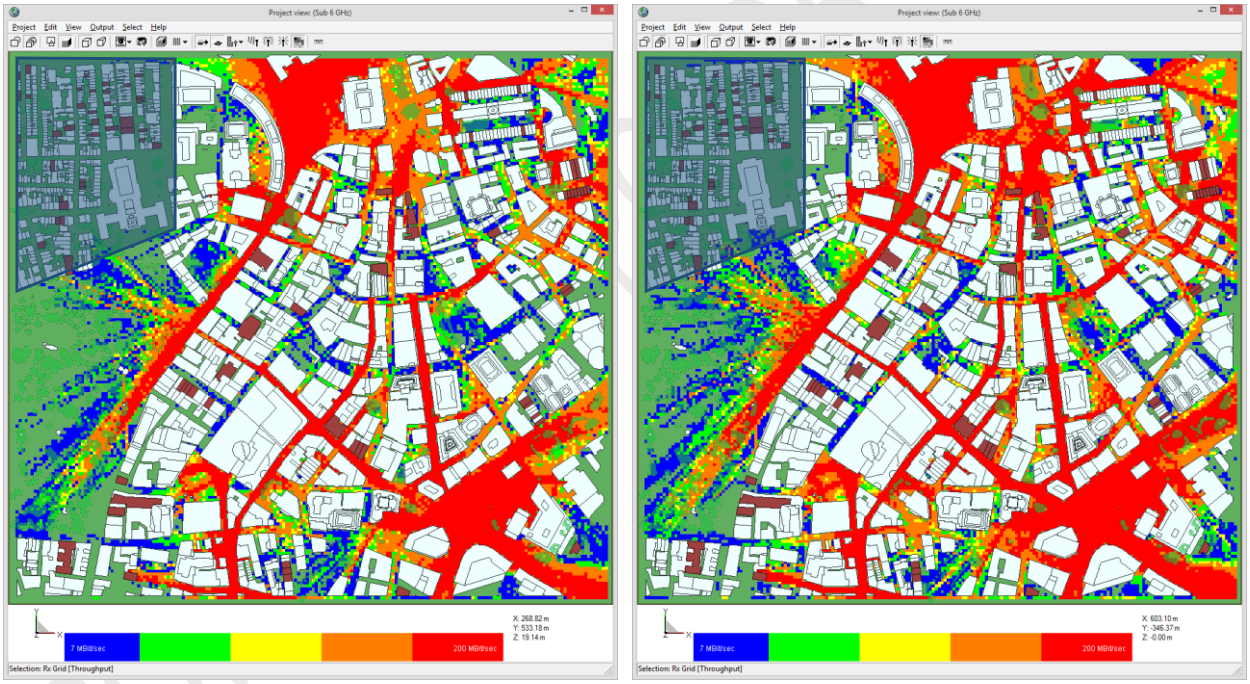

(a) Sub-6 GHz Throughput, 50th Percentile EIRP *(b) Sub-6 GHz Throughput, Peak EIRP*

Figure 7-39 Comparing Peak Throughput for Uplink at Sub-6 GHz, 50th Percentile vs. Peak EIRP

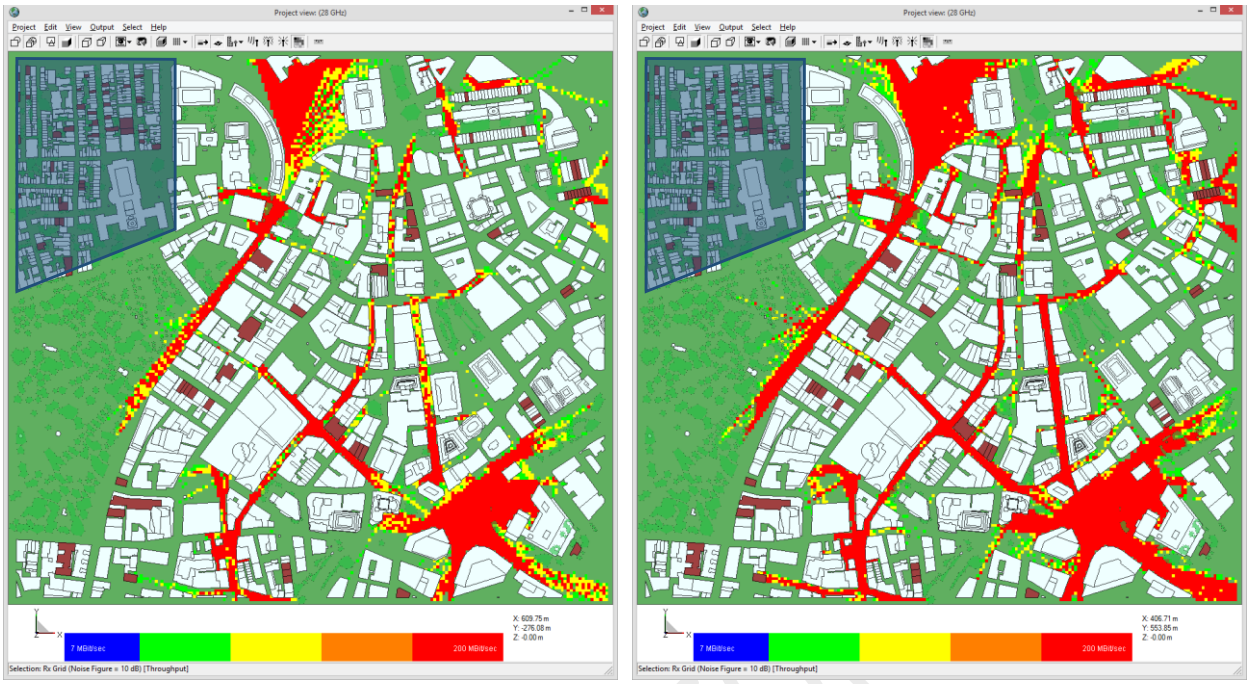

(c) 28 GHz Throughput, 50th Percentile EIRP *(d) 28 GHz Throughput, Peak EIRP*

Figure 7-40: Comparing Peak Throughput for Uplink at 28 GHz, 50th Percentile vs. Peak EIRP

A cumulative distribution of the uplink throughput throughout the area (outdoor only), is shown in Figure 7-41. Like the CDF for the downlink simulations, this shows less coverage at the 28 GHz band, but shows slightly higher throughput for the limited fraction of the area where coverage is strong. This includes places where the SINR and channel conditions for beamforming are sufficient that the system is able to achieve the highest uplink MCS of 16 QAM within the 400MHz bandwidth.

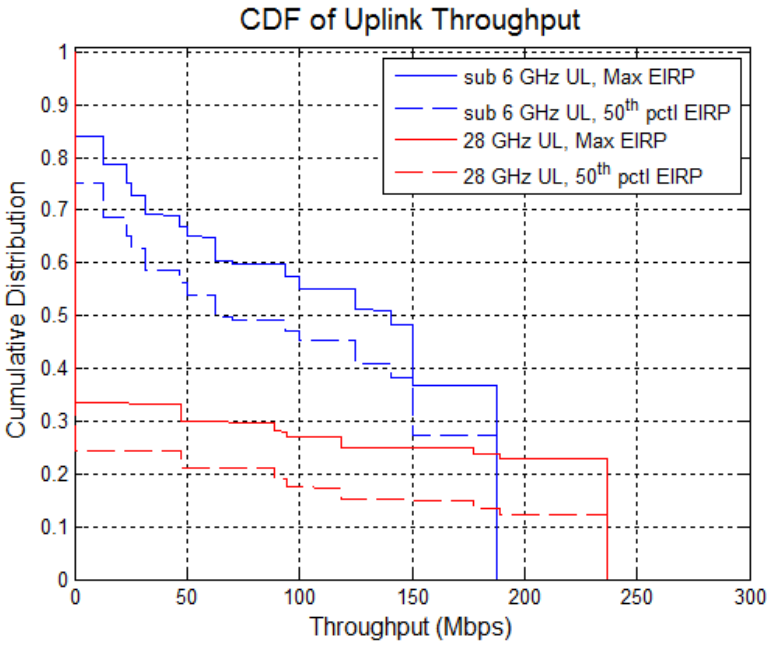

Figure 7-41 Comparison of the Cumulative Distribution of Uplink Throughput

Based on the results in the Table 7-10 and Figure 7-41 above, for a UL SLA of 7Mbps, mmWave would require approximately 2.5 to 3x the sites to cover same area as sub-6GHz.

7.2.3. Dual Connectivity between mmWave and Sub-6GHz

As seen in the previous sub-sections, the mmWave system is UL limited and thus the DL mmWave coverage is limited by its UL coverage. Hence, to improve overall performance and user experience using mmWave downlink, it is important to explore other options for uplink. 3GPP defines supplemental UL (SUL) in Sub-6GHz for the same purpose of improving overall coverage of 5G mmWave. Also, dual connectivity between mmWave and Sub-6GHz also help resolve this same issue. This section will look at simulation results of comparing mmWave DL vs Sub-6GHz UL coverage. The simulation assumptions for mmWave and Sub-6GHz were same as specified in previous sub-sections.

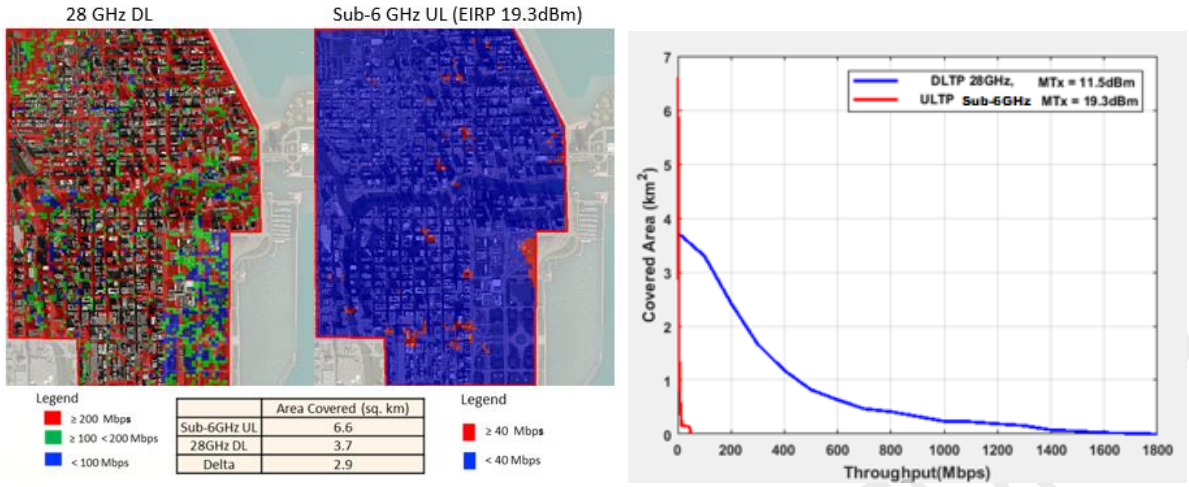

Figure 7-42 mmWave DL vs Sub-6GHz UL

As seen from plot and chart above (Figure 7-42), the system will no longer be UL coverage limited and can reap full capabilities of the mmWave DL. It would also be possible to switch between mmWave UL and Sub-6GHz SUL and hence use of mmWave UL near the cell for higher UL throughput while switching to Sub-6GHz UL for coverage needs. In such dual connectivity or SUL operation, mmWave system would require ~1.8x sites to match mmWave DL to sub-6GHz UL.

So far, it seems to make sense to use sub-6GHz for UL from a coverage perspective. However, that makes it important to look at it from a capacity perspective. To determine if sub-6GHz UL capacity is sufficient to carry mmWave DL traffic, we have assumed that mmWave NR uses FC2 alike slot structure. The charts below (Figure 7-43, Figure 7-44) illustrates peak mmWave DL throughput for various channel bandwidths (Blue bars). Assuming 5% Ack traffic (UL) for mmWave DL TCP based application's traffic (5% is considered to be conservative and is derived based on various application testing[69]), a 100 MHz of Sub-6GHz UL (TDD FC2 like) can accommodate mmWave DL peak throughput requirement (Single Layer) for up to 400MHz channel BW. In case of dual layer mmWave DL peak throughput requirement, even 160MHz sub-6GHz (TDD FC2 like) channel may not be sufficient for 400MHz mmWave channel BW. However, there is no restriction to use TDD FC2 alike UL in sub-6GHz for such scenario. One possibility would be to change the frame configuration of Sub-6GHz band to more UL intensive slots to support higher mmWave DL performance. Also, at the same time, make use of mmWave more DL intensive slot configuration. Another alternative would be to use Sub-6GHz FDD UL to pair with mmWave DL.

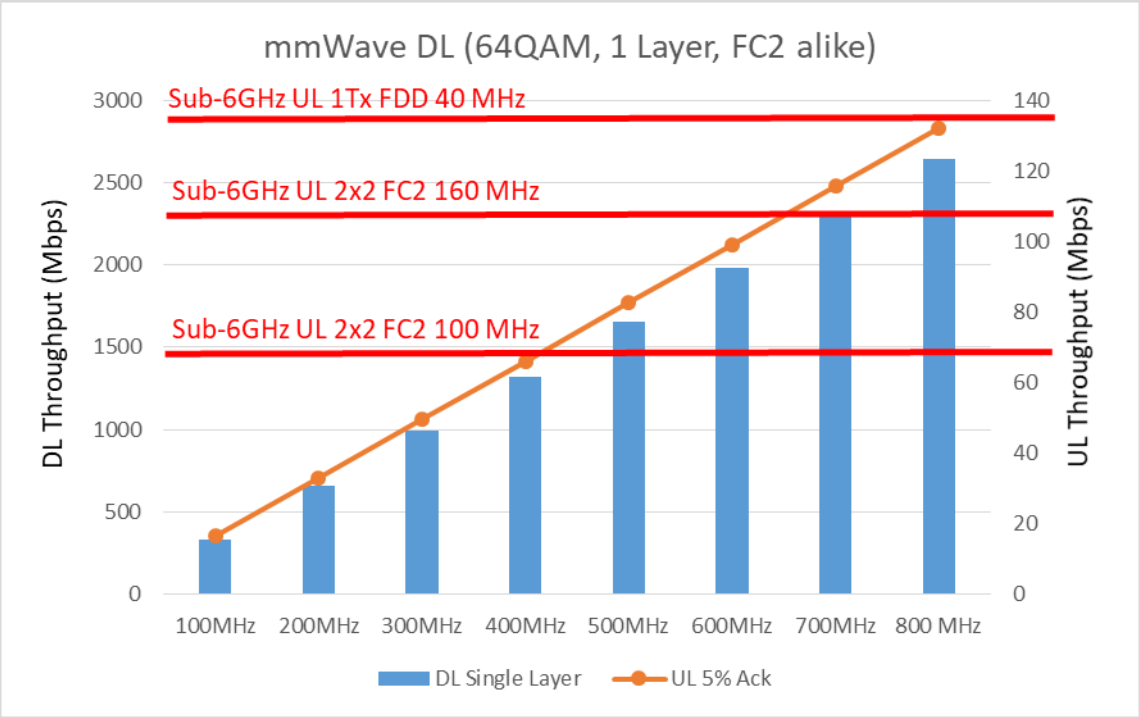

Figure 7-43 mmWave DL single layer peak performance

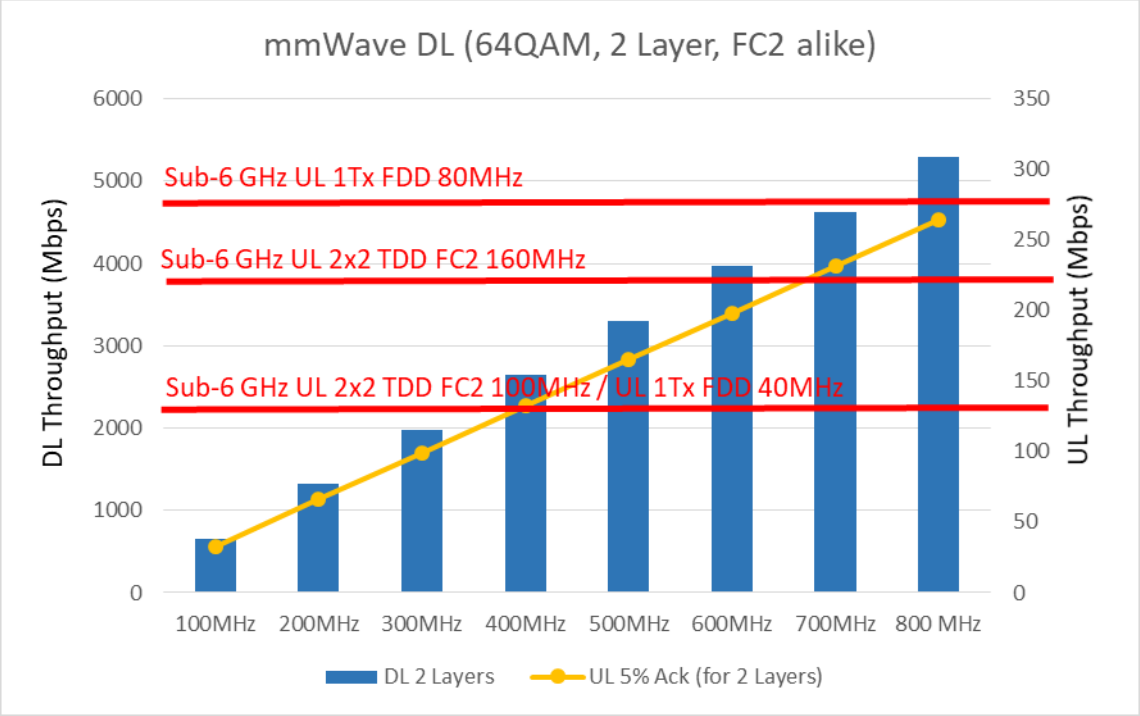

Figure 7-44 mmWave DL dual layer peak performance

As seen from the charts above, the use of 80MHz UL FDD in sub-6GHz would be more than sufficient to meet the mmWave DL throughput (2 layer) needs of 800MHz channel bandwidth, potentially even supporting higher/full DL intensive mmWave slot configuration. However, availability of ~40MHz or more of contiguous channel bandwidth in sub-6GHz FDD bands may be challenging for most operators. This would result in the use of inter-band carrier aggregation in UL which has its own challenges related to IMD, Tx power etc, causing concerns impact device power consumption.

Another point to clarify here is that the UL data could flow over lower bands using SUL. However, if SRS feedback is used for channel information, then DL mmWave channel performance may be limited. This can be overcome by using CSI-RS as a feedback mechanism. For dual connectivity operation, there would be a need of mmWave UL for HARQ and other control channel feedback. Further investigation of performance is required to better understand the de-coupling of UL from DL of mmWave.

7.2.4. Application performance considerations

As it has been learned so far that mmWave can provide the high capacity as required for 5G applications but at the same time there exists some coverage, mobility and reliability concerns, particularly in the case of standalone operation. These concerns are more important for mobile device form factor and use case, since it involves more frequent beam management procedures due to blockages. It is hence critical to understand the challenges that it brings to the adaptive control mechanisms in upper layer protocol / application layer performance. Initial real mmWave network performance evaluation by Signals Research Group [123] has also shown such performance instability due to mmWave signal as well as mobility management.

UDP is a connection-less protocol and therefore does not require upper layer feedback / acknowledgements. Hence, the use of UDP protocol may help determining the ideal network performance of mmWave system but may not deliver robust application layer performance under unstable / unreliable radio conditions. Most applications are TCP based and hence connection based. TCP offers reliable packet delivery (by sending ACK / feedback) as well as congestion control (by controlling the amount of data being transferred without an ACK). There are many different congestion control algorithms available that can dynamically change the congestion window based on ACK rate, bandwidth-delay product based, etc depending on link performance. The factors impacting TCP and latency performance include server location, mobility performance, TCP packet size / MTU, TCP buffer size and the congestion control mechanisms used. A detailed analysis on the impact of these factors on user performance was studied in [122]. However, many such controls may not be fast enough to adapt to the channel variations at mmWave frequencies and results in TCP slow start problem. Initial real mmWave network performance evaluation by Signals Research Group [123] has also shown that TCP slow start has an impact on throughput performance and there is significant difference in UDP and TCP performance. Such slow start operation cannot utilize available large instantaneous bandwidth. This paper [122] analyzed multiple mmWave deployment scenarios such as High-Speed (108km/h) and Dense Urban (10 UEs spread across the cell) using different congestion control algorithms and also provided means to improve TCP performance. The conclusion of the study [122] suggests that TCP benefit from shorter control latency.

When the RTT is high, TCP underutilizes the mmWave capacity. It also noted that multi-connectivity and advanced mobility management techniques can eliminate many of the reliability / latency concerns and result in robust TCP connection. The study also concludes that it is very challenging to properly dimension the buffer sizes for mmWave links due to rapid fluctuations and dramatic differences in bandwidth availability between LOS and NLOS conditions.

7.3. Summary

Overall, this section reviewed the mmWave coverage aspects. The propagation and penetration loss is ~50 dB higher compared to Sub-6GHz when accounting low E-glass and foliage loss (not accounting for hand/body loss). Besides penetration losses, outdoors coverage simulations were performed, analyzing the standalone mmWave scenario, comparing with Sub-6GHz and the use of Sub-6GHz UL with mmWave DL. The results demonstrate that mmWave coverage is UL limited and much shorter than sub-6GHz which makes it attractive to consider dual connectivity / SUL, using sub-6GHz UL.

8. Implementation considerations

The previous section discussed the coverage aspects of mmWave. This section will now dive into the deployment / implementation capabilities, configurations and considerations of mmWave system from technology, gNB and UE perspective. Massive MIMO / Beamforming is a de facto feature for mmWave and hence it is critical to analyze its performance, power consumption, size and cost. Other implementation considerations discussed in the section include channel BW, MCS, thermal dissipation as well as material technology status. This section will also illustrate mmWave capable products from various vendors.

8.1. User Mobility and channel considerations

User mobility pose several challenges, particularly at mmWave frequencies. Some of those challenges include lack of reliability, excessive handovers due to smaller coverage footprint and significant change in channel state / RF conditions even with small movements in the environment or the device. Initial real mmWave network performance evaluation by Signals Research Group [123] has also shown that quick body movements has an impact on device performance.

Doppler frequency shift is also a major factor than can affect mmWave Tx/Rx performance. mmWave uses higher SCS (120-240KHz) as compared to sub-6GHz (15-30KHz) which results in lower coherence time for the same UE velocity. The Doppler shift is inversely proportional to the channel coherence time ($T_{coh} = 1 / (2* f_d)$). As the carrier frequency increases in wireless systems, motion causes magnified Doppler effects. Doppler Effect is known to be 15-30 times greater at 28-60 GHz compared with sub-6GHz wireless systems [133]. Therefore the Doppler shift is higher at mmWave. The Doppler shift is caused by the relative velocity difference between Tx and Rx. Hence, high vehicular speeds could result in large Doppler shift. The max Doppler shift (f_d) is given as $f_d = f_c*(v/c)$ where f_c is the carrier frequency (Hz), v is the relative speed and c is the speed of light. For Example, at 28GHz carrier frequency and 500Km/h vehicular speed, the Doppler

speed will be ~12.97 KHz. The maximum frequency shift in the UL will be doubled because the UE transmit UL signal with its clock reference locked on the DL reception. Such Doppler shift has significant impact on receiver performance. One way to mitigate the Doppler Effect is to have additional reference signals but that adds overhead and impacts to overall system performance. Also, not all UEs travel at this high speed and hence system optimization much account for user behavior as well.

A good design and implementation of Beamforming can lower the impacts of user mobility. Delay spread and Inter-Symbol Interference (ISI) are caused by time dispersion / frequency selectivity in the channel. Wider transmit antenna aperture opens up for larger reflections and depending on the SCS / Cyclic prefix, the impact of delay spread / ISI could be very much higher. Beamforming transmission focusses in a more confined area which reduces the time dispersion / frequency selectivity in the channel at mmWave by narrowing the reflective / diffractive surface areas and thereby possibly lowering the overall channel delay spread.

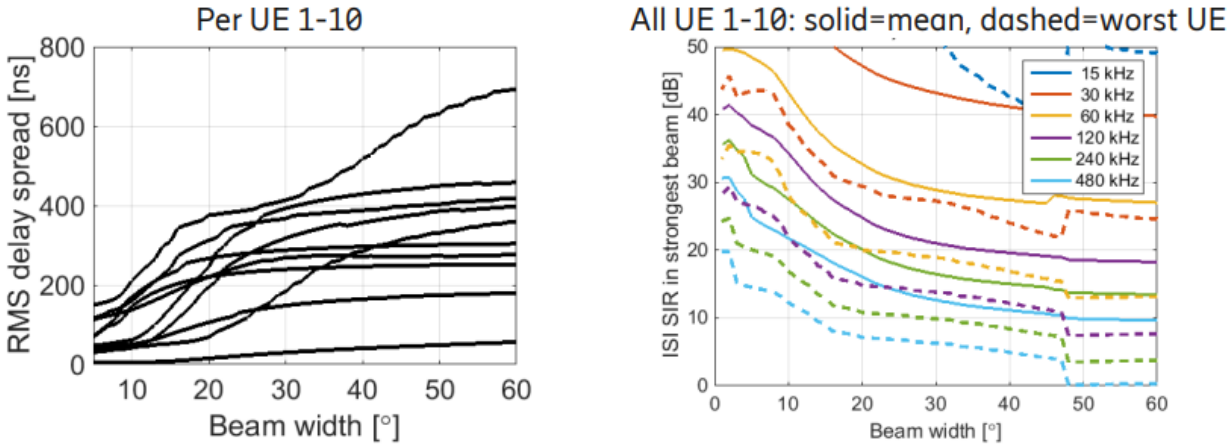

Figure 8-1 Delay spread and ISI Performance [138]

Figure 8-1 above shows delay spread and ISI results from the channel sounder measurements performed by Ericsson [138]. As it can be seen, narrow beamwidth results in lower delay spread and higher ISI SNR depending on UE position and LOS/NLOS.

Another chart below (Figure 8-2) from the same testing illustrates better ISI performance with beamforming compared to omni under LOS and NLOS.

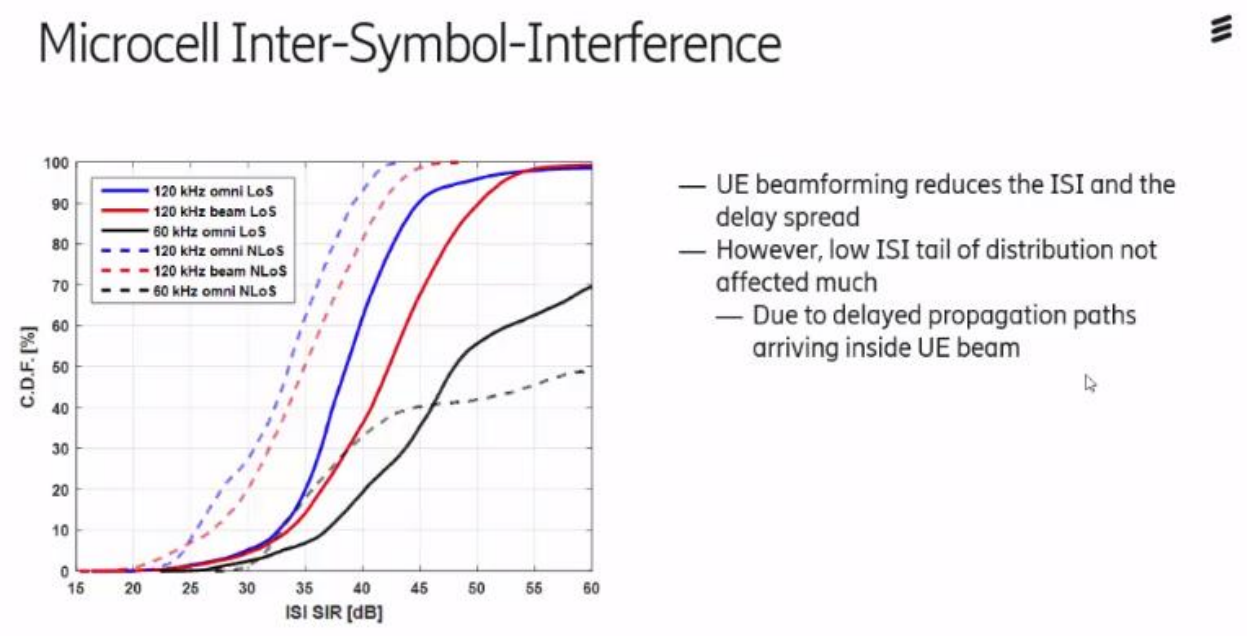

Figure 8-2 ISI Performance [138]

It is therefore important to explore beamforming techniques and their implementation consideration for the optimal design and deployment of mmWave network as discussed at length in subsequent subsections.

8.2. Antenna Arrays and Beamforming

One of the key tools for addressing signal losses at mmWave is the use of large antenna arrays. This gives more signal gain which can be used to overpower in the propagation to compensate for penetration losses at mmWave. Electrically large arrays are frequently regarded as antenna arrays that support more than 20dB of realized gain and are typically more than 16 square wavelengths in area. For 28GHz, this implies an antenna with physical antenna area of roughly 3 square inches. Therefore, antenna real-estate on the base station side will clearly not be a problem.

The downside to using higher gain antennas is that beamwidths narrow as gain increases. This is what has limited mmWave to fixed point to point links to date. It is critical that the antenna be able to scan the beam in order to cover multiple users. This scanning must take place at electronic speeds to render the scan operation invisible to end users. Therefore, electronically scanned, electrically large antenna arrays are a requirement for mmWave 5G communications.

The requirement for scanning imposes restrictions on how far apart the antenna elements can be spaced. In general, a well-designed electronically scanning antenna should never have more than a half-wavelength spacing between elements. Element spacing larger than this leads to undesired secondary beams appearing. These beams are not independently controllable from the main beam and thus cannot be signal processed out by any analog or digital technique. At one wavelength element spacing at least

one secondary beam always exists, reducing signal power by 3dB regardless of scan direction! In contrast, at half wavelength, the beam can be scanned over the entire forward hemisphere without this problem appearing.

There are a few different types of electrically large antenna arrays that can be considered for use in millimeter wave systems. The first one is a classic static antenna array. This setup is depicted schematically in Figure 8-3 and consists of a conventional modem/radio that is connected via a coaxial cable or waveguide to a fixed feed network. The feed network distributes energy to all the antenna elements and is responsible for delivering a known phase shift between the coaxial input and the antenna elements. Array elements can come in many forms such as dipole antennas, patch antennas, slots, spirals, etc. They are very well understood art and can be designed for a range of antenna patterns, polarizations and frequency responses. The obvious problem is that there is no mechanism, digital or analog, that causes these to scan in any way other than by frequency, which for most applications is undesirable.

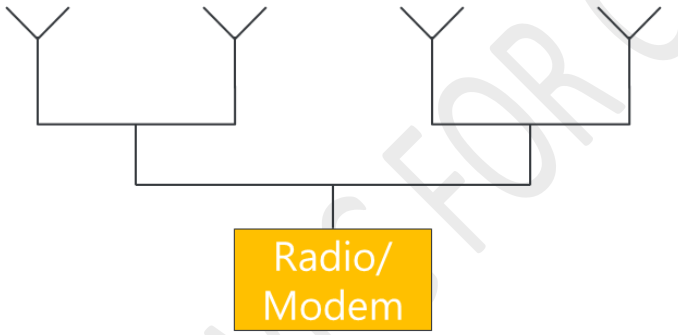

Figure 8-3 Schematic view of a static antenna array.

This type of antenna is unsuitable by itself due to the lack of scanning capability, but it does find use in hybrid architectures described later. Many vendors offer these types of antennas as commercial off the shelf (COTS) packages and are the mainstay of 4G antenna systems.

The second kind of electrically large antenna array is the classic phased array (**Analog Beamforming**). This architecture is well over 80 years old and is widely used in the defense industry. Historically this type of array has been very expensive to implement but recent advancements in highly integrated semiconductors have yielded significant price reductions. These types of arrays, on the outside, look very similar to static patch arrays but what is behind the antenna ground plane is quite different. The same feed network and modem/radio is present in the phased array. Here we have data converters translating the digital signals to and from broadband baseband or IF signals, connecting a radio transceiver performing the up and down conversion processes. At RF (example 28 GHz), we split the RF signal into several paths where we perform the beamforming, by controlling the phase of each path so that a beam is formed in the far field in the direction of the intended user. This enables a single beam to be steered per data path, so in theory we can serve one user per timeslot with this architecture. The choice of phase steers the antenna pattern in a precise way and can even do more advanced operations such as zero-

forcing (adaptive nulling in defense speak) and beam shaping. Unfortunately, phase shifters are lossy which results in PESAs (passive electronically steered arrays) not seeing much use in practice. AESAs (active electronically steered arrays) overcome this by placing amplification for both transmit and receive at the individual antenna element at the cost of no pattern selection prior to the receive LNA. This architecture preserves the noise figure and maximizes transmit power for the array and is shown in a Time Division Duplexing (TDD) scheme in Figure 8-4.

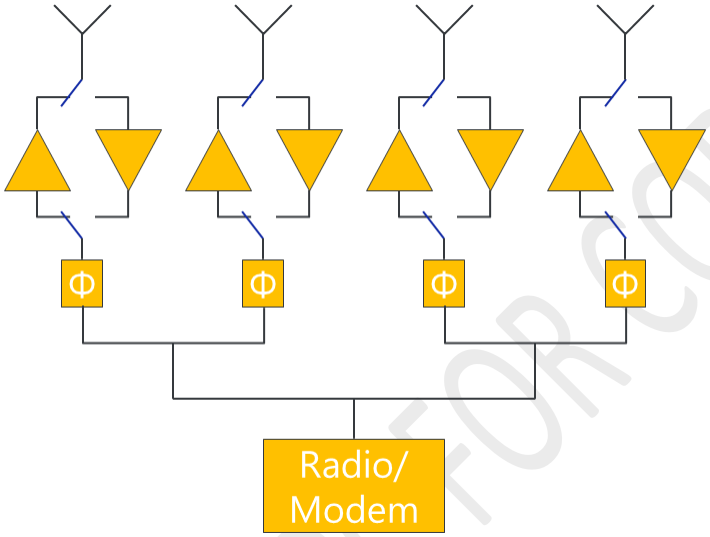

Figure 8-4 A canonical Phased Array Antenna Architecture (control circuits not shown)

Several companies are making advances in phased array chipsets. These chips usually package the phase shifter, amplifiers and power/control circuitry into a single packaged die. Anokiwave has partnered with Ball Aerospace to create a demonstration platform for mmWave phased arrays that has proven popular (See Figure 8-5). Sivers IMA, Phasor (not to be confused with Phazr), Intel and Qualcomm all have their own version of these chips as well. Frequently, four elements are driven by a single chip. Multiples of the chip are ganged up to form larger arrays. The chips are then driven by a straightforward processor that is interpreting the beam pointing commands from the radio.

Figure 8-5 A Ball Aerospace/Anokiwave 5G Prototyping system.[65]

Holographic beamformers (HBFs) are a new type of analog beam forming antenna architecture based on concepts from metamaterials. They operate on the principle of a variable impedance surface. Shown in Figure 8-6, a Radio/Modem feeds the HBF array. The elements are fed in series. Pure corporate feeds common in phased arrays do not work for HBF as a progressive phase is needed over the elements. The elements are oversampled (frequently at 1/5 of a wavelength spacing) and coupled to the feed line. Element control is achieved by tuning the impedance at the element via a varactor diode. Changing the varactor DC bias modulates the phase and amplitude of the element's radiation. Holographic Beamforming gets its name from the mathematics needed to calculate how to bias the elements to get the desired beam shape. It turns out that the same math needed to transform incoming light to a visual image is exactly that used for HBF but applied in the microwave regime.

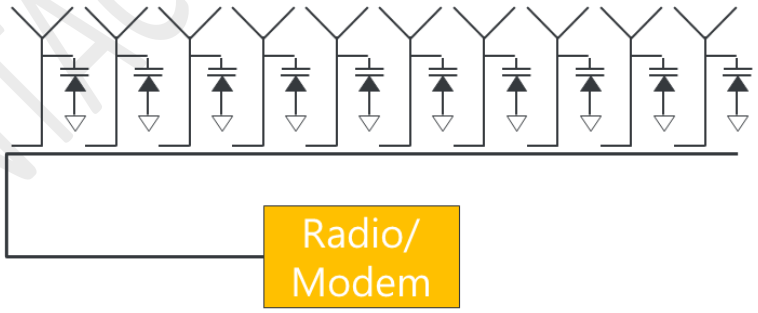

Figure 8-6 Schematic view of an HBF antenna array

HBF does not use distributed amplification within the array itself so the antenna structure is very simple. The HBF array is suitable for TDD and FDD operation and has fully reciprocal uplink and downlink characteristics. The HBF would be driven by a single PA/LNA combination rather than the distributed

approach used in phased arrays or digital beamformers. Signal linearity is a key advantage for HBF systems. It is far easier to linearize a single RF amplifier rather than contending linearization of an array. The simple parts needed for an HBF (varactor diodes, PCB, DC control circuitry, a single PA/LNA) make for a low cost, size, weight and power beamformer envelope. One key point to remember is that HBF supports two antenna ports per antenna (one for each polarization). HBF is not a digital beamformer so it cannot form more than two information streams from a single aperture. Thus it is not correct to think of an HBF antenna as a Massive MIMO antenna.

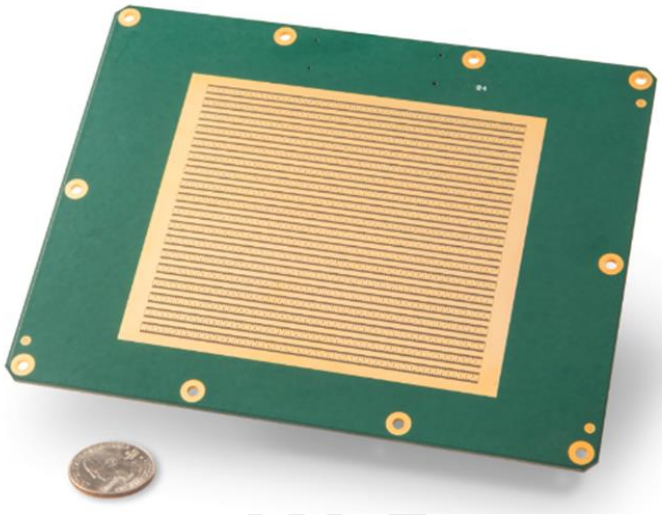

Figure 8-7 A view of the radiating surface of a 28GHz HBF antenna.

Another type of canonical antenna architecture is that of a digital beamformer. Well-designed digital beam forming antenna arrays look like phased arrays on the outside. A typical **digital beamforming** configuration is shown schematically in Figure 8-8 and it is easy to see that what is behind the antenna elements is quite different. In digital beamforming, the phase shift is purely implemented in the digital circuitry and then fed to the antenna array through an array of transceivers. Simply speaking, each radio transceiver is connected to a single antenna element, but in practice there could be several antenna elements per radio depending on the desired sector shape. The RF DAC/ADC pair is used to directly synthesize or digitize the RF signal on a per-antenna-element basis. This digitized information is transported via high speed bus to an N-channel coordinated radio system, where N is the number of antenna RF ports. This has several interesting theoretical advantages. The first is that the data can be processed in real time to determine direction of arrival and optimally adapt the transmission to the measured channel using this channel state information. Additionally, with large numbers of antenna elements, multiple data streams can be orthogonalized and processed as in Massive Multi-User MIMO. Thus, the digital approach enables highest capacity and flexibility and enables the roadmap to multi-user MIMO at mmWave frequency, similar to mid-band systems. However, it is highly complex and given currently available technology, will consume an excessive amount of DC power in the digital circuits to process the large amount of data. It is easy to imagine that if the capacity gains offered by this arrangement outpaces the hardware expense by a significant amount, it will see rapid adoption.

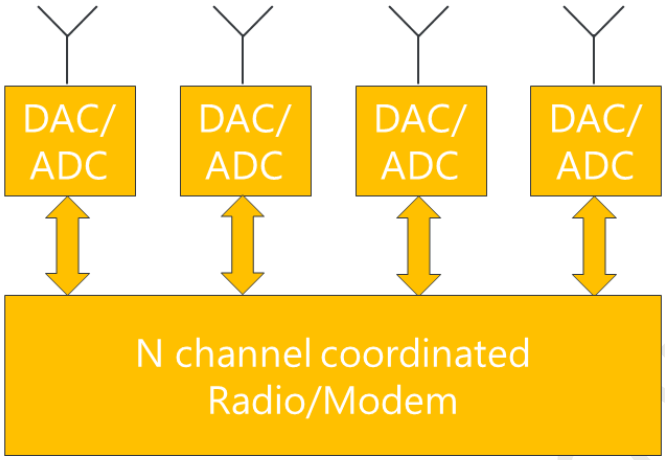

Figure 8-8 A schematic view of a digital beamformer

The problem with canonical digital beamformers is the need to digitize right at the antenna element to achieve their full potential. At sub-6 frequencies this is challenging but hardware is available. At mmWave the sampling rates on your ADC/DAC components need roughly double the carrier to achieve sufficient fidelity. This technique is theoretically possible. Metrology grade equipment where power and cost are not an issue can capture such signals in a small number of channels. However, they've got quite a way to go before they are commercially viable for large scale millimeter wave carrier deployments.

One technique used to reduce sampling requirements is to build an RF down/up converter into each element. With this method, the signals can be brought down to baseband which dramatically reduces the requirements on the DAC/ADC at the cost of the added RF components as well as some fidelity in the captured waveforms. Even at sub-6 GHz it is not uncommon to employ this technique to reduce the DAC/ADC requirements. At mmWave it appears to be mandatory as it is hard to imagine fully digitizing and processing a mmWave signal over multiple channels simultaneously with current technology.

Millimeter wave antennas will need large numbers of elements packed into a half wavelength lattice to achieve the antenna gain needed for mmWave link margins. The relative inefficiency of power amplifiers at mmWave (~20%) exacerbates this need since the antenna gain is needed to reach target EIRP while avoiding unacceptable power draw. As a result, antennas with hundreds of elements are needed. It is an unattractive option to try to build a fully digital beamformer with so many elements so industry is contemplating hybridization of the above canonical forms.

Finally, the last type of antenna architecture is the **Hybrid beamforming**. Hybrid digital-analog beam former which essentially combines digital pre-coding and analog beamforming to create several beams simultaneously in space (spatial multiplexing). By directing power toward the intended users with narrow beams, the basestation can re-use the same spectrum to simultaneously serve more than one user in a given timeslot. While there are a few different approaches to the hybrid beamformer reported in the many literatures, the sub-array approach is most practically implemented and is essentially a step and

repeat of analog beamformers. It has been shown that if the number of RF chains is twice the multiplexing order, the hybrid beamformer is capable of implementing any fully digital beamformer [101][102]. Currently reported systems support from 2 up to 8 digital streams in practice, which can be utilized to simultaneously support individual users, or alternatively provide 2 or more layers of MIMO to a lesser number of users. Several hybrid beamformers are appearing on the market today. Phazr and Ericsson have demonstrated a hybrid digital beamformers with static arrays. In these designs, the static arrays are large and provide significant antenna gain. The static arrays are overlapping and a low-number of RF ports is needed to drive them. In the case of Phazr's RABACK device, shown in Figure 8-9, each sector has radios that are driving four sub arrays containing 32 elements each. The scan capability is limited to within a 30° arc as the gain of the subarrays cannot be steered. Instead, MIMO beamforming is steering an even narrower beam within that arc. The limitation here is that many sectors are needed to achieve full coverage.

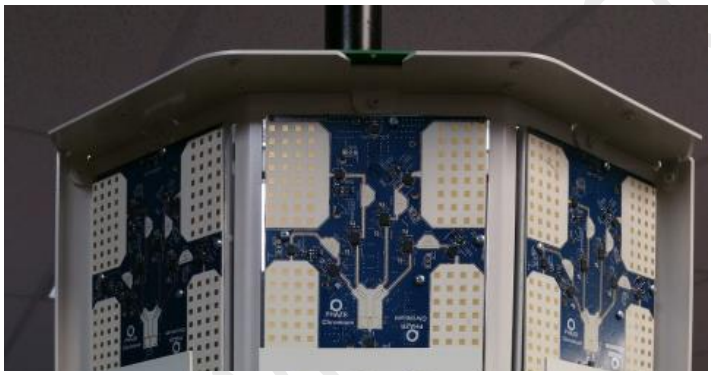

Figure 8-9 RABACK device (Phazr) showing 3 sectors with 4 static arrays per sector [66]

Pivotal Commware is developing a hybrid where the HBF panels replace these static antennas with steerable beamformers in what it calls Holographic MIMO™. This approach overcomes the scanning limitation, reducing the number of sub-arrays for full coverage. A similar approach using phased arrays in the place of the static antennas is being explored by many vendors such as NEC, Ericsson and presumably Huawei.

To summarize, there are number of possible combinations of antenna techniques that can be tried for mmWave operations. Actual deployment configuration will vary and will be tailored to customer requirements and industry developments.

8.3. Channel Bandwidths

The main benefit of mmWave bands is their large channel bandwidths (i.e >100MHz). This could result in higher throughputs in those bands. However, the wider channel bandwidths also pose significant challenges from a power consumption and thermal perspective on a smartphone. All the factors contributing to increased smartphone power consumption on a sub-6GHz smartphone (i.e. baseband, ADC, RFIC, PA efficiency, etc) become a magnitude higher, if not more, in mmWave space.

Also, the transmit signal power spread over a larger bandwidth may result in low link SINR which in turn limits coverage, making it more noise limited system instead.

With wider channel bandwidth (CBW) operation in 5G NR, the baseline power to transmit (at the gNB) and monitor (at the UE) the PDCCH increases significantly. The wider BW also increases the instantaneous power consumption, even though it helps with high data throughput. Also, the power efficiency of these wideband PA may be worse. All these would result in higher power consumption and in turn more heat dissipation.

Also, the transmit signal power spread over a larger bandwidth may result in low link SINR which in turn limits coverage, making it more noise limited system instead.

It is therefore important to understand the use case / throughput requirement and select appropriate use of channel BW to tradeoff power consumption.

The charts (Figure 8-10) below shows the DL/UL peak throughput with various channel BWs. Left chart assumes single layer (DL) operation while the right chart assume 2 layer (DL) peak performance. The blue line shows peak DL throughput and grey line reflects peak UL throughput in a TDD FC2 like frame configuration. The orange line indicate the required amount of UL throughput (TCP ACK) to support downlink TCP based applications requiring acknowledgements. The 5% UL Ack to DL TCP throughput is a conservative number and is derived based on testing of various apps under varies RF environments. Appropriate BW requirement should be generated based on these charts.

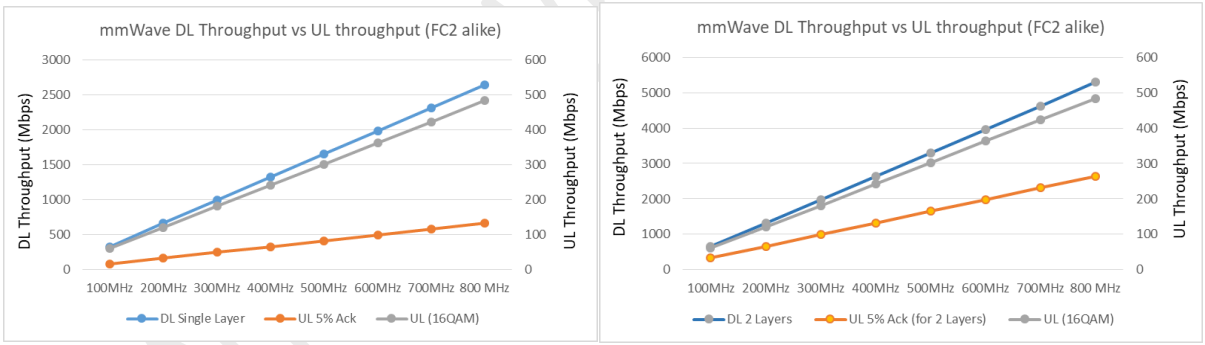

Figure 8-10 mmWave DL / UL Throughput – Single and Dual Layer

It can be seen from the Figure 8-10 above, the mmWave UL is capable of supporting mmWave DL throughput needs for the TCP based application. However, as seen from coverage analysis in section 7, the mmWave system is UL limited and hence cannot reap the wider channel BW benefits in downlink. An alternative would be to use sub-6GHz UL which can provide wider coverage. The Figure 8-11 below illustrates the sub-6GHz UL Bandwidth requirement to support mmWave DL throughputs.

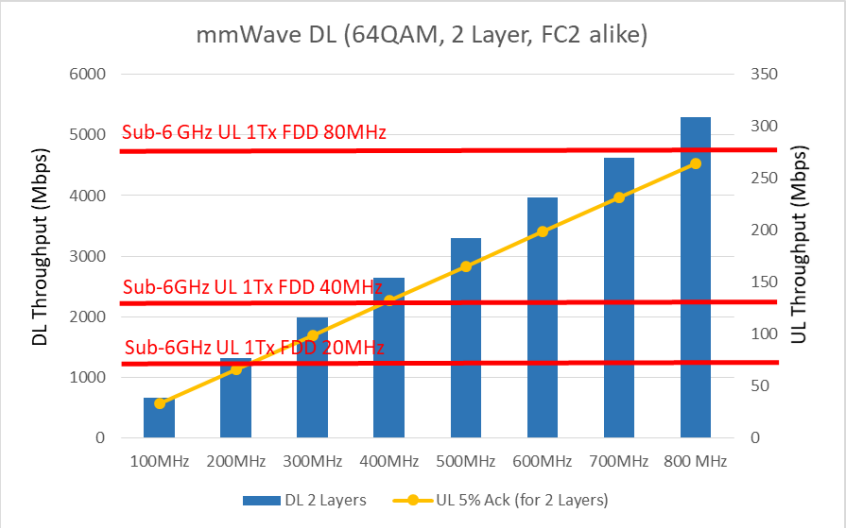

Figure 8-11 mmWave DL vs Sub-6GHz UL

As seen above, 20-40MHz of sub-6GHz channel BW is required to support 1-2Gbps of mmWave DL throughput, accounting TCP based applications. Use of Sub-6GHz for UL would eliminate some of the UL mmWave device power consumption concerns. However, availability of ~40MHz contiguous channel bandwidth in sub-6GHz bands may be challenging for most operators. This would result in the use of inter-band carrier aggregation in UL which has its own challenges related to IMD, Tx power etc, causing concerns impact device power consumption. Therefore, it is important to look at real deployments and analyze tradeoffs based on real network configurations.

8.4. MU-MIMO Capabilities

Due to shorter wavelength and the need for sharper beams (for coverage), the mmWave systems deploy larger number of antenna element in a given array. It is not feasible to support dedicated RF chains for these individual antenna elements, mainly limited by implementation constraints related to cost, power consumption and thermal dissipation associated with high speed ADC and PA inefficiencies. Analog beamforming has been mainly used in the past. This offers better coverage since all the antenna elements are used to construct a desired beam. But, that prevents mmWave from allocating MU-MIMO per transmission interval, and enforces a single stream to a single user.

An alternative to support more streams / MU-MIMO would be to use Hybrid beamforming, which can potentially support multiple Tx chains shared across the antenna elements.

From the Antenna array perspective, let's look at the potential MU-MIMO implementation configurations. The MU-MIMO could be implemented in different antenna configurations such as Single panel or multi-panel configuration as shown in Figure 8-12 [32] by Nokia. The main difference between the single panel array and the four-panel version is that the single panel array creates a single logical cross-pol RF beam (two-ports) at any given instant; whereas the four-panel array can create four logical cross-pol RF beams (eight-ports). Note that the eight beam ports formed in the four-panel array will have a wider beam

pattern and lower gain than the beams formed with the single panel array since the beams formed with the four-panel array are formed with fewer elements than the single-panel array which uses all the elements.

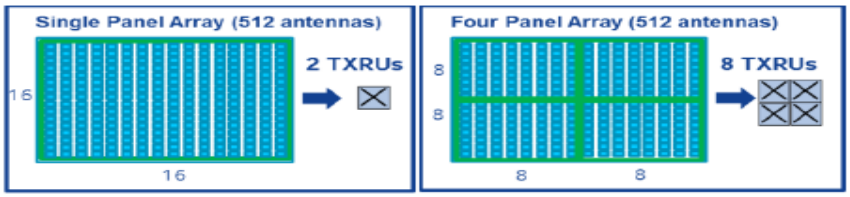

Hybrid Array designs: 16 rows x 16 columns of cross-pol antennas: 512 total antennas. Left: single panel design with two transceiver ports. Right: four-panel array with eight transceiver ports. Half wavelength spacing.

MU-MIMO operation with a hybrid array. Left: single panel array with parallel RF beams per UE. Right: four-panel hybrid array with a single RF weight vector per polarization per panel (one UE per panel).

Figure 8-12 MU-MIMO – Single Panel vs Multipanel Array – Nokia [32]

For a four-panel array with MU-MIMO, the cross-pol beam ports on each panel can be simultaneously aimed at individual UEs for a maximum of four co-scheduled UEs. However, with a single panel array, performing MU-MIMO in the RF domain is complex and would require multiple RF beams per polarization per panel (one per co-scheduled UE). Multiple RF beam weights per polarization per panel requires parallel RF Beams with summation devices behind the antenna elements which may pose cost and implementation difficulties. The single panel array case is considered as being more of theoretical interest as early hybrid array designs will likely not be implemented with multiple RF beams per polarization per panel.

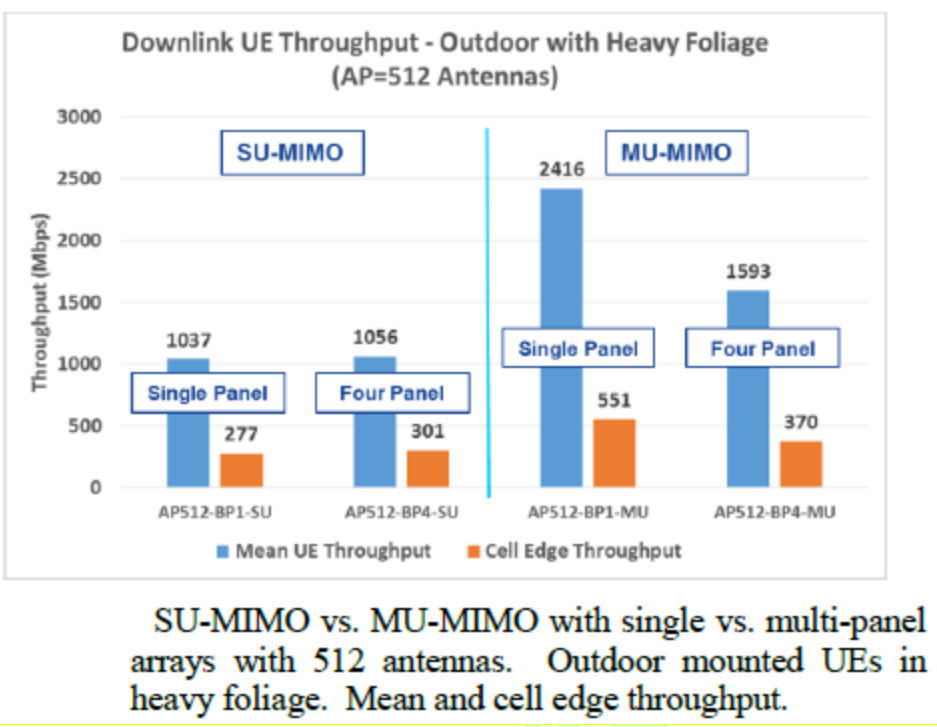

Figure 8-13 SU-MIMO vs MU-MIMO with Single vs Multipanel Arrays – Nokia [32]

As seen the Figure 8-13 [32], MU-MIMO showed much higher performance gains for single-panel arrays (though complex in design) compared to multi-panel arrays (130% vs 50%), largely due to the narrower RF beams that can be formed with the single panel compared to the beams formed by the smaller sub-panels. The SU-MIMO performance is similar between both the configurations.

It should be noted that the results above are based on outdoor CPE. In case of smartphones/handheld devices, the results would be quite different.

8.5. MCS Thresholds and limits

The higher order modulation requires better SNR in order to accurately receive the signal. As the density of the constellation goes up, it becomes more challenging to determine the digital character of the symbol versus others in the presence of significant noise and interference.

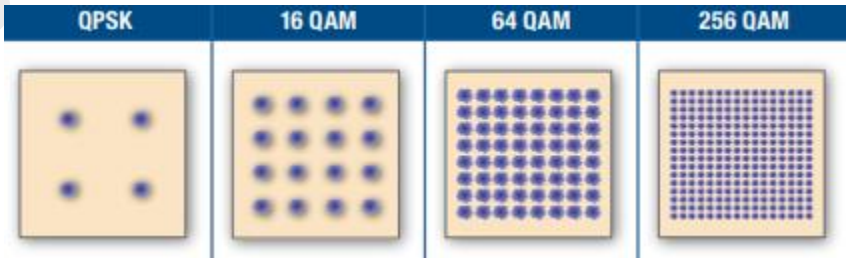

Figure 8-14 Modulation order – Skyworks [33]

This can be understood visually from the Figure 8-14 above that it could be more and more difficult to distinguish between the different points in the constellation. The Signal impairments [34] such as IQ impairments, phase noise, linear/non-linear compression, and frequency error increases with higher frequencies and wider bandwidths. These impairments can distort the modulated signal, making it difficult for the receiver to demodulate the signal accurately.

The EVM requirement for 256QAM is 3.5% as specified in 3GPP 38.104. This is very stringent requirement for the transmitter at mmWave frequencies. Initial real mmWave network performance evaluation by Signals Research Group [123] has also shown a MCS distribution with peak DL MCS of 64QAM.

Similarly, for UE UL, the EVM requirement for 64QAM is 8% as specified in 3GPP 38.101-2. This could also be stringent to meet at mmWave frequencies.

Therefore, with mmWave, achieving higher SINR may be challenging, also due to higher propagation / penetration loss, making it difficult to support 256QAM modulation in DL and 64QAM in UL.

8.6. Beam management

The mmWave band uses very high frequency which leads to higher propagation / penetration losses. To compensate for the losses, directional communication using antenna arrays is essential. Beamforming process combines signals from multiple antenna elements in an antenna array, so as to produce a narrow beam directed towards the receiver. This helps providing necessary gain to the RF link budget at these high frequencies. Beam management is therefore very important. 3GPP 5G NR specifications support Beam management operations for Initial Access as well as during idle/connected mode. Such operation include Beam Sweeping, Beam measurement, Beam selection and Beam reporting.

Beam sweeping refers to beam transmission in different directions over time, covering the entire cell area. Beam measurement and selection involves determination of best/suitable received beam over a specified period.

Figure 8-15 below illustrates initial access / control channel (SSB) beam management.

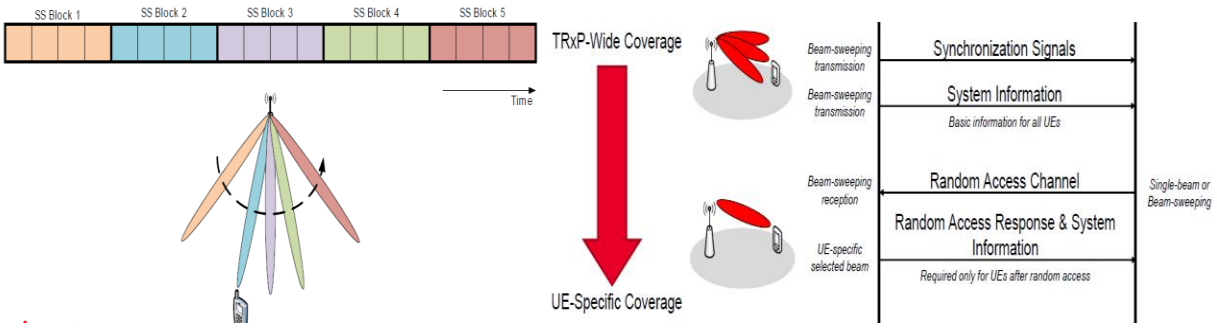

Figure 8-15 Beam Management – Keysight [35]

The Synchronization Signal (SS) burst is transmitted periodically by the gNB. One or multiple SSBs (beams) transmitted in different directions, together compose a SS Burst, confined in a 5ms duration (half frame) to reduce UE power consumption. The Max number of beams (L) per SS burst can be determined based on operating frequency (L=4 for <3GHz, L=8 for 3-6GHz, L=64 for 6-52.6GHz). The UE then finds the best beam, decodes the MIB/SIB using that SSB beam. The UE later attempts Random Access on the configured RACH resource specific to that beam index. The gNB would determine the specific beam used by the UE based on RACH resource. Similar process also applies to Idle mode.

Besides initial access / Idle mode, beam management is also supported in connected mode. Additional Cell/UE specific CSI-RS beams are configured for beam measurement. UE performs measurement on these CSI-RS beams as well as SSB beams to determine and reports best beams while in connected mode. Beam failure recovery process involves UE requesting for recovery by indicating a new SSB beam in a RACH procedure.

8.7. Single User Multi-Layer MIMO

The use of SM (Spatial Multiplexing / Multi-layer) or BF (Beamforming) can be determined based on the operating SNR. The SM (Spatial Multiplexing) uses multiple streams on a single carrier to increase the capacity per user, which is mostly effective in a high SNR region and where the channel provides sufficient diversity, or rank. Such scenario may be limited at mmWave frequencies due to propagation losses as well as other blockages.

SM operation requires the transmitter to split its power across the spatial streams. The SM would therefore provide less benefit under low SNR / cell edge region (e.g., power-limited channels with little interference) as it weakens each stream quality and causing higher bit errors that limit overall capacity gains. Thus, single layer may provide greater capacity (use of higher modulation) by increasing SNR in such region. mmWave systems will often be power-limited rather than bandwidth limited (due to much greater spectrum allocations and higher path loss associated with mmWave wavelengths), and will also often be noise-limited rather than interference-limited due to the use of BF to avoid co-channel interference while exploiting angle diversity [36]. Therefore, the Massive MIMO antenna design and spacing on these mmWave systems is usually optimized for better beamforming performance (coverage) instead of increasing independence of bit streams. From the UE perspective, having a single phased array operation and tight antenna element spacing could make it difficult to receive multiple uncorrelated signals as well.

8.8. Sector and Single User peak throughput

Based on some of the implementation considerations discussed above, here (Figure 8-16) is the peak achievable throughput in DL and UL for various mmWave channel bandwidths using TDD FC2 like frame configuration in a standalone operation mode. 400MHz CBW could achieve more than 1Gbps peak using single layer DL. With same 400CBW, UL peak throughput is little over 100Mbps.

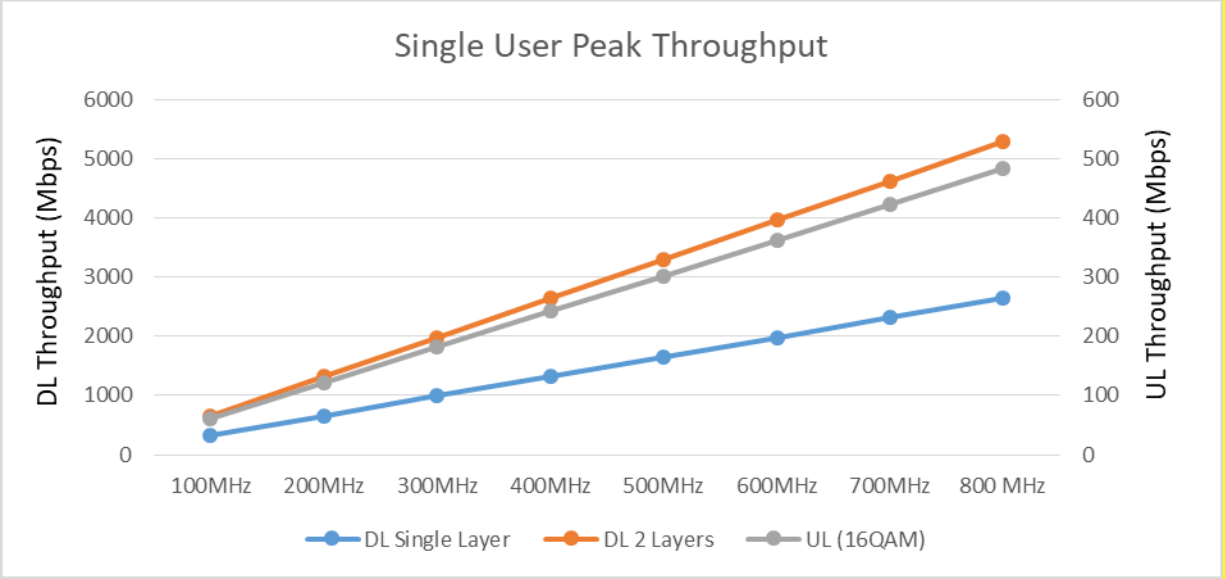

Figure 8-16 mmWave Single User Peak Throughput

The peak DL sector throughput is expected to be similar to the 2 layer single user throughput due to the limitations with the type of BF implementation i.e 2 layer MU-MIMO, at least in near term.

The theoretical peak mmWave DL spectral efficiency based on the chart above comes to ~4 b/Hz assuming 64QAM and single layer. This number is ~75% lower than the sub-6GHz DL peak spectral efficiency due to the use of 256QAM and 4 layers MIMO. It should also be noted that recently Signals Research Group performed practical mmWave measurements in the field using Verizon's mmWave network in Minneapolis and Chicago [124]. A total of 4 component carriers, each 100MHz wide were configured. The peak DL spectral efficiency of that mmWave was noted to be ~2b/s/Hz.

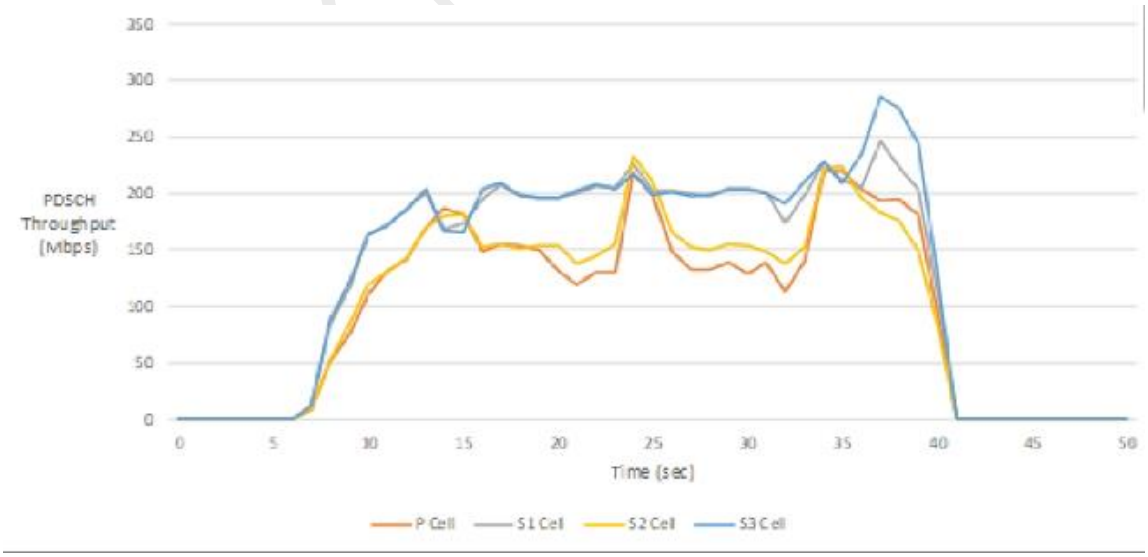

Figure 8-17 SRG testing - mmWave DL throughput in VZN network [124]

This shows that the practical case peak spectral efficiency (2b/Hz) may be ~50% lower than the assumed theory.

Figure 8-18 below has the sample cell throughput numbers from field testing by Ericsson in LOS and NLOS scenarios. The throughput results are similar under both cases (LOS and NLOS) above ~300m but for close to the cell location (~150m), the LOS shows significant advantage in terms of throughput performance. Cell radius ~33% lower in case of NLOS.

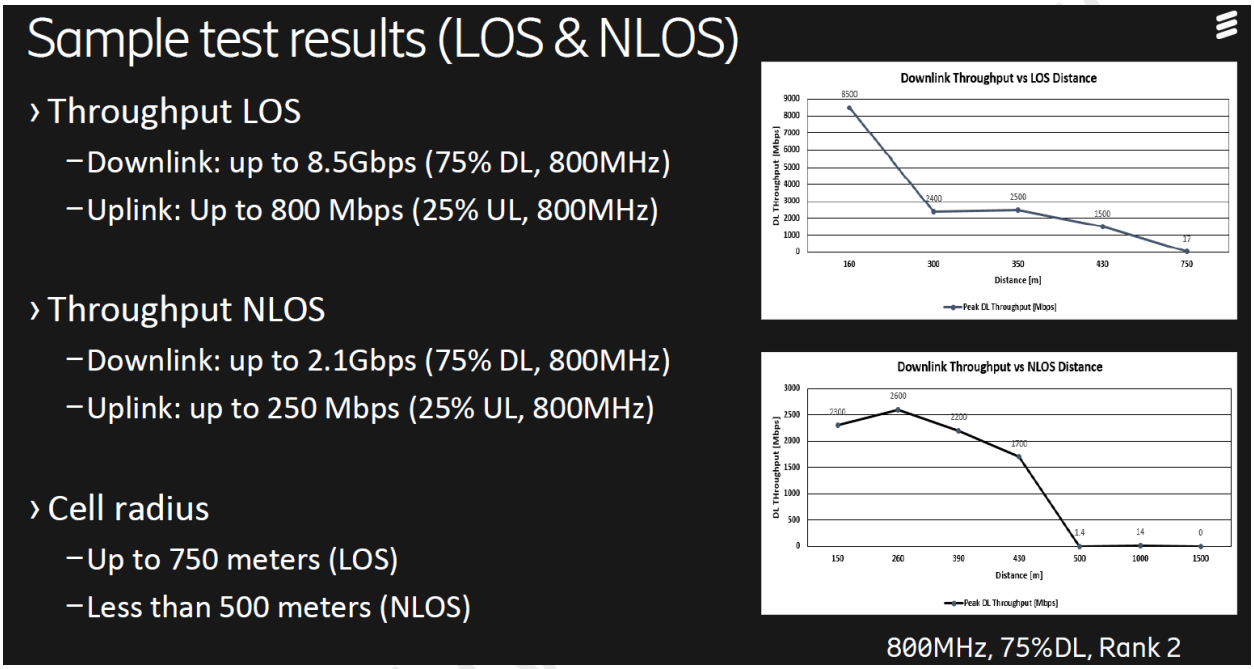

Figure 8-18 Downlink Throughput test results - Ericsson

To summarize, the peak performance would vary based on LOS / NLOS and the MIMO layer capability at the UE and the gNB.

8.9. gNB side Considerations

Previous subsections discussed overall functionality and capability considerations of overall system / technology. This subsection will focus on specific implementation considerations from a gNB perspective, discussing Massive MIMO antenna and beamforming considerations as well as impact on size and power consumption.

8.9.1. Nos. of Massive MIMO Antennas

mmWave renders itself, potential candidate to offer enormous capacity by virtue of providing very high number of transmitting and receiving antennas as well as enormous channel bandwidth. Marzetta propounded the idea of large-scale antenna array in mm wave propagation in his pioneering paper with reference to BSs. The paper [104] showed that in the limit of large number of antennas (theoretically

going to infinite numbers) , small scale fading effects vanish by virtue of channel hardening and channel vectors from the BS to the users tend to become orthogonal. As a result plain channel matched beamforming at base station permits serving several users at the same time – frequency resource slot with no interference. Only problem is due to pilot contamination, due to limited number of pilots, being reused in the network, leading to imperfect channel estimates.

One problem with massive MIMO systems is the cost and complexity of hardware to efficiently exploit large number of antennas in mm wave region.

Based on various vendor's mmWave products, the number of antenna elements at the gNB can vary from 128 to more than 1,000. More antennas can be integrated into a given area at mmWave frequencies, but the insertion losses, intrinsic power-overhead in radio-frequency (RF) generation (DAC/ADC), and amplification (PA) result in diminishing gains

Also, with mmWave, support for beam-sweeping is critical to estimate / identify the direction of interest. This procedure increases the overhead from CSI acquisition, which grows with the number of antennas since the beams become narrower and hence arising the need to support more beams.

Beamforming gain at mmWave is higher as compared to sub-6GHz since more number of antenna elements can be packed in the same form factor, resulting in a sharper beam. Also, this sharper beam can improve spatial separation between users and hence increase MU-MIMO performance.

8.9.2. Beamforming Considerations

As seen in section 8.1, the hybrid beamforming is achieved by a set of antenna arrays. Each antenna array consists of several antenna elements and each antenna array can be mapped with one RF Chain. Accordingly, the number of RF Chains or the number of arrays will determine the number of spatial layers that can be supported. Each array can generate an analog beam. The 3db beam width of each beam needs to be designed to achieve a target narrow beam gain. The center lobe gain of each beam is determined by the overall gain achieved by combining the gains from all the antenna elements of the array. The number of phase shifters and number of antenna elements will further determine the number of beam directions that can be generated. The number of beams direction along with the beamwidth will further determine the total coverage. The beams are implemented to span both the azimuth and elevation planes. The number of horizontal beams at different vertical planes and the number of such vertical planes determine the horizontal and vertical beam scan angle. Implementation can also consider different beambooks. Each beambook will map to different beam patterns. Beam patterns can be designed depending on deployment use cases associated with horizontal centric or vertical centric coverages as shown in the below Figure 8-19. Beambooks can be a configurable parameter or in more advanced systems the beambooks can be automatically adapted. In such adaptive beamforming, system can automatically learn based on performance metrics and close loop management, the required beambook to provide optimal coverage in any given cell.

Figure 8-19 Adaptive beambooks

Thus, such beamformer implementation is driven by many factors including segment shape and reach, power levels, path loss, thermal constraints etc., and is the section of the mmWave systems that requires some flexibility as the industry learns and matures. Even then, there will continue to be a variety of transmit power levels required to address deployment scenarios ranging from small cell to macro. 60 dBm EIRP is a commonly quoted transmit power target for FWA, but the number can be higher or lower depending on the desired reach of the basestation and the surrounding environment. Given the high variation in deployment scenarios, whether the area is highly treed, or composed of street canyons, or wide-open spaces, there will be a large range of path loss to contend with on a case by case basis. For example, in a dense urban deployment where LOS is assumed, the EIRP target may be as low as 50 dBm.

There are definition and published specifications as well as transmit power limits from the FCC by equipment class, and here we follow the 3GPP terminology for basestations (38.104). As illustrated in Figure 8-20 below, the class of equipment more or less defines the choice of technology for the power amplifier. While not an exact science, we can see that clearly the mobile user equipment (handset) is well suited for CMOS technology and a relatively low antenna count can achieve the required transmitter power. This type of radio will very highly integrated and power efficient to meet the needs of portable equipment. The local area basestation (small cell) and consumer premise equipment (transportable power) share similar requirements and span a range of technologies from CMOS on the low end of TX power requirements to SiGe BiCMOS for the higher end. The medium range basestations are ideally suited for SiGe BiCMOS technology to achieve a compact form factor. At the high end, for wide area basestation there is a range of technology that may be applied, and it comes down to the trade-offs of antenna size and technology cost. While SiGe BiCMOS can be applied in the 60 dBm EIRP range, GaAs or GaN power amplifiers are more practical for higher power.

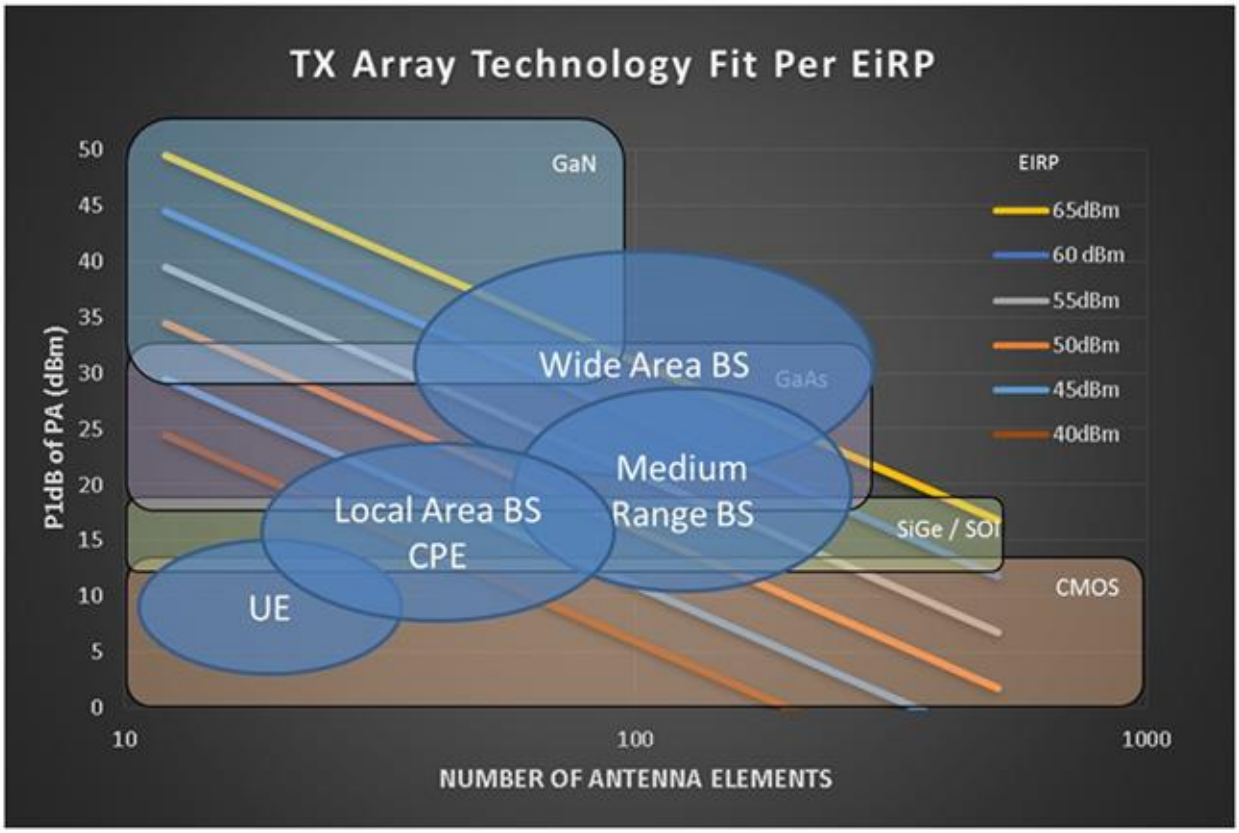

Figure 8-20 Technology fit per mmWave radio use case [31]

The above is snapshot of current technology, but much progress is being made in the industry and technology continues to improve. As mentioned in [37], one of the key challenges for the designer is to improve the DC power efficiency for mmWave power amplifiers. As new technologies and PA architectures emerge, the curves above will shift, and more highly integrated structures will be available for the high power basestations. A good overview of advancements in PA technology is presented in [38].

To summarize the beamformer section, let's reiterate the point made above. Currently there is not a one-size-fits all approach and one may need to design a variety of front-end designs to address the various use cases from small cells to macros.

8.9.3. Size / Power Consumption

mmWave femto/small cells are expected to increase power requirements, not reduce them which may be the opposite of the market pressure. Some of the reasons are as follows:

- There may be additional power inefficiencies and demands due to the processing (digital/hybrid beam forming, matrix-inversion, etc.).

- If additional transmit branches are needed (today's indoor small cells are 2T) then there will be more inefficient RF components. Most of the power consumption today are related to SoC and RF.

- The "Watts per bit per second" measurement increases the power consumption as a function of the throughput since it requires faster CPU and more utilized clock-cycles.

- The mmWave small cell SoC and platform hardware elements are immature at this time and will be less power friendly than the mature (10+ year old) LTE products available today.

- Supporting services like URLLC will require higher availability hardware which comes at additional cost and power consumption. This may need redundant hardware which will increase power consumption.

Use of MEC may mean more devices are "always connected" verses LTE small cells. These new service capabilities will increase the small cell utilization, and the resultant power consumption.

As mentioned in previous section, the DC power efficiency of beamformer is one of the major challenges facing the mmWave designer. The DC power efficiency limits the amount of power that may be transmitted and drives cost of both components and mechanical assembly.

At mmWave frequencies, only Phased Arrays and Holographic Beamformers are viable candidates. Massive MIMO is not mature enough for mmWave deployment. One common design point for gNBs is that of a 60dBm transmit EIRP (@P1dB), single polarization beamformer suitable for mmWave operation. Phased arrays targeted for this application are frequently 256 element transmit arrays (either 16 row and 16 column or 8 row and 32 column). The antenna array has 28dB of realized gain (29dB for a 'perfect' antenna array). Quad-element phased array chipsets becoming common in a variety of technology nodes. 64 of these driver chips would be needed to drive the 256 element array. Phased arrays distribute electronic gain to each element, resulting in a small transmit power requirement of 6.2mW per element for a total transmitted power of 32dBm. The combination of 32dBm electronic gain and 28dB antenna gain meets the 60dBm EIRP target. For Silicon based chips the expected Power Added Efficiency (PAE) is roughly 4% which means such an array will need at least 40W of DC input power. More efficient technology nodes exist (SiGe, GaAs, and GaN) but the cost generally scales with performance.

An HBF of equal aperture size to the phased array would have 640 total elements driven by a single high power amplifier (rather than distributed into the array). An HBF of this size would have 26dB of antenna gain and thus need a GaN power amplifier able to source 34dBm (2.5W). GaN is generally higher performance, with off the shelf power amps reaching 25% PAE. This single amplifier approach has the added benefit of being able to exploit digital predistortion techniques to linearize the PA which is normally impossible for phased arrays. HBF also has a small control overhead driven by the number of control ASICs needed for switching the element states. For an array of this size the control overhead is roughly 2.9W. This quantity is also present in Phased Arrays but is captured within the PAE of the chipset.

Both approaches have some elements in common and are omitted from this analysis. For example, both need drivers for control signal inputs, some light computation for manipulating the elements and some

optional feedback mechanisms for users (lights and sounds). These items generally have a power draw that is small compared to the RF power draw. This analysis also assumes that neither device needs an active cooling system which can be substantial. A summary of this analysis is shown in Table 8-1.

	Phased Array	HBF	Unit
Number of Unit Cells	256	640	#
Antenna Gain	28	26	dB
Number of RF chains	256	1	#
Transmit Power per chain	6.2	2512	mW
Total Transmit Power	1.58	2.51	W
Power Added Efficiency	4.0%	25.0%	%
DC Draw for RF	**39.6**	**10.0**	W
HBF Controller	**0**	**2.9**	W

Table 8-1 Difference between HBF and Phased Array power consumption

8.10. UE side Considerations

The previous subsection addressed key considerations from the gNB perspective. It is equally important to address UE side considerations, particular more so for the handheld form factor due to its size, power and thermal limitations. This section will discuss various such important considerations.

8.10.1. RF Front-End Architecture

RF Front end architecture design is a key aspect of a smartphone design, given the need to support various frequency bands. It has become even more important now that most smartphone manufacturers are aiming at supporting a global SKU that could be used worldwide and hence maintaining the overall cost. Also, supporting mmWave bands requires further considerations in terms of reducing front-end losses. This subsection will look at some of the RFFE aspects for supporting mmWave operation in a smartphone.

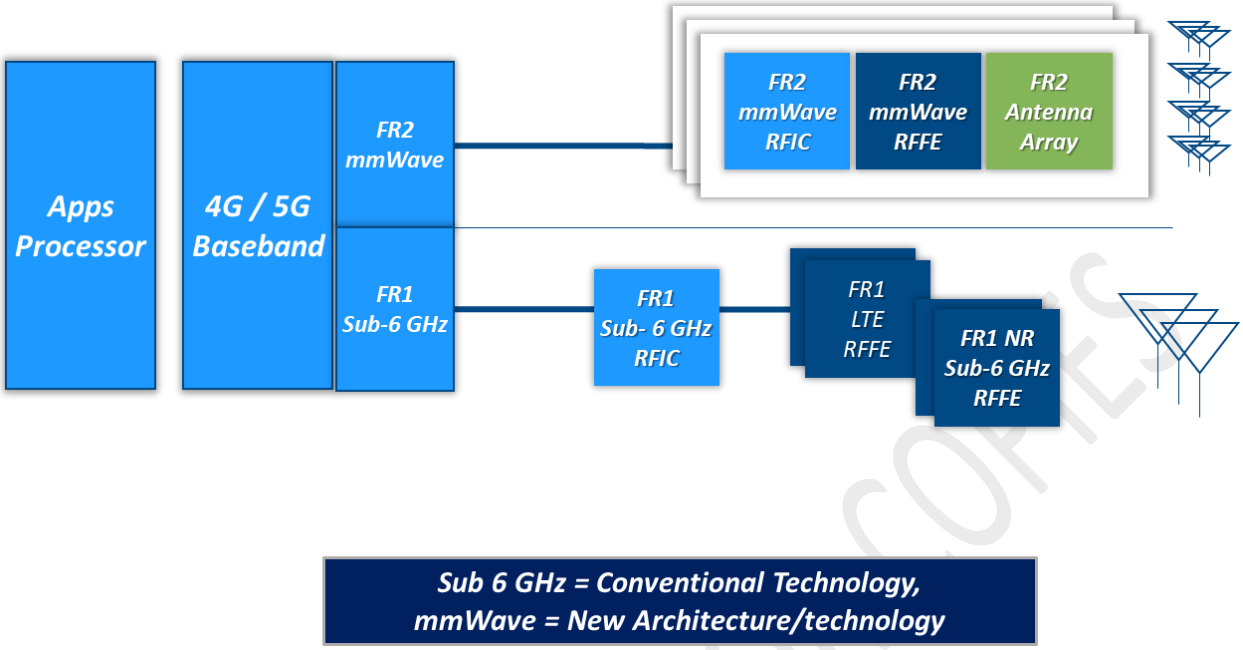

Figure 8-21 5G UE RFFE Block diagram

Figure 8-21 illustrate a block diagram of a UE support mmWave. The mmWave is expected to have a dedicated RFIC, RFFE and Antenna arrays. The combined 4G/5G SOC will have two seprated frequency domains- FR1 sub-6GHz and FR2 mmWave implimentations. The main difference required for mmWave will be integaral mmWave transciever- RFFE- and antenna array in combined package.

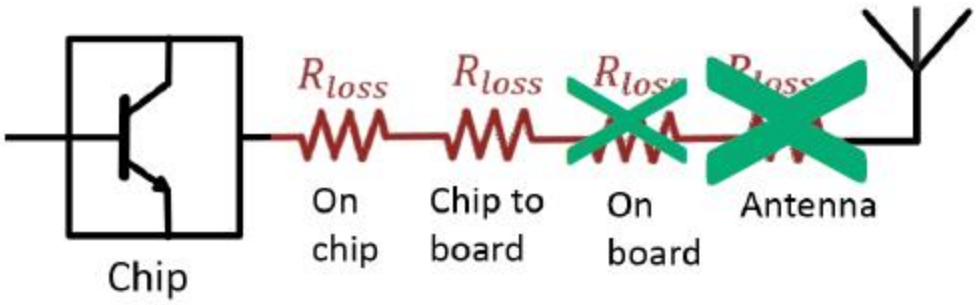

Figure 8-22 Minimizing loss for mmWave RFFE

The Figure 8-22 shows that co-integration or system-in-package placement of the antenna with the signal amplification (Tx/Rx) integrated circuits helps to reduce post – power amplifier loss. Signal transitions (signal reflections) from laminate to the RF board, signal loss in the board, and any transmission line losses to the antenna can be eliminated. For example, removing 2dB of loss will result in the recovery of 37% signal power. More significantly perhaps, if required power output can be reduced by 37% then power consumption and heat dissipation in the integrated circuit can be reduced (in accordance with the PAE of the power amplifier).

8.10.2. UE Co-existence with incumbents at mmWave

The 3GPP 5G NR Release 15 standard is designed to operate in the mm-wave frequency bands as listed in Table 8-2.

NR Operating Band	Frequency band
n257	26500 - 29500 MHz
n258	24250 - 27500 MHz
n260	37000 - 40000 MHz
n261	27500 - 28350 MHz

Table 8-2 Operating mm-wave frequency bands in the 3GPP NR R15 standard.

The Federal Communications Commission (FCC) has allocated licensed frequency spectrum for 5G applications in these sub-bands: 24.25–24.45, 24.75–25.25 and 27.5-28.35 GHz as discussed in Section 6. Adjacent to these frequency bands, there are multiple of incumbent systems which can interfere with the 5G systems. Furthermore, the 5G systems should fulfill the FCC regulations on emitted power to avoid interfering with these existing systems. Fixed Satellite Service (FSS) is one of the most predominant incumbent users which coexist in the 5G mm-wave frequency bands. This section of the Whitepaper provides an overview of the requirements on transmitted interferer levels as well as how the 5G system degrades in receive mode due to interference in adjacent channels. Furthermore, different ways to handle and improve the performance are also discussed.

Receiver blocking: A 5G mm-wave receiver can be blocked, or jammed, by an unwanted signal located in an adjacent channel. The blockers can either be another 5G NR signal or a signal from an incumbent

system. The 5G NR standard specifies that the User Equipment (UE) adjacent channel selectivity for the bands n257 and n258 should be 23dB, i.e. the reception should not be significantly degraded in presence of another 5G NR signal with a power level of 23 dB larger than the power of the wanted signal. A typical 5G NR receiver with analog beamforming is outlined in Figure 8-23, where the received signal is down-converted to zero IF. In the case of hybrid beamforming, where multiple data streams are received in parallel receivers, the filtering requirements will not be different from a pure analog beamformer.

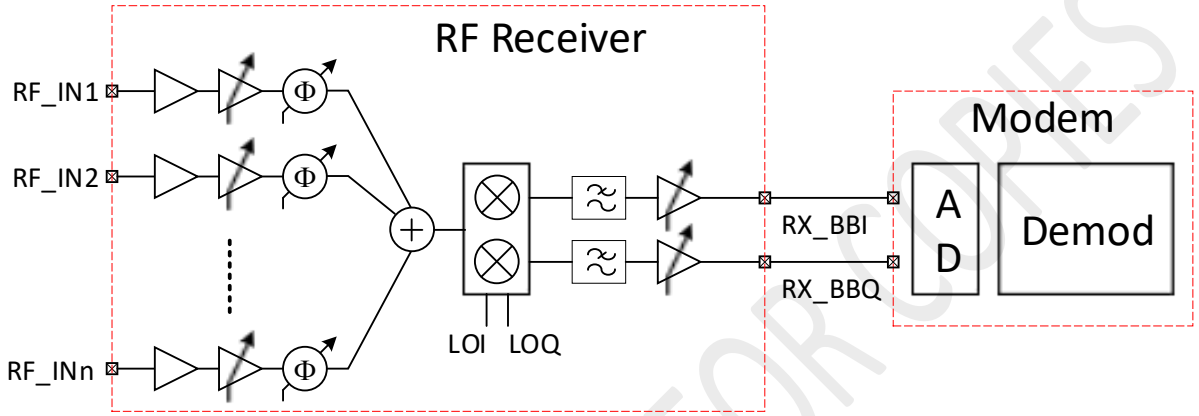

Figure 8-23 Block diagram of a typical beamforming receiver system

Even though some attempts can be found in scientific papers, implementing narrow band and tunable channel selective filters at RF frequency on silicon is not practical. The main reason why such filters are not found in mm-wave RFICs is the difficulty to implement high-Q resonant circuits with sufficient absolute accuracy. For instance, if a 100 MHz wide bandpass filter should be centered around a wanted channel in the 28GHz band, the spread of the absolute resonance frequency of the resonators in the filter should be significantly better than 1 percent, which is not possible without expensive calibration. What can be found in literature is to make use of so-called translational filters, which solves the problems with accuracy, but give raise to other issues instead. Hence, the adjacent channel selectivity of a 5G NR receiver can only be carried out in a selectivity filter located directly after the down-conversion mixers. The RF section of the receiver will therefore be sensitive to the entire 5G mm-wave frequency band and must handle the wanted signal as well as the interfering signals. A zero-IF architecture as shown in Figure 8-23 simplifies the implementation of the selectivity filters, since these can be implemented as programmable low-pass filters. In a low-IF architecture, the filters must be band-pass and are more difficult to implement.

The blocking performance of the receiver is also determined by the phase noise of the Local Oscillator (LO), since a strong signal in an adjacent channel can be mixed with the phase noise located in the adjacent channel and fall on top of the wanted signal after the mixer. This mechanism can be illustrated by a simple example. Assume that the phase noise profile of the synthesizer that generates the LO signal looks as shown in Figure 8-24 and that a 400MHz wide signal is present at the receiver input in an adjacent channel. Due to the distance from the wanted signal to the adjacent channel, it can be assumed that the noise from the synthesizer is flat. Furthermore, assume that the SNR level of the wanted channel is at least 25dB,

then the requirement of the noise floor of the synthesizer can be calculated to be < -25 - 86 – 23 = -134 dBc/Hz; where 25 dB is the required SNR, where 86 dB is the bandwidth in dB ($10 \log 400MHz$) and 23 dB is the requirement in the standard.

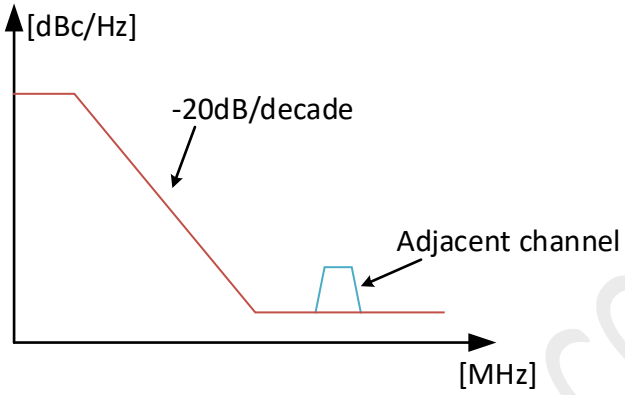

Figure 8-24 Phase noise profile of a typical synthesizer

In case the blocking signal originates from an incumbent system transmitting energy into the receive band, the 5G NR standard requires that the throughput of each carrier shall be ≥ 95% of the maximum throughput even with interfering signals present only 25 MHz apart and with levels just over 20 dB stronger than the wanted signal. Since such incumbent interferers are also present within the 5G mm-wave band, it is not feasible to suppress these in the RF domain prior to down-conversion. This requirement will therefore put additional requirements on the linearity performance of the RF section of the receiver as well as on the phase noise performance of the synthesizer.

To determine the requirements of the IF section of the receiver requires knowledge on the AD converter performance and its sampling rate. An AD converter with high sampling rate and large dynamic range requires less suppression of the blocking signals in the analog domain. An RF section with adequate linearity performance and a synthesizer with enough phase noise performance that fulfills the requirements in the 3GPP 5G NR standard is considered feasible to implement. However, due to very strong interferers outside the 5G NR frequency band, an RF band filter might be required to implement. Due to the large number of receiver inputs which are used for beamforming purposes, an RF band filter is typically implemented in the RF substrate in between the RF IC and the patch antenna, which adds constraints to the antenna board design. A typical frequency response of an RF band filter is shown in Figure 8-25.

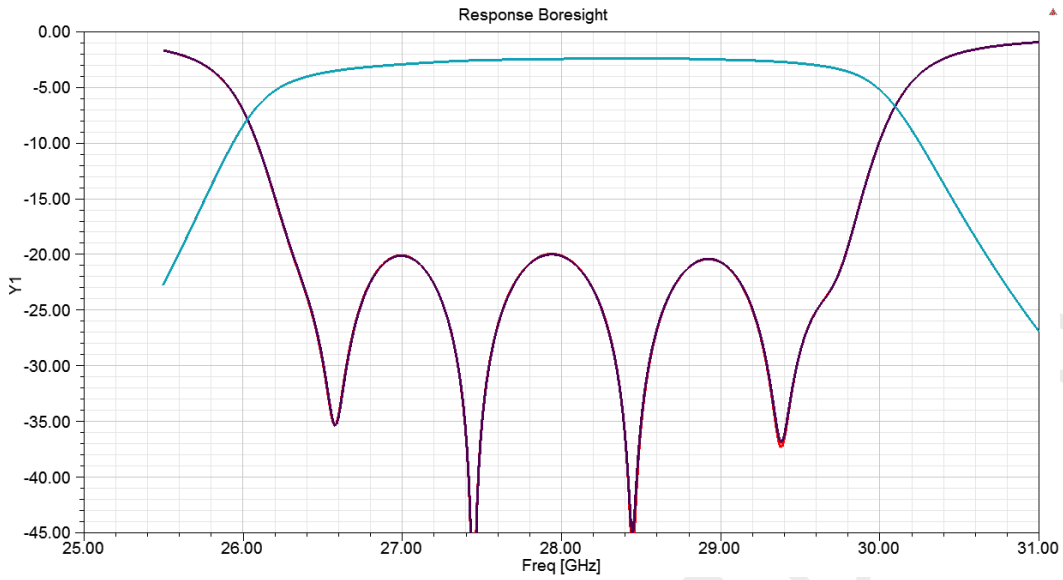

Figure 8-25 Typical filter response of an RF band filter. Courtesy of Kyocera International Inc.

RF spectrum emissions: A typical beamforming transmitter is shown in Figure 8-26. Unwanted emissions immediately outside the assigned channel will be generated due to the modulation in the digital modem as well as due to non-linearities in the transmitter. The out of band emission limit is thoroughly specified in the 5G NR standard in terms of a spectrum emission mask and an adjacent channel leakage power ratio. Additional requirements to protect specific bands are also considered in the standard. Furthermore, national government agencies, like FCC in the US and ETSI in Europe, are developing and implementing additional regulatory requirements on spurious emissions. The out of band spurious emission must be tested by a certified test house according standardized test methods to ensure that the national radiation limits are not exceeded, e.g. in the US according the Electronic Code of Federal Regulations, Title 47 and § 15.209 (often referred to as FCC 15.209).

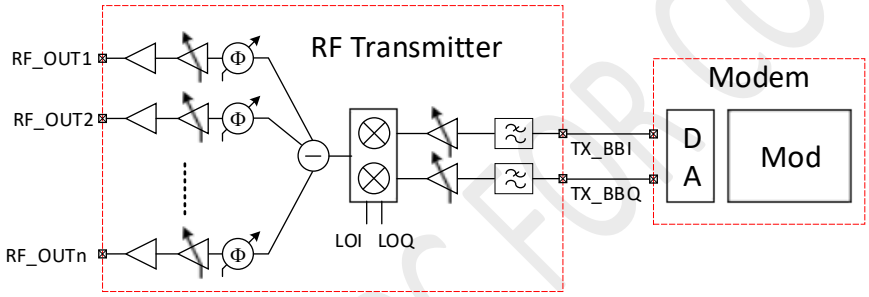

Figure 8-26 Block diagram of a typical beamforming transmitter system

The modulated spectrum is generated in the digital domain in the Modulator and is converted into the analog domain in the Digital to Analog Converter (DAC). The output signal from the DAC must be filtered by a reconstruction filter to remove image frequencies above the Nyquist limit. The reconstruction filter is often located as one of the first blocks in the RF Transmitter and it should have a bandwidth which is equal to the wanted channel bandwidth. Hence, in case of a 5G NR mm-wave system, the bandwidth of the reconstruction filter should be programmable to support the four different channel bandwidths in the standard (50, 100, 200 and 400 MHz). The RF Transmitter is preferably implemented with a direct up-conversion architecture as is shown in Figure 8-26, which means that the reconstruction can be implemented by a low pass filter with a bandwidth of half the channel bandwidth. The filter order is dependent on the performance and sampling rate of the Digital to Analog Converter.

A typical spectrum of a modulated 5G NR signal is illustrated in Figure 8-27, which consists of many OFDM modulated sub-carriers. Since the transmitter is not ideal, intermodulation between the sub-carriers will occur when the modulated signal is amplified, up-converted and phase-shifted. All odd-number of intermodulation (IM3, IM5, IM7 and so on) will result in intermodulation products falling in-band as well as in the adjacent channels. The power from these intermodulation products that ends up in the adjacent channel is referred to in the 5G NR standard as the Adjacent Channel Leakage power Ratio (ACLR) and is defined as the ratio of the filtered mean power centered on the assigned channel frequency to the filtered mean power centered on an adjacent channel frequency. The ACLR requirement is specified for a scenario

in which the adjacent carrier is another NR channel and should be > 17 dB for a mm-wave 5G NR signal. This requirement can only be fulfilled by a sufficiently linear transmitter, since RF channel filtering is not practical at mm-wave frequencies.

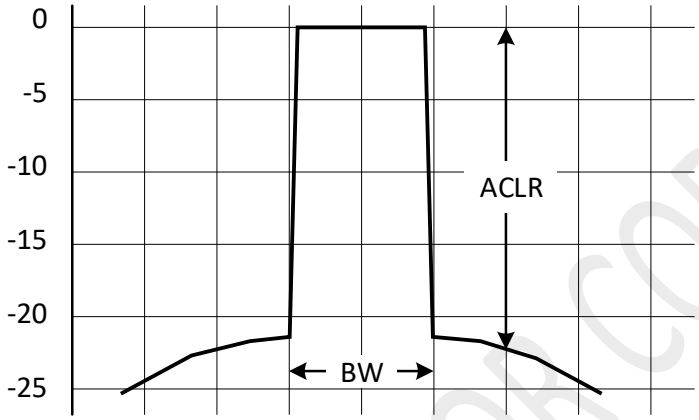

Figure 8-27 Typical spectrum of a 5G NR mm-wave signal

The general spurious requirements as specified in the 5G NR standard for User Equipment (UE) are found in **Table 8-3**. In addition to these general requirements, spurious requirements for coexistence with protected bands are specified as shown in **Table 8-3**.

Frequency Range	Maximum Level	Measurement bandwidth
30 MHz ≤ f < 1000 MHz	-36 dBm	100 kHz
1 GHz ≤ f < 12.75 GHz	-30 dBm	1 MHz
12.75 GHz ≤ f ≤ 2nd harmonic of the upper frequency edge of the UL operating band in GHz	-13 dBm	1 MHz

Table 8-3 Spurious emission limits

NR Band	Spurious emission					
	Protected band/frequency range	Frequency range (MHz)			Maximum Level (dBm)	MBW (MHz)
n257	NR Band n260	F_{DL_low}	-	F_{DL_high}	-2	100
	Frequency range	57000	-	66000	2	100
n258	Frequency range	57000	-	66000	2	100
n260	NR Band 257	F_{DL_low}	-	F_{DL_high}	-5	100
	NR Band 261	F_{DL_low}	-	F_{DL_high}	-5	100
	Frequency range	57000	-	66000	2	100
n261	NR Band 260	F_{DL_low}	-	F_{DL_high}	-2	100
	Frequency range	57000	-	66000	2	100
NOTE 1: F_{DL_low} and F_{DL_high} refer to each NR frequency band						

Table 8-4 Spurious emission requirements for UE coexistence.

In some cases, the network can signal to the UE to indicate that additional spurious requirements should be met. For instance, when "NS_201" is indicated in the cell, the power of any UE emission in the frequency band 23.6 – 24 GHz shall not exceed -8dBm measured in 200 MHz. The protection of this frequency band is intended to protect satellite passive services from interference. To fulfill this requirement is difficult without either stringent requirements on the transmitter or without a RF band filter located between the PA and the antenna.

Operation in the NR band n258, where the lowest frequency of operation is only 250MHz apart from 24GHz will therefore require additional filtering to ensure that the power limit in the restricted band is not exceeded. As can be seen from the filter response in Figure 8-25, the attenuation 250MHz from the band edge is limited to just below 10 dB, which implies that the standard will be very difficult to comply with for this specific use case. However, it is possible to improve the RF band filter response in order to increase its attenuation at the lower band edge.

8.10.3. Antenna Configurations

Achieving 3GPP UE EIRP and EIS specifications for 5G FR2 (millimeter wave frequencies) with acceptable power consumption requires significant antenna gain and the ability to steer that gain in desired directions to maintain and optimize the link (as shown in Figure 8-28 below).

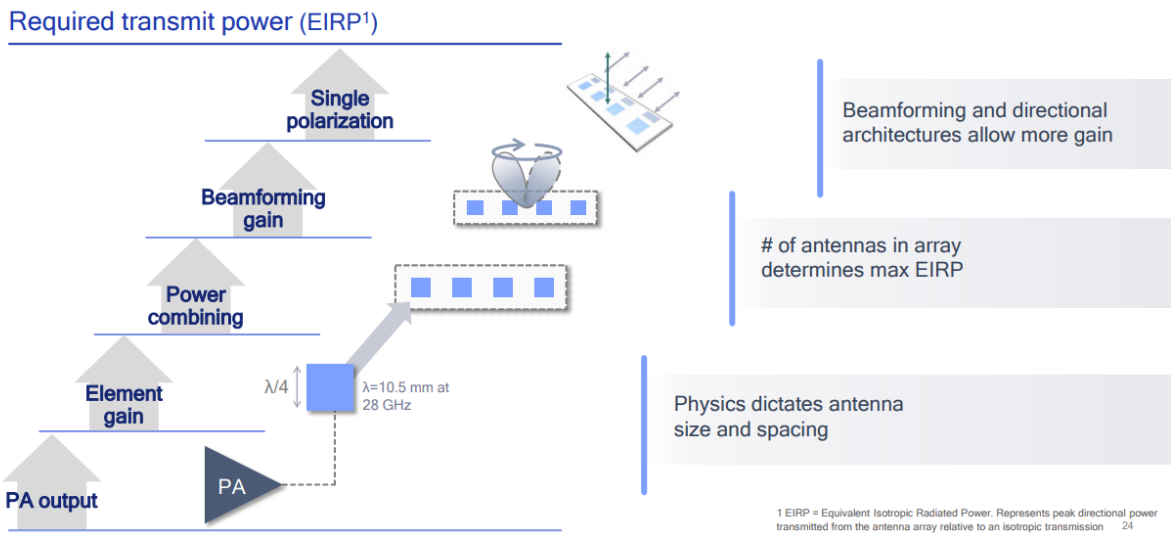

Figure 8-28 Factors to achieve required transmit power – Qualcomm [27]

The form factor of a mobile UE and the interaction with the user and environment strongly constrain practical implementations and realizable spherical coverage. Key considerations include the aspect ratio of the platform chassis, the display coverage of one or both large area sides, the cover materials, and collocation with FR1 antennas. Additionally, diversity in the quantity and location of antenna systems will typically be needed to achieve spherical coverage requirements in free-space and to improve robustness to user interactions.

This section will focus on these antenna configuration aspects.

Due to the very short wavelength at mmWave frequencies, a single half-wave dipole antenna would be only 4-5mm long. To achieve increased range, a small group of antenna elements (usually 4 or 8) are arranged in an array and phased to concentrate the transmitted power in a relatively narrow beam. Relative to transmitting the same total power from one antenna, the array achieves added gain of 10logN where N is the number of elements in the array. This gain applies in both transmit and receive. Antenna array factors that degrade the array performance from this ideal include direct coupling between the elements, surface waves with edge reflections, and differences in element patterns due to the finite overall structure size.

As mentioned earlier in this section, maintaining spherical coverage is key. For a handset, the antenna array will often be blocked by the user's hands, so it becomes important that additional arrays are implemented in different places around the handset case. Also as mention in section 5.2, 3GPP defines Sperical coverage in terms of EIRP CDF. It can be observed that the EIRP value at CDF = 50% vary dramatically with different phone factor, where the choice of phone case materials and the placement of antenna panel perform a serious impact on the CDF of EIRP for each device. Therefore, the integration of antenna arrays will be another critical point than the antenna array design itself.

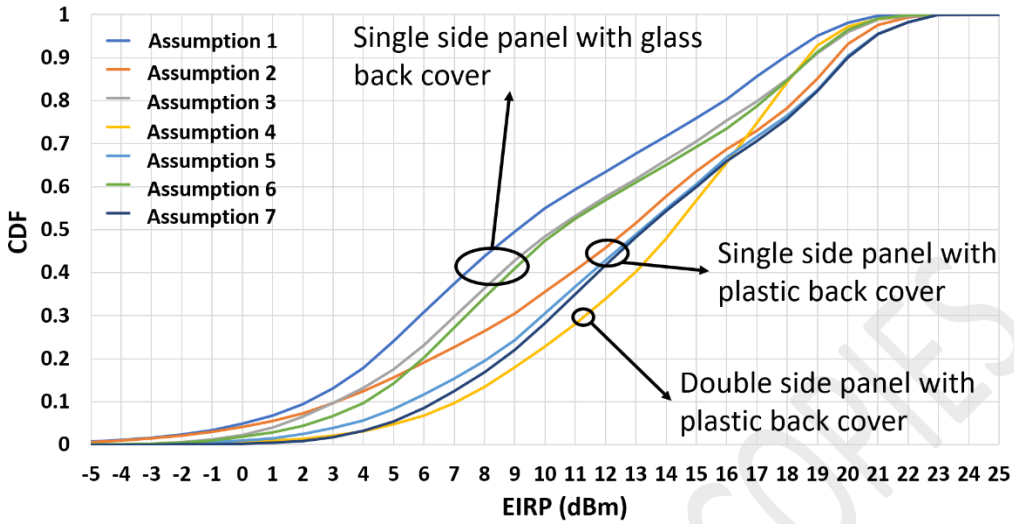

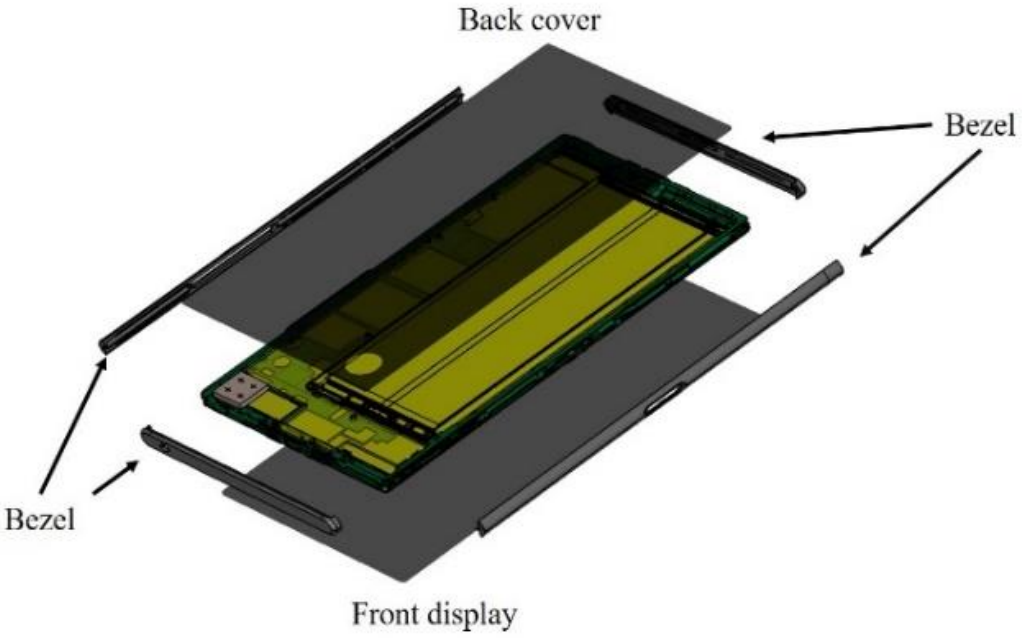

Figure 8-29 CDF distributions for a few realistic multi panel smartphone cases are simulated.

8.9.3.1. Dual/circular polarization antennas

The use of multiple operating arrays provide a mechanism for MIMO operation. In this case, the arrays beamform as needed in different directions into the multipath environment, to create multiple spatial channels, thus widening the total data pipe with proper decoding. If the individual antenna element is of a type that can be driven in orthogonal polarizations (as is the case for a patch antenna), the order of diversity or MIMO for the system can be further extended by driving these polarizations independently.

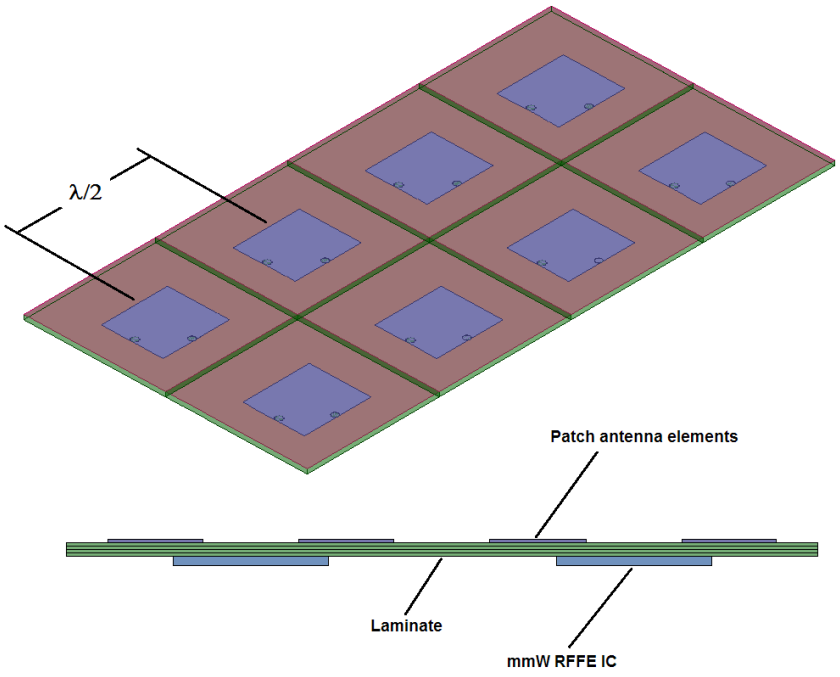

Figure 8-30 mmWave co-located RFFE/Antenna module – Skyworks.

Pictured here (Figure 8-30) is an example of a mmWave antenna array module. This example is a 2x4 array. The patch antennas are spaced center-to-center at a pitch of l/2, which is 5.4mm for 28GHz or 3.8mm for 39GHz. Looking closely at the antenna patches, two drive points can be seen on each, located on perpendicular sides. These are used to independently drive the two orthogonal modes that are available in each patch; these are often referred to as the "horizontal" (H) and "vertical" (V) modes. So effectively there are 16 independent antenna elements shown in this example. They may be served by two RFFE ICs, as shown, each 4H+4V, or a single RFFE IC of 8H+8V.

Although dual or circular polarization capability in the UE would bring diversity or MIMO benefits, they are not yet included in 3GPP requirements for the UE due to difficulties in effective implementation and the additional cost and complexity of the resulting system. Larger platforms may implement this as a differentiating factor.

Polarization diversity is far easier to implement in the UE than simultaneous dual polarization. Antenna elements can be switched to provide orthogonal polarizations but effective implementations along the edge of the UE present challenges due to the highly asymmetric ground plane.

To accomplish dual polarization antennas in UE´s presents challenges, at least for smartphones. The reason is, not only the mechanical design difficulty of integrating orthogonal feeds for the particular element design chosen, but also the presence of characteristic resonance modes from any conductors near the antenna metallic structure. Surface currents induced in chassis or PC-boards tend to de-polarize the radiated fields.

As an example, consider a dual-polarized endfire phased array for 5G handset devices at 28 GHz. The 4-element array has a low profile of 1.1 mm thickness and a small clearance of 2.7 mm. The array element is fed with Substrate Integrated Waveguide (SIW), which in the default mode works as a waveguide (WG) antenna with a vertically polarized radiation pattern. Two transition plates were used to improve the impedance matching of the WG antenna. The horizontal polarization is generated by exciting a two-patch transition. The other transition plate is modified as a group of triangle strips in order to minimize its reflection on the horizontal radiation patterns. A -10-dB simultaneously matched frequency bandwidth of 5.3% was achieved for both polarizations. At -6 dB matching limit, a simultaneous bandwidth of 25% was achieved. The end-fire gain ranges from 6.65 to 8.03 dBi and from 4.36 to 8.05 dBi for the horizontal polarization and the vertical polarization, respectively. Furthermore, both polarizations obtain the same gain when the proposed antenna scans within 0 and 40 degrees. Moreover, good agreement between simulations and measurements are shown in the below pictures.

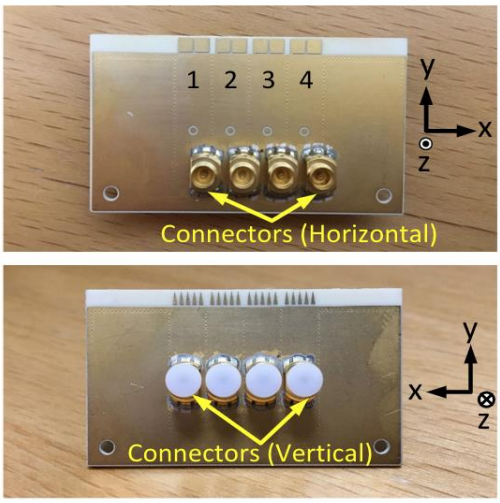

Figure 8-31 Prototype dual-polarized array [105]

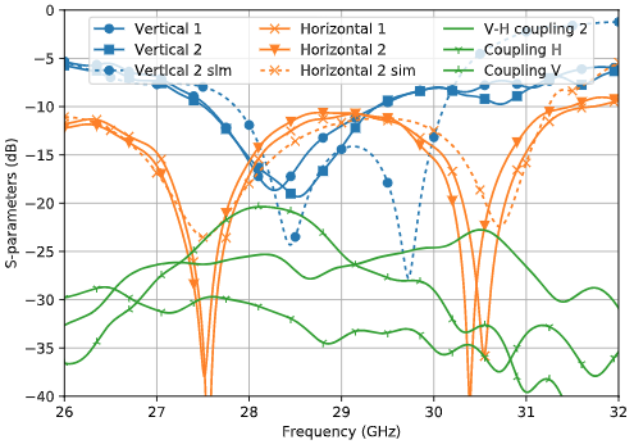

Figure 8-32 Measured and simulated reflection coefficients.

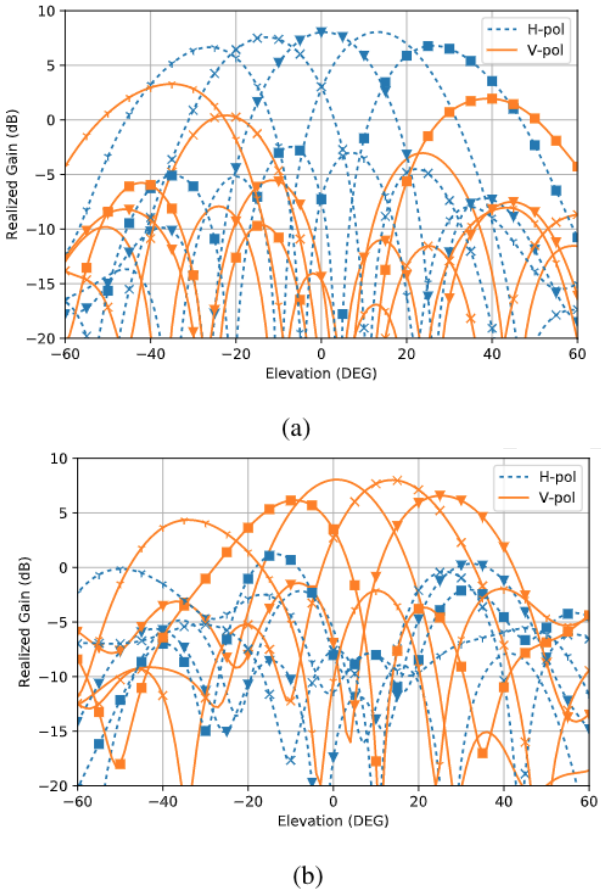

Figure 8-33 Scan patterns at 29 GHz: (a) H-mode, (b) V-mode

8.9.3.2. Reconfigurable antennas/arrays to realize large beam-scan coverage

Reconfigurability can be applied to several aspects of UE mmWave antennas.

1. Radiation pattern modifications for individual antenna elements
2. Switching between directional sub-elements
3. Polarization modifications.
4. Using 1 and/or 2 in an array to increase scan angle and reduce the arrays required for spherical coverage.

As an example of #4, consider an array where individual elements can be reconfigured for widely different radiation patterns, a 3D radiation pattern reconfigurable antenna (RPRA). These elements can be used in an array to form a reconfigurable phased array (RPA). For example, consider an element along an edge of a chassis that has three switchable radiation patterns: the broadside above the plane of the terminal, the opposite broadside below the terminal and an end-fire in the plane away from the edge. Each of the three different radiation patterns covers a different area in the Azimuth plane. The phasing is used to scan the

full RPA in the Elevation plane. By combining the beam switching and beam scanning, the RPA can provide much higher spatial coverage than conventional phased arrays, greatly reducing the number of arrays required for spherical coverage. By combining the beam switching and beam scanning, the proposed array can reach a large spatial coverage with less array elements compared to other approaches.

The beam switching was realized in prototypes using PIN diodes or with copper wire jumpers. Products based on this concept would use high-performance semiconductor or MEMS switches. Two examples of this approach follow, narrowband elements in an 8-element array and wideband elements in a 4-element array.

The narrowband approach [106] feeds each element with Substrate Integrated Waveguide for low loss and high isolation. Note that the RPA has a planar structure and requires small clearance on the ground plane for compatibility with mobile phone use. The 8-element RPA provides greater than 10 dBi gain and 1 GHz of bandwidth around 28 GHz.

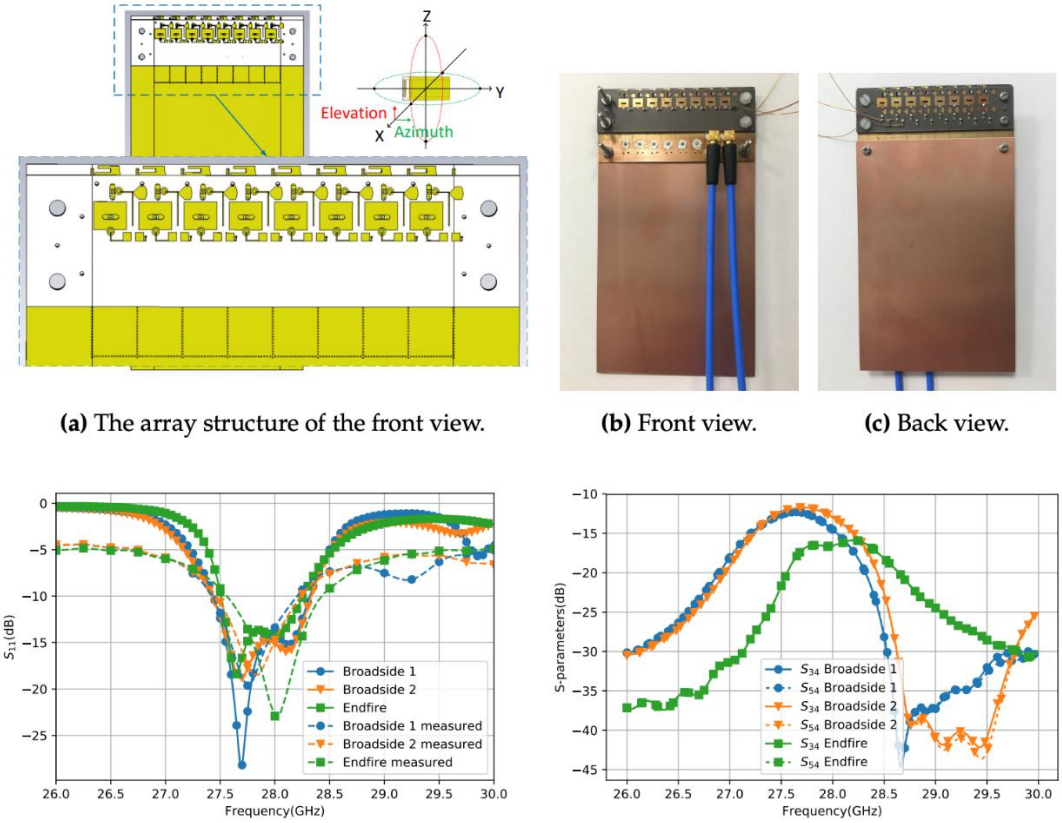

(a) The array structure of the front view. **(b)** Front view. **(c)** Back view.

(d) The simulated and measured reflection coefficiency of the middle element. **(e)** The simulated mutual coupling of the middle element.

Figure 8-34 Narrowband RPA configuration and performance [106]

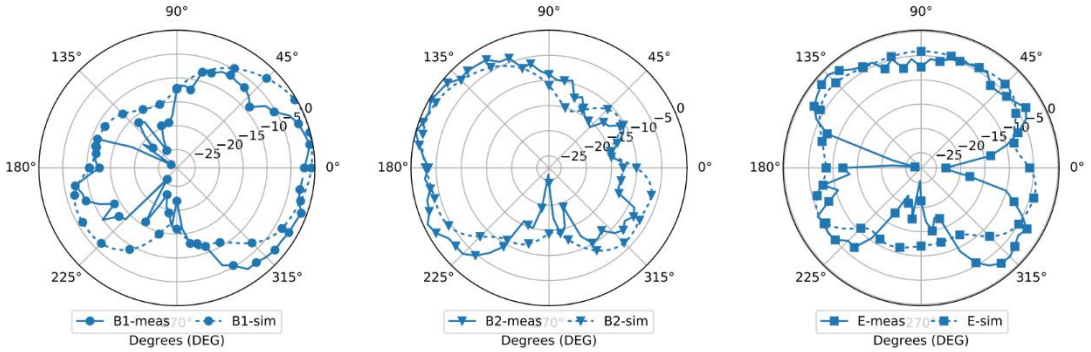

(a) Broadside 1 (b) Broadside 2 (c) Endfire

Figure 8-35 Simulated and measured radiation patterns with copper wire.

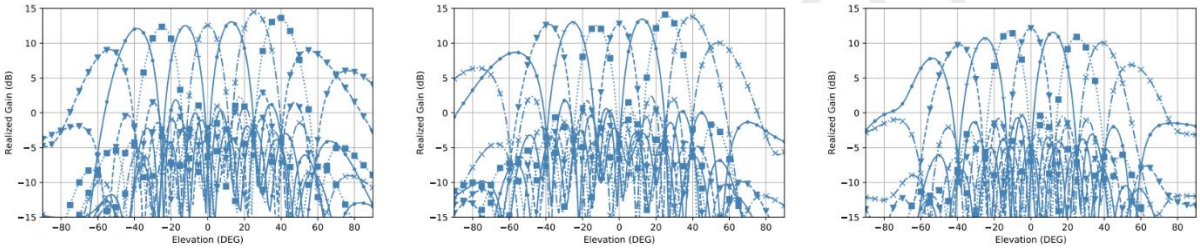

(a) Broadside 1 (b) Broadside 2 (c) Endfire

Figure 8-36 Array scan pattern in the elevation plane.

The wideband approach [107] uses a 4-element RPA built with RPRA elements with a wide working band from 24 GHz to 27.5 GHz, covering two of the primary frequency ranges for 5G. This array is also planar with a very small clearance of 3.4 mm. The beam switching is realized by applying two reconfigurable directors on both sides of the dipole. Three PIN diodes are mounted on each of the directors. The low loss of the PIN diodes is required for high radiation efficiency. The measured results show good agreement with the simulations as depicted in the following figures. The gain is lower than the narrowband as this array has only 4 elements.

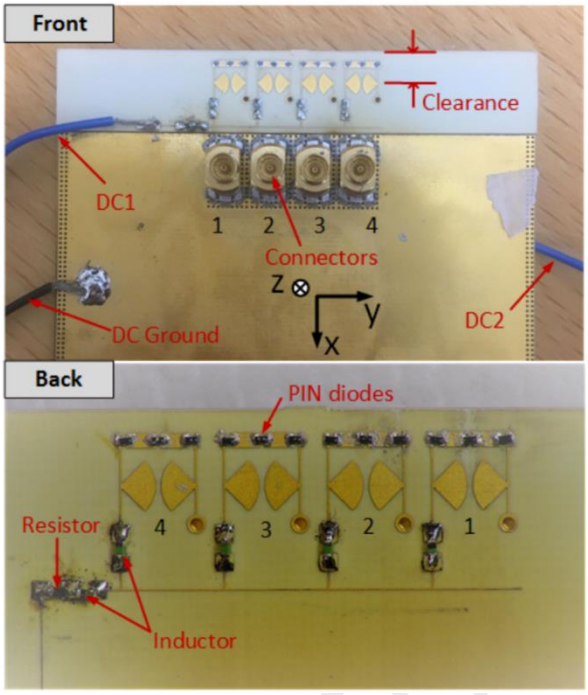

Figure 8-37 Structure of the proposed 4-element array [107]

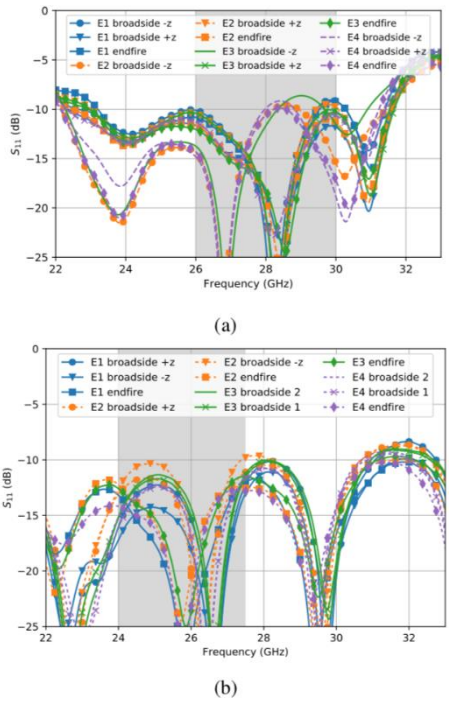

Figure 8-38 (a) Simulated and (b) Measured return loss.

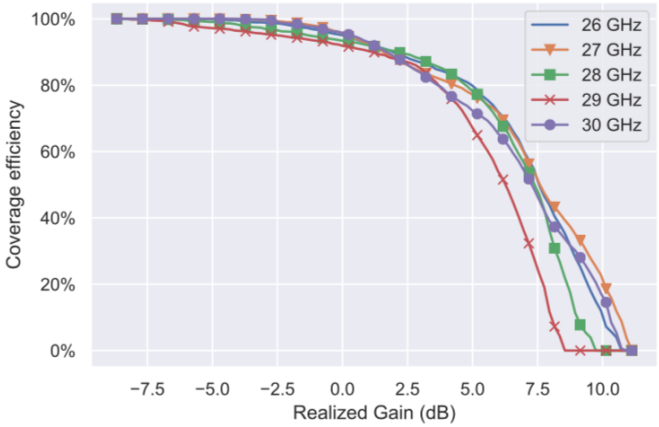

Figure 8-39 Simulated coverage efficiency within the operation bands.

8.9.3.3. Low-loss beam-steering antenna arrays without phase shifters

The insertion losses of commercially available semiconductor-based phase shifters at mmWave frequencies are too high for passive beam forming in UE arrays thus the arrays require active beam steering circuits. Also, the performance of phased arrays are also limited by the variation in delay with frequency of the phase shifters, leading to shifts in beam pointing over a wide bandwidth [110]. Moreover, the array element distance, which depends on the selected frequency, influences the gain at the lowest frequency and the coverage at the highest frequency of the interval. Smartphone mmWave antennas do not require very high directivity, only what is sufficient to provide the specified peak EiRP and wide spatial coverage, their element power beam-widths typically can stay in the range of 60°-90°. This means the number of beam states can be kept small, e.g. to 4-5 states per panel. While phased arrays can offer much higher resolutions, this is unnecessary for UE applications. In turn this implies beams can be controlled by simple switching schemes instead of phase shifters. Available switches offer <2 dB I.L. throughout 24-40 GHz compare to 4-7 dB phase shifter losses. Additionally, the beam direction of each setting does not depend on the alignment of multiple chains of electronics with and more consistent performance over environmental variation and over the terminal lifetime should be realized. This may also reduce test and calibration time.

The antenna configurations utilizing switching schemes can take any of the following forms:

- Single directive element (e.g. Yagi) antennas distributed around the UE chassis pointing in different directions
- Couplers and delay-lines with switches configured in a Butler Matrix formation for small array
- Various ESPAR arrays configured by switches or tuners

As an example, consider a wideband beam-steerable array using such hybrid high gain antennas selected by switches. The architecture, shown in Figure 8-40, consists of five microstrip-fed Quasi-Yagi antennas, characterized by unidirectional radiation and high gain, pointing in different directions. The distance between adjacent antennas varies to ensure low mutual coupling and reduce the spurious lobes. The antennas are printed symmetrically on both sides of the short edge of a Rogers RO3003 substrate, with

permittivity ε_r = 3, loss tangent δ = 0.001 and thickness 0.762 mm. The truncated ground plane acts as reflector and is contoured to follow the inclination of the corresponding antenna to maximize the gain. The driving dipoles are printed symmetrically on both faces of the substrate, with the half dipole in the bottom grounded to the ground plane and the half dipole on top connected to a microstrip line fed to an SPMS connector or a multi-throw switch in the demos. The reduced number of directors of the three central antennas allows to minimize the length of the clearance to 6.5 mm. The directors are printed on both sides of the substrate in order to maximize the directivity. In particular, ladder-like directors [111] are chosen for the central and the corner antennas and a bowtie dipole [112] for the three central antennas, in order to enhance the antenna gain and enlarge the bandwidth.

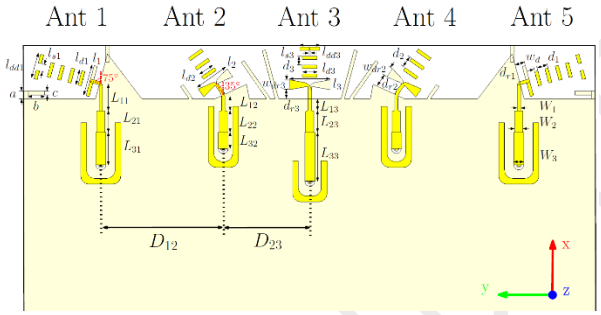

Figure 8-40 Geometric structure and parameters of the planar printed Quasi-Yagi antenna array [113]

The simulated S-parameter characteristics of the proposed design, reported in Figure 8-41(a), show that the Yagi-Uda antenna system covers a bandwidth of over 18 GHz in the band of 28 GHz and the isolation between neighboring elements is over 20 dB. Moreover, the realized gain of each component is above 7 dBi over the frequency band 26 – 40 GHz, as highlighted in Figure 8-41(b).

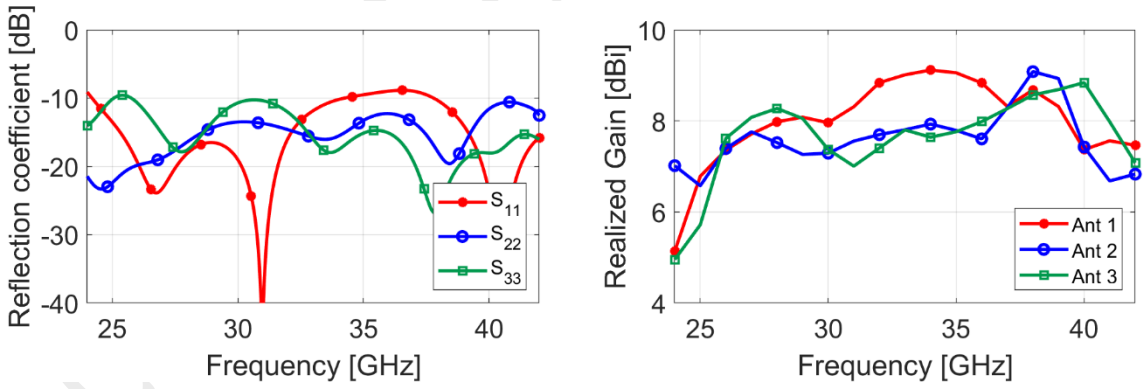

Figure 8-41 (a) Sim S-parameter characteristics (b) realized gain of Yagi-Uda antenna elements. [113]

The 2D-coverage property of the antennas system at 28 and 38 GHz is plotted in Figure 8-42. Each antenna scans a specific portion of the sphere, to cover the total span of 180°. As expected, the symmetric antennas generate symmetric radiation patterns, which become narrower at the higher frequencies (Figure 8-42(b)), increasing consequently the gain from 8 to 9 dBi.

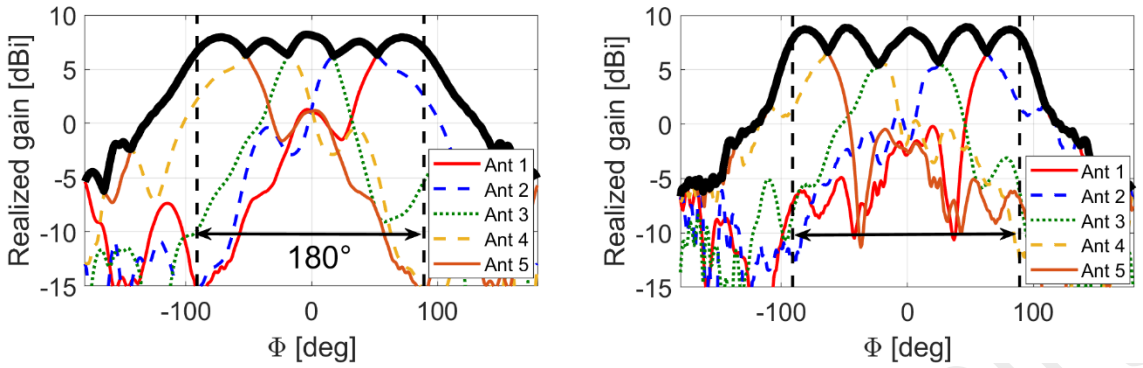

Figure 8-42 Spherical coverage of the 5-element antenna system at (a) 28 GHz and (b) 38 GHz. [113]

Thanks to the flexibility of the proposed antenna system, alternative placements of the antennas on the PCB have also be been evaluated in order to optimize the space, simplify the switching and minimize the feed length. A set of compact arrays of four elements at each corner represents a good trade-off between performance and dimensions, achieving the desired beam scanning at 28 GHz with high gain. The corner array also enables the most compact feed and switching solution.

Passive and active measurements of fabricated prototypes were performed with the MVG Starlab 50 GHz. The results of the passive measurements are in accordance with the simulations. The active measurements of the array connected to the FEM and integrated into a phone-case further confirm the radiation properties of the switchable antenna array at 28 GHz in a realistic scenario.

Another promising approach is using the ESPAR. Consider the simple configuration as shown in Figure 8-43, with one active element and two passive parasitic elements. By changing the reactive loading impedance of the parasitic elements, they can work either as a reflector or director as the loading is inductive or capacitive, respectively. The loading impedances can be effectively realized in many ways including switching between fixed loads, a programmable tuner or low-loss phase shifting circuit with short or open termination. The parasitic loads for the prototype were realized by a set of transmission lines of different lengths, each with a far end either shorted or open. The intent is to use a SPNT switch to select the desire load. The insertion loss of available SP4T switches is around 2.5 dB at 28 GHz. Since the switch is connected to the passive elements, the total impact to efficiency in the whole antenna system is less than 2dB. It is expected in a product implementation that the control and the parasitic loading would be integrated into a single integrated package and lower loss parasitic tuning would be employed.

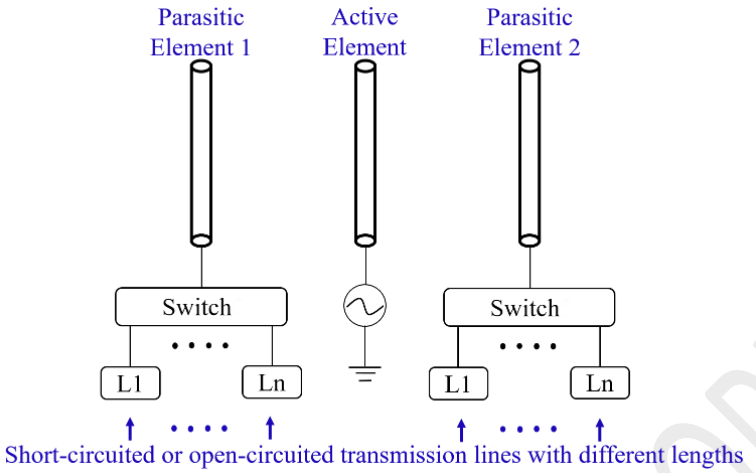

Figure 8-43 Beam steering with 2 passive parasitic elements.

The prototype antenna array with 2 passive parasitic elements is shown in Figure 8-44. In Figure 8-44(a), two beam-scanning arrays (i.e., array A and array B) are placed near the center of each long chassis edge. The different major parts in one array are shown in Figure 8-44(b) with surface copper, substrate and Polypropylene (PP) dielectric block hidden. The array consists of three monopoles. One monopole (out of three) is active and fed by substrate integrated waveguide (SIW), which is the only element connected to the RF port. The other two monopoles are passive and connected to the inputs of two switches via microstrip lines. The outputs of each switch are terminated with short-circuited microstrip lines of different lengths. By controlling the two switches, different reactive impedance can be loaded on two passive monopoles. The array volume is 2.5 × 2.5× 8.5 mm3. Each array has three monopoles with the inter-element distance of 3.5 mm. The height of each monopole is 2.5 mm. Note that the height can be further decreased by design variations, e.g. capacitive loading (add a small circular metal disc at the end of each monopole). The diameter of the monopoles and the width of the microstrip lines are 0.5 mm. Since the polarization of the monopoles is perpendicular to the chassis, strong surface currents are excited on the metal back cover that enlarges the gain of the small array. A PP block is applied as a supporting material for the monopoles. In Fig. 2 (d), the lengths of 5 short-circuited microstrip lines are L1=2.6 mm, L2=2.3 mm, L3=1.8 mm, L4=1.3 mm, L5=0.7 mm, respectively.

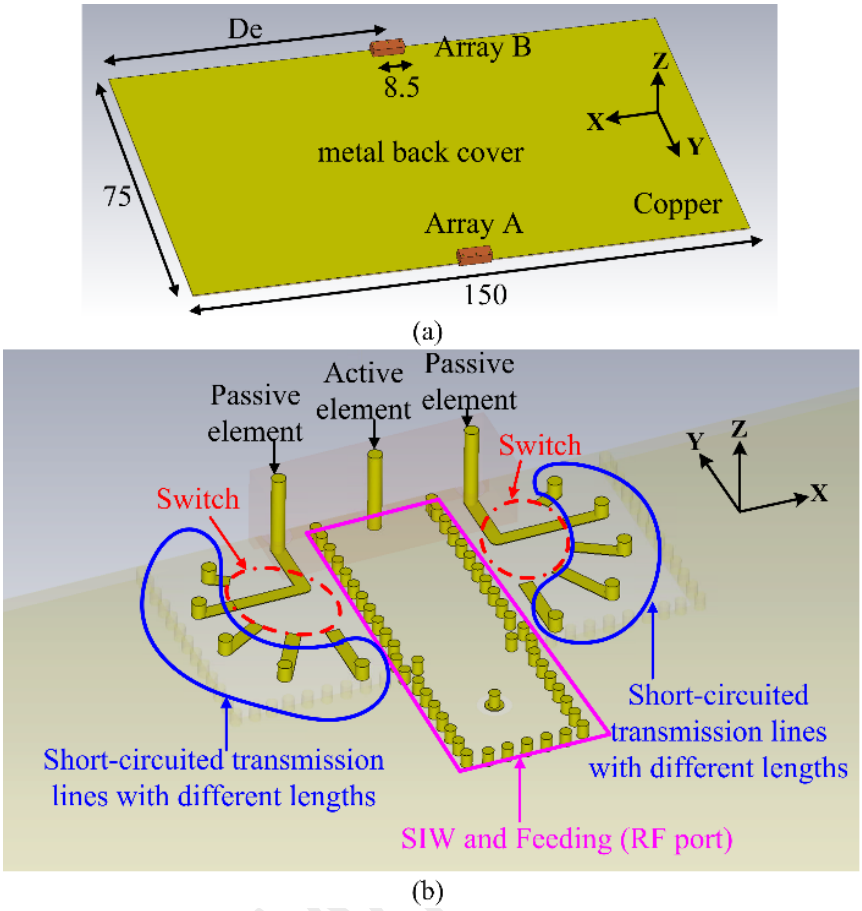

Figure 8-44 Proposed beam-steerable array: (a) 3-D view, (b) general view of 1 array [114]

Figure 8-45 shows the resulting radiation patterns when steering the beam with different loaded impedances to two parasitic elements. 180 degrees of beam steering is achieved. If we also apply another identical array on the other side of the ground plane, the beams of two arrays can cover all the directions in horizontal plane (360 degree). In Figure 8-46 and Figure 8-47, the realized gain and S parameters in different states are shown, respectively. The gain is over 9 dBi in the band of 28-29 GHz with return loss better than -14 dB across all states.

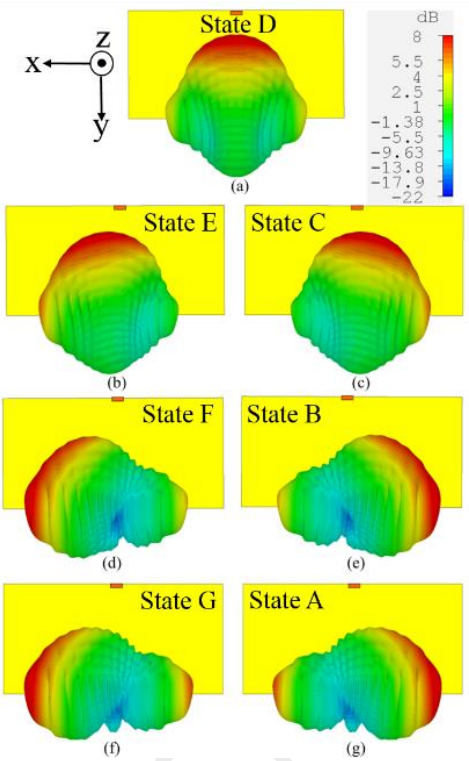

Figure 8-45 Simulated 3D radiation patterns at 28.5 GHz

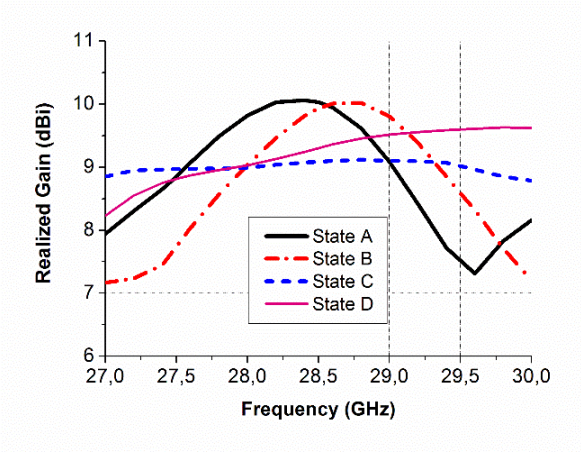

Figure 8-46 Simulated realized gain in different states

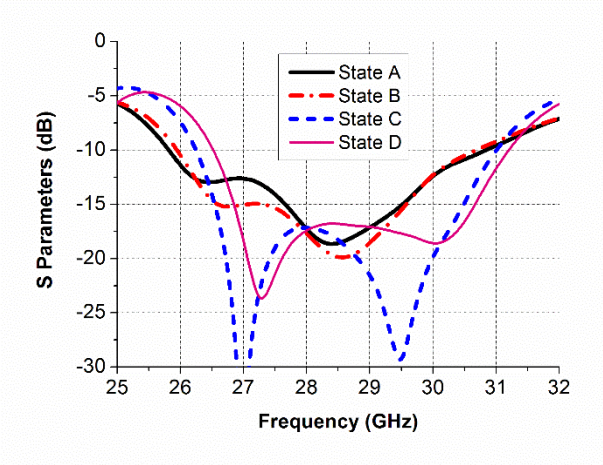

Figure 8-47 Return Loss in different states.

8.9.3.4. High performance beam steering components

The choice of architecture for beam forming in terminals depends strongly on the performance of the circuit elements available and their effective integration. For example, if small, high-performance switches were available, architectures with switches between the antenna elements and the active circuits would become feasible. Similarly, if integrated low-loss phase shifters were available (1dB or less), passive beam forming would become attractive, leading to reduced interference and easier calibration. Additionally, the need for beam-steering systems that preserve their performance over multiple FR2 bands may drive a need for mm-Wave tuning for matching the antenna elements and for side-lobe suppression. The multi-band requirement also will likely drive the need for tuning and/or reconfigurability throughout the signal chain.

As losses in mmWave circuits tend to be high, it is critical to place the amplification close to the radiating elements and minimize the loss of circuit elements between the two.

8.9.3.5. Multi band antennas

Antennas can either be designed for dual band resonances or for a single wide band to cover the currently proposed 28/39 GHz bands. Under discussion at 3GPP are extensions of these bands such that the most challenging global design would call for a 24.25 – 29.5 GHz and 37-43.5 GHz coverage. It is expected that region-specific UE´s will only cover portions of these bands. In addition to the bandwidth requirements of the antenna elements, another fundamental issue comes with array antennas is that in order to minimize surface waves and unwanted sidelobes, and thus focus the radiation energy in the desired direction, it is preferred to geometrically separate each element by a λ/2 distance. Note that λ/2 at 27 GHz corresponds to 5.6 mm (in air) but at 39 GHz this is 3.8 mm. In practice, a compromised separation design needs to be found or electrical adjustment is required in the effective element spacing.

8.9.3.6. Wideband/multi-band antennas/arrays with a small clearance

Many radiating elements at FR2 frequencies are highly loaded and thus are difficult to match over a large bandwidth with high efficiency. Space is also at a premium on the UE periphery. An example phased array uses an element that is designed to work around these limitations. This is a quad-mode end-fire planar wide scan angle antenna element with 1.2 mm clearance as shown in Figure 8-48. A previous wide scan angle antenna has been proposed [108] however that antenna element size was quite large. The compact antenna constructed in [109] only provided 4 GHz of bandwidth, whereas this antenna element can reach over 8 GHz bandwidth. Even after including a coax-to-differential stripline transition and MMPX connectors for testing, the impedance bandwidth at -7 dB match is around 12 GHz as shown in Figure 8-49.

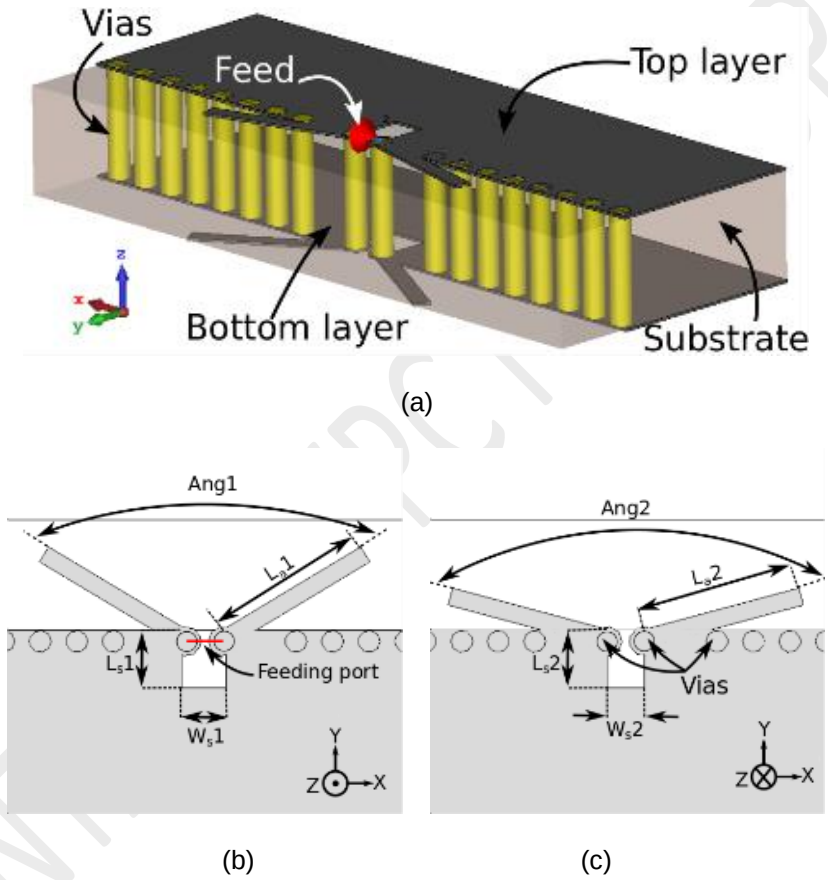

Figure 8-48 Antenna element geometry: (a) 3D view, (b) top layer, and (c) bottom layer.

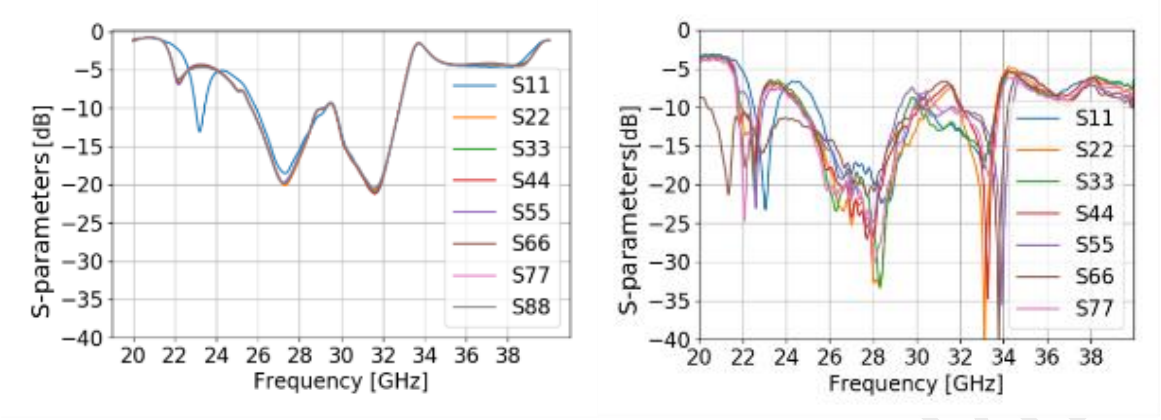

(a) (b)

Figure 8-49 (a) Simulated and (b) measured reflection coefficients of the proposed antenna array.

The intent is to efficiently combine these wide-band multi-mode array elements with different radiation patterns for each mode into a phased antenna array. However, in the array, similar and wide embedded radiation patterns are obtained for the all frequency ranges. This utilizes the neighboring elements to create alternative open loop current paths as in Figure 8-50 and thus, unwanted sidelobes within the operating frequency range of antenna are suppressed.

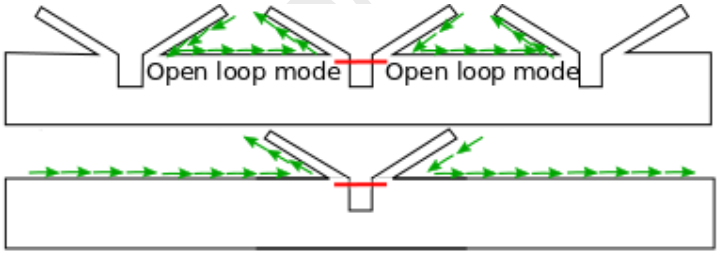

Figure 8-50 Open loop mode created by introducing neighboring elements.

The total scan pattern and coverage efficiency of the measured and simulated phased array antenna are calculated in the range from 25 to 33 GHz with a step of 1 GHz and a good agreement between measured and simulated results is observed in Figure 8-51. The mean coverage efficiency along the frequency range is very similar, but minor difference in variance of coverage efficiency is observed in the measurements. A coverage efficiency of around 50 % for the threshold gain of 5dBi is achieved in the chosen frequency range.

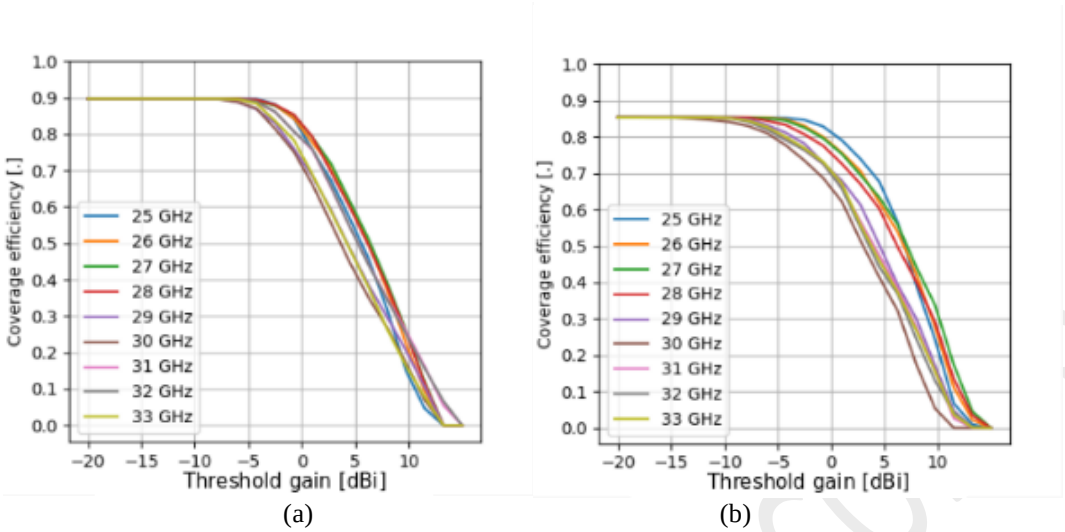

Figure 8-51 (a) Simulated and (b) measured coverage efficiency of the proposed antenna array.

8.9.3.7. Co-Integration of sub-6GHz antennas and 24-28 GHz antenna arrays

With the inclusion of 5G FR2 bands, new antennas must be added into in the highly limited space of handsets. FR1 antennas already occupy a large portion of the terminal periphery, particularly at the ends. Since the terminals must continue to support the FR1 frequency bands, solutions must be found for FR1 and FR2 antennas to share area and volume. An example of a mm-wave array is integrated with a 4G LTE planar inverted F-antenna (PIFA) [115]. An end-fire radiation pattern is obtained by adding a layer of grating strips between the mm-wave array and the low-frequency antenna. However, this design does not take into consideration the metal frame of many commercial phones, which is employed as a sub-6GHz antenna [116][117]. In [118], a large cut is made in the metal rim of the phone for the mm-wave module. The metal rim is used as LTE antenna, therefore both antenna types need to be co-designed not to affect each other. However, the metal frame limits the beam-steering capability of the mm-wave array, and only a $\pm 25°$ scan is achieved. Authors in [119] have proposed a mechanism to integrate the low-frequency metal-frame antenna with the mm-wave antenna. It consists in placing tilted layers of strips at both sides of the top frame of the handset. When the end-fire mm-wave array radiates the energy towards the bezel, most of the energy that is reflected on the frame is coupled to the strip layers. They act as parasitic radiators, which combine the electromagnetic waves in phase, as shown in Figure 8-52.

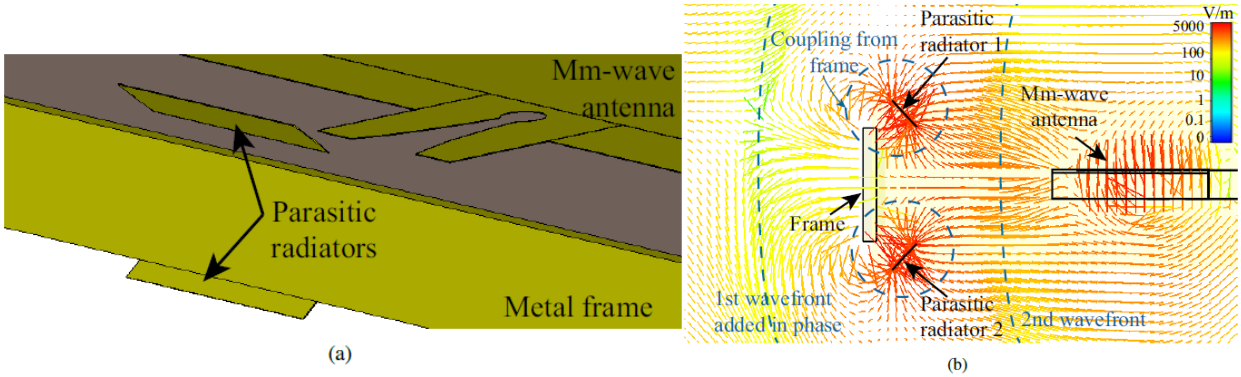

Figure 8-52 (a) mm-wave ant with frame & metal strips. (b) E-field of the mm-wave ant (side view) [119]

The two tilted layers of metal strips redirect the radiation in the end-fire direction across the target bandwidth, as shown in Figure 8-53. As shown in Figure 8-54, the mm-wave array in this solution is able to steer $\pm 60°$.

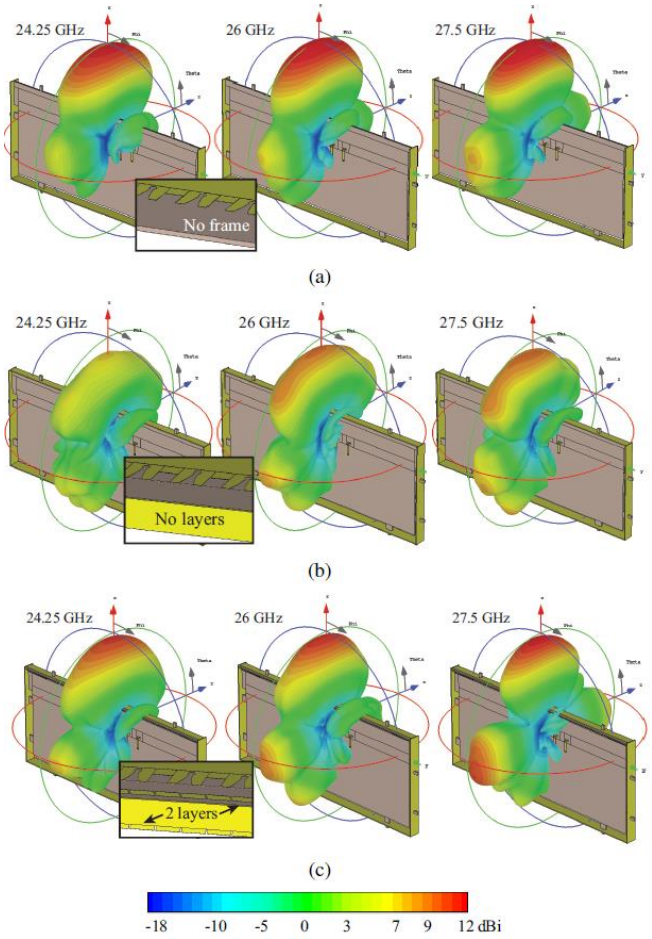

Figure 8-53 Radiation patterns with: (a) No frame. (b) No layers. (c) 2 layers [119]

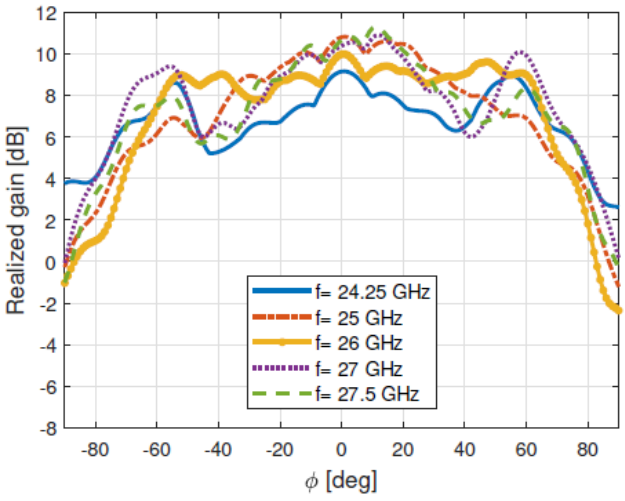

Figure 8-54 Simulated realized gain beam-steering envelope [119]

8.9.3.8. *Antenna module impact on user performance*

From performance viewpoint, in order to guarantee good coverage, the UE antenna performance must be independent of user handling of the device and LOS/NLOS operation. Qualcomm had performed antenna module testing (Figure 8-55 below) and found that with single antenna module, it can cover ~36% of overall spherical area, but when accounting hand blockage, the spherical coverage goes down to ~18%. This may not be enough to provide good isotropic coverage. However, it is not clear as to what are the absolute min and max gain values across the sphere just based on looking at the chart. As discussed above, to overcome the hand blockage issue and improve mmWave spherical coverage, use of multiple arrays in the phone plus a smart algorithm to select/combine arrays may be crucial. Initial real mmWave network performance evaluation by Signals Research Group [123] has shown some impacts (service interruptions) due to quick change of phones orientations. This could be due to delays in antenna module switching and / or beam management performance.

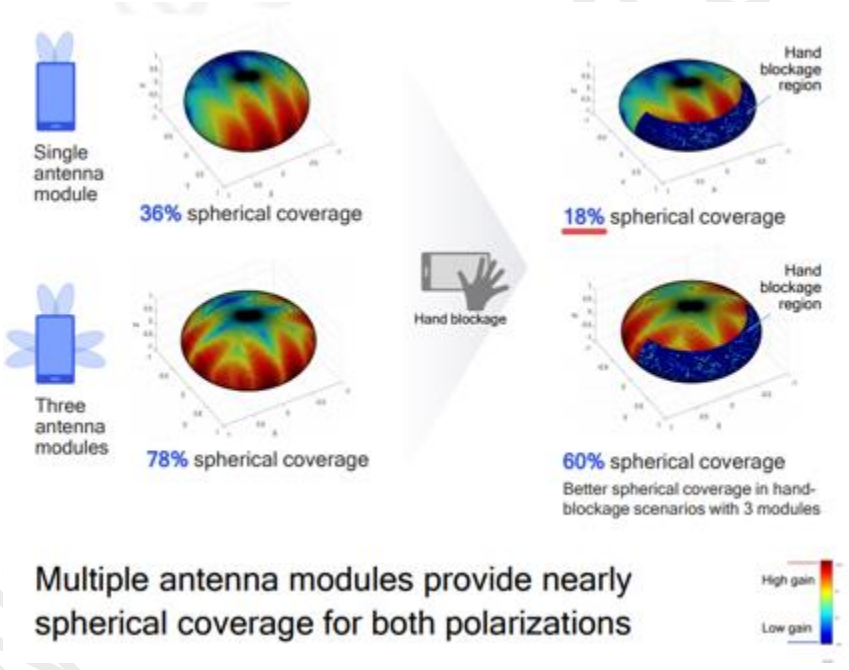

Figure 8-55 Hand Blockage performance impact – Qualcomm [27]

The Figure 8-56 below (Qualcomm) shows impact of number of antenna modules on user experience. In the DL cell edge scenario (MCL >135dB), use of 3 antenna modules could result in ~39% DL spectral efficiency gain and ~13% improvement in DL network capacity. However, it would be important to understand similar performance in UL as well, when available.

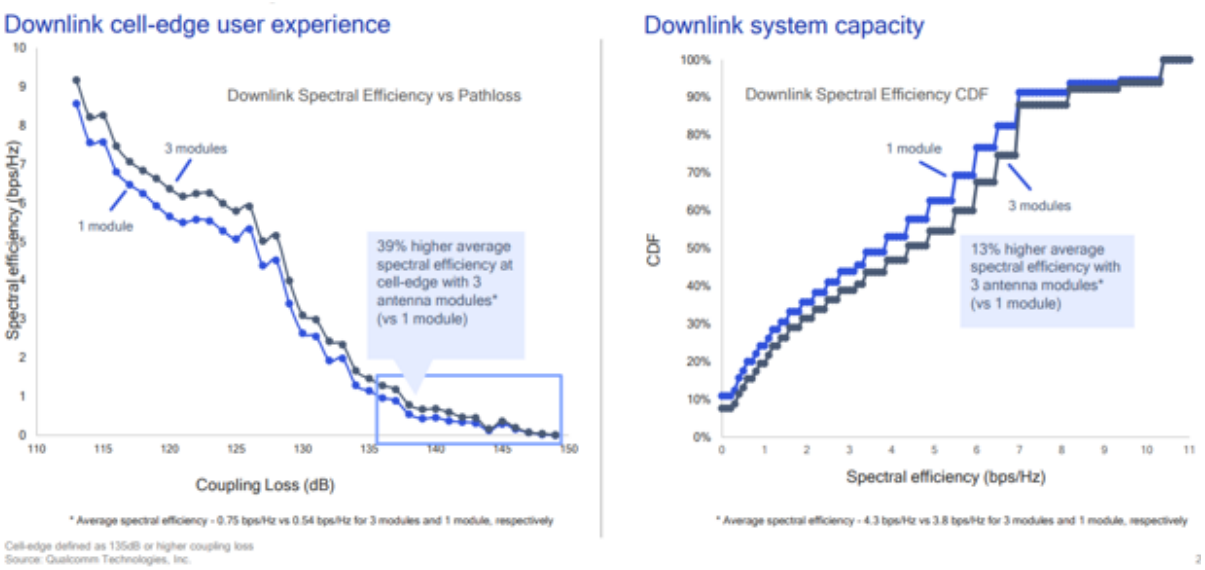

Figure 8-56 Antenna Module design performance – Qualcomm [27]

To summarize, mmWave handheld devices will require support for multiple antenna arrays of 1x4/2x2/2x4 elements configuration to mitigate hand blockage and improve overall user experience.

8.10.4. Power Consumption Constraints

Constraints on power consumption are one of the most challenging aspects of mmWave Mobility. UE customers value long time intervals between battery charging cycles. Consequently with each generation of UE devices, progressive improvements in battery technology concurrent with more flexibility in the means to charge those batteries is largely keeping pace with customer expectations. While 'bursty' type data communications has previously been shown to be efficient in respect of power consumption, and due to the wide channel bandwidths available in the FR2 bands, it is reasonable to propose that mmWave RF front-end power consumption must approximate the state-of-the-art sub-6GHz RF front-end power consumption once duty cycle is factored in. This may be a time-average of about 500mW for example, with the FR2-band uplink transmitter operated with duty cycle on the order of 10%.

At 28GHz, the FR2 UE of power class 3 ("PC3") must acheive a minimum of 22.4dBm Effective Isotropic Radiated Power (EIRP) while active, but it is limited to 23dBm total radiated power (TRP). In a typical case, the transmitter may achieve >30dBm EIRP while keeping just under the TRP limit, employing for example two 4-element arrays (possibly implemented as one array using vertical and horizontal polarizations).

In this case the required PA power per antenna element works out to about 17-18dBm, based on the following equation:

$$Po(dBm) = EIRP\ (dBm) - 20 \log_{10}(N_{ANT}\ \text{per array}) - 10 \log_{10}(N_{ARRAYS}) - G_{ANT}\ (dB) + \text{Post PA Losses (dB)}$$

where N_{ANT} is the number of antenna elements per array, N_{ARRAYS} is the number af arrays, and G_{ANT} is the antenna gain an individual antenna element. Some reasonable assumptions are G_{ANT} = 3dB, and post-PA losses = 2dB to 5dB, depending upon the type of RF switch, length and type of post-PA interconnect, enclosure material, etc.

We can then estimate the power consumption, being careful to note that widely-varying factors will include power amplifier efficiency, directivity of the antenna elements, power consumption in the RF synthesis blocks, etc. Given our example of 8 antenna elements driven by 8 PAs, and assuming ~15% backed-off PA efficiency, and that ~75% of the total power consumption of the mmWave RF front-end in transmit mode is, in fact, consumed by the PAs, then with 10% duty cycle our target of overall <500mW power consumption is met.

A recent academic review [67] of power amplifiers for mmWave 5G applications demonstrates that SOI technology leveraging stacked nMOS transistors can provide operation at 64QAM OFDM signals (with 800 MHz bandwidth and 8dB back-off at 28GHz) at 13dBm output power and more than 17% PAE without using digital predistortion.

While output signal amplification to ~14 – 18 dBm of linear RF power (P1dB ~22dBm) is a major factor in the power consumption contraints, additional power consumption in the transciever, LO generation (including LO buffering) and even digital processing for very wide bandwidth is significant compared to 5G FR1 or 4G with carrier aggregation. Consequently, mmWave data throughput should further be evaluated in terms of power consumption per bit/sec.

Besides the RFFE components considerations for power consumption, it is also important to understand / analyze other RF and technological aspects that could have an impact, especially for mobile / handheld use case since it involve the use of battery.

As we know that mmWave coverage is limited to few 100s of meters. The UEs are most likely to be in cell edge like scenario if not LOS due to various losses incurred. This would result in UE transmitting at higher/Max Tx power most of the time. This would particularly impact mobile device performance more due to higher hand / body blockage / losses.

mmWave 5G NR operation in a mobile use case, involve beam management for mobility purposes in both DL and UL. Mobility is more frequent with beams and mmWave due to smaller coverage area. Beam management involves constant monitoring, steering, measurement and switching of beams. This operation results in higher power consumption. Frequent measuring of such beams and providing channel state information feedback results in additional overhead and in turn impact battery life. Initial real mmWave network performance evaluation by Signals Research Group [123] has shown that a constant 1-2Mbps of UL data and a constant Tx power of 6dBm was used independent of user data. This may have a significant impact on device power consumption as device is required simultaneously to transmit on both mmWave and sub-6GHz frequencies at the same time (i.e. mmWave link sends PHY layer feedback for the

purpose of massive MIMO/beamforming functions while UL data transfer happens in sub-6GHz frequencies).

Also, mmWave bands support wider channel BW which can support higher throughputs in downlink and uplink. Higher throughput will in turn require higher baseband and AP processing capabilities in the device. This would result in more power drain. With wider CBW, the baseline power to monitor PDCCH increase significantly. Also, the use of higher SCS with mmWave would result in more stringent processing time budget due to shorter symbol length. Thus, the wider BW increases the instantaneous power consumption even though it helps with high data throughput. Also, the power efficiency of these wideband PA may be worse. It is also anticipated that early 5G systems will require the PA to operate in APT mode to accommodate the wider bandwidth signals, which in turn would result in higher power consumption.

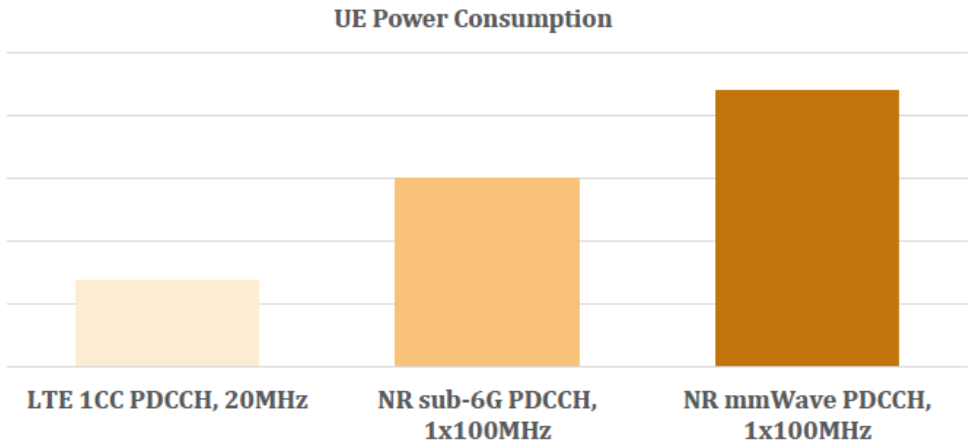

Figure 8-57 UE power consumption – Mediatek [40]

The chart (Figure 8-57) above from Mediatek illustrates the estimated power increase just to monitor PDCCH across with channel BW (up to 100 MHz). Supporting 400 MHz CBW would cause even higher increase in power consumption.

Having said that, there are couple of power saving techniques to counteract the channel BW increase, with the help of gNB. The key feature here would be to use the Bandwidth Parts (BWP) where the gNB could flexibly configure a shorter BWP to monitor PDCCH and switch to wider BW when there is data to send as shown in the Figure 8-58.

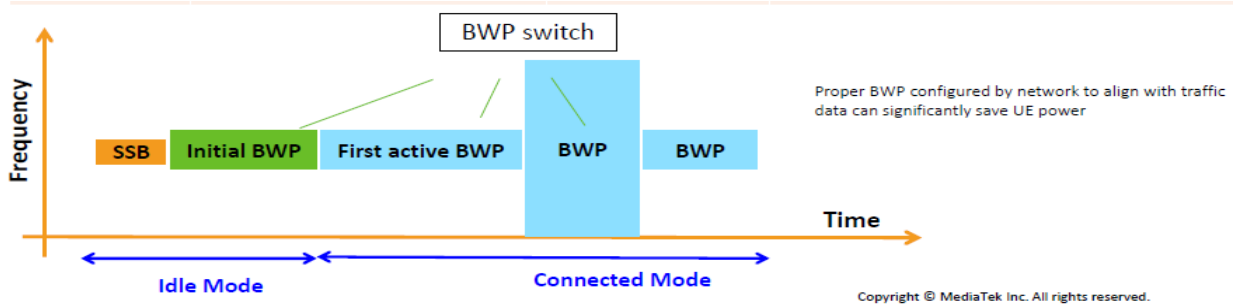

Figure 8-58 Adaptive BWP – Mediatek [40]

The power saving gain by BWP is expected to be 30-50% depending on the traffic type [40].

Another feature to help reduce power consumption would be to use cross slot scheduling where the UE can temporary turn Rx OFF during PDCCH decode since the data scheduling would not be in the same slot as seen in the Figure 8-59 below.

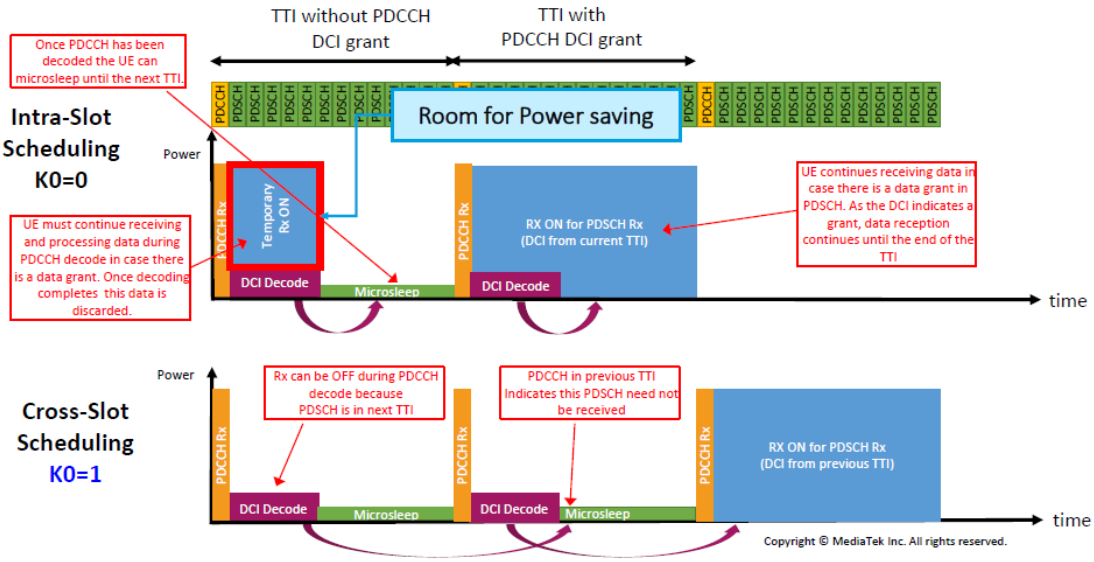

Figure 8-59 Cross Slot Scheduling – Mediatek [40]

The Table 8-5 below from VIVO summarize the impact of various 5G features on power consumption of various components with a device.

◆ Effect of 5G features on device power consumption

5G features	ATU	RFFE	RFIC	BP	AP	Level
Bandwidth	√	√	√	√	√	High
UL-MIMO	√	√	√	√	√	High
HPUE	√	√	√	√	√	High
BWP	√	√	√	√	√	High
DRX	√	√	√	√		High
Cross-slot scheduling	√	√	√	√		High
Numerology	√	√	√	√		High
Measurement	√	√	√	√		Medium
System information acquisition	√	√	√	√		Low
Paging	√	√	√	√		Low
RNA update	√	√	√	√		Low

Table 8-5 Effect of 5G features on device power consumption – VIVO [41]

This table is particularly related to Sub-6GHz deployment scenario. Therefore, UL-MIMO and HPUE may not be as relevant here since these features may not be feasible at mmWave frequencies due to complexity, cost or specifications. The use of wider BW has impact on most of the device components and this applies to mmWave as well. The higher frequency of beam measurement in mmWave channels could also have an impact on power consumption.

Furthermore, 3GPP Rel 16 is making efforts to create user profiles such as small data profile, large data profile, sporadic traffic profile etc, that could be signaled which can help improve overall power consumption depending on user configuration.

To summarize, this section discussed various source of power consumption and its impact on battery life which is particularly important for handheld devices. It also discussed some of the mitigation techniques that may help overall power consumption. Further evaluation of the real UEs being recently launched, is necessary in terms of power consumption as there are a lot of implementation dependencies and newer operational technology.

8.10.5. Thermal Dissipation considerations.

A challenging factor for mmWave mobility is thermal dissipation due to the fact that much more of the mmWave transciever is pushed into the front-end module perhaps integrated (or co-located) with the antenna elements. Consequently, temperature sensitive elements including functional blocks for up/down conversion may be exposed to the thermal load of the transmitter path. As was described in section 8.10.4, transmit path efficiency is expected to be between 5% and 20% such that 2- 4W of front-end power consumption transforms to heat generation of approximately the same proportion.

The chart below illustrates just the mmWave PA operation / efficiency.

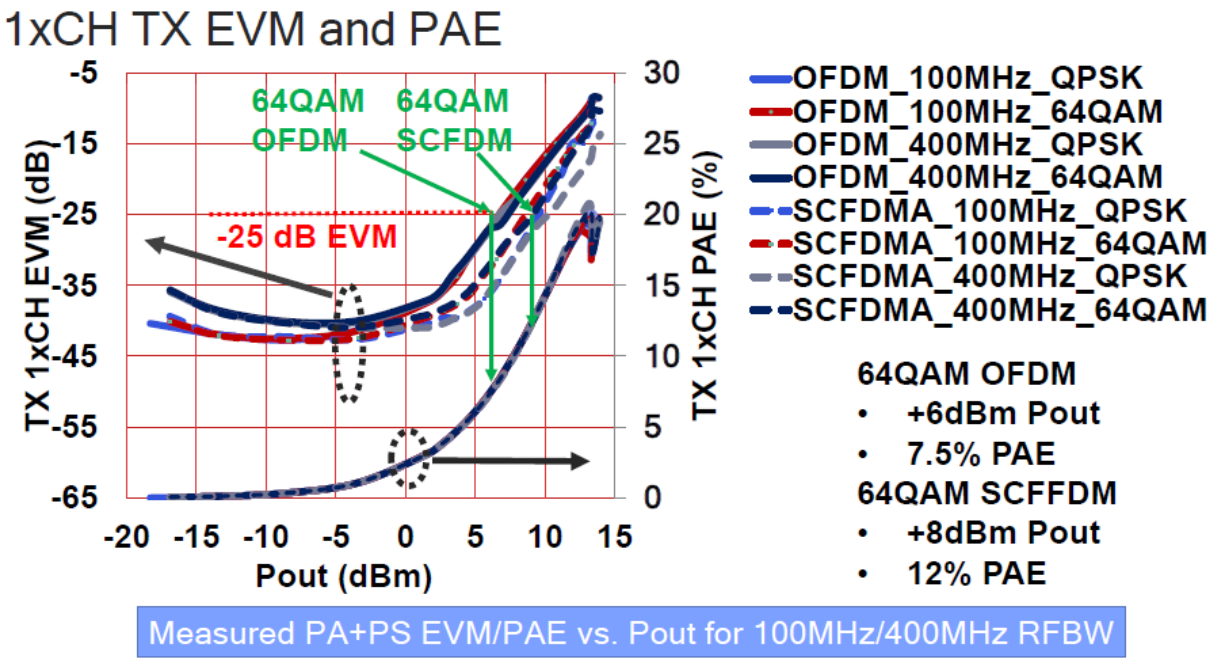

Figure 8-60 EVM and PAE for 100/400MHz BW – Qualcomm [29]

Based on the chart (Figure 8-60) above from Qualcomm, the max efficiency of the PA is less than 30%. This would result in higher power consumption which in turn results in higher heat dissipation.

Furthermore, mmWave communication may have additional necessity to address thermal dissipation due to wider channel BW / High data rate needing more power to crunch and process data. Also, the need for multiple transmitter/receivers (multiple active PAs / LNAs) feeding the antenna arrays could result in thermal dissipation. The concentration of thermal dissipation in some areas due to tightly coupled architecture where RFIC and Antennas are integrated on a single chipset as discussed above.

In the context of a UE, only passive heat dissipation methods can be used and no reduction in the temperature range of operaiton is permitted. Also, the placement of the front-end module and antenna elements within the form factor of the UE may introduce additional thermal management considerations. Hopefully, this thermal challenge could be addressed through optimal positioning of antenna module and use of appropriate materials for thermal energy spreading as illustrated by Qualcomm below (Figure 8-61).

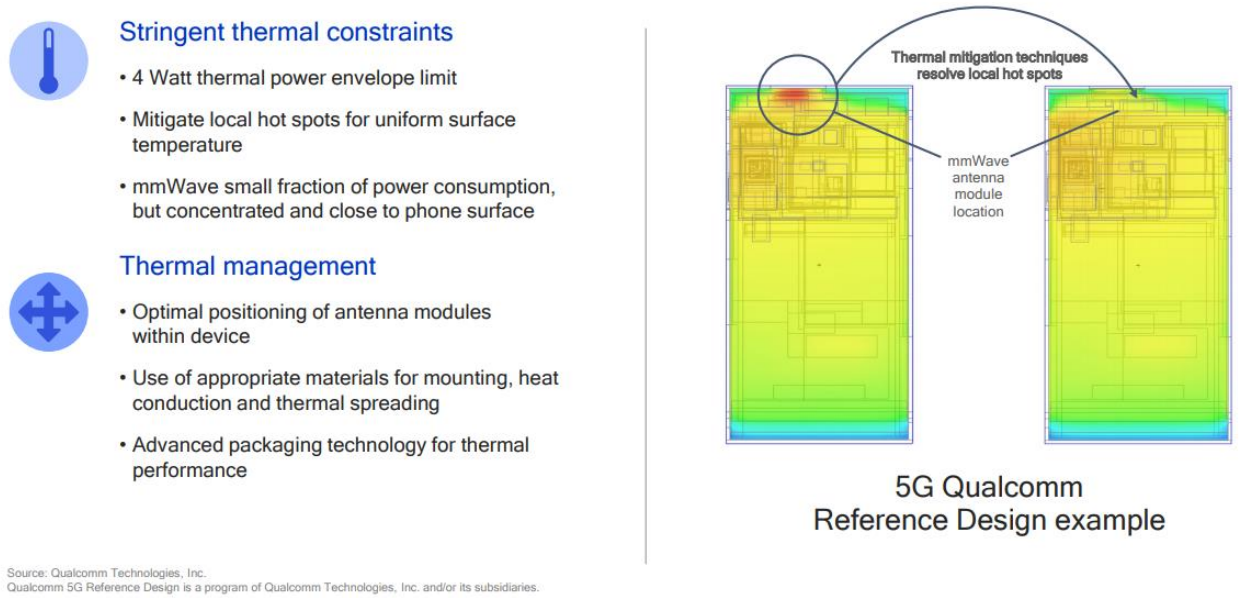

Figure 8-61 Addressing Thermal design challenge – Qualcomm [27]

To summarize, the tight integration of RF and Antenna module and the inefficiencies of various components would result in higher heat dissipation, mostly concentrated in specific areas instead of being spread across. Hence, the need for better component placement and use of appropriate mounting materials.

8.10.6. Device Size and Component placement considerations.

Device size is another key area for consideration, particularly important due to the need for Global SKU smartphone supporting wide range of bands and different operator requirements. This section will look at device integration, antenna placement and its impact of size aspects.

8.9.6.1. Device integration aspects

As we already know, LTE and mmWave frequencies are wide apart and hence prohibits to share antennas among them. Care must be taken such that LTE and mmWave antennas do not deteriorate each other's performance. As shown in Figure 8-62 below, mmWave antennas could be placed near the edges of the phone. The performance could be improved by avoiding blockage from phone's metal body and allowing radiation (RF) to conveniently pass through [42]. A plastic covering over the exposed antennas and between antenna elements could act as an isolator between mmWave and Sub-6GHz antennas. The plastic also decreases the wavelength of the signal being fed to the mmWave antenna, which allows for a smaller and more compact antenna structure.

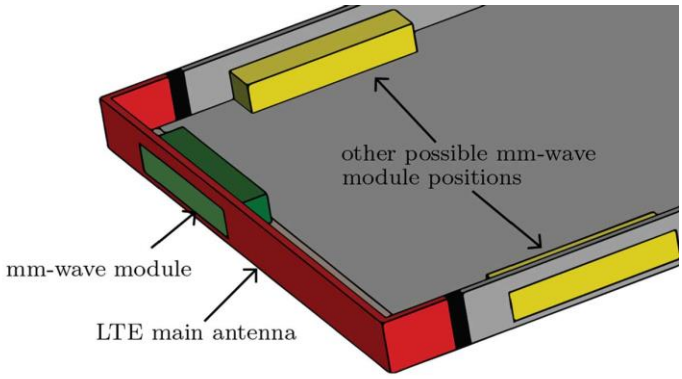

Figure 8-62 Antenna Placement [42]

Careful attention to proper integration of mmWave antennas into the mechanical structure of the UE is required maintain the radiating properties of the system. The mechanical integration must be considered an inherent part of the radiating system. Apart from the already mentioned characteristic resonance mode aspect mentioned in 8.9.3.1 subsection above, any dielectric material near the elements will require special care. Glass for instance has a permittivity of about 7 and will cause serious reflections and scattering of the beam.

mmWave antennas are affected by realistic mobile terminal environments, such as casing, glass, chassis, user's hand, and other components, resulting in distorted patterns for individual elements and distorted coverage for beam-scanning array antennas. Here is an example.

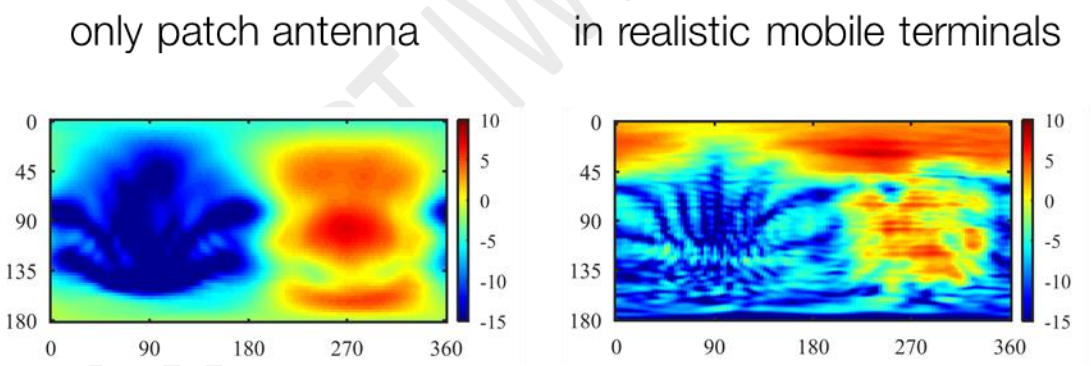

Figure 8-63 Beam scanning performance

The chassis design should be optimized for less surface waves to evolve and thus reduce the fine structure in the patterns. Additionally, the edges of the platform may be excited by the surface waves leading to strong sidelobes such as that seen above between 0 and 45 degrees. And the reflections from the cover lead to reduced energy in the main lobe and stronger excitation of the surface waves.

8.9.6.2. *Antenna configurations and locations around a mobile chassis for user blockage reduction*

In 5G mmWave mobile terminal applications, the user's body has a very high chance of creating blockage or shadow in the radiation patterns of handset antenna arrays as has been shown in [120] and [121]. It is necessary to determine the antenna array positions on the mobile phone ground plane where the best spatial coverage can be achieved when simulated with the user. The study used slot and Vivaldi antennas with broadside and end-fire radiation patterns respectively as shown in Figure 8-64(a). A total of 32 slots and 40 Vivaldi antennas have been placed on the ground plane and then a sliding array of four elements is constructed from any of four neighboring antenna elements. The proposed structure is then simulated in free space, talk, data and dual-hand modes with a homogeneous human phantom. By investigating the coverage efficiency variance and mean between the free space, talk, data, and dual-hand modes, the best positions have been found which have low variance and high mean. The normalized gain is shown in Figure 8-64(b) where the best array positions are normalized to a gain of 0.0. At the positions where the color bar value is -3.5 dBi, the mean gain will be at least 3.5 dBi lower than the best possible mean gain at the same coverage efficiency. It can clearly be seen that the best array positions are located around the corners of the mobile device. Note that if a right-handed phantom is used then the opposite (left) corners will give the best performance. Thus, it is recommended to place antenna on all four corners of the ground plane.

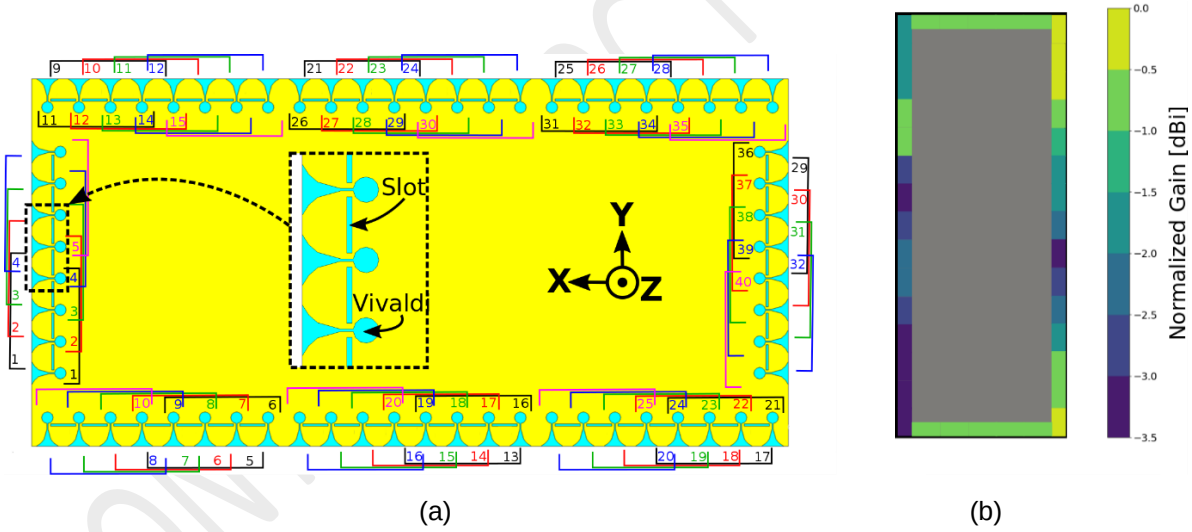

Figure 8-64 (a) proposed ant setup for best position (b) array performance on the ground plane edges.

Usually both the phase and the magnitude of each element should be measured without errors when calibrating and controlling arrays. To simplify this process in this work, the array beamforming is achieved by a SIW lens (Figure 8-65) so phase measurements are not needed and each input provides a specific beam configuration. In addition, for simplicity of fabrication and test and since end-fire radiation patterns are more preferred in practical applications, H-plane horn antennas are applied at the end of the lens and shown in Figure 8-65.

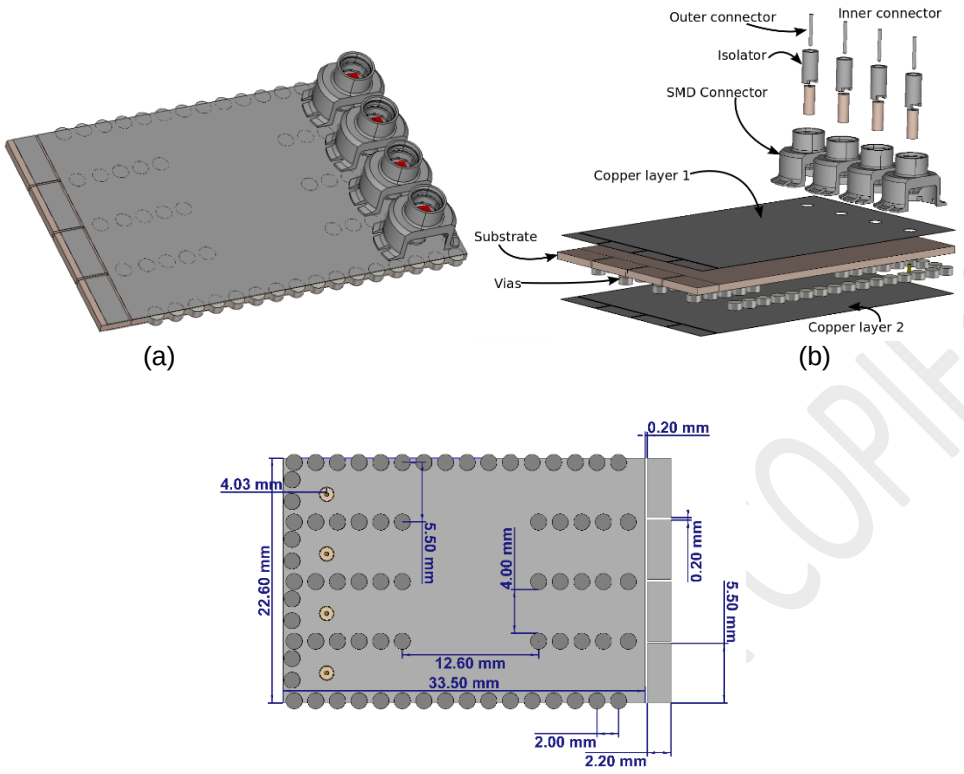

Figure 8-65 Antenna array with the lens (a) 3D view and, (b) exploded view, and (c) dimensions.

Two lenses are placed perpendicular to each other in one corner of the ground plane of the test terminal and then the terminal is rotated in measurement to orient the arrays in all four corners of the ground plane relative to the user. Thus a total of 8 sub-arrays are measured for each user setup as shown in Figure 8-66.

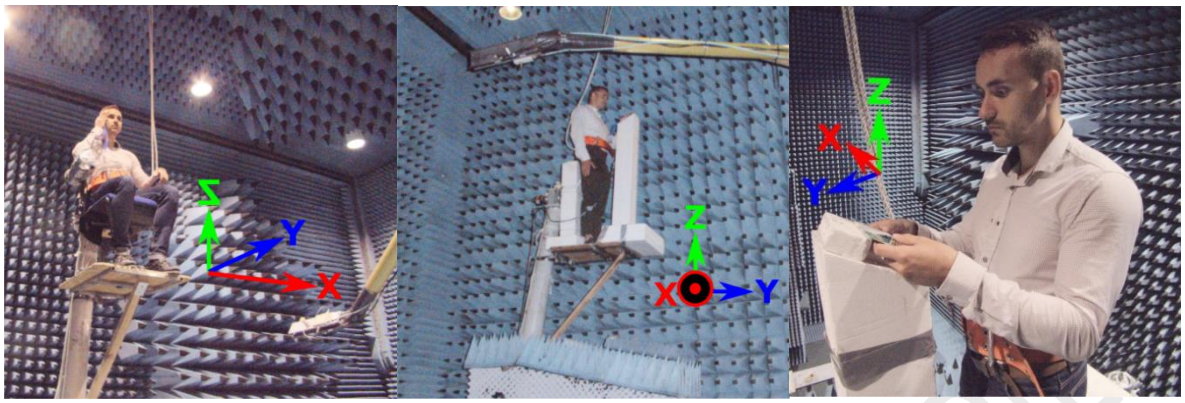

(a) (b) (c)

Figure 8-66 Measurement setup in (a) talk mode, (b) data mode, and (c) dual-hand mode.

The total scan patterns are calculated from the all 8 sub-arrays and then coverage efficiency curves are produced as shown in Figure 8-67. In Figure 8-67, the expected loss can be observed between setups with the user and the free space condition while the difference between the various user setups is significantly smaller**.** Also note that the gain threshold at 40% coverage efficiency is nearly the same for all conditions.

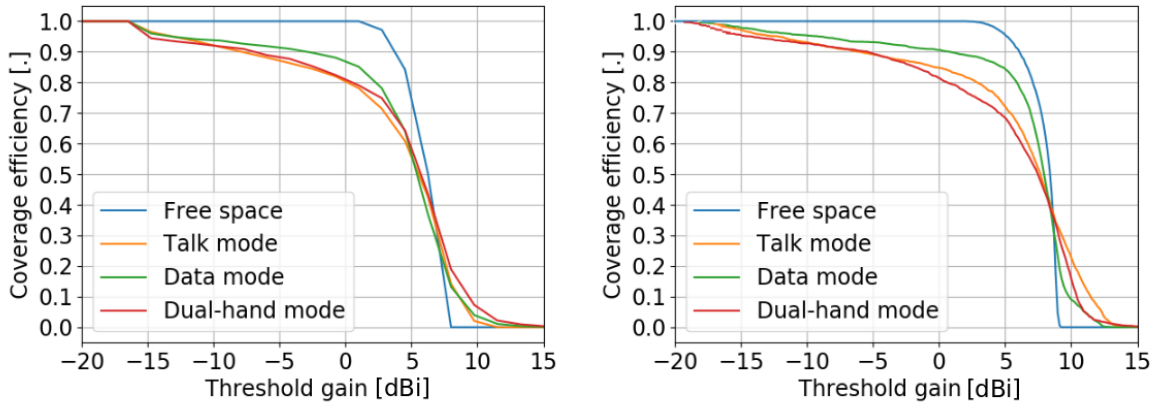

(a) (b)

Figure 8-67 (a) Simulated and (b) measured coverage efficiency of the proposed antenna array.

8.9.6.3. Device size

Also, to a degree, the front-end component size is dictated and limited to the antenna spacing and layout. Typically, antenna space of ~λ/2 is preferred. A linear array of 8 antenna elements, for example at 28GHz, will encourage a linear layout array of transmit/receive path components aligned to the antenna elements and commensurate in size. Consequently, in terms of a semiconductor die, a rectangular die might be encouraged in order to minimize (and equalize) the interconnect path between antenna port on the die and the antenna feed line. From a manufacturability perspective, an die x-y aspect ration below ~3 may be permitted by the wafer foundry but factors such as die thickness and subsequent post-dicing handling need to be considered very carefully for high volume production yeild.

There have been recent announcement by smartphones manufacturers on supporting mmWave. The size of these phones is larger or comparable to the plus sizes of iconic brands. The dimensions of Samsung's S10 5G are 6.4x3.04x0.31 inch with the screen size of 6.7". Another phone or to be specific "Mod" from Motorola support mmWave operation. The Motorola 5G Moto Mod packs Qualcomm's Snapdragon 855 SoC and integrates 10 antennas: four Qualcomm's QTM052 for mmWave radio, two antennas for sub-6 GHz connectivity, and four for 4G/LTE[101]. The dimensions of the device are 160 x 73.1 x 7.1 mm and the screen size is 6".

To summarize, the smartphones supporting mmWave are hitting the market, mostly having the screen size of more than 6 inch.

8.10.7. Standard based HW interfaces to handle connectivity

All the previous sub-sections have discussed component level considerations. Hi-speed communication interface among these various components within the device is equally important. For this purpose MIPI Alliance was formed which is a global, open membership organization that develops interface specifications for the mobile ecosystem. The organization currently has more than 15 working groups including battery interface, camera interface, RFFE working group, etc. The MIPI RF Front-End Control Interface, MIPI RFFE[SM], is a dedicated control interface for the RF front-end subsystem. It enhances the control of the complex RF subsystem environment, which has rigorous performance requirements and can include 10 to 20 components such as power amplifiers, antenna tuners, filters and switches as seen Figure 8-68 below.

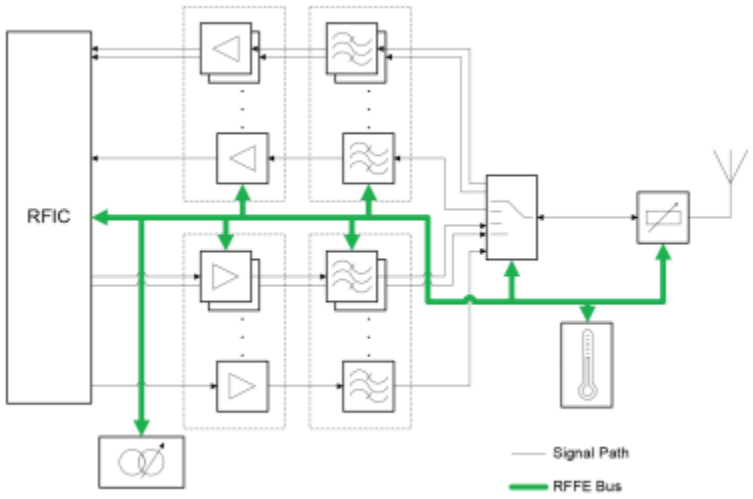

Figure 8-68 RFFE configuration

The interface can be applied to the full range of RF front-end components to simplify product design, configuration and integration, and to facilitate interoperability of components supplied by different vendors.

The current version for RFFE is MIPI RFFE v2.1 which features advancements in electrical & digital trace, flexible bus configuration and multiple message types. It is expected that current version maybe work well with 5G NR FR1 use case. However, there may be challenges using this version for FR2 / mmWave bands due to wider bandwidths, higher data rates and new type of use cases.

Various companies are working on FR2 RF front end control requirements to add the needed flexibility and programmability with respect to Tx/Rx paths, gains, PLL settings component calibrations. With higher frequencies comes the need for higher number of antenna elements, higher SCS, resulting in higher number of reconfiguration bits and enhanced latency requirements.

8.11. Technology Components / Materials considerations

In this section, we will discuss the effect of materials used in package, board and cover/enclosure for antenna and module (either small cell or user equipment) and also the impact of different semiconductor technologies in electronic chips to implement a mmWave 5G mobile radio.

8.11.1. Materials challenges at mmWave

While material science has always played an important part in communications systems, mmWave spectrum brings new challenges. For sub-6GHz applications, signal transmission is generally less impacted by the medium through which it is transmitted. The main reason for this is the amount of signal loss (more precisely, the loss tangent for a given permittivity) is proportional to frequency. If the same materials being used at 600MHz are built into 28GHz devices, the signal loss will be far greater. Whether the signal is travelling through a transmission line, radome, filter or other component, high losses necessitate new material requirements for mmWave applications.

Another point to consider is that with sub-6GHz applications, most components are considered electrically small compared to the wavelength of the signal. At mmWave frequencies however, this is not the case and complicates the design of structures like antenna radomes and smartphones. At mmWave frequencies, existing materials perform much differently and cannot necessarily be adapted with minor modifications. New materials, methods and solutions must be developed in order to meet the demands of 5G mmWave networks.

Antenna Radomes

Commoditized materials such as PVC, FRP and ASA have traditionally been used for sub-6GHz radome materials. They have proven to work well for antenna applications over the years and have good mechanical, thermal and dielectric properties below 6GHz. However, dielectric losses increase significantly for mmWave applications. One way to compensate for these losses is to decrease the thickness of the radome material. However, in order to reach an acceptable level of insertion loss, the material would be so thin that it would become fragile and not meet mechanical requirements. Therefore, alternative materials must be utilized that exhibit low loss while maintaining the mechanical properties required to protect the antenna elements.

A great deal of research has been performed in this area by the aerospace/defense industry although it does not necessarily translate well to base station antenna radome applications. Different mechanical and thermal requirements have significant cost implications that would not be attractive to 5G antenna OEMs. There are still various alternatives to traditional radome materials, such as syntactic foams, prepregs, or other composite constructions that perform well at higher frequencies. These materials allow more flexibility in tailoring the dielectric constant and loss tangent to meet the radome specification requirements, ensuring optimal performance. However, it is also likely that improved performance will come at a higher cost until sufficient scale is reached. A selection of materials can be seen in the table below, which illustrates the significant variation in loss tangent.

MATERIAL	BRAND NAMES	DIELECTRIC CONSTANT	LOSS TANGENT
Epoxy/fiberglass	G10, FR4	4.90	0.0190
Acetal	Delrin, Celon	3.70	0.0050
ABS	Lustran, Cycolac	3.23	0.0200
Nylon 6/6	Zytel	3.20	0.0210
Polyetherimide	Ultem	3.15	0.0013
Polystyrene	Styron	2.75	0.0005
Polycarbonate	Lexan	2.35	0.0100
UHMWPE	Dyneema	2.20	0.0004

Table 8-6 Materials performance [140]

It is also important to consider the thickness of radome. At 28GHz, it represents a significant proportion of one wavelength and is considered to be electrically large. As a result, reflections at the air/radome interface must be considered, particularly if the thickness is an odd multiple of a quarter-wavelength. In this case, the reflected waves will constructively interfere and further degrade performance. The permittivity, loss tangent and thickness of the radome material must be selected carefully in conjunction with the distance to the antenna elements to enable optimal performance.

User Equipment

Many of the issues discussed so far apply to smartphone applications as well. As user equipment devices trend towards increasing complexity, the demand for new material solutions also increases. In the Figure 8-69 below [44], the effect of the ABS cover can easily be seen and is not insignificant. The cover

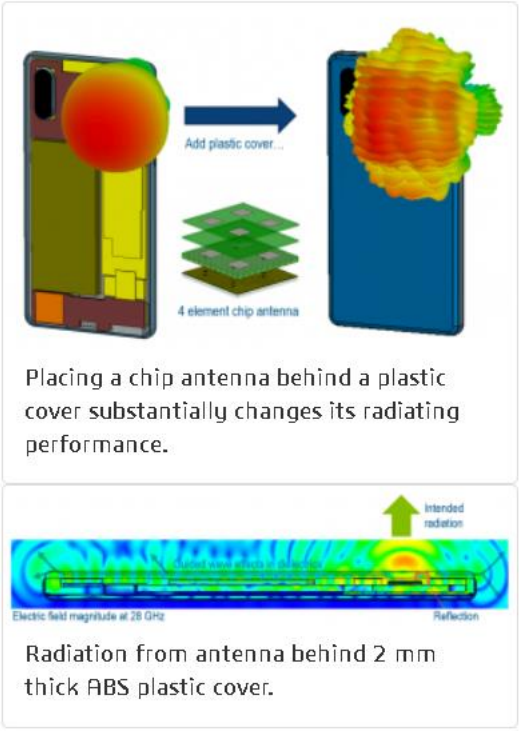

Figure 8-69 Effect of cover materials and thickness on mmWave antenna radiation efficiency

(as well as other components) must now be integrated into the antenna design and considered as a system. In fact, the cover behaves much like a base station antenna radome. The permittivity, thickness and distance between the antenna and cover must be designed to minimize reflections, insertion loss and pattern distortion.

8.11.2. Effects of board materials on mmWave phased array system

The phased array systems come with their own set of challenges. Due to the high losses at 28GHz, it is not feasible to utilize a separate enclosure for the electronics (or even collocated within the same enclosure) and so RFICs are mounted on the back of the PCB. This creates a very high density assembly, which is challenging from both an EMI/EMC as well as thermal perspective. For UE applications, the design of these arrays will certainly face even more difficult conditions. Typically, each RFIC will feed multiple antenna elements, configured as a sub-array and the RFICs will be fed from a common point. Because FR4 PCB substrates have such high loss (~1dB/cm) at 28GHz, it is necessary to convert to IF before signal transmission on board. However, with low loss PCB substrates using materials such as PTFE or LTCCs, it may not be necessary to convert to IF. Either material offers a good alternative to FR4 and can be used to improve the performance of both base station and user equipment devices.

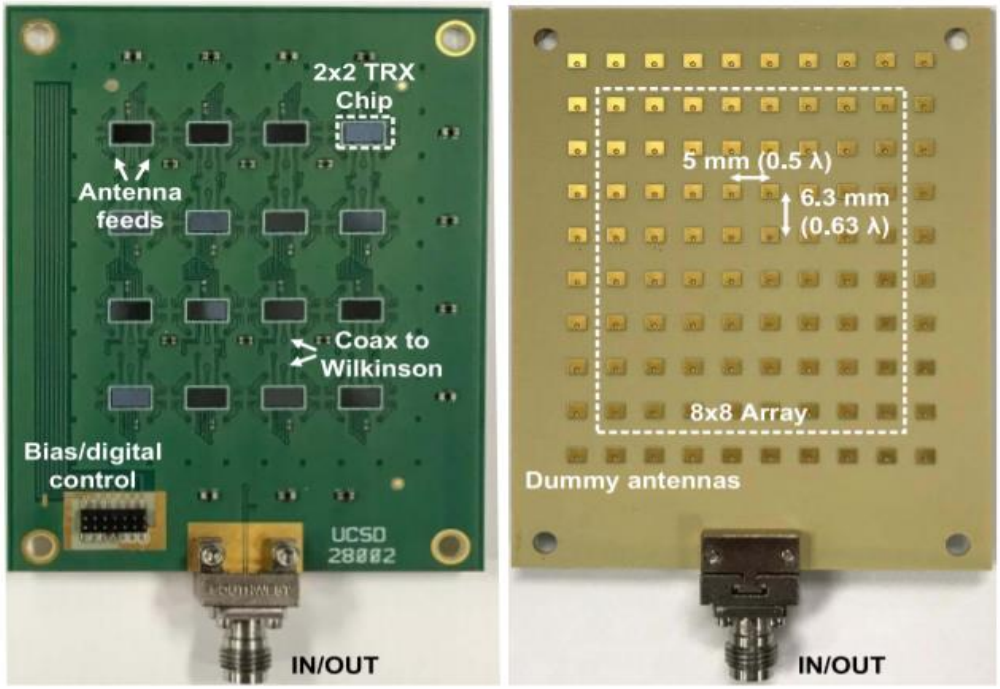

Figure 8-70 Phased array system board [139]

It is also important to consider the surface roughness of the plated Copper conductor. Since the skin depth is very small (0.39μm for Copper at 28GHz), excessive roughness will be a contributing factor to transmission line loss at mmWave frequencies. Technology exists to create a Copper conductor with very low surface roughness, however the tradeoff is that as roughness decreases, so does the level of adhesion to the substrate. Therefore, not only is the material used in mmWave PCB substrates important, but the manufacturing process is as well.

With regards to thermal loads, the RFICs will require paths for heat dissipation. A thermal interface material (grease, epoxy, pad or tape, depending on design requirements) placed between the RFIC and heatsink is absolutely necessary. Additional thermal interface materials may be required to draw heat from other areas on the PCB as well. On the opposite side of the PCB, the antenna elements also tend to generate a significant amount of heat. Because any material placed in front of the array will impact antenna performance, it is very difficult to dissipate this heat. In some infrastructure applications, active cooling may be required.

As with any electronic device, EMI/EMC issues must be considered and in a phased array this is particularly true. While the array is meant to behave as a group of independent elements intelligently combined in some manner, there will always be a level of mutual coupling between elements. This is caused in part by surface waves and will impact the gain and pattern of the array. For mid-band (e.g. 2.5GHz) phased arrays, a simple metal plate can be placed between the elements to provide the required isolation. However, at 28GHz this is not possible and therefore more advanced techniques and/or materials must be used. Metamaterial structures are becoming one of the more popular techniques to address this issue in recent

years. Rather than rely on the properties of the material itself, a repeating structure of unit cells determine the bulk properties and can be an effective tool in antenna design.

8.11.3. Semiconductor technologies for mmWave Handsets and Base Station radio

The gain of the phased array is proportional to the number of array elements (N). On the Receiver (Rx) side, the array gain improves receive sensitivity (SNR) by a factor of N, whereas on the Transmitter(Tx) side, the combination of array gain and additional power per element results in an N^2 increase in output power as compared to a single element. This fundamental property of the phased array enables a trade-off between semiconductor performance and the size of array needed to meet system requirements. In particular, the N^2 reduction in output power per element to achieve the same system EIRP targets makes silicon technologies an attractive choice for all but the highest power applications.

A variety of semiconductor technology platforms are available for mmWave radio implementations. From a historical context, less integrated platforms such as those based on III-Vs have been in use for over 10 years to implement single RF functions such as the power amplifier, a mixer and others. Serving primarily military applications, these semiconductor platforms are not well suited to highly integrated and compact consumer-grade wireless radio interface. Moreover, because of interaction with features having relatively small electrical length, multiple port interfaces and cable losses favor those front-end system partitions where more of the mmWave frequency synthesis and signal conditioning (e.g. phase shifters, amplification, etc.) is located close to the antenna elements.

Semiconductor technologies with requisite transistor performance for operation in the 5G mmWave frequencies include CMOS, SOI (partially and fully depleted versions), SiGe, GaAs, InP and GaN. These technologies span a wide range of power, performance, integration and cost capabilities and thus will address a diverse set of architecture and application requirements as indicated in Figure 8-71

Multiple semiconductor technology platforms can be considered candidates for implementing mmWave front-end functionality. To a large degree, this consideration and selection is dependent upon the system partitioning and the required integration /form factor demanded by the end radio system. Clearly, very small form factors such as UE devices will drive more highly integrated solutions and, consequently more highly integrated semiconductor platforms. Non-intuitively perhaps, integration into a form factor suitable for a smartphone is perhaps the greatest challenge in that fewer antenna elements can be used to achieve EIRP. Moreover, power efficiency of the transmit chain can be directly linked to battery life. Therefore, the chosen semiconductor technology must be able to provide relatively high RF power at each antenna element (~25dBm Psat) in consideration of 3-8 dB back-off for linear operation with OFDM-type signals. EIRP exceeding 23dBm is typically required and commensurate with sub-6GHz bands. Consequently, efficiency and constraints on circuit size drive more highly integrated chip-scale-package solutions where the number of chip to chip transitions (loss) is minimized.

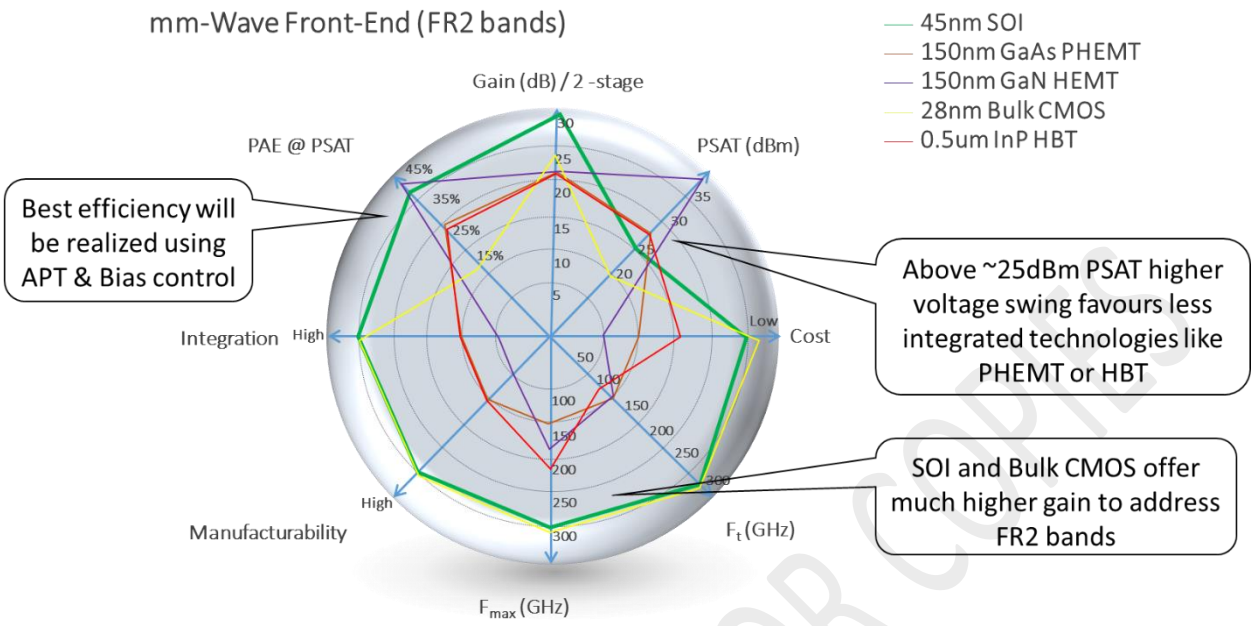

Figure 8-71 Charts showing comparison of different semiconductors for mmWave radio front end

As seen in the figure, while GaN HEMT platforms might offer the best Psat and PAE, the integration potential is very poor which drive the requirement for companion IC die to support ancillary functions (digital control, memory, biasing, etc.). Historically, choosing the best semiconductor platform for a particular function and then relying on system-in-package approaches has been highly successful. However, in the context of FR2 front-ends system integrators are demanding even more highly integrated single chip solutions. Fortunately, recent progress in nanometer scale Silicon-based semiconductor platforms provides us with a new set of options.

The introduction of advanced SiGe BiCMOS, bulk CMOS and silicon-on-insulator (SOI) platforms - featuring multiple levels of low-loss copper interconnect along with transistors with peak Ft/Fmax of over 300GHz is a 'just-in-time' occurrence that component providers can leverage for mmWave front-ends. Moreover, based on 12" wafers, these platforms offer the promise of compelling cost per mm2 which is consistent with consumer-grade wireless systems (VR headsets, laptops, etc.). The final compelling advantage of silicon-based technology platforms is manufacturability and relatively low parametric variation.

Base stations and handsets have different output power specifications and specifications are also quite different depending on chosen architecture (phase array complexity and system integration approach). Nowadays, all silicon and compound semiconductor technologies are competing for 5G mmWave base stations as well as handset.

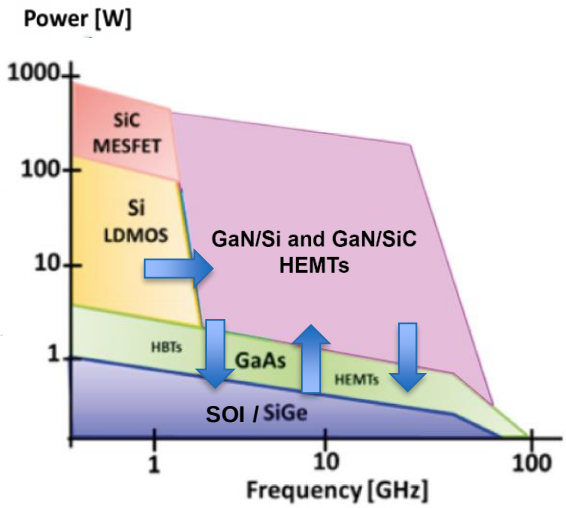

Source : Analog Devices, 2018 – w ith added comments

Figure 8-72 Tx Power vs Operating frequencies for Power amplifiers made on different Semiconductor

Cost and integration are key parameters. Silicon technologies have the advantage to be both cheap and allow system on chip integration versus compound semiconductors. Regarding cost, the analysis must be done at system and operating level. For example, even GaN on Silicon Carbide is 10 times more expensive than silicon bulk, silicon requires antenna phase array that are more complex in the order of 10 times to achieve similar performance. Silicon power efficiency will also be behind which will require heat sink systems which add cost and weight on top of overall system power consumption which costs as well. Detailed performance of different silicon technologies has been highlighted in the next section.

8.11.4. Key Figures of Merit (FOM's) for RF/mmWave circuits and systems

The general rule of thumb for technology requirement for adequate RF system performance is the transistor Ft and Fmax should to be minimum 5x and preferably 10x the operating frequency for acceptable gain and circuit margin. At the mmWave carrier frequency, for example at 39GHz 5G band, it means that a 200GHz Ft/Fmax is the minimum acceptable and 400GHz is preferred. Due to the high losses at mmWave, parasitics of active and passive elements are critical. Minimizing loss in the metal/dielectric stack is important for transmission lines (T/L) at the top metal levels and for efficiency in power combining networks. Thick metal and dielectric stacks are important in minimizing this loss. Substrate losses are also important; the quality factor of matching networks and T/L insertion loss improves with higher resistivity substrates. On the Rx side, transistor NFmin is important for low noise circuits; on the Tx side, breakdown voltage and safe operating area (SOA) are paramount for efficient power generation in the PA and for power handling in the antenna switch. For frequency generation, flicker (1/f) noise and the noise corner of the transistor is important for low phase noise VCO's.

Circuit FOM's:

LNA: NF, Gain, Linearity (IIP3), Power consumption

Switch: Insertion Loss, Isolation, Power handling, Linearity

PA: Psat/P1dB, Linear efficiency, Gain

Phase shifter: Loss, Power consumption

PLL: Phase noise, Power consumption

Mixer: Conversion gain

ADC/DAC: Energy/bit/MHz, Sampling rate, ENOB

We will compare different semiconductor technologies, mainly silicon Technologies w.r.t the above key circuit level FOM's

8.11.5. Silicon Technologies for mmWave Radio

RFCMOS

RF CMOS offerings provide enhanced modeling, design kit and process feature additions on mainstream digital CMOS platforms. The transistor performance is principally a result of the digital scaling. Starting at the 40nm node, CMOS ft and fmax exceeded 250GHz. Continued scaling has increased ft to 300GHz at the 28nm node and to 400GHz at 22nm, but fmax improvements have been a greater challenge due to the higher gate resistance (Rgate) of scaled dimensions. This has been exacerbated with the industry transition to HKMG at 28nm and FinFET at 22nm and below, with initial 28nm HKMG nodes only reaching an fmax of 150GHz. Continued optimization of gate stack and of FinFET layout (Fin and metal pitch and gate contact optimization) has been successful in reducing Rgate and has achieved both high ft and fmax, with Intel reporting 350/450GHz ft/fmax for a 22nm FF and GF achieving 350/350GHz with a 12nm FF. FinFET has higher mobility, higher drive current and higher self-gain compared to 28nm.

With CMOS comes integration of high density low power logic (1.5M logic gates/mm2 at 40nm increasing to >30M gates/mm2 at 12nm) capable of SOC integration of digitally intensive RF transceivers, analog front ends with filtering and data conversion, high speed SERDES and baseband modem processor/DSP.

A disadvantage of advanced CMOS is the low max operating voltage of scaled FET's, which limits the ability to efficiently generate and handle higher output power in front end circuits. As a result, peak output powers for 28GHz CMOS cascode PA's are in the range of 10-15dBm. Higher output power can be achieved with power combining networks of multiple amplifiers, but this also comes at the expense of PA efficiency. Antenna switches are also problematic in scaled CMOS due to the low breakdown voltage of the FET. ¼ wave transmission lines are an alternative, but insertion loss with a T/L is ~ 1dB higher than the best SOI and GaAs pHEMT technologies.

SOI

In SOI technology, CMOS transistors are built on a top layer of silicon isolated by a buried oxide (BOX) layer from the silicon substrate. The oxide isolation reduces FET junction capacitance to substrate and improves FET performance. As a result, transistor ft and fmax in an SOI technology are higher than in a comparable node planar CMOS technology. There are two flavors of SOI with excellent mmWave performance that are available, partially-depleted (PD) and fully-depleted (FD) SOI. PD-SOI and FD-SOI are distinguished by the thicknesses of the top silicon layer and the BOX. In common with RF CMOS, RF SOI technologies provide high frequency models, enhanced PDK's and optimized metal/dielectric stacks and features

PD-SOI

In PD- SOI, the top silicon is on the order of 50-100nm and the BOX is 100nm or larger. As the name implies, the silicon under the channel does not fully deplete of mobile charges, the transistor body can "float", and transistors are fully isolated from each other by the surrounding oxide (shallow trench on the sides and buried oxide underneath). Since the FET's are electrically isolated and there is no common substrate node as in bulk CMOS, FET's can be connected in series ("stacked") and biased such that the voltage is distributed equally across the stack. Stacking overcomes the low breakdown voltage (BVds) limitations of advanced node CMOS since the breakdown voltage of the stack is the sum of the BVds of the individual transistors in the stack. This is a significant benefit to front end circuit performance, resulting in higher PA output power and efficiency and improved antenna switch insertion loss and power handling. 45nm RFSOI PA's can deliver peak output power of 16-20dBm at 28GHz with high efficiency (>40% PAE), and Doherty designs with peak output power of 23dBm have been demonstrated.

Another advantage of PD-SOI with its isolated substrate is the capability to engineer the substrate for additional RF benefits. High resistivity (>1K ohm-cm) substrates reduce signal loss to the substrate and improve transmission line loss and Q of matching networks. Higher Q input matching networks result in lower LNA NF. In addition, engineered substrates with trap rich layers under the BOX reduce parasitic conduction mechanisms that otherwise will degrade switch harmonics and linearity.

GF has a 45nm PD-SOI in production that has been optimized for mmWave performance. NFET and PFET ft/fmax are 290/330GHz and 245/300GHz respectively. Metal/dielectric stacks are optimized for mmWave performance and offer single and dual ultra-thick 3u Cu levels for low loss transmission lines and combining networks and high Q passives. Other foundries have announced plans for 45nm and 65nm PD-SOI.

FD-SOI

In FD-SOI technology, transistors are built on a top layer of ultra-thin silicon isolated by an ultra-thin buried oxide layer from the substrate. The silicon and buried oxide thicknesses are in the 5-8nm and 10-30nm range respectively, which is an order of magnitude thinner than comparable PD-SOI layers. Because the silicon layer is so thin, the silicon under the channel becomes fully depleted of mobile charge carriers during operation. Because the buried oxide is also ultra-thin, the transistor characteristics can be

influenced from below by a bias on the back gate, thereby providing an additional terminal for device control that is unique to FD-SOI technology.

Since the silicon channel is ultra-thin and transistor Vt control can be accomplished via the back-gate, channel doping is not required, which improves mobility and reduces 1/f noise, device variation and mismatch. In digital circuits, forward back-gate bias is used to reduce Vt and increase transistor drive and switching speed, while reverse back-gate bias is used to increase Vt and reduce transistor leakage. In GF 22nm FD-SOI, back-gate bias provides 70mV/V of Vt control. This control enables ultra-low power digital circuits, with low voltage operation without speed loss in the on-state and low leakage in the off-state. For RF/analog circuits, back-gate control provides the designer with an additional device terminal that is not in the signal path and thus does not load the circuit. This enables new and powerful ways to dynamically calibrate and control RF/analog circuit performance that are unique to FD-SOI technology.

28nm and 22nm FD-SOI technologies are currently available, with 18nm and 12nm nodes next on foundry roadmaps. Because FD-SOI technology has the ultra-thin channel and does not require the source/drain engineering and channel Vt implants of bulk silicon, it requires fewer masking steps than comparable planar CMOS nodes. And because it is a planar technology, it is significantly less complex than the 3D FinFET fabrication. A 22nm FD-SOI process has approximately 20% fewer masking steps than 28nm bulk CMOS and approximately 35% fewer masking steps than 14nm FinFET CMOS. FD-SOI incurs the additional cost of the SOI substrate, but in aggregate, FD-SOI wafer cost is similar to 28nm CMOS.

The RF/mmWave performance of FD-SOI is excellent. GF's 22FDX technology has ft/fmax of 350/430GHz for the NFET and 270GHz/315GHz for the PFET. Due to the superior electrostatics of the fully depleted channel, the FET's have high gain efficiency (gm/Id) for excellent low power RF gain, delivering gm/I > 14 with ft>100GHz. NFmin at 28GHz is 0.43dB (vs 1.7dB for 28nm CMOS), and 1/f noise is 20f @ 1KHz [V^2*um^2/VHz], which is 8x lower than 28nm CMOS. This results in excellent mmWave LNA and VCO performance. At 22nm, CMOS logic density is 5.5M gates/mm2. An optimized metal/dielectric stack with dual ultra-thick metal levels provides low loss interconnects, transmission lines, transformers and power combiners. The combination of high performance low power 22nm logic with excellent mmWave front end circuit performance in FD-SOI enables highly integrated 5G SOC solutions. Integration can extend from the mmWave front end through the digital interface, including SERDES, data converter, IF/RF transceiver and beam former front end on a single FD-SOI IC. This is ideal for digital beam forming architectures where each antenna element has a full RF and analog chain. In analog/hybrid beam forming architectures, typical integration levels would be RF transceiver and mmWave front end.

SiGe

SiGe BiCMOS technology integrates a high performance silicon germanium heterojunction bipolar transistor (HBT) with RF CMOS. Compared to a high performance CMOS FET, the SiGe HBT has higher breakdown voltage, much lower 1/f noise and 1/f noise corner, much larger gm/device area, better transistor matching, better output conductance, and as a vertical transport device is less impacted by wiring parasitics and thus delivers higher performance to the transmission lines at the top of the

metal/dielectric stack. SiGe technology was developed for RF/mmWave applications, unlike RFCMOS where FET performance is optimized for logic and processor applications and RF features are added to the digital platform.

SiGe technologies have achieved higher ft and fmax than CMOS and SOI, with a record setting 505GHz ft / 720GHz fmax reported by IHP in an experimental SiGe bipolar-only process (Heinemann, IEDM 2016). In SiGe technology, ft improvement is achieved with vertical profile scaling, and fmax is separately optimized with lateral scaling and reduction of external parasitics. However, the performance level of a BiCMOS technology will be less than a stand-alone SiGe HBT process due to thermal cycle constraints and process interactions from the CMOS integration. The most advanced production BiCMOS processes today have 300-320GHz ft and 360-370GHz fmax (GF 90nm SiGe9HP and STM 55nm BiCMOS55, respectively). Next generation SiGe processes are targeting > 500GHz fmax. For example, IFX has announced a next generation 90nm SiGe BiCMOS platform with a 300GHz ft / 600GHz fmax target. (IMS 2017)

Summary of mmWave relevant Silicon Technologies

	CMOS	FD-SOI	PD-SOI	SiGe
Node	40nm – 12nm	22nm	45nm	250nm – 55nm
Logic Density	1.5 – 30M	12M	1.5M	0.1 - 1M
ft	250GHz - 350GHz	350GHz	290GHz	200GHz – 320GHz
fmax	250GHz – 350GHz	430GHz	390GHz	200GHz – 370GHz
CMOS Vdd	1.1 – 0.8V	0.9V	1.1V	
HBT BVceo / BVcbo (90nm)				1.7 / 5.3V
Substrate Resistivity	10	10	>1K	10 - 200
Wafer size	300	300	300	200 - 300
28GHz FEM performance				
LNA NF	2.0 dB (28nm)	1.4 dB	1.4 dB	2.1 dB
PA Psat	10 – 15 dBm	15 – 20 dBm	15 – 23 dBm	15 – 30 dBm
Switch IL		0.65 dB	0.65 dB	1.2 dB

Table 8-7 mmWave Silicon Technologies

Based on the above capabilities, different Semiconductor technologies can address different blocks of mmWave radio in a UE as shown below

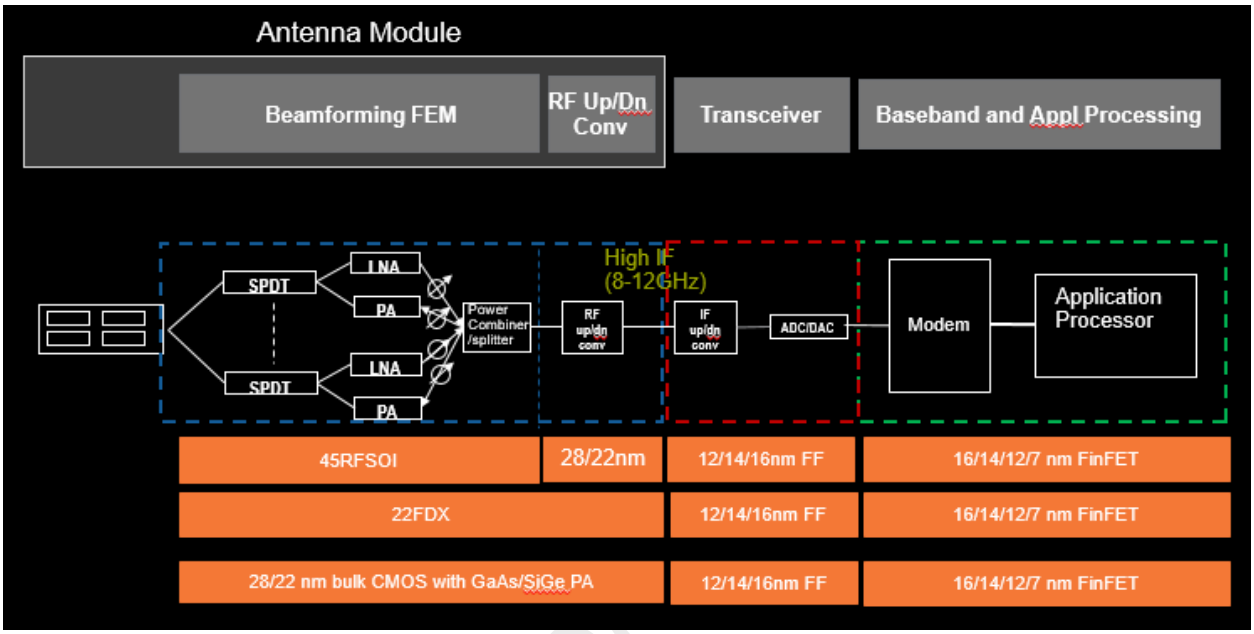

Figure 8-73 mmWave UE block diagram

8.11.1. Summary

The mmWave Radio hardware for mobile applications require use of new materials and technologies compared to sub-6GHz counterpart both for handset and base station equipment. Different beamforming architectures, chip partitioning options and TX power requirements can be addressed by different Semiconductor technologies. The phased array system enables use of Silicon technologies due to lower Tx power requirements from each Power Amplifier. PDSOI technology can address an integrated FEM for mmWave UE, while FDSOI can address an integrated FEM and Transceiver. Bulk CMOS will need either GaAs/GaN or SiGe Power amplifiers and RFSOI Switches to address the requirements.

8.12. Current Product Implementation

The previous sections thus far had looked at various implementation considerations / challenges with mmWave deployment. This section will now look at current and expected products from various gNB and UE vendors and some of the implementation details.

8.12.1. gNB solutions

This sub-section looks at RAN solutions. Several RAN vendors have well defined products and roadmap features to support mmWave bands. Some of the vendors details are as follows:

E/// has several products for 28/39GHz supporting different deployment scenarios such as pole/wall/strand mounts. The products support BW up to 800MHz and EIRP ranging between 55-60dBm.

Nokia's product configuration is illustrated below (Figure 8-74). All products support 2x2 MIMO. The EiRP of these products range between 50 – 60 dBm.

Radio Configurations for predictions

	AEUB	AEUD	AEUE	CMP	CMP Extension
Weight (lbs)	44.1 lbs	26.5 lbs	11 lbs	15 lbs	11 lbs
HxWxD (inch)	23.6 x 12.0 x 4.7	14.3 x 11.1 x 6.8	12.8 x 9.8 x 6.0	12.8 x 10.63 x 3.5	12.8 x 10.63 x 3
EIRP Average power (dBm)	60 dBm (Avg);	51 dBm (Avg);	51 dBm (Avg);	55 dBm (Avg)	55 dBm (Avg)
MIMO support	2x2 MIMO	2x2 MIMO	2x2 MIMO	2x2 MIMO	2x2 MIMO
Number of Antenna Elements	2 x 256 per panel	2 x 128 per panel	2 x 128 per panel	128 per panel	128 per panel
Number of H & V Phase Array Panels	2 single polarized 16x16 array/panel	2 single polarized 8x8 array/panel	2 single polarized 8x8 array/panel	2 single polarized 8x8 array/panel	2 single polarized 8x8 array/panel
Polarity structure (separate H&V or Cross Pol)	0° & 90°	0° & 90°	0° & 90°	0° & 90°	0° & 90°
# Beams	2 per panel	2 per panel	2 per panel	2 per panel	2 per panel
H & V Beamwidths (boresight)	(H) 6°; (V) 6°	(H) 12°; (V) 12°	(H) 12°; (V) 12°	(H) 12°; (V) 12°	(H) 12°; (V) 12°
H & V Steering Angles (3dB & 6dB points)	H-Steering: ±45° (3 dB); V-Steering: ±45° (3 dB)	H-Steering: ±90° (3 dB); ±105° (8 dB) V-Steering: ±45° (3 dB)	H-Steering: ±90° (3 dB); ±105° (8 dB) V-Steering: ±45° (3 dB)	H-Steering: ±45° (3 dB); ±60° (8 dB) V-Steering: ±15° (3 dB)	H-Steering: ±45° (3 dB); ±60° (8 dB) V-Steering: ±15° (3 dB)
Input Power Draw	420 Watts	370 Watts	60 Watts	200 Watts	55 Watts

* Assumptions subject to change to meet practical and field considerations

10 © 2018 Nokia NOKIA

Figure 8-74 mmWave Product Specs - Nokia

Samsung has an extensive commercial portfolio that continues to grow as operators look to new spectrum bands for 5G service support. In the mmWave spectrum our current commercial portfolio includes the 26GHz, 28GHz and 39GHz base stations based on the 5G NR standard, with features such as hybrid beam forming to provide market leading performance. In the sub-6GHz bands we have commercial solutions supporting 2.5GHz, 3.5GHz and the US CBRS band, all of which employ Massive MIMO 5GNR upgradeable architectures by a channel card addition in the digital unit(no tower climb) and a software push to dramatically increase capacity versus previous solutions. The 26GHz and 28GHz base stations as well as the 2.5GHz and 3.5GHz base stations are already commercially available and the additional products will be available later this year.

Figure 8-75 Samsung 28GHz Access Unit

8.12.2. Repeaters

In order to overcome some of mmWave short coverage, or outdoor to indoor penetration challenges, various companies are developing mmWave repeater type products of various configurations.

For instance, Pivotal Commware's Echo5G device is a layer 0 mmWave repeater optimized for the 28GHz band. It uses 4 independent HBF antennas to form four beams to an external gNB. The beams cover the uplink vertical polarization, uplink horizontal polarization, downlink vertical polarization and downlink horizontal polarization signal paths. Each signal path has a dedicated RF chain and is re-radiated through the glass by a single static antenna. The four static antennas are matched to typical glass window and re-radiate with a wide beam to assure coverage inside the home. Each signal path has roughly 60dB of electronic gain, 17dB of HBF gain and 6dB of glass-side static antenna gain.

This arrangement avoids the need for any RF down-conversion or baseband processing. The Echo5G automatically detects the base station and beamforms to it, eliminating the reflection loss due to base station beam angle of incidence in addition to providing significant gain from the HBF. The matched static antenna radiating directly into the glass provides additional link advantage. The unit consumes 14W of DC power and is wirelessly powered through the glass. This configuration allows user self-installation with minimal effort.

Figure 8-76. Exterior view of a pre-Echo5G prototype.

Echo5G pre-commercial units (Figure 9) have been tested in several environments with a US based carrier. One such trial took place on the second floor of a suburban apartment building shown in Figure 10. Two vendor base-stations (gNBs) located 700ft from the front of the apartment were used to serve traffic through the Echo5G to a third party mmWave CPE inside the home. An Echo5G was placed on the window closest to Location A and had line of sight to the base stations at an angle of roughly 45° from window broadside. Echo5G was able to interoperate with both gNBs and one of the gNBs was selected for use in additional locations.

8.12.3. UE Chipsets

From the UE chipsets, there have been announcements from multiple chipset partners on their product support for mmWave bands. This subsection will look at details from some of the vendors.

QCOM mmWave chipset solution (shown in Figure 8-77 below) is based on SDX50 (snapdragon 5G modem), capable of simultaneously interface with multiple QTM052 antenna modules through flex or co-ex cables. The QTM052 embeds 1 or multiple antenna arrays, includes SDX051 (mmWave RF transceiver integrating multiple PAs, LNAs, switches) and power management.

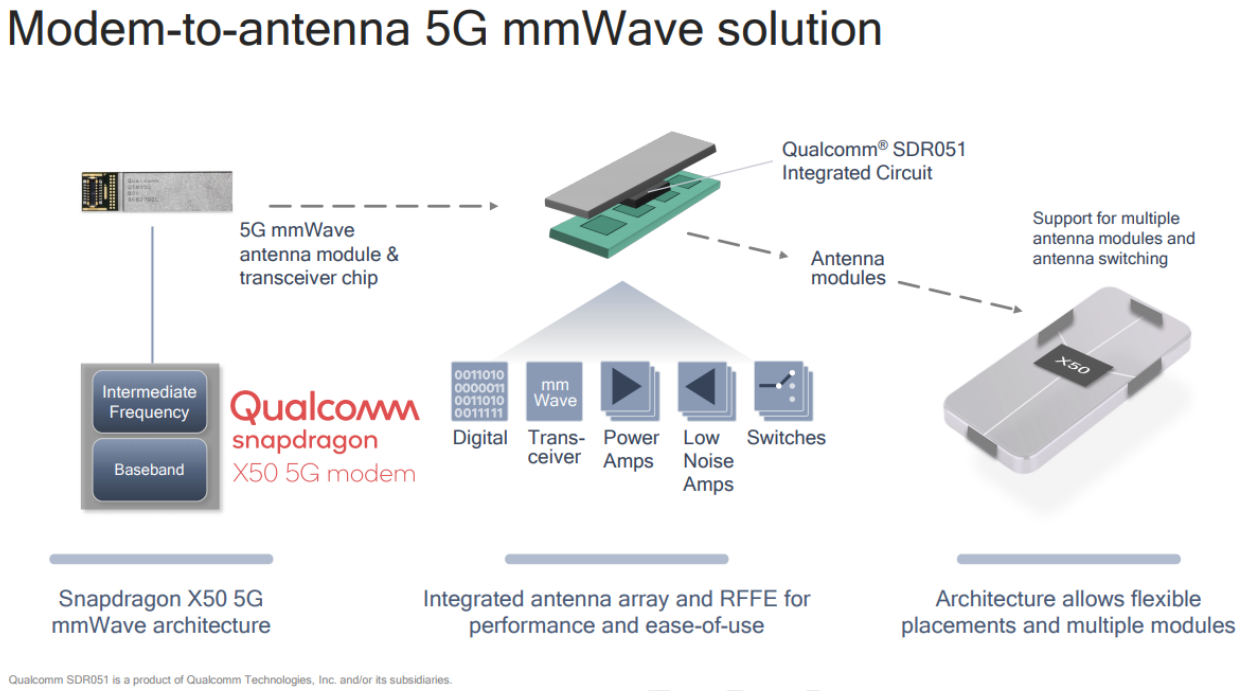

Figure 8-77 mmWave Solution – Qualcomm [27]

The QTM052 currently covers three 5G bands, handling up to 800 MHz aggregated carrier bandwidth in the 26.5 to 29.5 GHz band (n257) and covering the entire 27.5 to 28.35 GHz band (n261) and the entire 37 to 40 GHz band (n260)[70].

Intel has been shown various prototypes of mmWave solutions in terms of chipsets or RF-front end solution, but announced recently that they are not going to provide 5G modem solutions for smartphones anymore. It remains to be seen if products for other type of devices will be made by Intel in the future.

There is an understanding at the time of this writing that other companies like MediaTek or Samsung LSI may also provide support for mmWave solutions in the future.

9. Regulatory Acceptance Limits and Procedures

This section will focus on the regulatory aspects of mmWave deployments. The two major areas include the RF safety and Maximum output power.

9.1. Radio Frequency Safety

Human exposure to electromagnetic fields is a critical consideration for mobile system design, as its level will limit the maximum output power of mobile terminals and base stations. On the entire device level, the exposure compliance requirement for the 5G device is the sum of all simultaneous of sub-6GHz and

mmWave transmitters is less than 1. The sub-6GHz compliance is measured with specific absorption rate (SAR). The mmWave compliance is measured with power density (PD). The total exposure limit is

$$\sum_{i=100\,kHz}^{6\,GHz} \frac{SAR_i}{SAR_{limit}} + \sum_{i>6\,GHz}^{300\,GHz} \frac{PD_i}{PD_{limit}} \leq 1$$

where SAR_i is the measured SAR at frequency i, SAR_{limit} is the FCC lmit; PD_i is the measured PD at frequency i and PD_{limit} is the FCC limit.

There are two kinds of device defined by the regulator. US defines portable device as a transmitter designed to be used within 20 centimeters of the body of the user [88]. US also defines mobile device as a transmitting device designed to be used in other than fixed locations and to generally be used in such a way that a separation distance of at least 20 centimeters is normally maintained between the transmitter's radiating structure(s) and the body of the user or nearby persons[89].

Furthermore, portable devices that transmit at frequencies above 6 GHz are to be evaluated in terms of the maximum permissible exposure (MPE) limits specified in § 1.1310 and in § 1.1307(b). Measurements and calculations to demonstrate compliance with MPE field strength or power density limits for devices operating above 6 GHz should be made at a minimum distance of 5 cm from the radiating source.

The mmWave MPE limit FCC and International Commission defined currently are as followed:

FCC	IEEE C 95.1 – 2005 + IEEE C 95.1 – 2010a	
f ≥ 6 GHz	3 GHz ≤ f ≤ 30 GHz	f ≥ 30 GHz
10 W/m² (spatial peak)	10 W/m² (averaged over 100λ²)	10 W/m² (averaged over 100 cm²)
–	$18.56f^{0.699}$ (spatial peak)	200 W/m² (spatial peak)

Table 9-1 MPE Limit at mmWave

FCC issued interim guidance at TCB Council Workshop on Oct. 3 2018 to use 4 seconds as time window and 4 cm^2 as averaging area for 28 GHz and 39 GHz as shown in Table 9-2. A formal notice of ruling is expected in 2019.

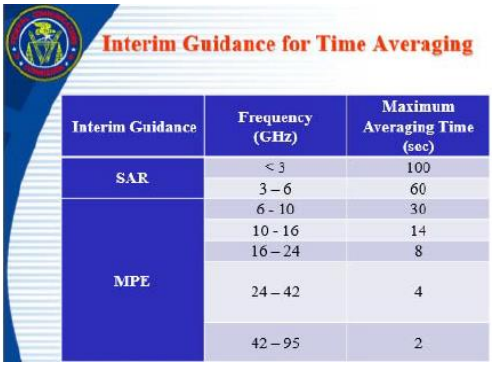

Interim Guidance	Frequency (GHz)	Maximum Averaging Time (sec)
SAR	< 3	100
	3 – 6	60
MPE	6 - 10	30
	10 - 16	14
	16 – 24	8
	24 – 42	4
	42 – 95	2

Table 9-2 FCC Interim Guidance

International Commission released a draft proposal on July 11th 2018 to use 20 W/m^2 as new limit and use 6 min as time window and 4 cm^2 as averaging area for sub-30 GHz and 1 cm^2 above 30 GHz as shown in Table 9-2. A 5G mmWave exposure standard IEC/IEEE 63195 addressing measurement techniques is under preparation and will be published in Q1 2021. Another standard IEC/IEEE 62704-5 will address related computational electric & magnetic field (EMF) methods. Since the mmWave systems depend on beam-forming, the already cumbersome near field power density measurement testing time will be multiplied by a factor equal to the number of beams unless some smart measurement algorithm can be found. Mobile Wireless Forum has defined research topics which cover several different aspects of EMF exposure issues.

6 GHz to 30 GHz	30 GHz to 300 GHz	
$55*f^{-0.177}$	$55*f^{-0.177}$	$110*f^{-0.177}$
Avg area: 4 cm^2	Avg area: 4 cm^2	Avg area: 1 cm^2

Table 9-3 IEEE Draft Power Density Limit

The exposure limits in Russia, China, Switzerland, and Italy, shown in Table 9-4 are much lower than those in the United States and most Western European countries.

Country/Guidelines	PD Restrictions for the General Public in W/m^2	PD Restrictions for the General Public in mW/cm^2	Frequency Range (GHz)	Basis
ICNIRP [17] (1998)	10	1	2–300	Science based
FCC [16] (1996)	10	1	1.5–100	Science based
China [32] (1987)*	0.1	0.01	0.3–300	Science based
Russia [33] (2003)	0.1	0.01	0.3–300	Science based
Switzerland [34] and [35] (2000)*	0.1	0.01	1.8–300	Precautionary
Italy [36] (2003)*	0.1	0.01	0.0001–300	Precautionary

Table 9-4 PD Limit at mmWave in China, Russia, Switzerland, Italy

9.2. Maximum Output Power

In term of maximum transmission power of UE in mmWave, FCC has set the max radiated total EIRP limit for mobile station as 43 dBm, including mobile handset, for mmWave bands from 28 GHz to 39 GHz. The EIRP measurement procedure has been defined.in KDB [91]

Also, FCC sets the max EIRP limit for transportable station (transmitting equipment that is not intended to be used while in motion, but rather at stationary locations) as 55 dBm. The corresponding EIRP measurement procedure for 28-39 GHz has been defined as followed:

- Radiated test facilities consisted of an indoor 3-meter semi-anechoic chamber. It was determined that separation of at least 14 cm is needed to ensure RF Exposure compliance.
- A raised turntable is used for radiated measurement. The turn table is a continuously rotatable, remote-controlled, metallic turntable and 2 meters in diameter.
- An 80cm tall test table is placed on top of the turn table. A pedestal is placed on top of the test table to bring the total table height to 1.5m for measurements above 1GHz.
- The receive measurement antenna is located meters from the EUT which is the far field of the EUT per formula (2*D^2)/wavelength, where D is the max diagonal dimension of the smartphone.
- Radiated power levels are investigated with the receive antenna horizontally and vertically polarized. The receive antenna was rotated on various angles to investigate worst case emissions.
- The maximized power level is recorded using the spectrum analyzer “Channel Power” function with the integration band set to the emissions’ occupied bandwidth. The EIRP is calculated from the raw power level measured with the spectrum analyzer: EIRP (dBm) = E (dBµV/m) + 20 log D − 104.8.

Figure 9-1 Anechoic Chamber

10. Test and measurements methodology for mmWave systems

The differences in propagation and penetration properties between sub-6 GHz and mmWave bands, together with the related differences in the specifications, mean that there are additional considerations

in testing and measurement methodology. This section addresses some these new considerations for mmWave.

10.1. UE Testing and Certification

Cellular communications systems have been developed and operated through multiple generations from the early days of GSM (2G) to today's successfully deployed LTE (4G) networks. 5G NR testing can therefore leverage established test procedures as well as a proven certification framework. Figure 10-1 illustrates the established process for user device testing in existing cellular technologies.

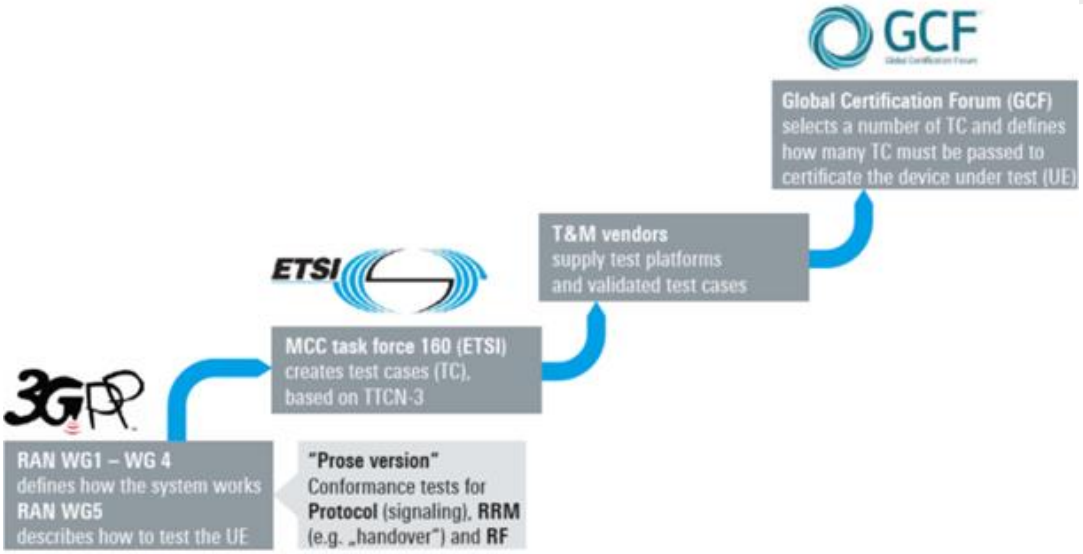

Figure 10-1 Certification process, from 3GPP to GCF

As the responsible standardization body, 3GPP creates the specification which provides a comprehensive definition of the complete system. More specifically, the 3GPP RAN4 and RAN5 working groups define the base station and user equipment requirements to be tested and verified. Obviously, regulatory conformance must be checked in accordance with the requirements of the local authority. In contrast, end-user devices can be operated in multiple mobile networks in different countries in a roaming scenario. This triggered the foundation of the Global Certification Forum (GCF). The GCF selects a number of test cases for a cellular technology in order to ensure a minimum level of performance for these devices. Independent test labs certify conformity with these requirements. The end-user device tests cover protocol (signaling) and three main categories on a high level.

The radio transmission and reception (i.e. RF) requirements define the transmitter capabilities (e.g. maximum output power and transmit quality such as EVM and frequency error) and receiver capabilities (e.g. the sensitivity of a device or its ability to maintain a certain throughput in the presence of an interferer or blocking signal). Both are closely related to the hardware implementation of the RF frontend. The second category summarizes the demodulation and channel state information reporting

performance. This is, in other words, the ability of a receiver to achieve a certain minimum throughput under various fading conditions. Furthermore, this relates to the required ability to measure and report the channel conditions. The third category verifies the support for radio resource management, i.e. support for handover and mobility scenarios. This is more closely related to the software implementation of the end-user device. Formulation of an unambiguous test case to verify a specific throughput requirement or a certain transceiver performance criterion (e.g. EVM) is a challenging task. To ensure interoperability, a common test language was created and further developed over time. The latest established version is known as TTCN-3. Using TTCN enables a joint description of all test cases, which are developed within ETSI MTC160 with voluntary contributions from the test industry. This general framework then allows test vendors to offer test platforms to execute these test cases. Finally, a certification organization like the Global Certification Forum (GCF – https://www.globalcertificationforum.org/) selects the most important test cases to ensure interoperability on a global scale. Founded in 1999, this membership organization brings together technical experts from the world's leading manufacturers, operators and the test industry. Note that on top of certification bodies like the GCF, various operators define their own test cases to ensure compatibility with their deployed networks. Thus, we may be tempted to conclude that 5G NR testing is straightforward and does not pose any major challenges after finalization of the technology design. However, although a stable framework exists, there are essential differences.

5G NR is the first cellular technology operating at frequencies in the cm-wave and mm-wave spectrum, requiring the application of advanced antenna technologies. This fact has a major impact since it means that over-the-air testing represents the default case (at least in the cm-wave and mm-wave spectrum). Both higher layer testing and core network testing are also affected.

10.2. Over the air testing, general aspects

Testing of base stations or user devices was established with the early 2G systems based primarily on conducted connections. Even on a component level, usually an RF connector was available allowing connection of a test instrument to measure the parameter of interest, e.g. a transmitter performance indicator such as EVM. Although the antenna implementation plays an equal and crucial role for the overall performance during operation in the field, testing was essentially done conducted. The reason is that most implementations (even up to operation of 4G networks) include passive antennas.

In an end-user device, the design of the antennas aims for an omnidirectional pattern away from the head. Although base station antennas aim for directional transmissions, for example, realizing 120° for a three-sector cell implementation, the design still targeted static antenna patterns.

The first over-the-air test methods were discussed in conjunction with the commercial adoption of MIMO schemes in user devices. The influence of the antenna implementation in combination with the precoding applied to the baseband demanded over-the-air test methods including emulation of real-world fading effects. The discussions on these test methods were extremely long-lasting and eventually resulted in additional OTA test cases for user devices. These additional test cases are specified in TS 37.544 and

generally include output power (TRP) and sensitivity tests. Likewise, the evolutionary step towards active antennas for base stations resulted in two over-the-air requirements. Initially, two distinct RF requirements (radiated output power and radiated sensitivity) were defined in TS 36.104. Reflecting the beam steering capability of active antenna systems, the base station manufacturer needs to verify these two radiated requirements (power and sensitivity) in all extreme steering positions and for the so-called reference beam peak direction.

Figure 10-2 illustrates the test procedure highlighting the beam peak direction and one of multiple possible extreme steering directions on an arbitrary surface.

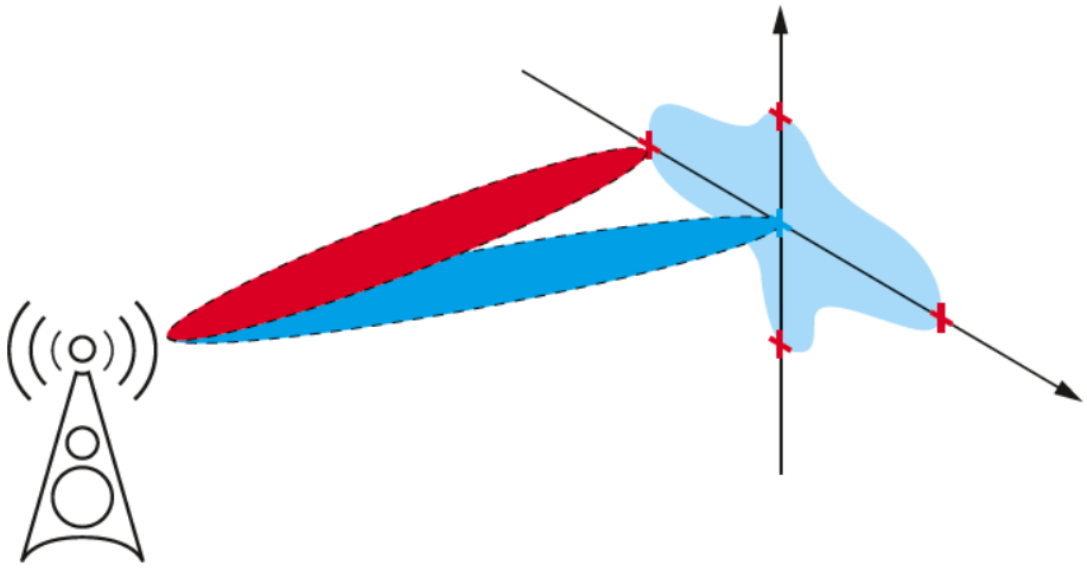

Figure 10-2 General principle of OTA testing. Five-point beam declaration procedure

Even with these initial steps in the direction of over-the-air testing, the described OTA test cases for both base stations and user devices are complementary ones. This reflected the need for taking the antenna implementation into account for specific requirements only. However, the vast majority of 2G through 4G testing is still executed in a conducted manner.

In an active antenna system, the transceiver frontends are integrated together with the antenna array, which means that traditional RF output ports are no longer available. Although it involves a generally lower number of applied antenna elements, the same challenges also apply when developing the transceiver for a user device. Therefore, over-the-air testing is no longer an add-on topic consisting of a limited number of test cases, but has become the default test case at least for FR2 frequencies.

This significantly affects the overall test procedures and requires access to the measurement uncertainty in over the air scenarios. In addition, shielding is typically required, not only to avoid influence from radiating sources near the DUT, but also to protect the test engineer from radiation.

The approach to OTA testing is different for base stations and user devices. Base station manufacturers need to declare the type of base station they are implementing. In contrast to base stations, for user devices the need for over-the-air testing depends on the frequency bands in which they operate. For FR1, most testing is still conducted since the availability of RF connectors is assumed. User devices supporting FR2 will be tested over the air only (see TS 38.101). The test methodology for over-the-air testing of user devices supporting FR2 was studied in TR 38.810. Generally, the test methodology distinguishes between UE RF testing, UE RRM testing and UE demodulation / CSI reporting. RF testing comprises transmitter and receiver requirements (section 6 and section 7 in TS 38.521 part 1, 2 and 3), e.g. maximum output power, modulation performance such as EVM, sensitivity or the ability to maintain a certain throughput performance in the presence of a blocking signal. RRM testing ensures the efficient use of the available radio resources. The requirements that are tested include, for example, cell reselection in idle mode and support for mobility (handover) in connected mode (see TS 38.533 for details). Finally, UE demodulation and CSI testing cover the baseband performance of the receiver under various fading conditions and the UE's ability to correctly measure and report channel state information (CSI) to the network. See TS 38.521 part 4 for details.

Generally, 3GPP requires all over-the-air measurements to be executed under far field conditions. For RF testing, two main test methods are permitted: the direct far field (DFF) and the indirect far field (IFF) method. Both use an anechoic chamber for shielding and require a positioning system such that the angle between the dual-polarized measurement antenna and the DUT has at least two axes of freedom and maintains a polarization reference. The DFF method ensures measurements at a sufficiently large distance according to the Fraunhofer distance. The IFF method uses a hardware transformation of the propagating waves to create plane waves, i.e. far field conditions, at the DUT at a shorter distance compared with the Fraunhofer distance. This reduces the required chamber size and thus reduces the complexity and cost of the test setup. Additionally, the IFF method allows for better control and parametrization (size, quality) of the Quiet Zone (QZ).

This solution is also known as a compact antenna test range (CATR) and is illustrated in Figure 10-3. Using Fermat's principle of least time, a planar wave can be focused on a single point using a parabolic mirror. If a measurement antenna is placed at this focal point, using the reciprocity principle, a plane wave can be generated since the parabolic mirror reflects a certain planar component of the incoming spherical wave from the measurement (or feed) antenna into the quiet zone where the DUT is placed.

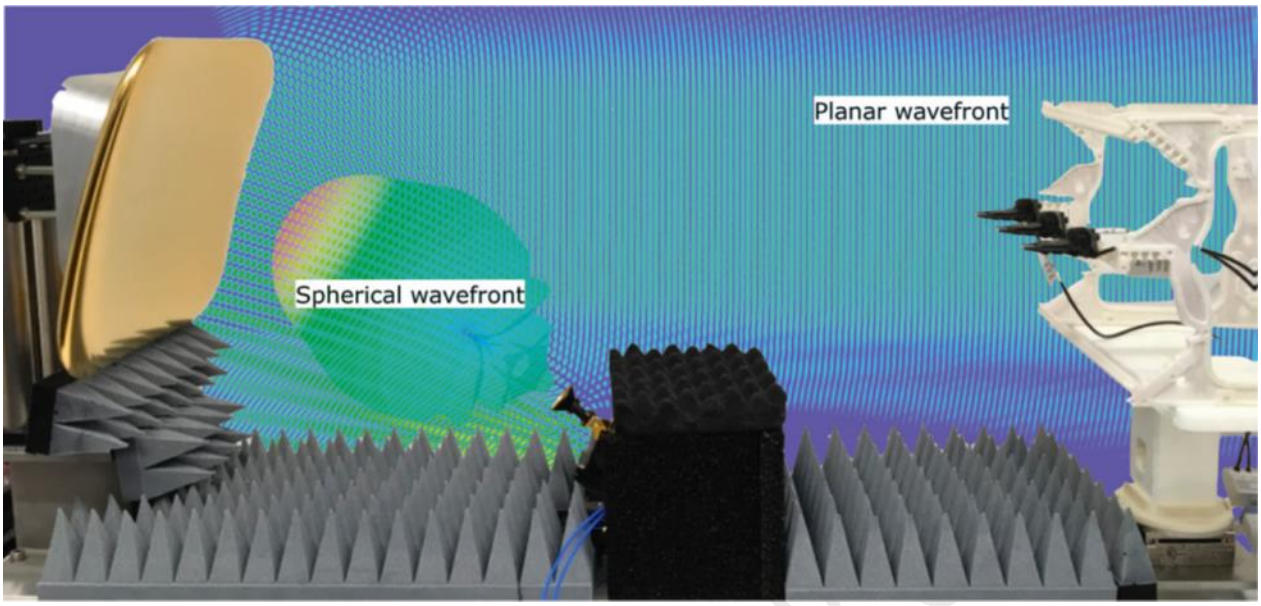

Figure 10-3 Compact antenna test range OTA measurement setup

A CATR reflector is typically built using a solid piece of aluminum to maintain the strict surface geometry requirements. End user device realization in FR2 allows for compact and rather light reflectors.

An implementation of the baseline test system for UE demodulation performance and channel state information reporting is sketched in Figure 10-4 (see TR 38.810 for details). Testing aims to verify the ability of a receiver to achieve a certain minimum throughput under various propagation conditions and involving different signal configurations (e.g. MIMO layers and modulation schemes).

In addition, the required ability to measure and report the experienced channel conditions is tested. Note that demodulation performance relates to the baseband capability of the end-user device receiver. The RF performance is verified throughout the RF testing steps as illustrated previously. Consequently, in 3GPP Release 15 demodulation performance and CSI reporting do not require far field conditions. Testing in the radiated near field is possible. The minimum measurement distance is defined as $R > 0.62 \sqrt{(D3/\lambda)}$. In the baseline test system, one transmission point, i.e. a single angle of arrival from the emulated eNB, with a dual-polarized antenna is directed to the UE within an anechoic chamber.

The positioning system is constructed in such a way that the angle between the dual-polarized measurement antenna and the DUT has at least two axes of freedom. Fading conditions, usually generated in the baseband of the communications tester, are modeled as a tapped delay line. Rank2 transmission, i.e. 2×2 MIMO, is required for some test scenarios and sufficient isolation between both polarizations must be ensured. In an initial step, the best beam is identified and locked for subsequent testing. For NSA test scenarios, an additional LTE link antenna is used to provide a stable LTE signal. The system applies to DUTs with a device size of $D \leq 15$ cm.

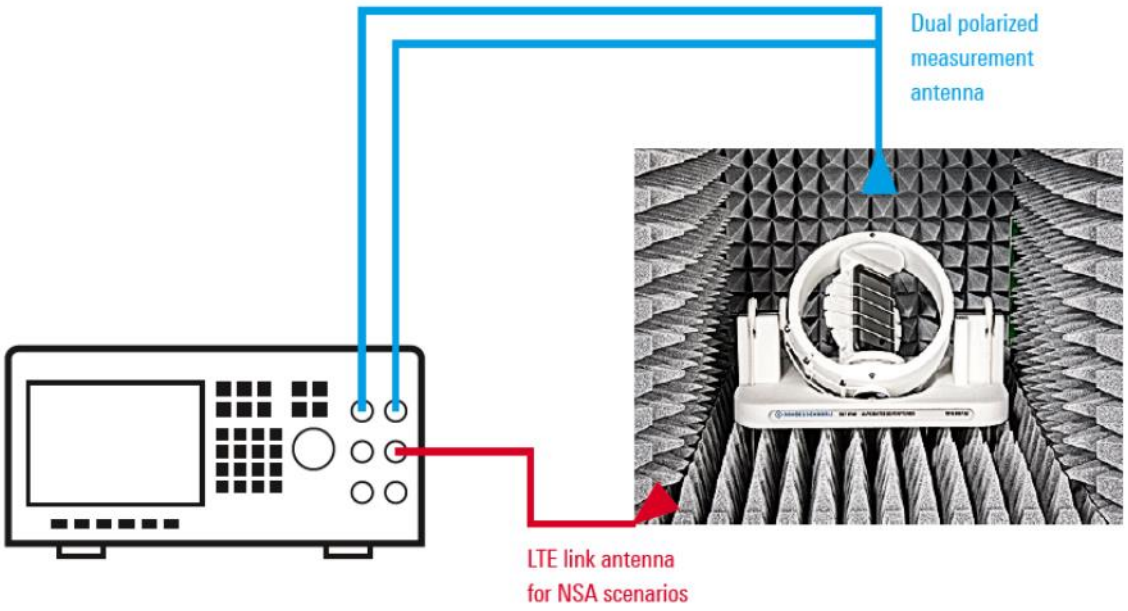

Figure 10-4 Test setup for UE demodulation and CSI reporting

Finally, support for Radio Resource Management (RRM) must be tested, i.e. support mobility scenarios like cell re-selection and handover. These RRM scenarios are particularly important since they also include testing of beamforming procedures. There is a trade-off between highly realistic emulation of a real-world network implementation and the need for cost- and time-efficient testing. An implementation of the generalized baseline test setup as described in TR 38.810 is sketched in Figure 10-5. It establishes an OTA link between the user device and several emulated base station sources, whereas as of 3GPP Release 15, up to at most two simultaneously active 5G NR transmission and reception points are used. Note that in case of a DFF and an IFF measurement setup, the maximum number of simultaneously active 5G NR transmission and reception points is two and one, respectively.

To account for different spatial directions of cells and beams involved in RRM procedures, 3GPP has concluded to a set of relative angular relationship between the – simultaneously or not – active transmission points as follows: 30°, 60°, 90°, 120°, and 150°. Potential spatial RRM requirements are expected to use angular offsets from this set, which shall be supported by the measurement setup accordingly. Again, the positioning system is constructed in such a way that the angle between the dual-polarized measurement antenna and the DUT has at least two axes of freedom and fading is applied using a tapped delay line model. Such a positioning system might allow for support of scenarios with continuous change of angle of arrival during the test.

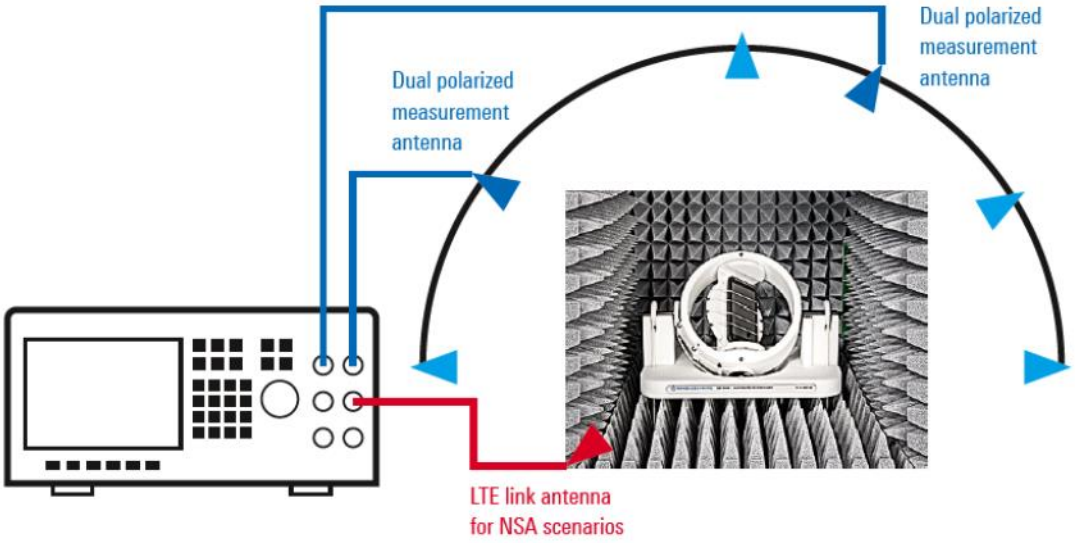

Figure 10-5 OTA test setup for RRM characteristics

FR2 over the air testing of end-user devices is a comprehensive task, requiring multiple test setups depending on the measurement application. For efficiency reasons, the number of test setups should be reduced as much as possible. In an R&D environment, CATR setups as illustrated in Figure 10-3 allow high flexibility to operate with different test instruments. In a conformance environment, solutions integrating shielding and the right choice of test instruments are essential. As an example, Figure 10-6 illustrates a compact solution that enables NSA RF, RRM (IFF with single TX/ RX) and UE demodulation / CSI reporting measurement applications in a single test setup.

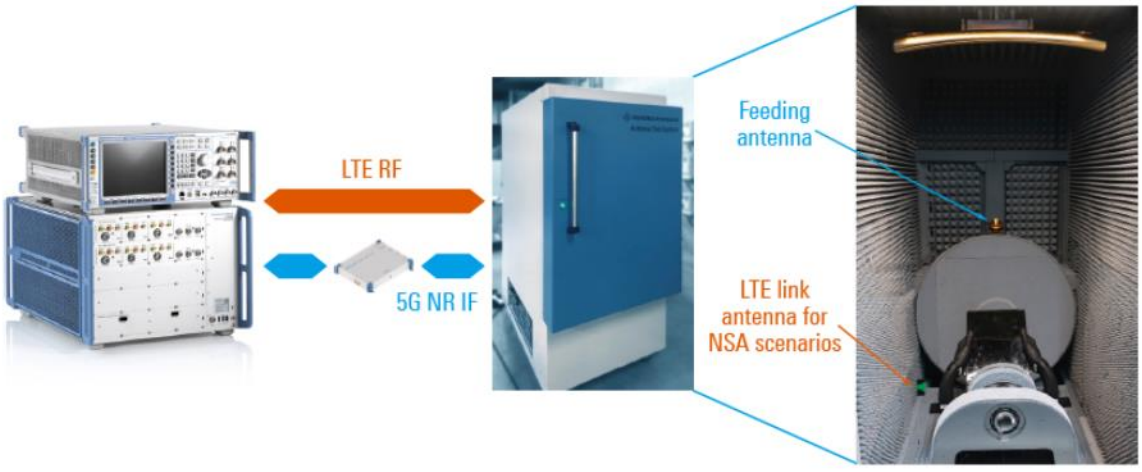

Figure 10-6 OTA test setup for UE RF testing, CSI reporting and RRM testing [129]

10.3. Near field/far field aspects

Generally, 3GPP requires over-the-air testing to be executed under far field conditions for accurate absolute power measurements. In the far field region of an antenna, radiated power decreases as the square of distance. Furthermore, each part of the electromagnetic (EM) field is associated with a change in the other part, and the ratio of the electric and magnetic field intensities is simply the wave impedance. Often, the far field is also described as the region where the electromagnetic waves have become planar waves as illustrated in the upper part of Figure 10-7.

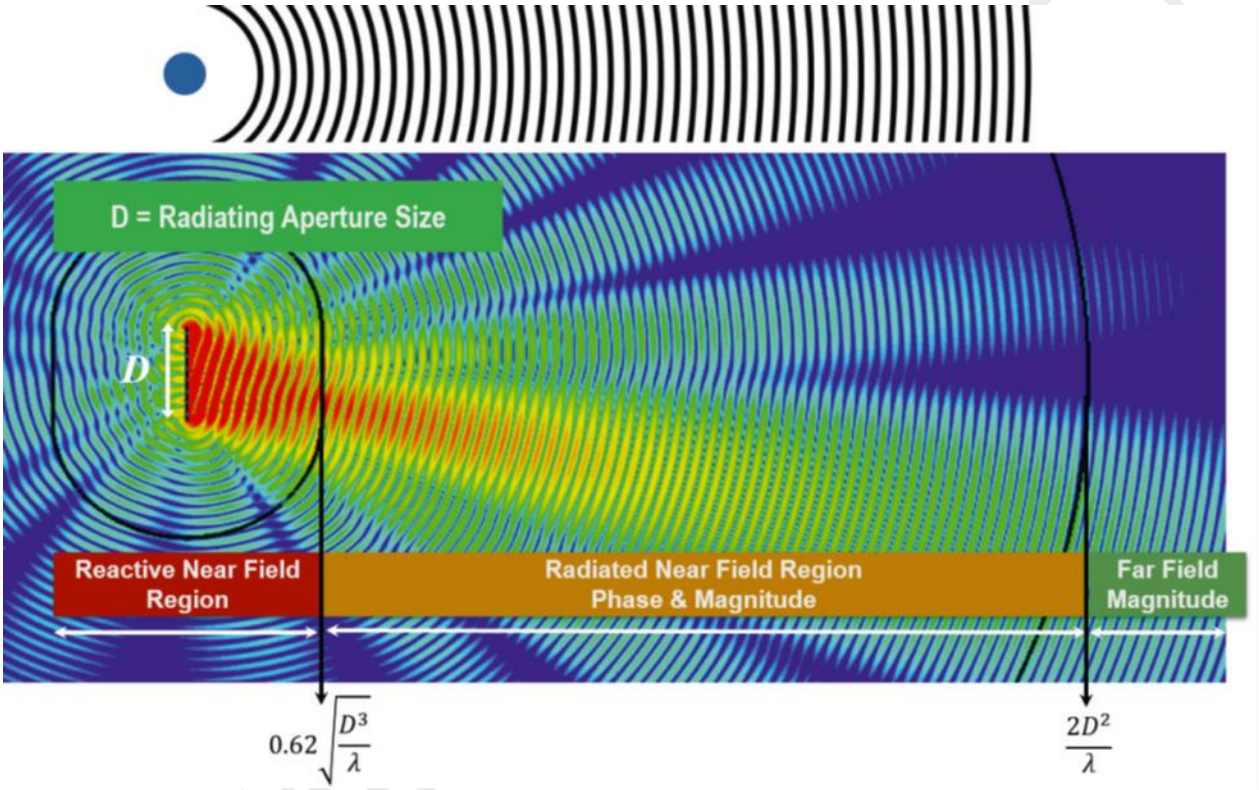

Figure 10-7 Near field and far field regions for an electromagnetically long antenna

In contrast, in the near field the relationship between E and H becomes very complex and all four polarization types can be present. Note that in the far field, electromagnetic waves are characterized by a single polarization type (horizontal, vertical, circular or elliptical). Furthermore, placing a measurement antenna in the reactive near field would lead to undefined results since any object in this region becomes part of the antenna system under test and interferes with the measurements.

The outer boundary of the reactive near field region is given by the formula in Fig. 1-11, assuming the radiator dimension D is greater than λ/2. Measuring in the radiated near field region is possible in general if both the phase and magnitude are determined. Based on this information, the near field to far field (NF-FF) transformation can be applied.

Since 3GPP requires far field measurements, the question is how to determine the far field distance. According to the literature, the far field is defined based on the Fraunhofer formula $r > 2D2/\lambda$. Here, D corresponds to the diameter of the smallest sphere that encloses the radiating parts of the device under test and λ is the wavelength at the applied frequency. For an illustration of far field distances at 28 GHz and 100 GHz depending on the parameter D, see Table 10-1.

D (in cm)	Frequency (in GHz)	Near/far boundary (in m)	Path loss (in dB)	Frequency (in GHz)	Near/far boundary (in m)	Path loss (in dB)
5	28	0.47	54.8	100	1.67	76.9
10		1.87	66.8		6.67	88.9
15		4.20	73.9		15.01	96
20		7.47	78.9		26.68	101
25		11.67	82.7		41.69	105
30		16.81	85.9		60.04	105

Table 10-1 Fraunhofer far field distance calculated for a traditional far field anechoic chamber

The Fraunhofer formula can be seen as the safe method to determine the far field distance. However, considering the transition from radiating near field to far field with gradually increasing characteristics of far field rather than an abrupt boundary, this criterion may be overly conservative. Furthermore, the far field distance determines the required chamber size, which is a major complexity and cost factor that must be kept in mind.

Investigations have shown that measurements are possible at distances that are shorter than the far field according to Fraunhofer, in particular if main beam testing is the focus. Two new expressions for far field distances based on assumptions for the maximum order of excited spherical harmonics are derived in [Ref. 1]. The resulting far field distance according to these expressions is on the order of 30 % compared with the Fraunhofer distance. The additional errors related to these much shorter distances are discussed in [Ref. 1]. Measurements performed in a compact anechoic chamber corroborate the findings.

The 3GPP technical report on NR test methods (see TR 38.810 for details) also includes an experimental method to determine the far field distance based on path loss measurements. By measuring the path loss gradient over a certain distance, the near/far field boundary can be found because the path loss exponent is different in the near field and the far field.

The results from an experiment conducted on an LTE device operated at 1.8 GHz are shown in Figure 10-8. The minimum far field distance can be found at the regression intercept point. However, TR 38.810 concludes that further work is required to determine whether this technique provides valid results for much higher frequencies and general device types.

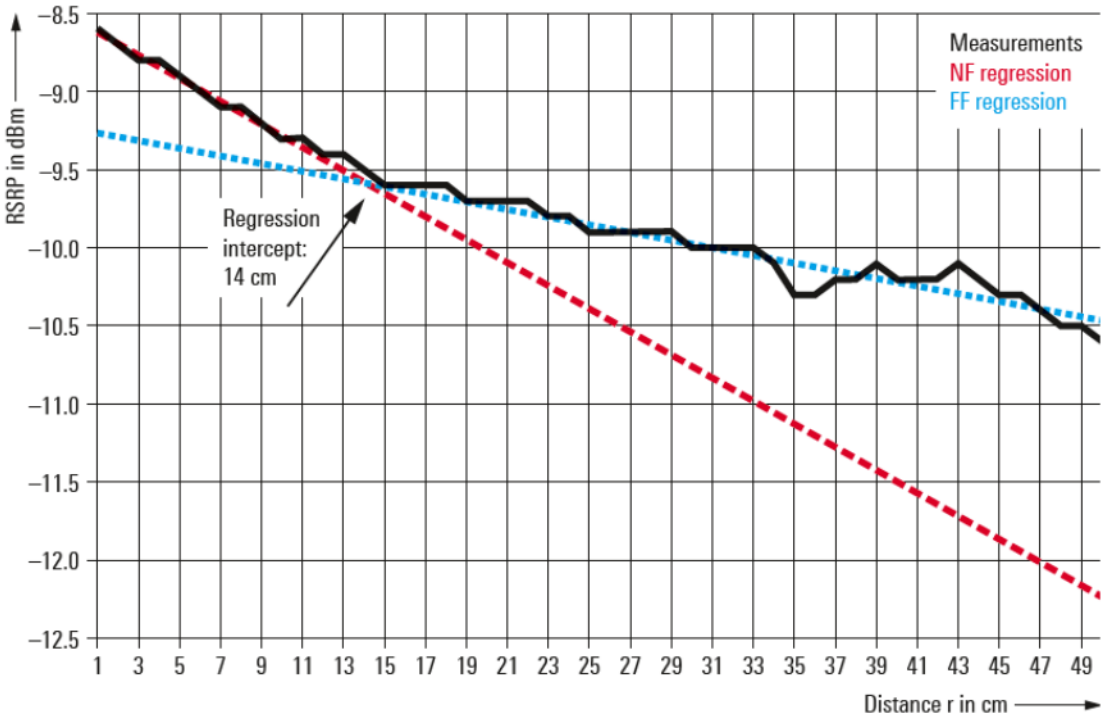

Figure 10-8 Measurements to determine the min far field distance for an LTE UE at 1.8 GHz (TR 38.810)

10.4. Field Testing and Optimization

Over the air testing of mmWave frequency bands, which can include walk test or drive tests, are required from the design phase through the integration phase. The design phase involves understanding the complete propagation profile for the mmWave signals and then using them for the modeling tuning exercise. This could involve continuous wave testing and modulated signal testing as well. Similar testing also needs to be done during site integration and then for day to day interference management and optimization.

5G introduces the concept of Synchronization Signal Block (SSB) Beams which are beams broadcast from the 5G base station (gNB). They enable the UE to discover nearby 5G gNBs. The UE then sets up a session with the gNB employing massive MIMO to form UE specific beams. Operators need to baseline the SSB coverage for mmWave based 5G network deployments, which involves in decoding the standards based NR technology. Once baselined then operators need to optimize the coverage of these SSB Beams which are performed through scanning receivers. Scanning receivers decode the SSB signals, providing an entire picture of the SSB RF landscape. Decoding the SSB beams allow scanning receivers to provide Primary/Secondary Synchronization and Physical Broadcast Channel Received Power, Received Quality and SINR for each SSB beam, as displayed below.

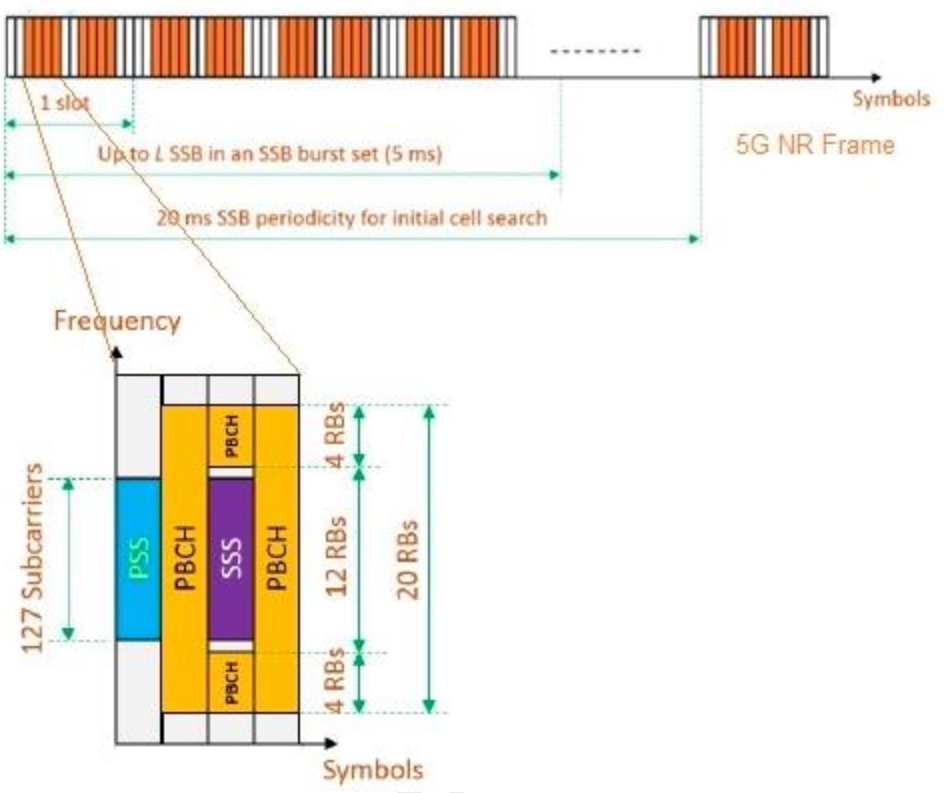

Figure 10-9. SSB signals

The bandwidth of the SSB is determined based on the sub carrier spacing used for the FR2 deployments which can either be 120KHz or 240KHz. The ability of a testing tool to report the maximum details of the SSB for multiple beams which can be up to 64 beams from each sector at any point is critical for the user to understand their RF environment and propagation profile of individual transmit beams. Since operators are now starting to deploy mobility and understand the level of their ubiquitous coverage with mmWave bands, data density drive and walk test is also critical. Users need to be aware of tool capabilities to support normal driving speeds above 40 mph (64 kmph) to support these types of measurements.

5G signal in FR2 are also highly susceptive to the topography, foliage and environment and hence the test methodology needs highly accurate devices with deep dynamic range which will enable the user to see low powered signals in the presence of high-powered ones to enable them to maximize spectral efficiency.

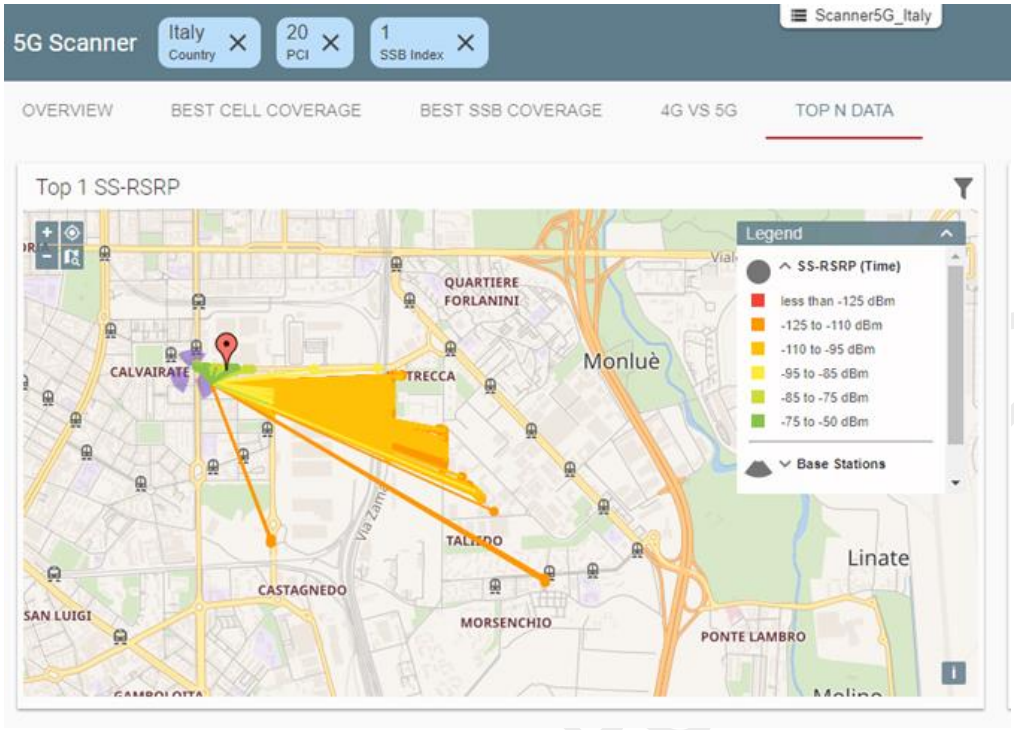

Figure 10-10 Screenshot from a measurement indicating the SSB beam coverage [130]

Figure above shows an example of a single SSB beam coverage based on a 5G scanner test output for the purpose of coverage illustration.

An important consideration for 5G test methodology using passive devices like scanning receiver is the antenna location for data collection. mmWave frequencies encounter high body absorption losses and require placing the antenna above the data collector's head to eliminate blockage resulting in an accurate baseline. While it's difficult to predict how end users will place their devices with respect to their body, it's important to properly baseline the network. When using omni-directional antennas for data collection, users need to be cognizant about the vertical beam widths of the antenna and need to factor the antenna gain and cable losses (which can be in the range of 3 dB per meter of cable in the mmWave band).

mmWave 5G networks have brought on many new unique challenges in measuring and optimizing the cellular network. Adding mobility brings on additional testing and deployment challenges. Testing tools are critical devices that enable operators to deploy, optimize and manage their networks.

10.4.1. Echo mmWave Repeater Field trial results

Echo5G pre-commercial units (Figure 10-11) have been tested in several environments with a US based carrier.

Figure 10-11 Exterior view of a pre-commercial Echo5G prototype

One such trial took place on the second floor of a suburban apartment building shown in Figure 10-12. Two vendor base-stations (gNBs) located 700ft from the front of the apartment were used to serve traffic through the Echo5G to a third party mmWave CPE inside the home. An Echo5G was placed on the window closest to Location A and had line of sight to the base stations at an angle of roughly 45° from window broadside. Echo5G was able to interoperate with both gNBs and one of the gNBs was selected for use in additional locations.

The CPE was moved to various locations nearby point A, B and C. Figure 10-13 summarizes the throughput results. The CPE supported a peak rate of 1Gbps (1000Mbps). With the Echo5G unit turned off, full rate was only observed by placing the CPE outside the home on the balcony. No locations indoors supported full rate with Echo5G turned off. Location C showed no connectivity at all. With Echo5G turned on, full rate experience was observed for most locations inside and even locations that previously had no connectivity showed substantial throughput. In this case the same forces that keep mmWave signals outside of the building were keeping the mmWave signal bouncing around inside the home. This is how throughput was observed in non-line of sight locations such as the bathroom adjacent to the master bedroom. SINR and BRSRP both showed 20 to 30dB improvement with Echo5G turned on.

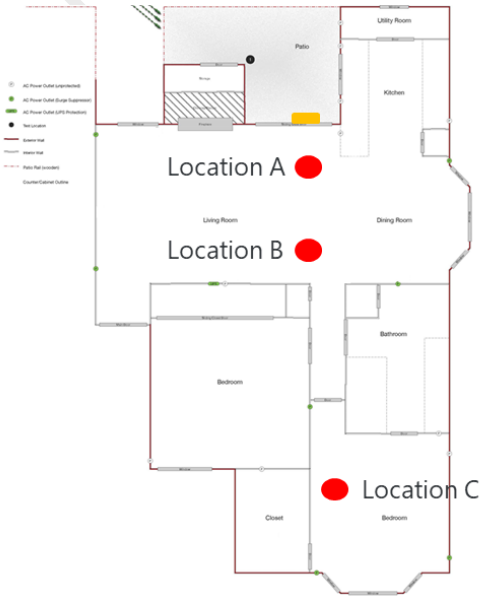

Figure 10-12 Floor plan for Echo5G field trial

The above figure is the floor plan using pre-commercial base stations, CPEs and Echo5G. The Echo is on the northern glass window (yellow rectangle). The CPE is moved to various locations inside the apartment.

		gNB Vendor 1		gNB Vendor 2	
		Baseline	With Echo	Baseline	With Echo
DL Throughput UDP (Mbps)	Location 1 - Balcony	1020	NA	1000	NA
	Location A	320	1000	510	1000
	Location A - L0.5	480	1000		
	Location A - L1	320	1000		
	Location A - L1.5	210	1000		
	Location A - L2	420	1000		
	Location A - L3	160	1000		
	Location A - L4	360	1000		
	Location A - L5	220	550		
	Location E	470	980		
	Location B	890	1000	440	1000
	Location B - R1	570	1030		
	Location B - R2	590	1010		
	Location B - R3	750	1010		
	Location B - R4	260	1020		
	Location C	NC	900	NC	950
	Location C - R0.5	NC	1000		
	Location C - R1	NC	670		
	Location C - R1.5	NC	210		

Figure 10-13 Throughput measurements at baseline (Echo5G turned off) and Echo5G on.

A second field trial took place within a multi-dwelling unit (MDU) on the 15th floor located in a dense urban environment. A single gNB was located 150ft from the dwelling and was -45° in elevation (the Echo had to steer down). As before, the CPE was moved around the dwelling on a grid shown in Figure 12 while BRSRP measurements were collected. As in the previous trial, BRSRP improvements of order 20 to 30dB were observed and all test locations saw connectivity at mmWave.

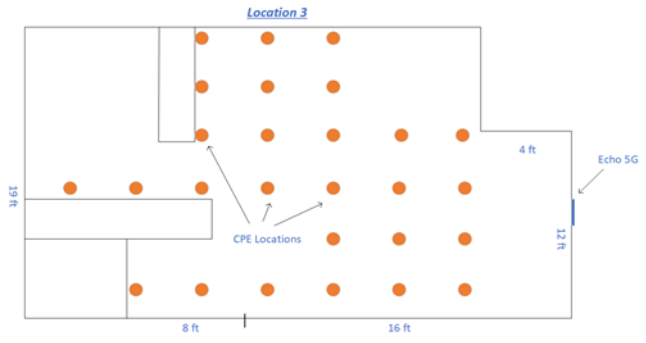

Figure 10-14 MDU layout and grid test locations (orange dots) within it.

BRSRP

ECHO OFF	distance from the wall					
distance from window	3'	6'	9'	12'	15'	18'
6'	-112	-115	-118	-116		
9'	-117	-100	-116	-115		
12'	-116	-117	-114	-115	-112	NS
15'			NC	NC	NC	NC
18'			NC	NC	NC	NC
21'			NC			
24'			NC			

ECHO ON	distance from the wall					
distance from window	3'	6'	9'	12'	15'	18'
6'	-92	-92	-86	-93		
9'	-92	-87	-96	-99		
12'	-93	-87	-100	-104	-94	-94
15'	-93		-92	-90	-94	-98
18'	-96		-94	-92	-91	-96
21'	-94		-94			
24'			-96			

Table 10-2 BRSRP measurements with Echo5G OFF (left) and Echo5G ON (right)

Echo5G availability is projected for Q3 of 2019. Trial results indicate it provides a significant link improvement between the gNB and CPE and expands coverage to include most of the home. This feature is critical to successful mmWave deployments. The number of gNBs needed to cover an area is the dominant factor in calculations of CAPEX and OPEX associated with a deployment. Echo5G reduces the number of initially needed base stations dramatically, with 1km distant line of sight links becoming possible even with outdoor to indoor penetration challenges.

11. Conclusions and Next Steps

The introduction of mmWave frequency bands is one of the key new 3GPP Rel.15 specifications, meant to address the deployment of 5G technologies. While mmWave frequencies have been used in the past for satellite or point-to-point and point-to-multipoint *backhaul* connections, this is the first time that those frequencies have become part of 3GPP global standards for the intended use of terrestrial mobile along fixed access networks. Such progression has been made possible through various technological advancements, including massive MIMO coupled with beamforming technologies, advancement in chipset processing power, and the overall RF front-end/antenna subsystem integration/innovation for base station equipment as well as user equipment.

The Mobile industry is in its infancy of embracing mmWave frequencies to address various use cases ranging from the relief of mobile network congestion in dense areas, to fixed wireless broadband access, industrial automation, and autonomous driving. Each of these use cases present their own challenges for using mmWave frequencies including the effective applicability along with the expected performance, robustness, and associated business cases. However, the initial deployments of mmWave spectrum for 5G in the US have shown the potential that exists to deploy these frequencies for the purpose of mobile networks.

This paper provides a technology-centric view on mmWave deployments in point-to-multi-point mobile networks and handheld consumer devices, such as smartphones. Topics related to the respective business cases, cost associated with deployment of mmWave frequencies, or the incremental cost to support mmWaves in smartphones etc, are outside the scope of this effort.

The limited propagation characteristics of mmWave spectrum due to their high frequency range, poor outdoor-to-indoor penetration due to building materials attenuation, as well as other environmental and weather factors have been well understood in the past. However, advancements in Massive-MIMO systems coupled with beamforming technologies related to fast beam-tracking, assignment, and switching intend to compensate for some of these shortcomings when mmWave spectrum is deployed in mobile networks.

The mmWave frequency simulation analysis presented in this paper shows that, depending on the simulation methodology used, a standalone mmWave mobile network would require 2.5-3 times more sites when compared to a sub 6-GHz deployment in order to ensure the same level of contiguous outdoor coverage in dense urban/metro areas. The number of sites for a standalone mmWave mobile network can be reduced by using EN-DC technology that combines an ability to bond sub-6GHz LTE/5-NR and mmWave 5G-NR for DL channels along with an ability to utilize sub-6GHz for UL data transfers. Such a scenario would require 1.78 times the number of mmWave sites when compared to a sub 6-GHz deployment in dense urban/metro areas. The use of EN-DC, on the other hand, would require an additional 20-40MHz of dedicated UL sub-6GHz spectrum to ensure an efficient deployment and to take full advantage of the large DL channel bandwidths available with mmWave. Separately, it should be noted that the deployment of mmWave frequencies outside the dense metro areas would require a much larger number of sites when compared to dense urban areas in order to ensure contiguous coverage, be it in standalone or EN-DC mode.

The deployment of mmWave frequencies in handheld devices, like smartphones, has required that advancements to be made in UE antenna technologies and their subsequent device integration in order to maintain the radiated properties of the system and consistent two-way reliable connectivity between the UE and base station through the beamforming mechanism. This paper highlights and analyzes various UE antenna technologies, such as phased-arrays, high-gain steering antennas, and reactive beam steering that could be used for such purposes.

The paper also analyses various technologies required to address high UE power consumption related to large channel bandwidth processing of mmWave bands. Some of these technologies, like high level of integration on UE RF front-end blocks are specific to mmWave frequencies, while others are more general to 5G and are band agnostic. Some of the technologies highlighted here include bandwidth part selection, cross-slot scheduling, and upcoming Rel. 16 user traffic profiling.

mmWave frequency bands require a different approach when it comes to gNB, UE, or overall system testing when compared to sub-6GHz bands, and this is mainly due to the need to run almost all RF conformance and performance tests in an OTA environment, as opposed to a conducted mode. This paper demonstrated that the test and measurements industry has made significant strides to meet those challenges and to provide cost-effective test solutions that are capable of measuring far-side performance through limited size environments.

Regulatory certification related to mmWave bands is also addressed in this paper and while the methodology is different from that of sub-6GHz bands, there is sufficient process and information defined to date, at least in the USA, that allow for gNB and UE regulatory processes to be completed. As of this writing, the first examples of smartphones that support mmWave spectrum have already been certified for the US market.

Deployments of mmWave frequency bands are currently underway in the US by two major operators and more deployments may materialize in other countries in the years to come. Various initial third-party evaluations of these initial deployments have highlighted some of the shortcoming and technological challenges presented in this paper, including coverage limitations, connection robustness, practical spectral efficiencies, smartphone battery life, etc. Like any new technology, the performance of these first deployments may be handicapped by suboptimal overall system implementation, something that maybe particularly true with operators rushing to be first to market with 5G.

Having said that, it is critical that the right lessons are gleaned from these initial deployments through a complete and thorough independent performance evaluation process. It is only through this process that appropriate technological advancement requirements, or new architectural solutions, will be identified and enable the industry to advance to the next phases of the technology. Wireless technology providers have consistently demonstrated that they are capable of meeting technical challenges over time through substantial R&D investment and dedication. Meeting those challenges within an acceptable cost model and performance structure in large scale mobile network deployments remains to be proven in the case of mmWave band frequencies.

As mentioned at the outset, the current version of this paper focuses largely on the mobility use case for mmWave addressing congestion relief in dense urban areas for eMBB. Subsequent versions of the paper will address technological specificities related to autonomous driving and industrial automation use cases. Those two use cases may require additional features in order to deal with short-range communication, high velocity movements, reliability of connection, and low latency requirements, features that may not be critical to the eMBB use case discussed in the current version of the paper.

12. List of Contributors

Company
3M
Global Foundries
PCTEL
Pivotal Commware
Qualcomm
Remcom
Rohde & Schwarz
Samsung
SiversIMA
Skyworks
Soitec
Sprint
Vodafone Group
WiSpry

13. List of acronyms

3GPP	3rd Generation Partnership Project
5GAA	5G Automotive Association
5GNR	5th Generation New Radio
ACK	Acknowledgement
ACLR	Adjacent Channel Leakage Ratio
ADC	Analog to Digital Converter
AR	Augmented Reality
ASA	Acrylic ester-Styrene-Acrylonitrile
BF	Beamforming
BiCMOS	Bipolar plus Complementary Metal–oxide–Semiconductor
BWP	Bandwidth Part
CATR	Compact Antenna Test Range
CBW	Channel Bandwidth
CPE	Customer-Premises Equipment
CSI-RS	Channel State Information-Reference Signal
DAC	Digital to Analog Converter
DFF	Direct Far Field
DSRC	Dedicated Short Range Communications
DUT	Device Under Test
EIRP	Effective Isotropic Radiated Power
EIS	Effective Isotropic Sensitivity
eMBB	Enhanced Mobile BroadBand
EMC	Electromagnetic Compatibility
EMI	Electromagnetic Interference
ENDC	EUTRA NR Dual Connectivity
ETSI	European Telecommunications Standards Institute
EVM	Error Vector Magnitude
FCC	Federal Communications Commission
FDD	Frequency Division Duplex
FEM	Front End Module
FinFET	Fin Field Effect Transistor
FOM	Figure Of Merits
FR2	Frequency Range
FRP	Fiberglass-Reinforced Plastic
FWA	Fixed Wireless Access
GaAS	Gallium Arsenide
GaN	Gallium Nitride
GCF	Global Certification Forum
gNB	Next Generation NodeB

GSM	Global System for Mobile Communications
GTI	Global TD-LTE Initiative
HARQ	Hybrid automatic repeat request
HEMT	High Electron Mobility Transistor
IEEE	Institute of Electrical and Electronics Engineers
IFF	Indirect Far Field
IMD	InterModulation Distortion
IoT	Internet Of Things
ISD	Inter-Site Distance
ITU	International Telecommunication Union
LMDS	Local Multipoint Distribution Service
LNA	Low-Noise Amplifier
LO	Local Oscillator
LOS	Line Of Sight
LTCC	Low Temperature Co-fired Ceramic
LTE	Long-Term Evolution
MCL	Maximum Coupling Loss
MCS	Modulation and Coding Scheme
MEC	Mobile Edge Computing
MEMS	Micro-Electro-Mechanical Systems
MIMO	Multiple Input Multiple Output
MIPI	Mobile Industry Processor Interface
MPR	Maximum Power Reduction
MTU	Maximum Transmission Unit
MU-MIMO	Multi-User MIMO
NSA	Non-StandAlone
OEM	Original Equipment Manufacturer
OFDM	Orthogonal Frequency-Division Multiplexing
OTA	Over The Air
PA	Power Amplifier
PAE	Power Amplifier Efficiency
PBCH	Physical Broadcast CHannel
PC3	Power Class 3
PCB	Printed Circuit Board
PDCCH	Physical Downlink Control CHannel
PRB	Physical Resource Block
PTFE	PolyTetraFluoroEthylene
PVC	PolyVinyl Chloride
QAM	Quadrature Amplitude Modulation
RACH	Random Access CHannel

RFFE	Radio Frequency Front End
RFIC	Radio Frequency Integrated Circuit
RRM	Radio Resource Management
SA	StandAlone
SCS	Sub-Carrier Spacing
SiGe	Silicon-Germanium
SINR	Signal-to-Interference-plus-Noise Ratio
SKU	Stock Keeping Unit
SLA	Service-Level Agreement
SOC	System On Chip
SOI	System On Insulator
SP4T	Single Pole 4 Throw
SPNT	Single Pole Multiple Throw
SSB	Synchronization Signal Block
SUL	Supplemental UpLink
SU-MIMO	Single User MIMO
TCP	Transmission Control Protocol
TDD	Time Division Duplex
TRP	Total Radiated Power
UDP	User Datagram Protocol
UE	User Equipment
URLLC	Ultra-Reliable Low Latency Communication
V2X	Vehicle to Everything
VCO	Voltage-Controlled Oscillator
VR	Virtual Reality

14. References

[1]	Cisco VNI Report, Feb 2019
[2]	Ericsson Mobility report, Nov 2018
[3]	https://www.gsma.com/futurenetworks/digest/leading-the-way-in-5g-fixed-wireless-access/
[4]	https://www.gsma.com/futurenetworks/wp-content/uploads/2018/08/Fixed-Wireless-Access-economic-potential-and-best-practices.pdf
[5]	https://www.gsmaintelligence.com/research/?file=0efdd9e7b6eb1c4ad9aa5d4c0c971e62&download
[6]	T. Cameron, "Bits to Beams: RF technology Evolution for 5G mmwave Radios", Microwave Journal, November 2018
[7]	The Carmel Group: Broadband Wireless Access Providers Prepare to Soar with Fixed Wireless THE BWA INDUSTRY REPORT: 2017
[8]	Toyota presentation: 1G of Vehicular Communications, 2016
[9]	5G Automotive Vision, 5GPPP/European Commission/ERTICO, Oct 2015.
[10]	3GPP TR 22.885 – V2X Use cases
[11]	https://enterpriseiotinsights.com/20190301/channels/news/lte-v2x-is-ready-to-roll-says-ford
[12]	http://www.marketsandmarkets.com/PressReleases/industrial-internet-of-things.asp
[13]	https://www.fiercewireless.com/wireless/25-charts-spectrum-ownership-united-states
[14]	https://docs.fcc.gov/public/attachments/DOC-355073A1.pdf
[15]	https://gsacom.com/download.php?id=6511
[16]	METIS channel model, METIS 2020, ICT-317667-METIS/D1.4, Feb, 2015
[17]	Nokia Small Cells Portforlio Update mmWave Overview
[18]	5G mmWave A challenge for device testing and how to solve it, Gunter Pfeifer, R&S Germany
[19]	Planning for 5G: Massive MIMO, mmWave Propagation, Coordinated MultiPoint..Putting it all Together with Predictuve Simulation, Remcom, IWPC Austin 2017
[20]	RF Propagation at 28 GHz, Samsung, IWPC Austin 2017
[21]	mmW for 5G Infrastructure - Which RF Challenges to Overcome?, Infineon, IWPC Autin 2017
[22]	Can a Fixed Wireless Last 100m Connection Really Compete with a Wired Connection and Will 5G Really Enable this Opportunity? By CableLabs/Arris
[23]	Nokia: The mmWave revolution - https://onestore.nokia.com/asset/200779
[24]	28 GHz Millimeter Wave Cellular Communication Measurements for Reflection and Penetration Loss in and around Buildings in New York City: NYU Wireless; http://faculty.poly.edu/~tsr/Publications/ICC_2013_Celinev2.pdf
[25]	5G on high frequencies and it's surroundings until 2020, Softbank, IWPC Madrid 2017.
[26]	mmWave and 5G A Service Provider's Soliloquy, Softbank, IWPC San Jose 2016
[27]	Breaking the wireless barriers to mobilize 5G NR mmWave, Qualcomm, Fierce Wireless Webinar, Jan 2019.

[28]	Millimeter Wave MIMO Prototype Measurements and Experimental Results, Qualcomm
[29]	5G UE Phased Array Design, Ozge Koymen, Qualcomm, Brooklyn 5G Summit, April 2018.
[30]	5G Pyeong-chang & the Way Forward, KT, Brooklyn 5G Summit, April 2018.
[31]	T. Cameron, “Bits to Beams: RF technology Evolution for 5G mmwave Radios”, Microwave Journal, November 2018.
[32]	Performance Characteristics of 5G mmWave Wireless-to-the-Home, Frederick W. Vook, Eugene Visotsky, Timothy A. Thomas, Amitava Ghosh, Nokia Bell Labs.
[33]	Skyworks: 5G in perspective Whitepaper
[34]	Top 5 Challenges for 5G New Radio Device Designers whitepaper, Keysight Technologies
[35]	Understanding 5G NR Physical layer – Keysight Technologies
[36]	MIMO for Millimeter-Wave Wireless Communications: Beamforming, Spatial Multiplexing, or Both?, Shu Sun, Theodore S. Rappaport, Robert W. Heath, Jr., Andrew Nix, and Sundeep Rangan
[37]	T. Cameron, 4.1 Invited: “Architectures and Technologies for the 5G mm-Wave Radio”, ISSCC 2018, Session 4, mm-Wave radios for 5G and Beyond
[38]	D. Y. C. Lie, J. C. Mayeda and J. Lopez, "A short survey on recent highly efficient cm-Wave 5G linear power amplifier design," 2017 IEEE 60th International Midwest Symposium on Circuits and Systems (MWSCAS), Boston, MA, 2017, pp. 13-16
[39]	5G mmWave Radio design for Mobile, Kamal Sahota, Qualcomm
[40]	5G Device Power Consumption - Challenges & Solutions, Mediatek, 23rd GTI Workshop, Vancouver, Nov 2018.
[41]	Considerations on 5G Device Power Consumption, Yuan Zhang, Vivo Mobile Communication Co Ltd, 23rd GTI Workshop, Vancouver, Nov 2018.
[42]	A New Phone Design to Facilitate the Shift From 4G to 5G, by Michelle Hampson, https://spectrum.ieee.org/tech-talk/telecom/wireless/a-new-phone-design-to-facilitate-the-shift-from-4g-to-5g
[43]	A 64-Element 28-GHz Phased-Array Transceiver With 52-dBm EIRP and 8–12-Gb/s 5G Link at 300 Meters Without Any Calibration (https://ieeexplore.ieee.org/document/8424053)
[44]	5G Antenna Design for Mobile Phones (https://blogs.3ds.com/simulia/5g-antenna-design-mobile-phones/)
[45]	Statistical Blockage Modeling and Robustness of Beamforming in Millimeter Wave Systems, Vasanthan Raghavan, Lida Akhoondzadeh-Asl, Vladimir Podshivalov, Joakim Hulten, M. Ali Tassoudji, Ozge Hizir Koymen, Ashwin Sampath, and Junyi Li, Qualcomm.
[46]	http://research.rewheel.fi/downloads/Capacity_utilization_fixed_mobile_broadband_substitution_potential_2017_PUBLIC.pdf
[47]	https://www.opensignal.com/sites/opensignal-com/files/data/reports/global/data-2019-02/the_5g_opportunity_report_february_2019.pdf
[48]	Evolution to 5G - An AT&T Perspective, by David Wolter, AT&T, 5G mmWave Opportunities and Challenges, 10/1/2017, Austin, TX USA (https://www.iwpc.org/DownloadDocument.aspx?DocumentID=5076)
[49]	https://arxiv.org/ftp/arxiv/papers/1803/1803.04163.pdf
[50]	http://5gaa.org/wp-content/uploads/2019/02/5GAA_White_Paper_on_C-V2X_Conclusions_based_on_Evaluation_of_Available_Architectural_Options.pdf
[51]	http://www.gtigroup.org/Resources/rep/2019-02-21/13325.html
[52]	https://www.verizonwireless.com/support/5g-home-faqs/
[53]	https://www.verizon.com/about/file/32255/download?token=6yr6fe6S
[54]	https://about.att.com/story/2019/50_days_of_5g.html

[55]	https://www.nasdaq.com/aspx/call-transcript.aspx?StoryId=4236791&Title=at-t-inc-t-ceo-randall-stephenson-on-q4-2018-results-earnings-call-transcript
[56]	https://www.eetasia.com/news/article/18120601-early-5g-solutions-showcased
[57]	https://venturebeat.com/2019/01/08/verizon-interview-our-true-5g-network-will-offer-a-better-experience-than-rivals/
[58]	https://www.tomsguide.com/us/moto-5g-mod-spring-release,news-29527.html
[59]	https://www.gsma.com/iot/wp-content/uploads/2018/09/201809_Industrial_IoT_Case_Study_Ericsson_Smart_Factory.pdf
[60]	https://news.ti.com/ti-unlocks-mmwave-technology-for-worldwide-industrial-market-through-new-60-ghz-sensor-portfolio
[61]	3GPP TS 22.261 Service requirements for the 5G system; Stage 1 http://www.3gpp.org/ftp//Specs/archive/22_series/22.261/22261-g60.zip
[62]	https://ieeexplore.ieee.org/iel7/35/7565175/07565190.pdf
[63]	Impact of shadow fading in a mmWave band wireless network by Maxime Flament (Chalmers University of Technology, Sweden) and Matthias Unbehaun (Royal Institute of Technology, Sweden): https://pdfs.semanticscholar.org/1420/ad8b30b7df59889452bf783aed2d7ecba6ef.pdf?_ga=2.93133208.403243193.1553005782-91779133.1550677963
[64]	mmWave measurement of RF Reflectors for 5G Green Communications by Tao Hong, Jin Yao, Cong Liu and Fei Qi. https://www.hindawi.com/journals/wcmc/2018/8217839/
[65]	https://www.microwavejournal.com/articles/28100-ghz-active-array-antenna-enables-rapid-5g-prototyping
[66]	Pairing Millimeter wave and Sub07 GHz Spectrum, PHAZR, Farooq Kahn's IWPC presentation, October 2017
[67]	Peter M. Asbeck, *et al.,* Power Amplifiers for mm-Wave 5G Applications: Technology Comparisons and CMOS-SOI Demonstration Circuits, IEEE Trans. Microwave Theory and Techniques, accepted and pending publication, March 2019.
[68]	https://medium.com/@DAQRI/motion-to-photon-latency-in-mobile-ar-and-vr-99f82c480926
[69]	https://www.qualcomm.com/media/documents/files/vr-and-ar-pushing-connectivity-limits.pdf
[70]	https://techneconomyblog.com/2017/01/22/5g-economics-the-tactile-internet-chapter-2/
[71]	https://arxiv.org/abs/1608.05384
[72]	https://blog.motorola.com/2018/08/02/motorola-connects-you-to-5g-first/
[73]	https://www.theverge.com/circuitbreaker/2019/3/13/18263615/verizon-moto-z3-5g-mod-price-release-date-smartphone
[74]	https://www.slashgear.com/5g-moto-mod-motorola-z3-verizon-add-on-fcc-approval-complex-design-release-16565998/
[75]	https://www.att.com/5g/emailsubscription
[76]	https://www.zvei.org/fileadmin/user_upload/Presse_und_Medien/Publikationen/2019/Maerz/5G_for_Connected_Industries_and_Automation/WP_5G_for_Connected_Industries_and_Automation_Download_19.03.19.pdf
[77]	https://venturebeat.com/2019/01/29/verizon-5g-home-wont-expand-until-second-half-of-2019/

[78]	https://www.researchgate.net/profile/Sakib_Khan2/publication/327032183_Feasibility_of_5G_mm-wave_communication_for_connected_autonomous_vehicles/links/5b73854192851ca6505dca60/Feasibility-of-5G-mm-wave-communication-for-connected-autonomous-vehicles.pdf?origin=publication_detail
[79]	https://www.mobileworldlive.com/featured-content/top-three/att-backs-away-from-fwa-5g/
[80]	https://www.sdxcentral.com/articles/news/att-changes-its-tune-on-5g-fixed-wireless/2018/09/
[81]	https://www.tutela.com/hubfs/Assets/Rewheel_Tutela_LTE_5G_performance_drivers_Europe_17022019_FINAL.pdf
[82]	https://spectrum.ieee.org/tech-talk/telecom/wireless/millimeter-waves-travel-more-than-10-kilometers-in-rural-virginia
[83]	https://www.akamai.com/uk/en/resources/visualizing-akamai/real-time-web-monitor.jsp
[84]	https://arxiv.org/pdf/1802.08027.pdf
[85]	http://www-file.huawei.com/-/media/CORPORATE/PDF/ilab/vr-ar-en.pdf
[86]	https://www.mobileworldlive.com/featured-content/top-three/att-backs-away-from-fwa-5g/
[87]	https://www.sdxcentral.com/articles/news/att-changes-its-tune-on-5g-fixed-wireless/2018/09/
[88]	https://www.law.cornell.edu/cfr/text/47/2.1093
[89]	https://www.law.cornell.edu/cfr/text/47/2.1091
[90]	https://venturebeat.com/2019/03/14/fcc-opens-24ghz-mmwave-5g-auction-includes-deals-for-rural-bidders/
[91]	971168 D01 Power Meas License Digital Systems v03r01 (https://apps.fcc.gov/kdb/GetAttachment.html?id=oa1c6R09aOUpAoM7bydRKg%3D%3D&desc=971168%20D01%20Power%20Meas%20License%20Digital%20Systems%20v03r01&tracking_number=47466)
[92]	https://www.engadget.com/2019/04/04/verizon-5g-network-testing-chicago-data-speeds/
[93]	https://www.nctatechnicalpapers.com/Paper/2018/2018-the-future-of-fixed-access/download
[94]	https://www.nctatechnicalpapers.com/Paper/2017/2017-can-a-fixed-wireless-last-100m-connection-really-compete-with-a-wired-connection-/download
[95]	https://www.theverge.com/2019/4/3/18293773/verizon-5g-wireless-network-rollout-chicago-minneapolis
[96]	https://www.cnet.com/news/testing-verizons-early-5g-speeds-3-major-issues-with-the-next-gen-data-network-and-how-to-fix-them/
[97]	https://www.ncbi.nlm.nih.gov/pmc/articles/PMC4629874/pdf/nihms-695510.pdf
[98]	https://www.commscope.com/Blog/A-Small-Solution-to-a-Big-PIM-Problem/
[99]	5G Mobile Systems and Smartphones, Sprint, IWPC Conference, Washington DC, March 2017
[100]	https://www.microwavejournal.com/articles/31448-first-5g-mmwave-antenna-module-for-smartphones
[101]	https://www.anandtech.com/show/14083/motorolas-5g-moto-mod-for-moto-z3-now-available

[102]	F. Sohrabi and W. Yu, "Hybrid digital and analog beamforming design for large-scale antenna arrays," in IEEE Journal of Selected Topics in Signal Processing, vol. 10, no. 3, pp. 501-513, Apr. 2016.
[103]	"Massive MIMO 5G Cellular Networks: mmWave vs µ-wave Frequencies", Stefano Buzzi and Carmen D'Andrea, University of Cassino and Lazio Meridionale, Italy.
[104]	T. L. Marzetta, "Noncooperative cellular wireless with unlimited numbers of base station antennas," in *IEEE Transactions on Wireless Communications*, vol. 9, no. 11, pp. 3590–3600, Nov. 2010.
[105]	J. Zhang, K. Zhao, L. Wang, S. Zhang, and G. F. Pedersen, "Dual-Polarized Phased Array with Endfire Radiation for 5G Handset Applications," IEEE Trans. Antennas Propag., 2019.(Submitted)
[106]	J. Zhang, S. Zhang, X. Li, Y. Fan, G. F. Pedersen, "3D Radiation Pattern Reconfigurable Phased Array for Transmission Angle Sensing in 5G Mobile Communication", Sensors, Vol. 18, No. 12, 4204, 01.12.2018.
[107]	J. Zhang, S. Zhang, and G. F. Pedersen, "A Dipole Phased Array with Reconfigurable Radiation Patterns for 5G Mobile Applications," IEEE Transactions on Vehicular Technology, 2019. (Submitted)
[108]	N. Ojaroudiparchin, M. Shen, and G. F. Pedersen, "Design of Vivaldi antenna array with end-fire beam steering function for 5G mobile terminals," 2015 23rd Telecommunications Forum Telfor (TELFOR), pp. 587–590, 2015
[109]	W. Hong, K. Baek, Y. Lee, and Y. G. Kim, "Design and analysis of a low-profile 28 GHz beam steering antenna solution for Future 5G cellular applications," Microwave Symposium (IMS), 2014 IEEE MTT-S International, pp. 1–4, Jun. 2014
[110]	L. Stark, "Microwave theory of phased-array antennas — a review," Proceedings of the IEEE, vol. 62, no. 12, pp. 1661–1701, 1974
[111]	L. Lu, K. Ma, F. Meng, and K. S. Yeo, "Design of a 60-ghz quasi-yagi antenna with novel ladder-like directors for gain and bandwidth enhancements," IEEE Antennas Wireless Propag. Lett., vol. 15, pp. 682–685, 2016.
[112]	H. Wang, Y. Chen, F. Liu, and X. Shi, "Wideband and compact quasi-yagi antenna with bowtie-shaped drivers," Electronics Letters, vol. 49, no. 20, pp. 1262–1264, 2013.
[113]	C. Di Paola, S. Zhang, K. Zhao, Y. Zhinong, T. Bolin, G. Pedersen, "Wideband Beam-Steerable Array with Hybrid High Gain Antennas for 5G Mobile Devices", IEEE Trans. Antennas Propag. (Submitted)
[114]	S. Zhang, I. Syrytsin, G. F. Pedersen, "Compact Beam-Steerable Antenna Array with Two Passive Parasitic Elements for 5G Mobile Terminals at 28 GHz." IEEE Transactions on Antennas and Propagation, 06.2018.
[115]	M. M. S. Taheri, A. Abdipour, S. Zhang and G. F. Pedersen, "Integrated Millimeter-Wave Wideband Endfire 5G Phased Array and Low-Frequency 4G LTE Antenna in Mobile Terminals," IEEE Transactions on Vehicular Technology, 2019.
[116]	C.-K. Chang, W.-J. Liao and C.-C. Tsai, "Metal Body-Integrated Open-End Slot-Antenna Designs for Handset LTE Uses," IEEE Transactions on Antennas and Propagation, vol. 64, no. 12, pp. 5436-5440, 2016.
[117]	Y.-L. Ban, Y.-F. Qiang, Z. Chen, K. Kang and J.-H. Guo, "A Dual-Loop Antenna Design for Hepta-Band WWAN/LTE Metal-Rimmed Smartphone Applications," IEEE Transactions on Antennas and Propagation, vol. 63, no. 1, pp. 48-58, 2015.

[118]	J. Kurvinen, H. Kähkönen, A. Lehtovuori, J. Ala-Laurinaho and V. Viikari, "Co-Designed mm-Wave and LTE Handset Antennas," IEEE Transactions on Antennas and Propagation, vol. 67, no. 3, pp. 1545-1553, 2019.
[119]	R. Rodríguez-Cano, S. Zhang, K. Zhao and G. F. Pedersen, "Reduction of Main Beam-Blockage in an Integrated 5G Array with a Metal-Frame Antenna," IEEE Transactions on Antennas and Propagation, 2019.
[120]	I. Syrytsin, S. Zhang, G. F. Pedersen, K. Zhao, T. Bolin, and Z. Ying, "Statistical investigation of the user effects on mobile terminal antennas for 5G applications," IEEE Trans. Antennas Propag., vol. 65, pp. 6596–6605, Dec 2017.
[121]	I. Syrytsin, S. Zhang, G. F. Pedersen, and Z. Ying, "User effects on the circular polarization of 5G mobile terminal antennas," IEEE Trans. Antennas Propag., vol. 66, pp. 4906–4911, Sep. 2018.
[122]	M. Zheng, M. Polese, M Mezzavilla, J. Zhu, S. Rangan, S. Panwar, and M. Zorzi, "Will TCP work in mmWave 5G Cellular Networks?".
[123]	"5G: The Greatest Show on Earth" by Signals Research Group.
[124]	Signals Research Group, Signals Flash report, April 4, 2019.
[125]	3GPP TS 38.306 v15.5.0 (2019-03), NR; *User Equipment (UE) radio access capabilities (Release 15)*. 3rd Generation Partnership Project, Technical Specification Group Radio Access Network, March 2019.
[126]	ITU-R p.527-3, "Electrical Characteristics of the Surface of the Earth," March 1992.
[127]	ITU-R p.2040-1 "Effects of building materials and structures on radiowave propagation above about 100 MHz," July, 2015.
[128]	Mark A. Weissberger, "An initial critical summary of models for predicting the attenuation of radio waves by trees," ESD-TR-81-101, IIT Research Institute Final Report, 1982.
[129]	5G NR Fundamentals, Procedures and T&M aspects - Technology book edited by Rohde&Schwarz, 2019
[130]	ROMES coverage measurement software - operating manual. Rohde&Schwarz, April 2019
[131]	https://arxiv.org/pdf/1903.08712.pdf
[132]	https://www.hindawi.com/journals/jat/2017/2750452/
[133]	https://www.itu.int/dms_pub/itu-r/opb/rep/R-REP-M.2376-2015-PDF-E.pdf
[134]	https://www.federalregister.gov/documents/2017/01/12/2016-31059/federal-motor-vehicle-safety-standards-v2v-communications
[135]	https://www.theverge.com/2017/11/1/16592704/vehicle-to-vehicle-communications-mandate-trump
[136]	https://arxiv.org/pdf/1712.01754.pdf
[137]	3GPP TS 22.186 v16.1.0 (2018-12), Enhancement of 3GPP support for V2X scenarios
[138]	"Beamforming Impact on Time Dispersion – Measured Result", Bo Goransson, IWPC Oct 2018, Austin Tx.
[139]	"A 64-Element 28-GHz Phased-Array Transceiver With 52-dBm EIRP and 8–12-Gb/s 5G Link at 300 Meters Without Any Calibration", Figure 9
[140]	"5G Cellular Electromagnetic Window Considerations", Table 2